

Profiling of the micro-RNA Landscape in Human Vascular Smooth Muscle Cells and Exosomes during Replicative Senescence

by

Nguyen Duong Ngoc Diem

A thesis submitted to the School of Pharmacy
University of Nottingham
In Partial Fulfilment of the Requirements for the
Degree of Doctor of Philosophy

November 2020

I. LIST OF PUBLICATIONS

1. Soh FCO, Kee JH, Thein MY, Ying YL, Le CF, **Nguyen D**, Goh BH, Pung SY* and Pung YF*. (2018) Antibacterial activity by ZnO nanorods and ZnO nanodisks: A model used to illustrate “Nanotoxicity Threshold”. *J Ind Eng Chem.* 62: 333-340.

(Impact factor: 4.978)

(DOI: 10.1016/j.jiec.2018.01.013)

*Corresponding author

2. Ho JS, Aziz AI, Pung YF*, Chew HY, Pung SY, Ying YL, **Nguyen D**, and Lim CS. (2020) Potent antifungal activity of ZnO Nanoparticles on *R. mucilaginosa* is mediated by reactive oxygen species and zinc ion. *IOSR-JEN.* 10(4): 44-57.

*Corresponding author

3. **Diem Nguyen Duong Ngoc**, William M Chilian, Shamsul Mohd Zain, Muhammad Fauzi Daud and Yuh Fen Pung. 2020. Micro-RNA Regulation of Vascular Smooth Muscle Cells and Its Significance in Cardiovascular Diseases.

Manuscript under review by Canadian Journal of Physiology and Pharmacology. Impact factor: 2.04.

4. **Diem Nguyen Duong Ngoc**, William M Chilian, Shamsul Mohd Zain, Muhammad Fauzi Daud and Yuh Fen Pung. 2020. Decrease of hsa-miR-155-5p expression levels in human vascular smooth muscle cells and exosomes during replicative senescence.

Manuscript under preparation for submission to American Journal of Physiology – Heart and Circulatory Physiology. Impact factor: 4.0.

II. LIST OF CONFERENCES

1. Wong YC, **Nguyen D**, Pung SY, Chilian WM and Pung YF. Ultrafine particle induced oxidative stress and impaired the ability of human peripheral blood mononuclear cells to differentiate into circulating angiogenic cells. 28th Intervarsity Biochemistry Seminar UCSI, 13 May 2017, Kuala Lumpur, Malaysia
2. **Nguyen D**, Chilian WM, Pan Y and Pung YF. Replicative senescence validation in human vascular smooth muscle cells. 3rd Annual Biomedical Science Postgraduate Research Symposium UNMC, 21 July 2017, Kuala Lumpur, Malaysia
3. **Nguyen D**, Chilian WM, Pan Y and Pung YF. Distinguishing Senescence Phenotypes via Qualitative and Quantitative Analyses in Human Vascular Smooth Muscle Cells. PGR Student Conference Support Poster Competition UNMC, 15 September 2017, Kuala Lumpur, Malaysia.
4. Ho JS, Ying YL, **Nguyen D**, Pung SY, and Pung YF. Comparative study on the antifungal properties of the in-house synthesized ZnO and WO_x nanoparticles, and the nano hybrids on *Rhodotorula mucilaginosa*. 29th Intervarsity Biochemistry Seminar Taylor's University, 12 May 2018, Kuala Lumpur, Malaysia
5. Chew HY, Ying YL, **Nguyen D**, Pung SY, and Pung YF. Comparing antibacterial activities of newly engineered Zinc oxide nanoparticles, Tungsten oxide nanoparticles and Zinc oxide-Tungsten oxide nanohybrids against *Staphylococcus aureus*. 29th Intervarsity Biochemistry Seminar Taylor's University, 12 May 2018, Kuala Lumpur, Malaysia
6. Nurul Husna I, **Nguyen D**, Rayan S, Nashiru B, Chilian WM and Pung YF. Curcumin reduces oxidative stress induced by wood smoke and promotes differentiation of peripheral blood mononuclear cells into endothelial progenitor cells. 9th Malaysian Biomedical Science Symposium University Malaya, 12 to 13 May 2018, Kuala Lumpur, Malaysia
7. Azzahraa Izzati A, Ying YL, **Nguyen D**, Pung SY, and Pung YF. Assessing the antibacterial activities of Zinc oxide, Tungsten oxide, Zinc oxide-tungsten oxide nanoparticles towards *Staphylococcus aureus*. 9th Malaysian Biomedical Science Symposium University Malaya, 12 to 13 May 2018, Kuala Lumpur, Malaysia
8. **Nguyen D**, Chilian WM, Pan Y and Pung YF. Dysregulated micro-RNAs in senescent human vascular smooth muscle cells. 2nd FoS PGR Research Showcase UNMC, 20 June 2018, Kuala Lumpur, Malaysia
9. **Nguyen D**, Chilian WM, Pan Y and Pung YF. Small molecules, Big Tools – MicroRNA as Biomarkers for Hypertension. International Conference on Biochemistry, Molecular Biology and Biotechnology, 15-16 August 2018, Kuala Lumpur, Malaysia

10. Lofti Abdellatif ZA, **Nguyen D** and Pung YF. Curcumin reduces wood smoke extract-induced damage in human endothelial progenitor cells. 30th Intersociety Biochemistry Seminar University of Nottingham Malaysia, 4 May 2019, Kuala Lumpur, Malaysia
11. **Nguyen D**, Chilian WM, Pan Y and Pung YF. Understanding the cardiovascular risk of aging: Elucidating miRNA biomarkers for aging in arteries. Faculty of Science and Engineering Post-graduate Research Showcase 2019 University of Nottingham Malaysia, 23 Sept 2019, Kuala Lumpur, Malaysia
 - (Ms Nguyen D won second prize for the poster presentation category)
12. **Nguyen D**, Chilian WM and Pung YF. MicroRNAome Profiling on Senescent Human Vascular Smooth Muscle Cells. American Heart Association, 16-18 Nov 2019, Philadelphia PA
 - **Nguyen D**, Chilian WM and Pung YF. MicroRNAome Profiling on Senescent Human Vascular Smooth Muscle Cells, *Circulation*. 140 (2019) A15116–A15116. https://doi.org/10.1161/circ.140.suppl_1.15116
 - (Top 50 abstracts for the Atherosclerosis, Thrombosis and Vascular Biology Council)
 - (2019 Paul Dudley White International Scholar Award, American Heart Association)
13. **Nguyen D**, Chilian WM and Pung YF. Uncovering Dysregulated Micro-RNA Expression in Senescent Human Vascular Smooth Muscle Cells: Impacts on Cellular Communication and Vascular Aging, *FASEB J.* 34 (2020). <https://doi.org/10.1096/fasebj.2020.34.s1.00333>.
 - (2020 Experimental Biology Travel award, Biochemistry and Molecular council)

III. ACKNOWLEDGEMENT

First, I would like to extend my gratitude to The University of Nottingham Malaysia for granting me the opportunity for a post-graduate research program here at this beautiful campus. Here was where I have learned many valuable lessons, connected with many wonderful people and improved myself greatly as a researcher.

In order for me to be at this point, writing these words, I am most sincerely thankful to Dr. Pung Yuh Fen, my main supervisor and my mentor. I am forever grateful for your support and insights. You always inspired me with your lectures during my undergrad and you have continued to do so throughout my PhD journey. I thank you for all the difficult times and the good times, the delicious food, the discipline and tough love. With the knowledge that you have passed on to me, I have become a better researcher than I ever thought I would be. I wish you nothing but the best and I hope we can still stay in touch after my PhD.

Another person whose guidance I will always cherish, Prof. William M Chilian, my co-supervisor. Although I regrettably missed the chance to meet you in person, thank you for always being so supportive with your feedback and enlightening me on how to be a proper researcher. I hope you will always be well and I hope we will still have the chance to in the near future.

I would also like to extend my sincere thanks to Dr. Shamsul Mohd Zain for always being so supportive during my PhD journey, from always helping me when I was working in UM to always participating in events at UNM to giving very helpful feedback on my manuscripts. May you always have good data for high impact publications and a successful research career.

I would like to send my gratitude to the admin staff and lab technicians of the Faculty of Science and Engineering, especially Sharon, Fifi, Radha, Siak Chung, Asma and Siti for being

always so helpful despite their busy schedules. I am also extending my appreciation to the Hall Tutor and Hall Warden group. Thank you for letting me be a part of the group. I have learned many new skills by being a hall tutor and I will definitely never forget the experience we had together while overcoming two floods and one pandemic. I wish you all well and all the best.

To the badminton crew, Ernest, Jasmine, Majid, Grace, Eric, Laheji, Omid, Edwin, Jenna, Paulina, Leon, Shi Hui, Yi, you guys are awesome! Thank you for taking good care of me and being a fun part of my memories. I was lucky to have met you guys and may everyone graduate with flying colors.

To Ricardo, I would like to send my thanks for all the times you believed in me when I did not believe in myself and gave me confidence from the confidence you had in me. Thank you for always reaching out to help, for showing me kindness when it is due and for letting me see that the possibilities are endless.

To Mahmoud, my fellow hall tutor and a great friend. Thank you for always cheering me on and taking care of me during my difficult times. Thank you for always helping me and being the friend that I can always talk to and rely on. I hope you will achieve what you set out to do and I wish all the best for you.

To my two great friends, Raymond and Jessica. Thank you for always looking out for me and helping me through my darkest times. I always enjoyed the time we spent together and the conversations we had. You make me a better person. May you both finish smoothly and I know you will achieve great things ahead.

To Anusha, one of the strongest women I know, who I am so very lucky to have as a dear friend. Thank you for always being there, for being so empowering and supportive. You gave me the strength that I needed when things got bad. Always be the strong and empowering

person that you are to inspire others the way you inspired me. I cannot wait to eat lobsters with you and May Zie in Mauritius.

To May Zie, the one who has walked this path with me since day one. Malaysia would not be as good a place and my PhD would not be as memorable a journey without you. Thank you for all the laughter, the tears, the advice, the company. Thank you for being the best friend anyone could ever ask for. May our friendship only get stronger with time like fine wine and may you achieve all that you want in your future endeavors. Here is to the exciting journey that awaits us.

To my family and friends back home, Uncle Gary, Thao, Tra, Dang and all the people who have given me unrelenting support and had absolute faith in me. Thank you for always being there and giving me strength to move on. I hope to always have your back the way you have had mine. I would not know what I would do without you in my life.

With all the hard work and achievements, I would like to dedicate everything to the most important person in my life, my mother, who has dedicated everything she had to me. Thank you for teaching me the value of resilience and unconditional love so that my wounds heal quicker every time I fall down. Words cannot express how grateful I am to be your daughter and I hope to grow more into the person who would make you prouder with every passing day. Sending you all my love.

IV. TABLE OF CONTENTS

Chapter 1. Introduction.....	1
1.1. <i>Background, Rationale and Hypothesis of Study</i>	1
1.2. <i>Aim and Objectives of Study.....</i>	4
1.2.1. Aim.....	4
1.2.2. Objectives.....	4
Chapter 2. Literature Review.....	5
2.1. <i>Arterial Stiffness and Early Vascular Aging in Hypertension.....</i>	5
2.1.1. Arterial Stiffness in Hypertension	5
2.1.2. Early Vascular Aging.....	6
2.2. <i>Vascular Smooth Muscle Cells and Aging.....</i>	7
2.2.1. Phenotypes and Phenotypic Switching	7
2.2.2. Replicative and Stress-Induced Senescence.....	8
2.2.3. Molecular Signalling Pathways of Cellular Senescence	12
2.3. <i>Micro-RNAs and their Roles in VSMC Regulation and Communication.....</i>	16
2.3.1. The Discovery of micro-RNAs	16
2.3.2. The Biogenesis of miRNAs.....	17
2.3.3. Interactions Between miRNA and Target mRNA via the miRNA-RNA-induced Silencing Complex.....	19
2.3.4. The Unconventional Roles of miRNAs.....	20
2.3.5. Evidence of miRNA Intracellular Signaling in Vascular Smooth Muscle Cells	24
2.4. <i>Introduction to Intercellular Communication via Exosomes.....</i>	31
2.4.1. Exosomal Biogenesis and Export	31
2.4.2. Micro-RNA Sorting and Loading into Exosomes	32
2.4.3. MiRNA Extracellular Signaling via the Exosomal Axis.....	34
2.4.4. Exosomal miRNA Studies in Clinical Research	37

2.5. Current Drawbacks and Potential of miRNAs in Research and Clinical Settings	38
2.5.1. Technical Drawbacks.....	38
2.5.2. Origin of Circulating miRNAs: Cell-type-specific miRNA Profiles	39
2.5.3. Circulating miRNAs: Cell-free or Exosomal?	40
2.5.4. The Latent Potential of miRNAs.....	40
Chapter 3. Materials and Methods.....	41
3.1. Characterization of Replicative Senescence in Human Vascular Smooth Muscle Cells.....	41
3.1.1. Materials	41
3.1.2. Subject Selection	41
3.1.3. Human Vascular Smooth Muscle Cell Culture and Morphological Analysis	42
3.1.4. Human Vascular Smooth Muscle Cell Passaging and Cryopreservation	42
3.1.5. Senescence-Associated β -galactosidase Staining	43
3.1.6. Total RNA Extraction from Human Vascular Smooth Muscle Cells for Senescence- Associated Gene Expression Analysis	43
3.1.7. Complementary DNA Synthesis for Quantitative Polymerase Chain Reaction.....	44
3.1.8. Genomic DNA Extraction from Human Vascular Smooth Muscle Cells for Relative Telomere Length Measurement.....	44
3.1.9. Primer Validation via Absolute Quantification and Gel Electrophoresis.....	45
3.1.10. Senescence-Associated Gene Expression.....	47
3.1.11. Relative Telomere Length Measurement	48
3.2. Isolation and Characterization of Human Vascular Smooth Muscle Cell-Derived Exosomes....	50
3.2.1. Materials	50
3.2.2. Exosome Isolation from Conditioned Media using Sucrose Cushion	50
3.2.3. Scanning Electron Microscopy.....	50
3.2.4. Transmission Electron Microscopy	51
3.2.5. Lowry Protein Assay.....	51
3.2.6. Immunoblotting.....	52

3.3. <i>Whole-Genome Small RNA Next-Generation Sequencing</i>	53
3.3.1. Total RNA Extraction from Human Vascular Smooth Muscle Cells and Human Vascular Smooth Muscle Cell-Derived Exosomes for Next-Generation Sequencing	53
3.3.2. RNA and DNA Quality Control using Qubit Fluorometer	53
3.3.3. RNA and DNA Quality Control using BioAnalyzer	54
3.3.4. Whole Genome Small RNA Next-Generation Sequencing.....	54
3.4. <i>Primary and Secondary Data Analysis of Whole-Genome Small RNA Next-Generation Sequencing</i>	57
3.5. <i>miRNA Target Prediction and Pathway Analyses</i>	60
3.6. <i>Validation of Differentially Expressed miRNAs in Human Vascular Smooth Muscle Cells</i>	61
3.6.1. Materials	61
3.6.2. Total RNA Reverse Transcription Targeting Matured miRNAs	61
3.6.3. Primer Design and Validation for Differentially Expressed miRNA Validation.....	62
3.6.4. miRNA Differential Expression Validation	62
3.7. <i>Statistical Analysis</i>	63
Chapter 4. Results	64
4.1. <i>Characterization of Replicative Senescence in Human Vascular Smooth Muscle Cells</i>	64
4.1.1. Human Vascular Smooth Muscle Cell Morphology during Senescence	64
4.1.2. Senescence-associated β -galactosidase Activities in Human Vascular Smooth Muscle Cells during Senescence.....	64
4.1.3. Gene Expression in Human Vascular Smooth Muscle Cells during Senescence	65
4.1.4. Relative Telomere Length of Human Vascular Smooth Muscle Cells during Senescence .	65
4.2. <i>Characterization of Exosomes Isolated from Human Vascular Smooth Muscle Cell Conditioned Media</i>	70
4.2.1. Scanning Electron Microscopy.....	70
4.2.2. Transmission Electron Microscopy	70
4.2.3. Immunoblotting.....	70

4.3. Optimization of Small RNA Library Prep prior to Sequencing	73
4.4. Primary and Secondary Data Analysis of Whole-Genome Small RNA Next-Generation Sequencing.....	75
4.5. Intracellular and Exosomal miRNAs in Human Vascular Smooth Muscle Cells during Replicative Senescence.....	84
4.5.1. Differential Expression Analysis and Validation of Intracellular and Exosomal miRNAs in Senescent Human Vascular Smooth Muscle Cells.....	84
4.5.2. Validation of Differentially Expressed miRNAs in Senescent Human Vascular Smooth Muscle Cells and Exosomes	91
4.5.3. Predicted Target Genes of Differentially Expressed miRNAs.....	95
4.5.4. Gene Ontology Categorization of Predicted Target Genes of Differentially Expressed miRNAs	100
4.5.5. Pathway Analysis of Predicted Targets of Differentially Expressed miRNAs	107
4.5.6. Regulatory Interaction Network of Differentially Expressed miRNAs and Their Target Genes.....	111
Chapter 5. Discussion	121
5.1. Human Vascular Smooth Muscle Cells Replicative Senescence Characterization	121
5.2. Human VSMC-Derived Exosome Isolation and Characterization	126
5.2.1. Differences in Proliferative and Senescent hVSMC-Derived Exosomes.....	127
5.3. Genome-wide Small RNA Landscape in Young and Old Human Vascular Smooth Muscle Cells and Their Exosomes during Replicative Senescence	129
5.3.1. Highly Variable RNA Profiles in Human Vascular Smooth Muscle Cells during Replicative Senescence	129
5.3.2. RNA Profiles of Human Vascular Smooth Muscle Cell-Derived Exosomes	131
5.3.3. Other Non-coding RNA classes and Their Association with Cellular Senescence in Vascular-Related Diseases	133

5.3.4. Overcoming Limitations and disadvantages of Irregular RNA Profiles in Senescent hVSMCs and hVSMC-derived exosomes.....	135
<i>5.4. Differentially Expressed Intracellular miRNAs in Human Vascular Smooth Muscle Cells during Replicative Senescence</i>	<i>138</i>
5.4.1. Upregulation of Intracellular hsa-miR-664a-3p, hsa-miR-664a-5p, hsa-miR-664b-3p and hsa-miR-4485-3p and the Negative Regulation of Cellular Phosphate Metabolism, Subcellular Localization and Transport.....	138
5.4.2. Upregulation of Intracellular hsa-miR-664a-3p, hsa-miR-664a-5p, hsa-miR-664b-3p and hsa-miR-4485-3p in the Regulation of Toll-like receptor and MAPK Signaling Pathways in hVSMCs during Replicative Senescence	142
5.4.3. Downregulation of Intracellular hsa-miR-155-5p and hsa-miR-20a-5p Promoted Cytoskeletal Reorganization and Cell Cycle Arrest	143
5.4.4. Downregulation of Intracellular hsa-miR-155-5p and hsa-miR-20a-5p Dampened hVSMC Stress Response during Replicative Senescence	145
5.4.5. Downregulation of Intracellular hsa-miR-155-5p and hsa-miR-20a-5p Promoted TGF- β Accumulation but Inhibited TGF- β signaling Pathway in hVSMCs during Replicative Senescence	146
5.4.6. Downregulation of intracellular hsa-miR-155-5p and hsa-miR-20a-5p activated PI3K/Akt signaling in human vascular smooth muscle cells during replicative senescence.....	147
<i>5.5. Differentially Expressed Exosomal miRNAs in Human Vascular Smooth Muscle Cell-Derived Exosomes during Replicative Senescence.....</i>	<i>149</i>
5.5.1. The Potential of Exosomal hsa-miR-7704 in hVSMC-derived Exosomes during Replicative Senescence	149
5.5.2. Downregulation of Exosomal miRNAs hsa-miR-155-5p and hsa-miR-146b-5p as an Intercellular Signal to Mitigate hVSMC Proliferation and Proinflammatory Signaling	150
<i>5.6. Significant Downregulation of hsa-miR-155-5p Expression in Senescent hVSMCs and Their Exosomes</i>	<i>152</i>
<i>5.7. Senescent hVSMCs Trying to Escape Death?</i>	<i>154</i>

Chapter 6. Limitations, Conclusion and Future Work	156
6.1. <i>Limitations</i>	156
6.2. <i>Conclusion</i>	157
6.3. <i>Future work</i>	159
6.3.1. Direct Interactions and Functional Studies Derived from the Profiling of the miRNA Landscape within hVSMCs and Exosomes during Replicative Senescence	159
6.3.2. Long Intergenic Non-coding RNA Profiling in Young and Senescent hVSMC-Derived Exosomes.....	161
6.3.3. Exosome Composition of Senescent hVSMCs and Uptake by Recipient Cells	161
6.3.4. Linking Differentially Expressed miRNAs from Replicative Senescent hVSMCs to Arterial Stiffness and Hypertension	161
Chapter 7. References	163
Chapter 8. Appendix	187
8.1. <i>Cycling conditions and reaction setup for relative telomere length measurement</i>	187
8.2. <i>Sample summary</i>	188
8.3. <i>Target genes of Differentially Expressed miRNAs</i>	189
8.4. <i>Gene ontology categorization and enrichment analysis</i>	203
8.4.1. Intracellular upregulated miRNA target genes GO categorization.....	203
8.4.2. Intracellular downregulated miRNA target genes GO categorization.....	209
8.4.3. Exosomal upregulated miRNA target genes GO categorization	216
8.4.4. Exosomal downregulated miRNA target genes GO categorization.....	218

V. LIST OF FIGURES

Figure 2.2-1: A simplified presentation of the cell cycle.	13
Figure 2.3-1: MiRNAs are prominent intracellular regulators of important cellular events, such as phenotypic switching, senescence, vascular calcification and neointimal formation.	30
Figure 2.4-1: Biogenesis of miRNAs and their loading into endosomes, which are released as exosomes into the extracellular matrix via exocytosis.	36
Figure 3.1-1 Calculation for T/S Ratios.	49
Figure 3.2-1 Stacking sandwich for protein transfer.	52
Figure 3.3-1: Truseq Small RNA Library preparation workflow.	55
Figure 3.3-2: Optimization of DNA elution for NGS library prep.	56
Figure 3.4-1: Secondary analysis using the CAP-miRSeq workflow adapted from Sun <i>et al.</i> (2014).	59
Figure 4.1-1: A qualitative comparison between proliferating and senescent hVSMCs in terms of morphology and SA β -galactosidase activities under a bright field microscope.	67
Figure 4.1-2: Relative fold change of the expression of the senescence-associated genes <i>CDKN2A</i> , <i>CDKN1A</i> and <i>CDKN1B</i> encoding p16 ^{INK4α} , p21 ^{Cip1} and p27 ^{Kip1} in old samples.	68
Figure 4.1-3: Relative telomere length of young and old samples.	69
Figure 4.2-1: Ultrastructure of exosomes from scanning electron microscope and transmission electron microscope.	71
Figure 4.2-2: Immunoblotting via Western Blot against the protein TSG101.	72
Figure 4.3-1: Optimization of native PAGE for NGS library prep.	74
Figure 4.4-1: Per base sequence quality of intracellular and exosomal miRNAs post-trimming.	76
Figure 4.4-2: Per sequence quality scores of intracellular and exosomal miRNAs post-trimming.	77
Figure 4.4-3: Per base N content of intracellular and exosomal miRNAs post-trimming.	78
Figure 4.4-4: Sequence length distribution of intracellular and exosomal miRNAs post-trimming.	79
Figure 4.4-5: RNA profiling of intracellular hVSMCs.	81
Figure 4.4-6: RNA profiling of hVSMC-derived exosomes.	82
Figure 4.4-7: Data distribution analyses.	83

Figure 4.5-1: Heat map representing significant differentially expressed intracellular miRNAs of hVSMCs	85
Figure 4.5-2: Heat map representing significant differentially expressed exosomal miRNAs in hVSMC-derived exosomes	86
Figure 4.5-3: Differential expression of young compared to old intracellular miRNAs.....	87
Figure 4.5-4: Differential expression of young compared to old exosomal miRNAs.....	88
Figure 4.5-5: Structure of differentially expressed miRNAs generated by miRDeep2.	90
Figure 4.5-6: Validation of upregulated intracellular miRNAs in senescent hVSMCs.....	92
Figure 4.5-7: Validation of downregulated intracellular miRNAs in senescent hVSMCs.....	93
Figure 4.5-8: Validation of downregulated exosomal miRNAs in senescent hVSMC-derived exosomes.....	94
Figure 4.5-9: GO Enrichment Analysis of target genes of intracellular upregulated miRNAs.....	102
Figure 4.5-10: GO Enrichment Analysis of target genes of intracellular downregulated miRNAs..	103
Figure 4.5-11: GO Categorization of target genes of upregulated exosomal <i>hsa-miR-7704</i>	104
Figure 4.5-12: GO Enrichment Analysis of gene targets of exosomal downregulated miRNAs.....	105
Figure 4.5-13: GO Enrichment analysis of the target genes of <i>hsa-miR-155-5p</i>	106
Figure 4.5-14: Most enriched pathways associated with target genes of intracellular miRNAs.	109
Figure 4.5-15: Most enriched pathways associated with target genes of exosomal miRNAs.	110
Figure 4.5-16: miRNA-mRNA target interaction network of downregulated intracellular <i>miR-155-5p</i> and <i>miR-20a-5p</i>	113
Figure 4.5-17: miRNA-RNA target interaction network of upregulated intracellular miRNAs.	114
Figure 4.5-18: miRNA-RNA target interaction network of downregulated exosomal miRNAs.	115
Figure 4.5-19: miRNA-RNA target interaction network of upregulated exosomal <i>hsa-miR-7704</i> . .	116
Figure 4.5-20: PPI network of significantly enriched target genes of intracellular upregulated miRNAs.....	118
Figure 4.5-21: PPI network of significantly enriched target genes of intracellular downregulated miRNAs.....	119
Figure 4.5-22: PPI network of significantly enriched target genes of exosomal downregulated miRNAs.	120

Figure 5.1-1: A simplified diagram of senescence-associated signaling pathways. 124

Figure 6.2-1: Schematic diagram of miRNA intracellular and exosomal regulation of hVSMC during replicative senescence. 158

VI. LIST OF TABLES

Table 1. Intracellular miRNA regulatory effects on VSMCs.	22
Table 2. Primer sequences for SA gene expression analysis.	47
Table 3. Primer sequences for telomere length measurement.	48
Table 4: Primer assays for differentially expressed miRNA validation.	62
Table 5: Dysregulated miRNAs in senescent hVSMCs.	89
Table 6: Dysregulated miRNAs in exosomes derived from senescent hVSMCs.	89
Table 7: Highlight of target genes filtered from GO and KEGG enrichment analyses.	96
Table 8. Cycling conditions for Tel Assay.	187
Table 9. Reaction setup for 36B4 assay.	187
Table 10. Reaction setup for Tel Assay.	187
Table 11: Summary of sequenced reads of all samples.	188
Table 12: Validated target genes of differentially expressed miRNAs reported by miRWalk.	189
Table 13: Biological processes of intracellular upregulated miRNA targets (Top 50).	203
Table 14: Molecular functions of intracellular upregulated miRNA targets.	206
Table 15: Cellular components associated with intracellular upregulated miRNA targets.	208
Table 16: Biological processes of downregulated miRNA targets (Top 50).	209
Table 17: Molecular functions of intracellular downregulated miRNA targets (Top 50).	212
Table 18: Cellular components associated with intracellular downregulated miRNA targets (Top 50).	214
Table 19: GO biological processes associated with target genes of upregulated <i>hsa-miR-7704</i>	216
Table 20: GO molecular functions associated with target genes of upregulated <i>hsa-miR-7704</i>	217
Table 21: GO cellular components associated with target genes of upregulated <i>hsa-miR-7704</i> . ..	217
Table 22: Biological processes of downregulated exosomal miRNA target genes (Top 50).	218
Table 23: Molecular functions of downregulated exosomal miRNA target genes.	221
Table 24: Cellular components of downregulated exosomal miRNA target genes.	222

VII. LIST OF ABBREVIATIONS

AMPK	AMP-activated protein kinase
ATM	Ataxia telangiectasia mutated
ATP	adenosine triphosphate
ATR	ATM and Rad3-related
BP	biological process
BSA	bovine serum albumin
CAD	coronary artery disease
CC	cellular component
CVD	cardiovascular disease
DDR	DNA damage response
DNA	deoxyribonucleic acid
FBS	fetal bovine serum
FDR	false discovery rate
GO	gene ontology
HRP	horseradish peroxidase
INK4	inhibitors of CDK4
MAPK	mitogen-activated phosphate kinase
MF	molecular function

miRNA	micro-ribonucleic acid
PRR	pattern-recognition receptor
PTM	post-translational modification
QC	quality control
qPCR	quantitative polymerase chain reaction
RNA	ribonucleic acid
ROS	reactive oxygen species
rpm	revolution per minute
RS	replicative senescence
RT	room temperature
SA	senescence-associated
SEM	scanning electron microscopy
SIPS	stress-induced premature senescence
TEM	transmission electron microscopy
TLR	toll-like receptor
TRIF	TIR-domain-containing adapter-inducing interferon- β
TSG101	tumour susceptibility gene 101

VIII. ABSTRACT

Vascular aging is highly associated with cardiovascular morbidity and mortality and vascular smooth muscle cell (VSMC) senescence is one of its key contributors. During senescence, VSMCs intracellular regulations as well as intercellular communication are altered. However, intracellular and intercellular signaling in senescent VSMCs are not fully explored. MicroRNAs (miRNAs) cellular posttranscriptional regulators as well as potential intercellular messengers and understanding miRNA intracellular and intercellular regulation via the exosomal axis during VSMC senescence may elucidate the molecular mechanistic link between vascular aging and early adverse vascular remodeling. This study aimed to identify dysregulated miRNA expression within senescent VSMCs as well as senescent VSMC-derived exosomes. Healthy and senescent human VSMCs (hVSMCs) were cultured *in vitro* and exosomes secreted by these cells were isolated via ultracentrifugation. Subsequently, cellular and exosomal miRNAs were isolated and used for library preparation of whole-genome small RNA next-generation sequencing (NGS). Post-sequencing and differential expression analyses compared the miRNA profiles between healthy and senescent hVSMCs as well as their derived exosomes. Thereafter, NGS data were validated using real-time polymerase chain reaction (qPCR). Additionally, target prediction, gene ontology and pathway enrichment analyses were performed. In senescent hVSMCs, eight significant differentially expressed mature miRNAs were identified ($n= 4$, $q < 0.05$). Bioinformatic analyses showed correlation between upregulated miRNAs, *hsa-miR-664a-3p*, *hsa-miR-664a-5p*, *hsa-miR-664b-3p* and *hsa-miR-4485-3p*, with altered cellular metabolism and transport, with changes in ATP binding and reduced stress response. Meanwhile, downregulated miRNAs, *hsa-miR-155-5p* and *hsa-miR-20a-5p* might associate with cell cycle arrest at G1/S phase, reduced stress response and increased levels of oxidative stress. On the other hand, three significant differentially expressed miRNAs were found in senescent

hVSMC-derived exosomes. Data suggested that the upregulated exosomal miRNA *hsa-miR-7704* might involve in intercellular communication via the exosomal signaling axis. Concurrently, downregulation of exosomal miRNAs *hsa-miR-155-5p* and *hsa-miR-146b-5p* promoted cell cycle arrest and evaded from immune clearance. Interestingly, there was a consistent observation of *hsa-miR-155-5p* downregulation in both senescent hVSMCs and their secreted exosomes. Further analyses with the other dysregulated miRs suggested *hsa-miR-155-5p* involvement in the Smad/TGF- β and PI3K/Akt/mTOR signaling pathways. Differentially expressed intracellular and exosomal miRNAs might be involved in the regulation of cell survival in senescent hVSMCs via the TGF- β signaling pathway. Finally, changes in miRNA signaling in senescent hVSMCs reflected association with vascular aging and therefore might pose as a potential link between early vascular aging and cardiovascular diseases.

Keywords: hypertension, exosomes, replicative senescence, biomarker.

Chapter 1. Introduction

1.1. Background, Rationale and Hypothesis of Study

Cardiovascular disease (CVD) refers to conditions affecting the heart and blood vessels in humans and is among the leading causes of death worldwide(196). CVDs consist of a group of different but relatable heart and blood vessel diseases that can develop under two main types of risk factor: modifiable and non-modifiable. Currently, hypertension, a non-communicable disease, is one of the most important modifiable risk factors for premature CVDs (30).

Hypertension is the state of abnormally high blood pressure and is often under-diagnosed, thus usually referred as a silent killer due to its lack of signs and/or symptoms. According to the World Health Organization (WHO), 1.13 billion people have hypertension, affecting one in four men and one in five women globally (304). In Malaysia, the National Health and Morbidity Survey (NHMS) in 2015 recorded 6.1 million adults with hypertension at a similar prevalence rate of 30.3 per cent, with only half were aware that they had hypertension (1). These alarming statistics are often underestimated as hypertension is a chronic disease that does not result in instant morbidity and mortality. Therefore, its severity is often overlooked by majority of the public.

Currently, the most favourable method of hypertension diagnosis is blood pressure measurement as it is cost-effective, accurate and non-invasive. Although one is considered to be prehypertensive if their measurement falls between 120/80 – 139/89mmHg, these values are subjective while patients are objective and are different in many dynamics (55). Additionally, this technique can only be used to diagnose prehypertension and hypertension, but not the early development of hypertension that precedes prehypertension.

As the world population is gravitating towards a more sedentary lifestyle and rich diet, a rise in hypertension is imminent and a universal method for accurate diagnosis of early development of hypertension has not been established. Therefore, it is important that such method is developed for the specific diagnosis of early development of hypertension. Rather than getting long term treatment with hypertensive drugs which can be costly and debilitating to the patient's quality of life, early hypertensive diagnosis can raise awareness and encourage patients to make appropriate lifestyle changes, which would intervene hypertension development and progression. The early development of hypertension diagnostic test can be incorporated into an annual health check-up program which will be cost effective and fuss-free as the results will be interpreted by the practitioner and returned to the patient, similar to that of a blood examination.

The first step towards developing an early development of hypertension diagnostic tool for hypertension involves the detection and identification of potential biomarkers that are specific to the condition, robust in nature and clinically significant. It is widely recognized that hypertension is influenced by arterial stiffness, which is closely related to aging (262). Although high correlations have been found between arterial stiffness and aging, no solid evidence of any specific mechanism or pathway has been concluded as a direct connection between arterial stiffness and aging (108).

The development of hypertension involves the vasculature and the blood vessel wall thickest layer, *tunica media*, consists of vascular smooth muscle cells (VSMCs), whose health greatly reflects the health of the blood vessel. In healthy conditions, VSMCs are differentiated and acquire a contractile phenotype. Contractile VSMCs possess elasticity and tensile strength to maintain vascular tone and accommodate high pressure exerted on the vascular wall by the tensile stress. In pathological conditions, contractile VSMCs receive autocrine and/or paracrine signaling and switch to a synthetic phenotype characterized by the downregulation

of the smooth muscle (SM) marker genes, i.e. α -SM actin and SM MHC proteins, and the upregulation of the osteogenic genes, i.e. osteopontin, collagen I and bone morphogenic proteins (BMPs)(118, 332). VSMC phenotypic switching is heavily regulated and a crucial step to maintain balance between contractile and synthetic VSMC phenotypes. Synthetic VSMCs can exit the cell cycle and go into senescence upon induction to stress or exhaustion of replicative capacity, which are referred to as stress-induced premature senescence and replicative senescence, respectively.

In recent years, an increasing body of miRNA and VSMC signaling research has emerged as a new layer of cellular regulation during vascular pathogenesis(51, 102, 165, 166, 245, 271, 328). Micro-RNAs (miRNAs) have attracted considerable attention in vascular research. MiRNAs are regulatory RNA molecules that play a major role in post-transcriptional modification, which regulate gene expression via gene silencing pathways. Unique miRNA expression profiles have been identified in different tissues, suggesting the potential use of miRNAs as specific biomarkers for diagnosis of pathological tissues. Furthermore, accumulating evidence suggested that miRNAs could be secreted to the extracellular matrix or bloodstream to facilitate intercellular communication(60, 129, 130, 133, 160, 273, 340). Despite ample reports, the roles of miRNAs in VSMC regulation, particularly in senescence, are not fully deciphered. Based on the currently available literature, we hypothesized that miRNAs are abnormally regulated in hVSMCs and their exosomes during replicative senescence.

Understanding miRNA regulation of VSMCs in aging has important implications in hypertension development and progression. Insights into the cellular mechanisms and signaling pathways involved in the pathological progression of hypertension will be highly useful in devising strategies for accurate diagnosis of disease onset, improved prognosis and precise therapeutic interventions.

1.2. Aim and Objectives of Study

1.2.1. Aim

The principle aim of this study is to discover a set of potential biomarkers for early diagnosis of arterial stiffness in order to intervene and hamper the development of hypertension. In order to achieve this aim, the study was sectioned into multiple phases with different but complementing objectives. The first phase involved the fundamental characterization and profiling of hVSMC miRNAs to identify underlying pathways associated with miRNA regulation and signaling during replicative senescence. The second phase involved functional studies and validation of the biological significance of the identified miRNAs and their target genes. Lastly, the final phase involved clinical screening and comparison between healthy and early hypertensive subjects using a panel of the miRNA identified. The current study focused on the first phase of the whole study.

1.2.2. Objectives

In order to complete the first phase of the study, four main objectives were proposed:

- To distinguish hVSMC replicative senescence from stress-induced premature senescence *in vitro*;
- To isolate and characterize hVSMC-derived exosomes from 'conditioned' media of young and old hVSMC *in vitro* cultures;
- To profile and compare the miRNA landscape in hVSMC and exosomes during proliferation and replicative senescence.
- To identify potential signaling pathways associated with differentially expressed miRNAs in hVSMC and exosomes during replicative senescence.

Chapter 2. Literature Review

2.1. Arterial Stiffness and Early Vascular Aging in Hypertension

Patients with essential hypertension have an increased risk of CVD, not only by elevated blood pressure, but also due to the fact that hypertension often clusters with other risk factors, such as arterial stiffness and early vascular aging. A common interpretation of known relations between arterial stiffness and hypertension is that elevated blood pressure increases stress in the aortic wall, which accelerates elastin degradation (44, 205, 260). Thus, hypertension is perceived as an accelerated form of vascular aging that leads to arterial stiffness (186).

2.1.1. Arterial Stiffness in Hypertension

Although the causality between increased arterial stiffness and hypertension is complex due to many factors (e.g., aging, diet, life style), recent studies in humans and animals suggest that increased arterial stiffness can precede hypertension (207). In clinical studies, a consistent observation of arterial stiffness preceding hypertension was also observed in the Framingham Heart Cohort Study (125). However, the biological mechanisms and cellular processes whereby increased arterial stiffness alone can lead to hypertension are still unclear, encouraging further investigation. An important note to takeaway is that while hypertension can predict arterial stiffness, arterial stiffness can also foretell hypertension (202).

There are a few different ways to measure arterial stiffness, but the methods that are most cited to be the gold standard for arterial stiffness measurement are elevated carotid-femoral pulse wave velocity (CFPWV) and conventional pulse pressure calculations (303). Pulse pressure depends aortic geometry and peak aortic flow, whereas CFPWV measures of aortic

wall stiffness. Currently, the measurement of arterial stiffness remains a research tool that has not been implemented in routine clinical practice. However, growing evidence of clinical value and further advances in technology suggest that arterial stiffness measurement and interpretation will be a useful tool for clinical use in the near future (151, 303).

On a molecular level, various factors contribute to arterial stiffness. In stiffened vessels, elastin fibre content decreases while collagen deposition increases. This is considered to be causal change leading to arterial stiffness as collagen is much stiffer than that of elastin. Therefore, as more collagen is present in the extracellular matrix of the blood vessel, it makes the vessel become more rigid and harden (289). Arterial stiffness is also influenced by the activity or inactivity of certain matrix metalloproteinases and semicarbazide-sensitive amine oxidase (SSAO) (183). For instance, matrix metalloproteinase 9 was found to facilitate collagen degradation as a compensatory mechanism when blood pressure is raised due to an increase in arterial stiffness (220). However, in some pathological conditions, this mechanism is faulty thus resulting in raised blood pressure for a prolonged period. Cell-matrix interaction is one of the key players in the modulation of arterial stiffness. Arterial stiffness may be due to the thickening of the arterial walls as well as calcification of the arterial vascular smooth muscle cells (177).

2.1.2. Early Vascular Aging

Aging is a natural phenomenon and vascular aging plays a central role in facilitating age-related vascular diseases, which contribute to morbidity and mortality of CVDs (83). As a person ages, their blood vessels undergo structural modifications which make them more susceptible to the development of arterial stiffness (262). The concept of early vascular aging (EVA) syndrome was first described in 2008 (201, 203), which has been followed by different studies that explored vascular aging to look for new mechanisms and treatment targets. The core component of EVA is reported to be arterial stiffness, which could be measured by

elevated CFPWV along the aorta directly with some modern technical devices that have been reported to be mostly reliable (240, 288).

One way to combat against EVA is to look for factors that protect from EVA, such as diagnostic biomarkers. Detection of vascular aging could be better defined and understood using advanced phenotyping using genetics and omics. On that note, EVA and arterial stiffness have been associated with changes in vascular smooth muscle cells (VSMCs) that involved cytoskeletal reorganization, inflammatory responses and intercellular communication, among many other signaling pathways (147, 202).

2.2. Vascular Smooth Muscle Cells and Aging

2.2.1. Phenotypes and Phenotypic Switching

Human vascular smooth muscle cells (hVSMCs) play a very important role in regulating and maintaining the appropriate blood pressure by modulating their contractility. However, they also have significant influence on the tissue microenvironment and contributions towards vascular remodelling (210).

Under normal conditions, the majority of hVSMCs differentiate into a contractile phenotype where hemodynamic stability is favoured. The contractile phenotype is a reversible differentiated state of hVSMCs (81). Senescent hVSMCs obey the evolutionary of aging, whereby they exhibit antagonistic pleiotropy, in which cellular senescence can be both protective and deleterious towards the cell at the same time(39). An example of the harmful aspect of cellular senescence is the senescence associated secretory phenotype (SASP) of hVSMCs (58). During cellular senescence or pre-senescence, hVSMCs transform themselves back into their active, proliferative and synthetic state equivalent to that seen during vasculogenesis of the fetus (209).

SASP hVSMCs encompass many factors which can be simplified into three main categories: soluble signalling factors, secreted proteases and secreted insoluble proteins (extracellular matrix components). These factors contribute to SASP potent paracrine effects and microenvironment remodelling capabilities (58). SASP has an altered set of secretome which can be referred to as senescence-messaging secretome. A study by Dupont *et al.* (2005) has identified a set of secreted proteins related to the synthetic phenotype of human aortic vascular smooth muscle cells using proteomics approach (76). The results showed the presence of cytoskeletal proteins involved in cellular structural remodelling and also cellular calcification. This serves as an exemplary study and experimental design to base on for the discovery and identification of biomarkers of hypertension, starting from the secretomic analyses of senescence hVSMCs.

2.2.2. Replicative and Stress-Induced Senescence

Cellular senescence is an irreversible cell-cycle arrest mechanism of cells to cease cell proliferation at an appropriate time as a protective measure against the growth of damaged and/or abnormal cells in mammals (284). It is proposed that, as cells senesce, the gene pool becomes depleted and cell regeneration rate declines. As a result, the organs and tissues involved in cellular senescence degenerate with some classic manifestations being: thinned skin, osteoporosis, hair fall, and other common features of aged tissues (235).

It is important to note that senescent cells are neither quiescent nor terminally differentiated (29). They are fully viable even though there are some distinct features that set them apart from other functionally dividing cells. Some senescent characteristics include: enlarged morphology, telomere shortening, positive senescence-associated β -galactosidase staining, increased p16^{INK4 α} expression, senescence associated heterochromatin foci formation, mitochondrial dysfunction, and secretion of growth factors, cytokines, proteases and other factors (235), some of which will be further discussed. Cellular senescence is neither

restricted to a specific pathway nor does the senescent phenotype always possess all the senescent features mentioned. Nevertheless, cells do undergo senescence in two main ways: replicative senescence or stress-induced premature senescence (SIPS) (58, 189).

Replicative senescence, also referred to as the 'Hayflick limit' in which a cell only divides for a finite number of times (98). Hayflick suggested cellular senescence to also be the result of intrinsic factors and not only by external catabolic factors that Carrel had concluded previously (40, 96). The impactful finding provided a robust foundation for studies attempting to link cellular senescence via intrinsic pathways with aging and possible age-related diseases. It was established soon after that telomere shortening was one of the major intrinsic mechanisms that drove cells towards replicative senescence (38).

A cell's proliferation capacity cannot be justified only by 'time', 'culture longevity' or 'age'. Rather, it is defined by the rate of DNA replication (97). Eventually, the concept of chromosome protection via telomeres was deduced from classic cytogenetic studies (176, 195). This was an impactful discovery as telomeres can accurately foretell cellular senescence in a quantitative manner. The concept also includes telomere protection of the DNA ends from chromosome fusion (27).

Telomeres are double-stranded, non-coding tandem repeats of six nucleotides – TTAGGG – at the end of a chromosome (28, 192). The tandem repeats are followed by 3' G-rich single-stranded overhangs which are highly important for telomere maintenance and regulation. The telomeres are thought to fold themselves into two types of loop: The T loop and the D loop. The telomere DNA folds back to itself to form the T loop and the 3' G-rich overhang associates with the double-stranded telomere DNA to form a triple-stranded D loop (211).

The T and D loops interact with a range of protein-protein interacting network to form a Shelterin complex. This mechanism can also be referred to as 'telomere capping'. Shelterin is a negative regulator of telomere length extension which consists of 6 different proteins:

TRF1, TRF2, RAP80, POT1, TPP1 and TIN2. It acts as a platform that interacts with and recruits other signaling molecules from various different pathways in order to perform telomere protective and maintenance mechanisms (164). Interestingly, 3' G-rich overhangs interaction with double-stranded telomeric DNA can also form G-quadruplexes. These G-quadruplex of telomeric DNA ensures normal progression of replicative cellular senescence, partly facilitating telomere shortening after each successive replication, maintaining normal cellular proliferation (171).

The conserved telomeric sequences are not replicated by DNA polymerase and thus becomes shorter over time. When the short telomeric capping is recognized, DNA damage response mechanisms and cell cycle arrest are initiated in a similar fashion to that of double stranded breaks (DSB) (109). The point of cell cycle arrest due to cellular response to telomere shortening, or telomere attrition, is referred to as the Hayflick limit (208, 297).

The understanding of telomere attrition allows for the development of experimental designs which aim to measure the telomere length of a cell in order to assess its type of senescence. The assessment of telomere length not only assists in differentiating between replicative senescence and stress induced premature senescence, it is also applicable on other pathological conditions and is a useful parameter for the studies of the disease mechanism and prognosis. Relative telomere length comparison between samples was first proposed by Cawthon *et al.* (43).

Other methods of telomere length measurement include absolute telomere length (aTL) qPCR, metaphase quantitative fluorescent *in situ* hybridization (Q-FISH), interphase Q-FISH, flow-FISH, primed *in situ* hybridization protection assay and single strand 3' overhang measurement (189). Despite its significance in cellular senescence, cells can sometimes undergo senescence without the signals of telomere attrition.

Cells can undergo senescence without the signaling from telomere attrition via stress-induced premature senescence (SIPS). SIPS is characterized as an abrupt and abnormal cell cycle arrest. It is a prompt mechanism that protects the tissue or organ from harmful effects of abnormally growing cells, not allowing them to reach the Hayflick limit (278). SIPS can be the result of a collective group of risk factors such as oxidative stress, mitochondrial damage, DNA damage response and oncogenic signalling.

SIPS can be most commonly induced by oxidative stress *in vitro* via the release of reactive oxygen species (ROS). Some examples of ROS include: superoxides, peroxides, hydroxyl radicals and singlet oxygen. ROS are small, effervescent and highly reactive oxygen-containing molecules and therefore are major senescence and apoptosis inducers. They inflict oxidative damage onto macromolecules such as proteins, lipids and nucleic acids. Of all the different types of ROS, hydroxyl radicals are considered to be the most destructive as they are reactive with almost every other molecule and are very common by-products of hydrogen peroxide (H_2O_2), which is abundantly produced by the enzyme superoxide dismutase (SOD) (274). Ironically, SOD plays a very important role in clearing out superoxide anions, massively produced by respiratory complexes I and III of the mitochondrial electron transport chain (ETC) (33).

DNA damage is a form of cellular insult and stress. Lesions in the DNA can be inflicted upon the genome via many factors, including environmental toxins, Fenton reactions, oxidative damage or radiation exposure such as ultraviolet (UV) rays (53). These damaging factors often result in different forms of DNA damage, ranging from base lesions, DNA cross-linking, to DNA strand breaks (162). The latter can be separated into 2 types: single-strand breaks (SSB) and double-strand breaks (DSB) with DSB being the most severe form of DNA damage. DNA damage results in disturbed replication forks, ultimately interfering with cellular replication and normal cell cycle progress. Furthermore, it has also been linked to

mutagenesis, recombination and chromosome rearrangements within the genome (112, 113, 161). All in all, DBS is highly hazardous for the cell whereby unrepaired DBS can lead to apoptosis and misrepaired DBS can lead to chromosomal alteration, both of which are deleterious for the cell (135).

Although telomere attrition is not involved in SIPS, the telomeres play an important role as a sensor in prematurely aging cells, enhancing the sensitivity and efficiency of the DNA damage response (DDR) in general. It has been observed in recent studies that telomeres are able to sense genotoxic stress and activate SIPS (264). The DDR within a cell is crucial for the maintenance of cell viability and functionality. DDR tackles the DNA damage stress via multiple pathways but the most significant, important and established is the Ataxia telangiectasia mutated/ATM and Rad3-related (ATM/ATR) pathway. Prolonged and chronic DDR will result in the arrest of the cell cycle and entry into cellular senescence.

The expression of oncogenic genes, such as the *Ras* oncogenes, will induce SIPS. As Ras protein triggers aberrant and abundant DNA replication during the S phase, the DDR becomes activated and stops cell cycle progression and trigger entry to cellular senescence or apoptosis (228). Cellular senescence from this particular senescent signalling pathway is also usually referred to as oncogene-induced senescence (OIS) (45).

2.2.3. Molecular Signalling Pathways of Cellular Senescence

2.2.3.1. Cell Cycle Checkpoints

The eukaryotic cell cycle is a vital cellular progression and is tightly regulated to maintain the integrity of the genomic material being passed down to daughter cells. Classically, the cell cycle is divided in to five phases: 2 gap phases (G1 and G2), synthetic phase (S), mitotic phase (M) and G0 phase (216).

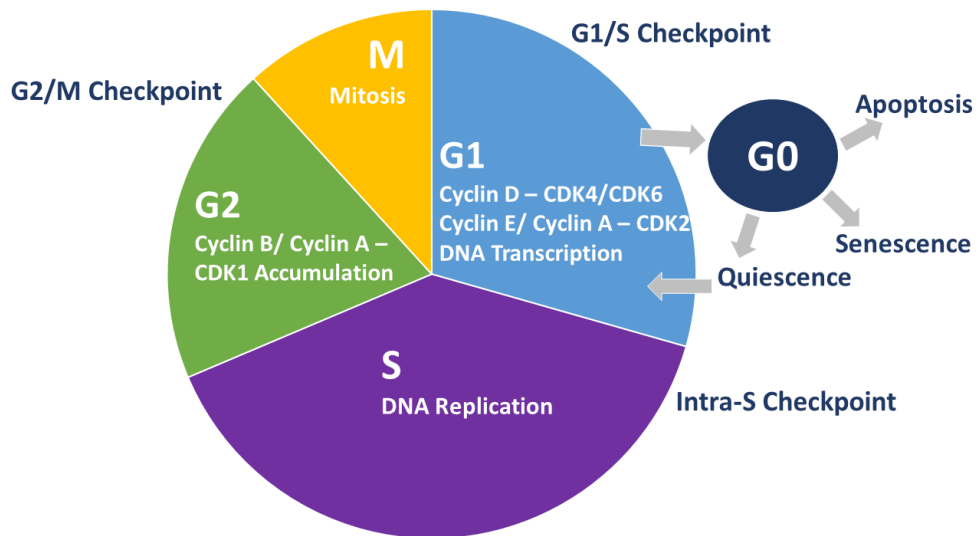


Figure 2.2-1: A simplified presentation of the cell cycle. The gap phases (G1 and G2) exist to prepare the cells for upcoming DNA replication (S phase) and segregation (M phase) respectively. Cell cycle progression is primarily driven by cyclin and cyclin-dependent kinases (CDKs). In G1, Cyclin D – CDK4/CDK6 and cyclin E/cyclin A – CDK2 complexes drive cell into S phase where DNA replication takes place. During G2, cyclin B/cyclin A – CDK1 complexes are the major driving forces into the M phase of the cell cycle where cells undergo mitosis and cytokinesis to produce two daughter cells. These new cells then either commit to the cell cycle or exit to G0 phase which results in either cellular quiescence (reversible), senescence (irreversible) or apoptosis. Checkpoints are introduced at several stages of the cell cycle to repair the genetic material and regulate the cell cycle progress.

In order to regulate cell cycle progression, checkpoints are introduced in between the phases (Figure 2.2-1). Important checkpoints of the cell cycle include: G1/S checkpoint, intra-S checkpoint, G2/M checkpoint and post-mitotic checkpoint. Cell cycle arrest induction by checkpoints is most commonly induced by DNA damage and the DDR. In line with the focus of this review, only the relationship between cell cycle checkpoints and cellular senescence will be discussed.

It is proposed that G1/S checkpoint is the most sensitive in terms of sensing DNA damage whereby one single DSB can induce cell cycle arrest (65). Although cellular senescence can be activated by all checkpoints, the G1/S checkpoint is the most powerful driving mechanism as inhibition of CDK2 as well as CDK4/CDK6, which are highly active in the G1 phase, can robustly send cells into senescence (163). However, it is important to note that cell cycle

arrest via cycle checkpoints does not always result in cellular senescence. Cells can also resume the cycle progression or undergo apoptosis. A collective response of signalling pathways determine cellular entry into senescence. As an overview, the cell cycle checkpoints trigger cycle arrest in a similar fashion in which the ATM/ATR pathway is activated, leading to downstream activations of the p53, p16^{INK4α} and the pRb pathways which are the master regulators of cellular senescence (24).

2.2.3.2. ATM/ATR Pathway

As DNA damage and DDR is involved in most cell cycle checkpoints, the DNA-PK/ATM/ATR pathway plays a pivotal role in the negative regulation of the cell cycle towards mitotic progression. The ATM enzyme phosphorylates p53, which results in p53 dissociation from its negative regulators MDM2/MDM4 and helps p53 escape proteolytic degradation (7).

2.2.3.3. p53/p21^{Cip1} and p27^{Kip1} Pathway

During DDR, there is an increase in stabilization and activation of the p53 protein. P53 proceeds to initiate the transcription of the gene *CDKN1A* encoding protein p21^{Cip1}, which inhibits the CDK1/CDK2 complexes. Therefore, active p21^{Cip1} inhibits cell cycle progression from G1 to S and G2 to M phase (243). Increase in another protein, p27^{Kip1}, inhibits CDK4 and CDK2, allowing retinoblastoma proteins (pRb) to become activated and ultimately halting cell cycle progression from G1 to S phase (223).

2.2.3.4. p16^{INK4α}/pRb/E2F Pathway

p16^{INK4α} is a 16kDa protein and a member of the inhibitors of CDK4 (INK4) family of CDK inhibitors and is overexpressed in replicative senescence (35, 94). P16^{INK4α} acts to inhibit CDK4 and CDK6 by binding directly to them, preventing their phosphorylation of pRb (249). Unphosphorylated pRb is activated and binds to E2F, a group of transcription factors, to repress the transcription of genes that are involved in DNA-replicating S phase (101). These

events restrict cell cycle progression from G1 to S phase and retain the cell at the G1/S phase checkpoint.

Additionally, the p16^{INK4α}/pRb pathway also acts to stabilize p53. P16^{INK4α}-encoding gene *CDKN2A* mRNA can be translated into two different proteins due to its two overlapping reading frames, producing either p16^{INK4α} or p14^{ARF}. P14^{ARF} inhibits the E3 ubiquitin ligase activities of MDM2 which leads to the stabilization of p53. This results in the downstream signaling cascade initiated by p53 to prevent cell cycle progression and retain its status at the checkpoint until all DNA damage is repaired. Conclusively, increase in transcription of *CDKN2A* is one of the first steps that ties the two pathways of p53 and p16^{INK4α} together, allowing them to tightly regulate cell cycle progress at cell cycle checkpoints and become powerful factors that drive cellular senescence.

Understanding of these senescent associated signaling pathways allows our experimental design and analysis of differential expression of these proteins to validate the senescence phenotype of the hVSMCs in replicative senescence.

2.2.3.5. Senescence-Associated β -galactosidase Activity

Senescent cells express a type of senescence-associated β -galactosidase (SA β -gal) with its activity detectable at pH6, which is not found in other pre-senescent, quiescent or terminally differentiated cells (72). In experimental studies, SA β -gal staining is one of the most common techniques used for qualitative validation of cellular senescence. Although associated with cellular senescence, little was known about the origin of SA β -gal in senescent cells. It was later on discovered that the SA β -gal was the product of the *GLB1* gene encoding for lysosomal β -D-galactosidase, indicating the enzyme is lysosome-derived. However, cells are able to undergo senescence despite negative SA β -gal activities which implies that it is not essential for the induction of cellular senescence. Rather, increased SA β -gal levels is the

result of senescence where it is overexpressed, which emphasises increased lysosomal mass of senescent cells (153).

2.3. Micro-RNAs and their Roles in VSMC Regulation and Communication

2.3.1. *The Discovery of micro-RNAs*

Since the completion of the Human Genome Project (2000), only 1.5 % of the entire human genome was found to be protein-coding genes. Intense research on the non-coding DNA regions of the genome has found ample evidence that these regions greatly contributed to natural selection, genetic individuality, gene and protein conservation, expression and regulation(219). One such breakthrough in the study of non-coding DNA of the genome is the discovery of a particular type of short non-coding RNA, later named micro-RNA.

Micro-RNAs, or miRNAs, belong to a conserved class of endogenous, small, non-coding and single-stranded RNAs, normally 19 to 24 nucleotides in length(25). Lee *et al.* (1993) first discovered miRNAs in a study on *Caenorhabditis elegans* whereby lin-4 miRNA was found to negatively regulate the translation of lin-14 mRNA(156). Later, studies reported the same inhibitory interactions occurring between the let-7 miRNA and the translation of the lin-41 mRNA(229, 254). The topic gained more attention when miRNAs were found to be evolutionarily conserved in many other organisms, including humans(218). In humans, miRNAs were reported to be cell-type-specific, which contributed to tissue-specific expression of miRNAs and emphasized their signature regulation of gene expression in different tissues(258). More importantly, dysregulation of miRNAs has been found to associate with important human diseases, most popularly cancer, vascular diseases and immune diseases.

To date, over 2000 mature miRNAs in humans have been sequenced and deposited on the most established miRNA database – miRBase(142). Almost all discovered miRNAs follow a

standard nomenclature system that can be easily accessible on miRBase (11). As our understanding of miRNAs grows, it is important to note that miRNA nomenclature can evolve throughout the years and it is essential to revisit the nomenclature updates in order to standardize miRNA naming prior to publications.

The discovery of miRNA has contributed greatly to the understanding of the 'junk' DNA's biochemical values for the past couple of decades. These tiny regulators have elevated our understanding of gene regulation to a new level, leaving big impacts on human pathological and therapeutic exploratory research. Upon miRNA discovery, the next important step was to elucidate their biogenesis and functional pathways. Many biogenesis pathways of miRNAs has been proposed. At the moment, these pathways are unofficially classified into 'canonical' and 'non-canonical' pathways. In terms of function, miRNAs have been most well-perceived in the RNA interference pathway, which involves a sequential and specific gene-silencing mechanism, from miRNA biogenesis to mRNA binding and silencing (6).

2.3.2. The Biogenesis of miRNAs

In order to become a fully functional mature miRNA, the transcript needs to undergo a few processing steps. MiRNA biogenesis can occur via two different pathways, most commonly referred to as the canonical and non-canonical pathways.

2.3.2.1. The 'canonical' pathway

In the canonical pathway, the biogenesis of miRNAs consists of 5 main events: primary miRNA transcription, nuclear processing, nuclear export, cytoplasmic pre-miRNA processing and mi-RISC complex formation(90).

The synthesis of miRNA starts with the transcription of primary miRNA (pri-miRNA) from the non-coding region of the genomic DNA. The pri-miRNA consists of a stem of 33-35bp, a terminal loop and single-stranded RNA segments at both the 5' and 3' sites. During nuclear

processing, the Microprocessor complex, comprised of the proteins Drosha and DGCR8, processes and cleaves the pri-miRNA to produce a 70-nucleotide-long precursor miRNA(87, 157).

Precursor miRNAs (pre-miRNAs) consist mainly of the 5p species and a minority of the 3p species, both with a 2-nt overhang at the 3' end that acts as a recognition site for exportin-5. Nuclear export takes place when exportin-5 transports the pre-miRNA from the nucleus to the cytoplasm. Cytoplasmic pre-miRNA processing followed whereby the enzyme Dicer then cleaves at ~20nt upstream of the overhang to form a miRNA duplex intermediate (a double-stranded RNA fragment)(319). The duplex consists of a guide-strand, selected by an Argonaute (Ago) protein to become the mature miRNA, and a passenger strand, which is eventually degraded(181, 206). Mature miRNAs originating from the 5'-arm of the pre-miRNA hairpin loop are denoted with a "-5p" while those originated from the 3'-arm of the loop are denoted with a "-3p" suffix (71).

The mature miRNA is incorporated into an RNA-induced silencing complex (RISC) via members of the Ago protein family. When incorporated with mature miRNA, the complex is termed mi-RISC. The mi-RISC uses the mature miRNA as a template to recognize complementary target mRNA for translation repression(334).

2.3.2.2. The 'non-canonical' pathway

Apart from the canonical pathway of miRNA biogenesis, mature miRNAs may also derive from other pathways that do not require all of the processing enzymes involved in the canonical pathway. These miRNAs are often referred to as non-canonical miRNAs. Non-canonical miRNAs may derive from several sources, such as short introns, small nucleolar RNAs (snoRNAs), endogenous short hairpin RNAs and tRNAs(2). Unlike canonical miRNA biogenesis, the non-canonical pathways are often independent from Drosha/DGCR8 processing, yet, heavily relies on Dicer activities(138, 239).

The biogenesis of mature miRNAs can be influenced by several factors, affecting miRNA processing at different levels of miRNA biogenesis. Mature miRNA expression can be influenced by single-nucleotide polymorphisms (SNPs), miRNA tailing via uridylation or adenylation, RNA editing, RNA methylation and miRNA stability (13, 19, 123, 198, 214, 326).

2.3.3. Interactions Between miRNA and Target mRNA via the miRNA-RNA-induced Silencing Complex

MiRNAs repress gene expression at a post-transcriptional level, which may include either mRNA destabilization or translational repression or both, with translational repression being their key action(42). Translational repression activities of the miRNAs take place in several steps: formation of the miRISC, target mRNA binding, translation initiation repression and/or mRNA degradation (**Figure 2.4-1** – Step 5-8). Regardless of the sequential order in which the steps occur, the main events leading to miRNA functional outcomes are those carried out by the miRISC. A fully assembled miRISC usually consists of Ago proteins, GW182, Ccr4-Not deadenylase complex, DDX6 helicase, and the mature miRNA. Translational repression involves the pairing of miRISC to the mRNA target followed by decapping and deadenylation of the mRNA. The perfect pairing between miRNA canonical seed region to the target mRNA, also known as the canonical seed pairing, is a major determining factor of successful translational repression. The seed sequence spans from nucleotides 2 to 8 from the 5' end of the mature miRNA(248). Meanwhile, the non-canonical seed pairing involves imperfect complementary base-pairing, which leads to weakened seed binding stability and attenuates translational repression activities of the miRISC(294).

Following target mRNA binding, the protein GW182 within the miRISC recruits the Ccr4-NOT complex, which interacts with the DEAD-box RNA helicases and participates in the decapping and deadenylation of the target mRNA. Despite inconsistent evidence, the eIF4A2 helicase was proposed to act as a RNA clamp, which would inhibit 43S ribosome scanning of the target

mRNA 3'UTR and hamper mRNA translational initiation(20, 179). Meanwhile, another study has argued that miRISC and the CCR4–NOT complex silence mRNA targets independently of 43S ribosomal scanning(144). Another helicase, DDX6, has been suggested to enhance mRNA decapping(301). In humans, DDX6 might constitute the miRISC and depletion of DDX6 resulted in a slight decrease of miRNA-mediated translational repression in mRNA targets(52). Most recently, it was elucidated that the eIF4a2 helicase inhibited CNOT7 activity, which disallowed the Ccr4-NOT complex to carry out target mRNA deadenylation. Concurrently, DDX6 helicase competed for binding and enhanced CNOT7 activity, accelerating mRNA degradation(180).

Apart from the Ago proteins that recruit mature miRNAs, the RISC consists of the GW repeat-containing protein GW182 (TNRC6A-C in humans), which interacts with Ago proteins and poly(A)-binding proteins, as well as recruiting the Ccr4-NOT and PAN2-PAN3 complexes upon mRNA binding. These complexes trigger deadenylation of the mRNA thus mediating mRNA degradation(34, 47, 79).

Whether translational repression and mRNA degradation occur simultaneously or in a timely sequential manner is still debatable. Overall observation of many studies proposed that translational repression is compulsory before mRNA degradation can occur. Nevertheless, degradation is not always the fate of miRISC-bound mRNAs as their reactivation has been observed(302).

2.3.4. The Unconventional Roles of miRNAs

Despite being structurally well conserved, miRNA functions are not thoroughly understood. MiRNA-mRNA interactions may indirectly promote gene expression through the activation or suppression of related genes or proteins (Table 1). Meanwhile, proteins, the end-targets of miRNA translational inhibition, are capable of controlling miRNA biogenesis in return(46).

More unconventionally, miRNAs have been found to be translocated from the cytoplasm back into the nucleus by importin 8 to interfere with RNA processing and modulate the biogenesis of other miRNAs, or the same miRNA themselves(182, 299). Another unconventional role of miRNAs is their ability to be exported from their host cell into the extracellular environment, such as the extracellular matrix and the bloodstream, and enter other cells to regulate protein expressions(255). Such miRNAs are referred to as circulating miRNAs and are emerging targets for biomarker detection in many human diseases, including CVDs.

Table 1. Intracellular miRNA regulatory effects on VSMCs.

Phenotypic Switching

Expression	miRNA	Target	Pathway	Effects	Reference
Decrease	22	MECP2/HDAC4/EVI1	Multiple	Downregulated when undergoing phenotypic switching; Recover expression of SMA marker genes when overexpressed; Overall a mediator for VSMC plasticity and neointimal formation.	Yang <i>et al.</i> (2018)
Decrease	124	Sp1 mRNA		Induces VSMC proliferation	Tang <i>et al.</i> (2017)
Increase	145	KLF5/ Myocardin	Myocardin-CARG box transcription initiation	Inhibits phenotypic switching	Cheng <i>et al.</i> (2009), Zhang <i>et al.</i> (2016)
Summary: Increased expression of <i>miR-22</i> , <i>miR-124</i> and <i>miR-145</i> can reverse VSMC phenotypic switching, favouring the contractile phenotype.					

Cellular Senescence

Expression	miRNA	Target	Pathway	Effects	Reference
Increase	34a	SIRT1 mRNA	p21/SASP release	Induces senescence	Badi <i>et al.</i> (2015)
Increase	143	Unknown, regulatory effects on MEF2A expression	Akt signalling	Induces senescence	W. Zhao <i>et al.</i> (2015)
Summary: Increased expression of <i>miR-34a</i> and <i>miR-143</i> promotes VSMC senescence via multiple pathways.					

Vascular Calcification

Expression	miRNA	Target	Pathway	Effects	Reference
Decrease	133b/211	RUNX2	MAPK/SMAD	Induces calcification	Panizo <i>et al.</i> (2016)
Decrease	30b/133a/143	RUNX2/Osterix/SMAD1	Wnt/ β -catenin	Induces calcification	N. Liu <i>et al.</i> (2008); Louvet <i>et al.</i> (2016)
Increase	204	RUNX2	MAPK/SMAD	Induces calcification	Cui <i>et al.</i> (2012)
Increase	29b	RUNX2	MAPK/SMAD	Induces calcification	Panizo <i>et al.</i> (2016)
Increase	32	PTEN/RUNX2	PI3K/MAPK/SMAD	Induces calcification	J. Liu <i>et al.</i> (2017)

Summary: Dysregulation of miRNAs induces VSMC calcification mainly via MAPK/SMAD-related pathways

Stenosis and Neointimal Hyperplasia

Expression	miRNA	Target	Pathway	Effects	Reference
Decrease	19b	Lysyl oxidase	Collagen fibril cross-linking (CCL)	Increases collagen cross-linking, which induces left ventricular stiffness. Potential biomarker.	Beaumont <i>et al.</i> (2017)
Increase	26a	MAPK6	TGF- β /SMAD	Reduces neointimal hyperplasia	J. Liu <i>et al.</i> (2017); Tan <i>et al.</i> (2017)
Increase	195	CDC42/CCND1/FGF1	p38/NFkB	Reduces VSMC proliferation, migration and synthesis of IL1 β , IL6 and IL8.	Wang <i>et al.</i> (2012)

Summary: Decreased miR-19b levels might be a biomarker of neointimal hyperplasia while increased miR-26a and miR-195 levels reduces neointimal hyperplasia

2.3.5. Evidence of miRNA Intracellular Signaling in Vascular Smooth Muscle Cells

MiRNAs can negatively regulate different targets in different cell types(165). For instance, *miR-133* promotes growth in myoblasts while suppressing proliferation in VSMCs and cardiomyocytes(150, 166, 277). In VSMCs, miRNAs are prominent intracellular regulators of important cellular events, such as phenotypic switching, senescence, vascular calcification and neointimal formation.

2.3.5.1. Regulation of miRNAs in Vascular Smooth Muscle Cell Phenotypic Switching

Pathological cues such as aging, oxidative stress, inflammation, and mechanical injury induce phenotypic changes of VSMCs, leading to cell proliferation, migration and extracellular matrix (ECM) remodelling which collectively constitute to phenotypic switching(37, 84). During phenotypic switching, contractile VSMC transforms into a synthetic phenotype, which is characterized by the downregulation of the smooth muscle (SM) marker genes, i.e., α -SM actin and SM MHC proteins, and the upregulation of the osteogenic genes, i.e., osteopontin, collagen I and bone morphogenic proteins (BMPs)(118, 332).

MiR-145 is a novel smooth muscle cell (SMC) phenotypic marker and modulator that modulates VSMC phenotypic switching(51, 336). An *in vitro* study on mice reported increased *miR-145* expression indirectly promotes the expression of the SMC marker genes (i.e., alpha-SM actin, calponin and SM-MHC), thus favouring the contractile phenotype, by modulating the expression of Kruppel-like Factor 5 (KLF5) and its downstream signaling molecule, i.e., myocardin(51). Phenotypic modulation by *miR-145* was further demonstrated *in vivo*, whereby restoration of *miR-145* expression led to inhibition of neointimal growth in mouse balloon-injured arteries(51).

Thereafter, Zhang *et al.* (2016) reported a significant regulatory role of *miR-145* in the phenotypic switching of human VSMCs in the 'normal region' of aorta from atherosclerotic

patients(336). In aortic VSMC samples from atherosclerotic patients, decreased *miR-145* expression was observed with increased expression of KLF5 and decreased myocardin. After VSMC transduction with *miR-145*-mimetics, VSMCs from atherosclerotic patients showed significant decrease of KLF5 gene and protein expression, coupled with increased myocardin expression. In other words, increased expression of *miR-145* was able to restore KLF5 and myocardin expression levels in the atherosclerotic VSMC samples to those of non-atherosclerotic controls(336). Altogether, this evidence suggested that increased levels of *miR-145* may prevent the switching of VSMCs to their synthetic phenotype, thus exerting vaso-protective effects.

In a clinical study, Tang *et al.* (2017) showed downregulation of *miR-124* in the aortic media collected from patients with vascular proliferative diseases. The decreased *miR-124* levels were observed in proliferative aortic VSMCs, which reduces inhibition of the specificity protein 1 (Sp1) gene expression and promotes phenotypic switching(271).

Another report involved simultaneous miRNA regulation of VSMC phenotypic switching and neointimal formation. Yang *et al.* (2017) demonstrated that *miR-22* is a novel mediator of VSMC plasticity as well as neointimal hyperplasia. The *in vivo*, *ex vivo* and *in vitro* wire-injured mouse model analyses showed that *miR-22* significantly decreased in injured arteries and mouse VSMCs undergoing phenotypic switching. A decrease in *miR-22* expression was observed as the SMC markers diminished through the cell culture passages, suggesting a loss of *miR-22* function during phenotypic switching. The loss of *miR-22* leads to reduced inhibition of methyl CpG binding protein 2 (MECP2), histone deacetylase 4 (HDAC4), and the oncoprotein ecotropic virus integration site 1 (EVI1) gene expression, which subsequently promotes phenotypic switching. When overexpressed, *miR-22* reduces MECP2, HDAC4 and EVI1 expression while recovering the expression of SMC marker genes (ie. SM α -actin and SM-MHC). Most notably, *miR-22* delivered the same therapeutic effects when locally applied

to the site of wire-injury, preventing restenosis and neointimal formation by inhibiting VSMC phenotypic switching. Furthermore, inverse levels of *miR-22* and MEPC2/EVI1 were observed in diseased and healthy human femoral arteries. In other words, *miR-22*, together with MEPC2 and EVI1, might be promising biomarkers for proliferative vascular diseases. As such, local delivery of *miR-22* might be a potential therapeutic strategy for the prevention of post-angioplasty restenosis(316).

As a whole, increased expression of *miR-145*, *miR-124* and *miR-22* function as repressors of VSMC phenotypic switching that prevent the transition from contractile VSMCs into the synthetic state via modulation of SMC marker genes.

2.3.5.2. *MiRNA Regulation of Vascular Smooth Muscle Cell Senescence*

Cellular senescence is an irreversible cell-cycle arrest as a protective measure against the growth of damaged and/or abnormal cells in mammals(284). Senescent cells are neither quiescent nor terminally differentiated, they are fully viable even though there are some distinct features that set them apart from other functionally dividing cells(29). Some senescence characteristics include enlarged morphology, shortened telomere length, increased senescence-associated (SA) β -galactosidase activity, increased p16INK4 α expression, increased SA heterochromatin foci formation, increased mitochondrial dysfunction and increased secretion of growth factors, cytokines, proteases and other factors(235). It is well recognized that VSMC senescence is associated with pathological conditions of the cardiovascular system.

MiR-34a is linked to the senescence of several cell types, such as cardiac, endothelial progenitor cells, as well as VSMCs. *MiR-34a* was found highly expressed in the aortas of old mice and its target, the protein sirtuin 1 (SIRT1), was greatly downregulated. In replicative senescent VSMCs, increased *miR-34a* levels caused enhanced SA p21 expression, as well as pro-inflammatory senescence-associated synthetic phenotype (SASP) factors (i.e. IL1 β ,

MCP1, IL6 and IL8). Restoration of SIRT1 levels could rescue the *miR-34a*-induced VSMC senescence. However, it could not revert the SASP and the production of pro-inflammatory factors. These results indicated that *miR-34a* affects VSMCs through multiple mechanisms that may be independent from one another. It is plausible that single therapeutic targeting of *miR-34a* may prevent its downstream effects on multiple pathways(17).

MiRNAs can function in synergy with other proteins to induce VSMC senescence. Zhao *et al.* (2015) discovered a synergistic interaction between *miR-143* and myocyte enhancer factor 2A (MEF2A) in which overexpression of both factors promotes VSMC senescence while overexpression of one or the other factor does not yield prominent senescence induction(338). MEF2A promotes miR-143 expression via the mediation of the transcription factor KLS2 while miR-143 overexpression rescues MEF2A knockdown in VSMCs. This compensatory mechanism suggested *miR-143* also possesses regulatory effects on MEF2A expression(338). However, the mechanisms linking these events and cellular senescence are still unclear.

2.3.5.3. MiRNA Association with Vascular Calcification

Vascular calcification is the pathological accumulation of minerals in the vascular system and several different miRNAs have been found to contribute to vascular calcification via multiple pathways(306). *MiR-204* was found to regulate β -glycerophosphate-induced VSMC calcification through runt-related transcription factor-2 (RUNX2), both *in vitro* and *in vivo* using Kunming mice(64). Another *in vivo* study revealed that increased levels of *miR-29b* and decreased levels of *miR-133b* and *miR-211* directly influence VSMC calcification, induced by high phosphorus microenvironment through interactions with RUNX2(212).

A recent study found that *miR-32* promoted calcification in VSMCs by enhancing the expression of calcification markers such as bone morphogenetic protein-2 (BMP2), RUNX2, osteopontin, and the bone-specific phosphoprotein matrix GLA protein *in vitro*(165).

Moreover, *miR-32* modulated vascular calcification progression by activating phosphoinositide 3-kinase (PI3K) signaling and increasing RUNX2 expression and phosphorylation by targeting the 3'-untranslated region of phosphatase and tensin homolog mRNA (PTEN) in mouse VSMCs. Most importantly, plasma *miR-32* levels from patients with coronary artery disease with coronary artery calcification (CAC) were higher than those observed in non-CAC patients(165).

A recent *in vitro* study has successfully prevented inorganic phosphate (Pi)-induced vascular calcification by using magnesium (Mg²⁺) to recover the expression of *miR-30b*, *miR-133a* and *miR-143*, which was dampened by Pi(170). This finding implied that miRNAs are not only important for their biological functions but also useful as therapeutic targets.

2.3.5.4. *MiRNA Expression and Signaling during Stenosis and Neointimal Hyperplasia*

Beaumont *et al.* (2017) examined several miRNAs for the correlation between their expression and aortic stenosis (AS) development in 28 patients with severe AS(22). It was discovered that *miR-19b* was significantly repressed thus favouring increased expression and activity of lysyl oxidase, an enzyme responsible for collagen fibril cross-linking (CCL) in the myocardium. As a result, there was an increase of CCL which in turn increases left ventricular stiffness in the heart of the AS patients, an important determining factor of heart failure. Therefore, it was proposed that *miR19-b* could be a potential biomarker for AS patients with heart failure(22).

Using multiple approaches, Wang *et al.* (2012) reported *miR-195* significantly reduces VSMC proliferation and synthesis of inflammatory cytokines (i.e. IL1 β , IL6 and IL8) via direct interaction with CDC42, a protein commonly expressed in neointima, CCND1 and FGF1(295). Direct repression of the *CDC42* gene by *miR-195* suppressed neointimal formation after balloon angioplasty in rats. The results indicated that *miR-195* played an important role in the inhibition of VSMC proliferation in atherosclerotic plaques, as well as the attenuated

neointimal formation after aortic injuries. Therefore, it can be a valuable therapeutic candidate to minimize neointimal hyperplasia in patients undergoing balloon angioplasty.

MiR-26a is another example of miRNA multiple-target inhibition. *MiR-26a* was discovered to promote VSMC proliferation while inhibiting cellular differentiation and apoptosis and altering TGF- β /SMAD signaling interactive pathway. In *in vivo* mouse models with abdominal aortic aneurysm (AAA), downregulation of *miR-26a* was observed together with enhanced switching of VSMCs from contractile to synthetic phenotype. Therefore, the downregulation of *miR-26a* might have positive effects on aneurysm stability and prevents aneurysm rupture(165). Another *in vivo* study showed direct translational inhibition of *miR-26a* on MAPK6 mRNA that minimized neointimal hyperplasia after vein graft surgery in rats(269). A close connection could be drawn between these two studies that miR-26a exerts its preventative effects by minimizing phenotypic switching of VSMCs to the synthetic phenotype. These reports suggested that one miRNA could be used locally at different target sites to induce specifically desired therapeutic effects (**Figure 2.3-1**).

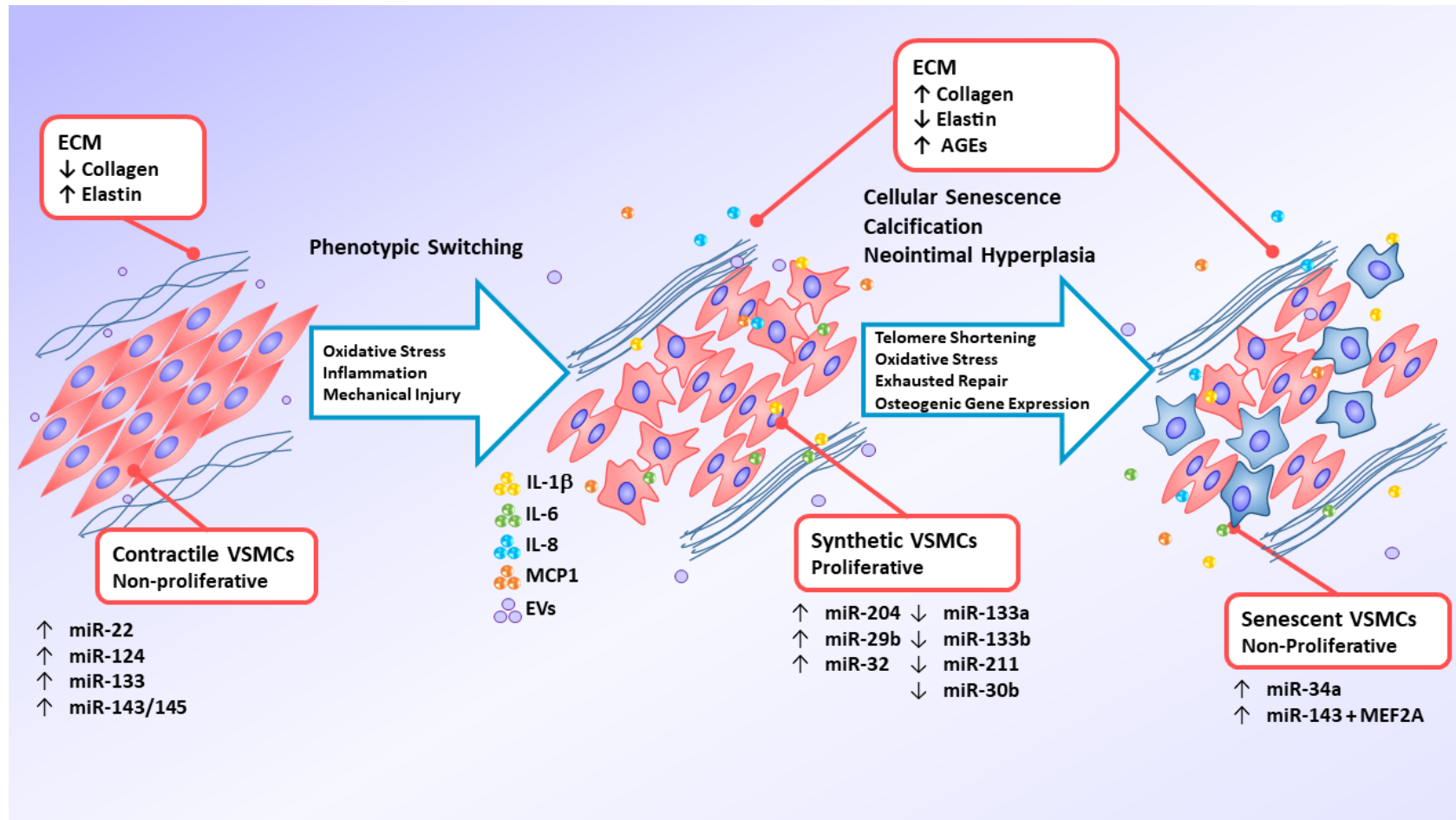


Figure 2.3-1: MiRNAs are prominent intracellular regulators of important cellular events, such as phenotypic switching, senescence, vascular calcification and neointimal formation. Pathological cues such as aging, oxidative stress, inflammation, and mechanical injury induce phenotypic changes of VSMCs, leading to cell proliferation, migration and extracellular matrix (ECM) remodelling, which collectively constitute to phenotypic switching.

2.4. Introduction to Intercellular Communication via Exosomes

2.4.1. Exosomal Biogenesis and Export

Extracellular vesicles (EVs) are slowly emerging targets of molecular and pathogenesis research. Most often, EVs originate from either endosomes or plasma membranes, which consist of exosomes, microvesicles and apoptotic bodies(227). Likewise, VSMCs undergoing phenotypic switching secrete an abundant amount of cytokines and EVs as a mean of cellular communication and signalling. In particular, exosome release from VSMCs has accumulated significant research interest.

It is generally accepted that exosomes consist of a heterogeneous population with diameter ranging from 40-100nm or lesser than 150nm(105). However, studies have reported differing exosome sizes from different cell types, and VSMC-derived exosomes were characterized to be ~170nm in diameter on average(32). Unlike other EVs secreted via direct budding of the plasma membrane, exosomes are packaged inside the late-endosome, also known as multivesicular body (MVB) within the cell and released upon MVB fusion with the plasma membrane(95). Within the MVB, intraluminal vesicles (ILVs) are formed via back-fusion or internal budding. When the MVB limiting membrane fuses with the cytoplasmic membrane, ILVs are released as exosomes(16). Exosomes are not only enriched with cholesterol and cytoplasmic proteins, they also carry genetic materials (mRNA and small RNAs, including micro-RNA) for inter-cellular communication(282). The ability to facilitate cell-to-cell communication makes exosomes truly meaningful as a target for diagnostic and therapeutic research (**Figure 2.4-1**).

The complete mechanism of exosome biogenesis and release has not been fully elucidated. With the current understanding, exosome biogenesis and release can be mediated by either

endosomal sorting complex required for transport (ESCRT)-dependent or ESCRT-independent mechanisms.

The ESCRT-dependent machinery has been the main apparatus in MVB and exosomal biogenesis. The ESCRT machinery consists of four major complexes (ESCRT-0 to -III), each playing different roles: from sequestering mono-ubiquitinated proteins to facilitating membrane budding and scission. When released into the extracellular matrix, exosomes carry ESCRT components within their lumen, particularly the ESCRT-I subunit TSG101(173). Knocking down ESCRT components inhibit exosome biogenesis and release, suggesting exosome biogenesis and release depend greatly on the ESCRT machinery.

On the other hand, ESCRT-independent mechanism was proposed by Trajkovic *et al.* (2008), where ceramide was found to take part in intra-endosomal membrane transport and exosome formation via hydrolysis, catalysed by sphingomyelin phosphodiesterase 3 (SMPD3), independent from the ESCRT machinery. The study concluded that ceramide facilitated the specific biogenesis of certain exosomal sub-populations and distinguished them from ILVs formed for lysosomal degradation(173). A complementing study by Kapustin *et al.* (2015) demonstrated that the inhibition of SMPD3 attenuated exosome production but did not completely paralyze exosome release(129). Altogether, the biological function of the ESCRT-independent mechanism was rather complementary to the ESCRT-dependent biogenesis than being an independent pathway.

2.4.2. Micro-RNA Sorting and Loading into Exosomes

Apart from the two prominent mechanisms for exosome biogenesis, additional information connecting them to other mechanisms is lacking. Most importantly, the understanding of how genetic materials, such as miRNAs, could be selectively packaged into the exosomes still remains incomplete and requires further studies. Nevertheless, it is certain that loading of

miRNAs is strongly dependent on the ESCRT, the surface molecules of exosomal membranes and the specific binding motifs of the miRNAs themselves. As previously reported, the Ago proteins of the miRISC mediated the transfer of mature miRNAs to processing bodies (P-bodies), followed by P-bodies fusion with late endosomes, which spontaneously underwent back-fusion to form ILVs that were secreted into the extracellular space as exosomes via membrane fusion between MVBs and the cytoplasmic membrane(331).

A more in-depth description of this loading mechanism, proposed by Janas *et al.* (2015), involved the lipid-mediated formation of raft-like regions in the MVB limiting membrane, followed by lipid-induced inward budding of the raft-like regions and ultimately the binding of miRNAs to the inward-budding raft-like region(120). It has been reported that miRNAs were produced in excess compared to Ago protein levels, thus, miRNAs may undergo different interactions with other molecules rather than with just Ago proteins alone(119). One such example is the speculation that miRNAs were delivered to raft-like regions for binding by RNA-binding proteins (RBPs), such as hnRNPA2B1, which possess high affinity towards ceramide-rich membrane regions like the raft-like regions of the MVB limiting membrane(287). The specific sorting mechanism of miRNA loading into exosomes is as elusive as miR-MVB binding mechanism. Recent reports described specific sorting of miRNA for exosome loading via human ELAV protein Hur and RNA-binding protein SYNCRIP in hepatocytes(193, 242). The later study also reported that exosomal loading was greatly determined by the heXO miRNA extra-seed motif(242).

In the past decade, special attention has been paid to VSMC exosomal research, focusing on vascular calcification, atherosclerosis and restenosis(129–133). Elucidating specific miRNA loading mechanisms into exosomes will increase our understanding of exosomal signalling and may allow accurate manipulation of specific miRNA-exosome loading to facilitate more studies on exosomal miRNA therapeutic potentials in vascular research.

2.4.3. MiRNA Extracellular Signaling via the Exosomal Axis

Despite the numerous reports highlighting the potentials of circulating miRNAs, much less data exist to explain the precise underlying processes that facilitate VSMC cell-to-cell communication, the secretion of a particular exosome-derived miRNA from the host VSMC and the type of recipient cells targeted by the dysregulated exosome-derived miRNA expression. Several studies have attempted to elucidate the significant signaling mechanisms affected by circulating miRNAs that make them excellent mediators of communication between VSMCs and other cell types. For instance, growing evidence of communication and regulation between VSMCs and endothelial cells (ECs) via the exosomal signaling axis involving miRNAs was reported(102, 160, 339).

An *in vivo* study by Hergenreider *et al.* (2012) discovered a sequence of inter-cellular communications between ECs and VSMCs via miRNAs, which exerted an athero-protective mechanism in response to shear stress(102). In short, shear stress activated the transcription factor Kruppel-like Factor 2 (KLF2) in ECs. KLF2-active ECs released exosomes enriched with miR-143/145, which controlled target-gene expression in VSMCs and facilitated their phenotypic switching favouring the contractile phenotype, resulting in reduced atherosclerotic lesion formation in ApoE^{-/-} mice aorta(102).

Zhou *et al.* (2013) reported the transfer of *miR-126* and Ago2 protein from ECs to VSMCs, which promoted VSMC turnover *in vitro*(343). This transfer was reduced by atheroprotective laminar shear stress. Increased expression of *miR-126* was observed at areas where laminar shear stress is low, which are the areas more susceptible to neointimal lesion formation during the progression of restenosis and atherosclerosis(343). Therefore, *miR-126* could be used as a biomarker for neointimal hyperplasia detection as well as a therapeutic target to mitigate neointimal formation.

Another study by Zhao *et al.* (2016) demonstrated intercellular signaling between VSMC and ECs via miRNA transfer maintained vascular homeostasis(339). Briefly, the transcription factor X-box binding protein-1 (XBP1) mRNA was spliced differently in response to vascular injury. This alternative splicing led to increased intra- and extracellular *miR-150* expressions, which transferred from VSMCs to ECs and mediated EC migration via VEGF-A/VEGFR/PI3K/Akt pathway activation to promote vascular remodelling after injury(339).

An *in vitro* and *in vivo* study by Shan *et al.* (2015) identified a significant amount of *miR-223* found only in bone marrow-derived blood cells and VSMCs of apo-E knockout mice and patients with atherosclerosis(250). In the *miR-223* knockout mice, atherosclerotic lesions were exacerbated. This finding suggested that blood cells could signal VSMCs via miRNA transfer by secreting miRNAs into the serum in order to protect the vascular walls against atherosclerosis(250).

Overall, there is a lack of cell-cell communication studies between VSMC and other cell types on the molecular level. Further extracellular miRNA research is necessary to understand how VSMCs can communicate with each other, as well as with other cells within the blood vessels.

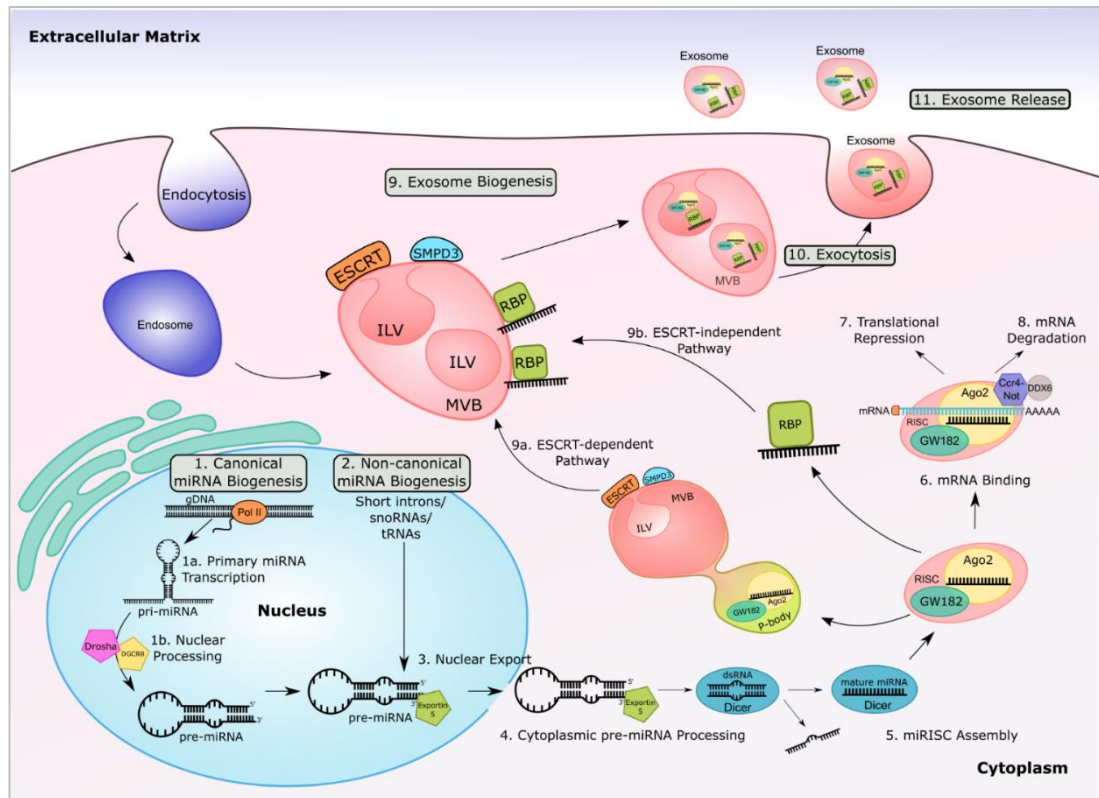


Figure 2.4-1: Biogenesis of miRNAs and their loading into endosomes, which are released as exosomes into the extracellular matrix via exocytosis. In the canonical pathway, the biogenesis of miRNAs consists of 5 main events: primary miRNA transcription, nuclear processing, nuclear export, cytoplasmic precursor miRNA processing and miRNA-RISC (miRISC) complex formation (Step 1, 3-5). Non-canonical miRNA biogenesis is often independent from Drosha/DGCR8 processing yet still reliant on Dicer activities (Step 2-5). Exosomes are packaged inside the late-endosome, also known as multivesicular body (MVB) within the cell and released upon MVB fusion with the plasma membrane. Within the MVB, intraluminal vesicles (ILVs) are formed via back-fusion or internal budding. When the MVB limiting membrane fuses with the cytoplasmic membrane, ILVs are released as exosomes (Steps 9-11).

2.4.4. Exosomal miRNA Studies in Clinical Research

As with every field of study, there are drawbacks and limitations to the extent in which the nature of miRNAs can be understood and clinically applied. Most miRNA studies have been case-controlled with small populations. As such, there is a lack of large cohort studies regarding miRNAs and their correlation to a particular vascular disease. However, this temporary drawback can be resolved with time. As of recently, Karakas *et al.* (2017) has reported the results of the large AtheroGene study, which involved screening a set of miRNAs from 1112 patients with documented coronary artery disease (CAD) throughout 4 years. Data analyses identified three circulating miRNAs: *miR-132*, *miR-140-3p* and *miR-210* that were able to predict cardiovascular death, specifically predicting mortality in secondary prevention settings, and represent valuable markers for risk estimation in CAD(134). This study proved to show that many large-scale studies might be currently ongoing, providing broader results in the near future.

Despite their great necessity, large-scale studies should be accompanied by thorough analyses and reproducible predictive values of the identified miRNAs. For instance, Zampetaki *et al.* (2012) identified *miR-126*, *miR-197* and *miR-223* as predictive markers for risk of myocardial infarction from a large-scale study in primary prevention settings. However, sub-analysis of this finding showed no predictive ability for early or late adverse cardiovascular events(134, 245, 328). Many *in vivo* experiments reported the dysregulated expression of miRNAs but did not perform target interaction and molecular mechanistic studies. The development of standardized research guidelines for miRNA discovery, functional and therapeutic value assessment might improve the quality of miRNA predictive and therapeutic assessment in vascular research.

2.5. Current Drawbacks and Potential of miRNAs in Research and Clinical Settings

MiRNA studies in CVD research come with several challenges that need to be addressed in order to push the boundaries of our understanding of miRNA biological significance and its prospective applications. These challenges involve technical drawbacks in miRNA detection, origin of identified exosomal miRNAs and distinction between cell-free and exosomal miRNA for accurate miRNA profiling. Nonetheless, these challenges cannot overshadow the imminent potential of miRNAs as valuable translational tools for diagnostics and therapy of CVD.

2.5.1. Technical Drawbacks

The first technical drawback involves the prediction of miRNA interactions with its target(s). While computational analysis plays an important role in predicting miRNA interactions with its target(s), experimental miRNA research validates and contributes to the accuracy of the database. Currently, computational prediction of canonical miRNA targets is most commonly used, which relies solely on the seed sequence and theoretical binding free energies between the seed sequence and target mRNA[94]. Insights into the seed sequence composition and length may improve the accuracy of these predictions[64, 90]. However, a congruent principle of miRNA target prediction remains unestablished. More research-based data on direct interactions, especially in CVD conditions, is needed to help with bioinformatics prediction.

Another technical drawback affects miRNA application in routine clinical settings. Due to their small size, high sequence homology and low levels in samples, miRNA detection remains relatively complex and time consuming. Early standard method of miRNA detection was Northern Blotting, which was laborious and not sensitive enough. In current time, miRNA detection has improved by using real-time quantitative polymerase chain reaction (RT-

qPCR), microarray or next-generation sequencing (NGS). However, these methods are time consuming and the data analyses are complicated. In this regard, another drawback would be the lack of a rapid detection method in cases of emergency, such as diagnosing patients with myocardial infarction. Fortunately, studies are under way to improve miRNA detection time using different assay formats that can yield results from 3hrs to only 15mins[33, 39, 54]. These studies remain nascent and are still at the proof-of-concept phase. Techniques such as nanomaterial-based detection, rolling circular amplification or enzyme-free amplification, among many others, are being developed to circumvent existing problems of current miRNA detection methods[98].

2.5.2. Origin of Circulating miRNAs: Cell-type-specific miRNA Profiles

One limiting factor of circulating miRNA studies involves the identification of the tissue where the dysregulated miRNA(s) originate. A large fraction of circulating miRNAs originates from blood or endothelial cells and the amount of circulating miRNAs is dependent on the size of the originating tissue. Fortunately, VSMCs comprise the thickest layer of the vascular wall and exosomal transfer of miRNA from VSMCs to ECs had been reported[108]. Therefore, it is likely that changes in VSMC exosomal miRNA expression could be easier identified compared to other originating tissue or organ. Nevertheless, exosome miRNA profiling of healthy VSMCs and other cell types would highly assist the origin mapping of circulating miRNA identified from patient samples. MiRNA profiling data are commonly deposited in the Gene Expression Omnibus (GEO) of the National Center for Biotechnology Information (NCBI) (<https://www.ncbi.nlm.nih.gov/geo/>). However, specific exosomal miRNA profiles of VSMCs in different conditions are much more scarce compared to those of ECs, thus indicating the need for establishing a cell-type-specific exosomal miRNA profile for VSMCs.

2.5.3. Circulating miRNAs: Cell-free or Exosomal?

It is important to discuss the present inconsistency in circulating miRNA profiling. As circulating miRNAs consist of either cell-free miRNAs or encapsulated miRNAs (i.e. in exosomes or other vesicles), it is necessary to standardize the exosome isolation method prior to profiling, in order to ensure the altered miRNA expression profile belongs to a specific population. Profiling total circulating miRNAs from blood plasma, for example, may not be reliable, as the results obtained would not be able to determine if the dysregulated miRNAs are cell-free or encapsulated, or a combination of both. Regardless, profiling miRNAs of a particular population of vesicles (i.e. exosomes) would provide more accurate results, although the laboratory procedures would be much more complex and could be considered a major drawback when translating into routine clinical practice[62].

2.5.4. The Latent Potential of miRNAs

The potential application of miRNA(s) as diagnostic and therapeutic targets is promising. While intracellular miRNAs pose as potential therapeutic targets, extracellular circulating miRNAs (exosomal or cell-free) represent suitable candidates as diagnostic biomarkers for CVDs. The application of miRNAs in clinical settings represent a new leaf in the era of precision medicine. Several miRNAs have been validated and are now undergoing clinical trials with *miR-34* mimic and *miR-122* being the most prominent and are at phase 1 for cancer treatment and phase 2 for hepatitis treatment respectively[34, 75]. MiRagen, a RNA-based therapeutics company, is in the process of developing MRG-110, which targets and inhibits *miR-92a* in order to promote vasculogenesis and healing after ischemic stroke (<http://www.miragen.com/pipeline>). In the near future, more miRNAs are expected to undergo clinical trials either as therapeutic targets or diagnostic biomarkers, both of which would contribute to solidify miRNA usage potential.

Chapter 3. Materials and Methods

3.1. Characterization of Replicative Senescence in Human Vascular Smooth Muscle Cells

3.1.1. Materials

Human vascular smooth muscle cells (hVSMCs) from four individuals were obtained from Hospital Serdang. Ethics were approved by Medical Research and Ethics Committee (MREC), Ministry of Health, Malaysia. All chemical and reagents were obtained with highest purity from Sigma Aldrich (St. Louis, MO).

3.1.2. Subject Selection

Subjects selected were Malaysian Chinese male of more than 30 years of age with a normal BMI range and diagnosed with any form of CVD (**Table 2**).

Table 2: Subject demographic table.

Subject	Age	Sex	Height (m)	Weight (kg)	BMI	BMI Range	Ethnic Group	Diagnosis
16D-54M-5A	54	M	172	59.7	20.17982693	Normal	Chinese	Ischemic Heart Disease
16D-54M-5L	54	M	172	59.7	20.17982693	Normal	Chinese	Ischemic Heart Disease
16D-54M-7A	54	M	164	63.8	23.72099941	Normal	Chinese	Coronary Artery Disease
16D-54M-7L	54	M	164	63.8	23.72099941	Normal	Chinese	Coronary Artery Disease

3.1.3. Human Vascular Smooth Muscle Cell Culture and Morphological Analysis

HVSMCs were first maintained in Smooth Muscle Basal Medium (SmBM) then underwent gradual SmBM replacement with Dulbecco's Modified Eagle Medium (DMEM), supplemented with 2 % L-glutamine, 1 % penicillin-streptomycin and 10 % fetal bovine serum (FBS). Media was changed every 48 hr. If hVSMCs could not become confluent within a month, they were considered to be senescent and subjected to subsequent qualitative and quantitative analyses such as senescence-associated (SA) β -galactosidase staining, differential gene expression and relative telomere length measurement to ascertain hVSMC replicative senescence. The morphology of senescent hVSMCs was assessed using Nikon Eclipse TS100 inverted light microscope (Nikon, Japan). Throughout the thesis, simplified terms of 'young' and 'old' samples will be used to refer to samples consisting proliferating hVSMCs and replicative senescent hVSMCs, respectively.

3.1.4. Human Vascular Smooth Muscle Cell Passaging and Cryopreservation

Old media was removed and discarded. Cells were washed with 1x Dulbecco's phosphate buffered saline (DPBS) warmed to 37°C, detached from the flask surface with 0.5% trypsin and incubated at 37°C, 5% CO₂ for 3 min. The flask was tapped gently for complete detachment of cells and checked using the Nikon Eclipse TS100 inverted light microscope (Nikon, Japan). Trypsinized cells are neutralized with 10% DMEM (DMEM, 10% FBS), transferred to a 15ml tube and centrifuged at 230 x *g* for 5 min at RT. Supernatant was removed and discarded. For passaging, cell pellet was resuspended with 10% DMEM, counted and aliquoted into new flasks accordingly. For cryopreservation, cell pellet was resuspended in cryo-medium (50% of 10% DMEM, 40% FBS and 10% dimethylsulfoxide (DMSO)) and aliquoted into cryovials. Vials were put into Mr. Frosty and stored at -80°C overnight and transferred into LN₂ cryotank the next day for long-term storage.

3.1.5. Senescence-Associated β -galactosidase Staining

During the harvesting of young and old hVSMCs, five thousand cells were taken from each sample, seeded onto a sterile coverslip placed in a 6-well plate and incubated for 16 hr at 37°C, 5% CO₂. After incubation, conditioned medium was removed and cells were fixed with 2% paraformaldehyde for 3 min, washed with 1x phosphate buffered saline (PBS) and incubated with a staining solution (1mg/ml bromochloroindoxyl galactoside (X-gal), 40mM citric acid/phosphate buffer, 5mM potassium ferricyanide, 5mM potassium ferrocyanide, 150mM NaCl, 2mM MgCl₂, pH 6.0) for 16 hr at 37°C, without CO₂. After staining, the seeded coverslip was washed with 1xPBS, dried in 90% and 100% methanol respectively and mounted onto a microscope slide using DPX Mountant (Sigma Aldrich, St Louis, MO). Slides were stored away from light overnight and the edges of the coverslip were sealed the next day using nail polish to prevent sample contact with air. Samples were viewed using the Eclipse 80i bright-field microscope (Nikon, Japan).

3.1.6. Total RNA Extraction from Human Vascular Smooth Muscle Cells for Senescence-Associated Gene Expression Analysis

Culture of young and old hVSMCs from T75 flasks were trypsinized, spun down in a 1.5ml microfuge tube, washed twice with 1 x Dulbecco's phosphate buffered saline (DPBS) and counted. Cells were spun down again, with supernatant removed and cells pellet was lysed gently in 750 μ l of Qiazol (Qiagen, Germany). Samples were then immediately kept at -80°C until extraction. Extraction methods were followed according to the protocol provided by Qiagen with minor modifications. Briefly, 150 μ l of chloroform was added to the sample lysed in Qiazol and incubated at RT for 3 min. Then, sample was spun down at 12000 x *g* for 15 min at 4°C and the aqueous phase was transferred to a new tube. An amount of 5 μ g of glycogen was added to the sample, followed by 375 μ l of 100% isopropanol and vortexed to mix. Sample was incubated at room temp for 10 min and spun down at 12000 x *g* for 10 min at

4°C. The supernatant was carefully removed and discarded. A volume of 750µl of 75% ethanol was added to the tube containing the sample, followed by centrifugation at 7500 x g for 5 min at 4°C. Supernatant was removed and discarded completely. Pellet containing total RNA was left to air dry until it appeared as a transparent gel-like pellet. Pellet containing total RNA was resuspended with 15µl of RNase-free water and total RNA was quantified using Epoch microplate spectrophotometer (BioTek Instruments, Winooski, VT). Total RNA was either used immediately for complementary DNA (cDNA) synthesis or stored at -80°C until further use.

3.1.7. Complementary DNA Synthesis for Quantitative Polymerase Chain Reaction

Quantinova Reverse Transcription Kit (Qiagen, Germany) was used. First, genomic DNA (gDNA) was removed by combining gDNA Removal Mix, RNase-free water and template RNA, with each reaction containing 5µg of total RNA template. The gDNA removal mix was incubated for 2 min at 45°C and placed on ice. For reverse transcription, the RT Mix was prepared on ice, combining RT Enzyme, RT Mix and template RNA with gDNA removed. The reverse transcription was performed using the Mastercycler Nexus Gradient Thermal Cycler (Eppendorf, Germany). The reactions were set to anneal for 3 min at 25°C, followed by reverse transcription for 10 min at 45°C and inactivation for 5 min at 85°C. Newly synthesized cDNA library was immediately placed on ice and stored at -20°C.

3.1.8. Genomic DNA Extraction from Human Vascular Smooth Muscle Cells for Relative Telomere Length Measurement

Genomic DNA (gDNA) isolation was performed based on Qiazol's manufacture protocol with slight modifications. Briefly, aqueous phase was removed as much as possible after incubating and spinning down the Qiazol-chloroform-sample homogenate mentioned in 3.1.6. A volume of 225µl of 100% ethanol was added to each sample, inverted to mix and

incubated for 3 min at RT. The samples were then centrifuged at 2000 x *g* for 5 min at 4°C. Phenol-ethanol supernatant were removed, transferred to a new tube and stored at -80°C for protein extraction. Meanwhile, the pellet was washed with 750µl of 0.1M sodium citrate in 10% ethanol by incubating for 30 min at RT with occasional mixing. Then, the sample was centrifuged at 2000 x *g* for 5 min at 4°C. The sample was washed and centrifuged one more time with the same conditions. Sample was then continuously washed with 1125µl of 75% ethanol via incubation for 20 min at RT with occasional mixing and centrifuged at 200 x *g* for 5 min at 4°C. Supernatant was removed and discarded. Sample was air-dried for 15 min at RT. Pellet containing gDNA was resuspended in 10ml of 8mM NaOH and centrifuged at 12000 x *g* for 10 min at 4°C. Supernatant containing gDNA was removed and transferred to a new tube and neutralized to pH7.0 using 1x Tris-EDTA buffer and stored at -20°C for future use. Isolated gDNA was quantified using Epoch microplate spectrophotometer (BioTek Instruments, Winooski, VT).

3.1.9. Primer Validation via Absolute Quantification and Gel Electrophoresis

Absolute quantification real-time PCR was carried out using KAPA SYBR FAST qPCR Kit Master Mix Universal (2x) on the Eco Real-time PCR System (Illumina, San Diego CA). The reactions were setup with final concentrations of 1x SYBR FAST Master Mix, 200nM forward primer, 200nM reverse primer and a range of cDNA concentrations. Five 5-fold dilutions of template cDNA were prepared and added to the master mix (100, 10, 1, 0.1 and 0.01ng) accordingly. The reactions were amplified with heat activation at 95°C for 3 min, followed by 40 cycles of denaturation at 95°C for 3 sec with annealing and extension at 60°C for 30 sec. Finally, the melt curve was generated by capturing the fluorescent signal every 1 sec as the temperature rose from 60°C to 95°C. A standard curve was generated after the run and the gradient and R² value of each primer pair were calculated in order to assess the primer pair's efficiency.

The products of the qPCR were run on 3% agarose gel in 1 x Tris/Borate/EDTA (TBE) Buffer. Theoretical product size was obtained from PrimerBLAST during primer design. 100bp DNA ladder (Promega) was used for all gels. After electrophoresis, the gel was captured using Bio-Rad Molecular Imager Gel Doc XR System (Bio-Rad, USA) and viewed using Quantity One 1-D Analysis Software (Bio-Rad, USA). The gel image and melt curve were used to assess the primer pair's specificity.

3.1.10. Senescence-Associated Gene Expression

Table 3. Primer sequences for SA gene expression analysis.

Gene	Protein	Primer (5'-3')	Amplicon	Reference
<i>CDKN1A</i>	P21 ^{Cip1}	F : GCAGACCAGCATGACAGATTT R : GGATTAGGGCTTCCTCTTGGA	70	Saramäki <i>et al.</i> (2006)
<i>CDKN2A</i>	P16 ^{INK4a}	F : GAAGGTCCCTCAGACATCCC R : AAACCTACGAAAGCGGGGTGG	136	Yamakoshi <i>et al.</i> (2009)
<i>CDKN1B</i>	P27 ^{Kip1}	F : CCGGTGGACCACGAAGAGT R : GCTCGCCTCTTCCATGTCTC	66	Roy <i>et al.</i> (2007)
<i>36B4</i>	RPLP0	F : CAGCAAGTGGGAAGGTGTAATCC R : CCCATTCTATCATCAACGGGTACAA	75	Cawthorne <i>et al.</i> (2002)

Primer specificity was checked using Primer Basic Local Alignment Search Tool (PrimerBLAST). Primers were synthesized by Integrated DNA Technologies (IDT, Singapore). Relative quantification qPCR was carried out using KAPA SYBR FAST qPCR Kit Master Mix Universal (2x) on the Eco Real-time PCR System (Illumina, San Diego CA). The reactions were setup with final concentrations of 1x SYBR FAST Master Mix, 200nM forward primer, 200nM reverse primer and 1ng of the template cDNA. The gene *36B4* was used as the reference gene. Standard curves and fold-change calculations were analysed using EcoStudy software (Illumina, San Diego CA). The reactions were run with heat activation at 95°C for 3 min, followed by 40 cycles of denaturation at 95°C for 3 sec with annealing and extension at 60°C. Finally, the melt curve was generated by capturing the fluorescent signal every 1 sec as the temperature rose from 60°C to 95°C.

3.1.11. Relative Telomere Length Measurement

Table 4. Primer sequences for telomere length measurement.

Gene	Protein	Primer (5'-3')	Amplicon	Reference
<i>36B4</i>	RPLP0	F : CAGCAAGTGGGAAGGTGTAATCC R : CCCATTCTATCATCAACGGGTACA A	75	Cawthorne <i>et al.</i> (2002)
<i>Telomere</i>	N/A	F : GGTTTTTGAGGGTGAGGGTGAGGG TGAGGGTGAGGGT R : TCCCGACTATCCCTATCCCTATCC CTATCCCTATCCCTA	75-500	Cawthorne <i>et al.</i> (2002)

Reference gDNA was extracted from saliva using the Oragene Kit (Qiagen, Germany). Relative telomere length measurement was performed as previously described (43). Relative quantification qPCR was carried out using KAPA SYBR FAST qPCR Kit Master Mix Universal (2x) on the Eco Real-time PCR System (Illumina, San Diego CA). The single copy gene and the telomere, represented by '36B4' and 'Tel' assays respectively, were run separately due to differences in their cycling conditions and reaction setup (details shown in **Appendix 8.1**).

For the 'Tel' assay, the reactions were setup with final concentrations of 1x SYBR FAST Master Mix, 270nM forward primer, 900nM reverse primer and 1ng of the template gDNA. The 'Tel' assay was amplified starting with initial heat activation at 95°C for 10 min, followed by 30 cycles of denaturation at 95°C for 15 sec with annealing and extension at 60°C for 2 min. The melt curve was then generated by capturing the fluorescent signal every 1 sec as the temperature rose from 60°C to 95°C.

For the '36B4' assay, the reactions were setup with final concentrations of 1x SYBR FAST Master Mix, 300nM forward primer, 500nM reverse primer and 1ng of the template gDNA. The '36B4' assay was amplified starting with initial heat activation at 95°C for 10 min, followed by 30 cycles of denaturation at 95°C for 15 sec with annealing and extension at 58°C for 1 min. The melt curve was then generated by capturing the fluorescent signal every 1 sec

as the temperature rose from 58°C to 95°C. Relative measurement was performed using telomere to single copy gene (T/S) ratios between young and old samples against the reference sample accordingly.

ΔCt_{young}	$= Ct_{\text{Tel}}_{(\text{young})} - Ct_{\text{36B4}}_{(\text{young})}$
ΔCt_{Ref}	$= Ct_{\text{Tel}}_{(\text{Ref})} - Ct_{\text{36B4}}_{(\text{Ref})}$
$\Delta\Delta Ct_{\text{young}}$	$= \Delta Ct_{\text{young}} - \Delta Ct_{\text{Ref}}$
Relative T/S Ratio _(young vs Ref)	$= 2^{-\Delta\Delta Ct_{\text{young}}}$
ΔCt_{old}	$= Ct_{\text{Tel}}_{(\text{old})} - Ct_{\text{36B4}}_{(\text{old})}$
$\Delta\Delta Ct_{\text{old}}$	$= \Delta Ct_{\text{old}} - \Delta Ct_{\text{Ref}}$
Relative T/S Ratio _(old vs Ref)	$= 2^{-\Delta\Delta Ct_{\text{old}}}$
<div style="border: 1px solid black; background-color: yellow; padding: 5px; display: inline-block;"> <p>Expected Result $2^{-\Delta\Delta Ct_{\text{young}}} > 2^{-\Delta\Delta Ct_{\text{old}}}$</p> </div>	
<small>*Ref = Reference gDNA</small>	

Figure 3.1-1 Calculation for T/S Ratios.

3.2. Isolation and Characterization of Human Vascular Smooth Muscle Cell-Derived Exosomes

3.2.1. Materials

TSG101 monoclonal primary antibodies, catalogue number MA1-23296, and Goat anti-Mouse IgG (H+L) Secondary Antibody, HRP, catalogue number 31430, were both purchased from Invitrogen (Carlsbad CA).

3.2.2. Exosome Isolation from Conditioned Media using Sucrose Cushion

Serum-starved conditioned media was collected after 48 hr of serum starvation of hVSMCs and centrifuged at 1,000 rpm, 2,000 rpm and 4,000 rpm for 10 to 15 min at 4°C to remove cells, apoptotic bodies and large debris. A volume of 120ml of conditioned media from 12 x T75 flasks per sample was centrifuged at 100,000 x *g* for 90 min at 4°C using the SW41Ti Rotor (Beckman Coulter, Brea CA) with 60 % sucrose cushion. Interphase was collected and centrifuged again with the sucrose cushion at 110,000 x *g* for 12 hr at 4°C. The interphase enriched with exosomes was collected, washed and pelleted with 1 x PBS at 110,000 x *g* for 2 hr at 4°C. Pellet containing exosomes were resuspended in either 100 µl of 4% glutaraldehyde, 60 µl RIPA buffer or 750 µl Qiazol (Qiagen, Germany) for scanning and transmission electron microscopy, immunoblotting, or RNA extraction (described in **3.3.1**) respectively.

3.2.3. Scanning Electron Microscopy

Freshly isolated exosome pellets were fixed in 4 % glutaraldehyde and dropped onto a stub covered with carbon tape and aluminium foil, respectively, and air-dried. The surface was sputtered with gold-carbon for 30secs using sputter coater (Leica Microsystems, Germany)

with argon gas for sputtering. The stub was imaged under low beam energies (5.0-10.0 kV) using Quanta FEG 650 SEM (FEI, Holland).

3.2.4. Transmission Electron Microscopy

Freshly isolated exosome pellets were fixed in 60 μ l of 4 % glutaraldehyde and dropped onto a copper grid and set for 5 min. Excess liquid was wiped away using Whatman filter paper, Grade 1. A negative staining solution of 2 % phosphotungstic acid (PTA) was then dropped onto the copper grid and incubated for 5 min and removed using the filter paper. The copper grid was air-dried in a desiccated chamber. Sample was imaged using transmission electron microscope LEO LIBRA-120 (Zeiss, Germany) at 120kV and viewed using Soft Image (SI) Viewer.

3.2.5. Lowry Protein Assay

Total protein was quantified using the Lowry protein assay. Briefly, bovine serum albumin (BSA) standards were diluted from 10mg/ml BSA stock to make 10 different final concentrations of 20, 40, 60, 80, 100, 120, 140, 160, 180 and 200 μ g/ml. Total protein samples were diluted in 1/10 fractions. Standards and samples were pipetted accordingly into a flat-bottom 96-well plate, followed by the addition of an equal volume of alkaline-copper working reagent (0.5 % w/v copper sulphate pentahydrate, 2.7 % Na/K tartrate with 10 volumes of 10 % w/v Na₂CO₃ anhydrous in 0.5M NaOH). Mixtures were incubated for 30mins followed by the addition of an equal volume of a final concentration of 1 x Folin-Ciocalteu reagent (Sigma Aldrich, St Louis, MO). The plate was incubated for another 20mins before reading at 650nm using Epoch microplate spectrophotometer (BioTek Instruments, Winooski, VT).

3.2.6. Immunoblotting

Exosome pellets were resuspended in 60 μ l RIPA buffer, added with 6x loading buffer and boiled for 5 min at 100°C. Equal amount of total protein from all samples, based on the Lowry protein assay, were loaded and run on a 12 % SDS-PAGE gel at 80V for 2 hr. While gel was running, ice cold transfer buffer (25mM Tris, 190mM glycine and 20 % methanol) was prepared. Polyvinylidene difluoride (PVDF) membrane was activated by subsequently soaking in ice-cold 100 % methanol for 5 min, rinsed with MilliQ water and incubated ice-cold transfer buffer until used for stacking, respectively. SDS-PAGE was stacked and transferred to a PVDF membrane at 25V for 7 min using Thermo Fisher Pierce G2 Fast Blotter (Thermo Fisher Scientific, Waltham MA) (**Figure 3.2-1**).

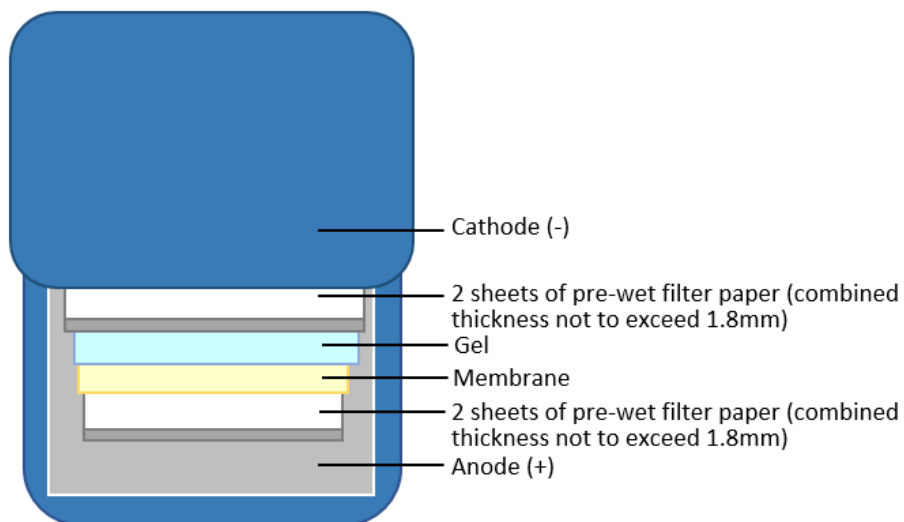


Figure 3.2-1 Stacking sandwich for protein transfer.

After the transfer, the PVDF membrane was blocked with 5 % BSA in 0.2 % TBST for 45 min at RT, incubated with 1:1000 TSG101 primary antibody in 0.2 % TBST overnight at 4°C. The membrane was washed thrice with 0.2 % TBST for 10-15 min each time, incubated with 1:15000 HRP-conjugated anti-mouse secondary antibody in 5 % BSA and 0.2 % TBST for 1 hr. The membrane was washed again six times with 0.2 % TBST, 10 min each time. Finally, the membrane was detected using enhanced chemiluminescent substrates for Western Blot,

WESTAR Supernova (Cyanagen, Italy) and captured using the ChemiDoc XRS+ System (Bio-Rad, Hercules CA).

3.3. Whole-Genome Small RNA Next-Generation Sequencing

3.3.1. Total RNA Extraction from Human Vascular Smooth Muscle Cells and Human Vascular Smooth Muscle Cell-Derived Exosomes for Next-Generation Sequencing

RNA extraction was carried out using miRNeasy Micro Kit (QIAGEN, Germany). Briefly, exosome and cell pellet were homogenized in Qiazol and incubated for 5 min. A volume of 150µl chloroform was added to the homogenate, incubated for 5 min at RT and centrifuged at 12000 x g for 5 min at 4°C for phase separation. The aqueous phase was transferred to a new tube and added with 100 % ethanol and then passed through a spin column. The spin column was then washed with Buffer RWT, Buffer RPE and 80 % ethanol before eluted with RNase-free water. Total RNA concentration and integrity were assessed using Qubit fluorometer (Invitrogen, Carlsbad CA) and Bioanalyzer (Agilent Technologies, Santa Clara CA).

3.3.2. RNA and DNA Quality Control using Qubit Fluorometer

Quality control (QC) of RNA and DNA libraries were performed following manufacturer's protocols using Qubit™ RNA HS Assay Kit and Qubit™ DNA HS Assay Kit, respectively. Qubit Working Solution was prepared by mixing Qubit reagent and Qubit buffer at 1:200 ratio. Standards and user samples (i.e. RNA or DNA) were added to different tubes accordingly and topped up to a final volume of 200µl with Qubit Working Solution. The tubes were vortexed to mix and incubated for 2 min at RT before reading using the Qubit fluorometer (Invitrogen, Carlsbad CA). Qubit readings of samples were used for sample dilution prior to RNA and DNA QC using BioAnalyzer (Agilent Technologies, Santa Clara CA).

3.3.3. RNA and DNA Quality Control using BioAnalyzer

RNA Pico Chip, Small RNA Chip and High Sensitivity DNA Chip were used for cellular RNA, exosomal RNA and DNA, respectively. Final QC was performed using Agilent BioAnalyzer 2100 instrument and the 2100 Expert Software (Agilent Technologies, Santa Clara CA).

3.3.4. Whole Genome Small RNA Next-Generation Sequencing

Libraries for sequencing was prepared according to the manufacturer's protocol TruSeq Small RNA Library Prep (**Figure 3.3-1**) (Illumina, San Diego CA). Briefly, total RNA was ligated with adapters, reverse transcribed and amplified. Amplified cDNA libraries were separated according to size using 6% native PAGE (**Figure 4.3-1**). Bands with sizes between 160-145bp were excised. The gel containing the excised band was broken via centrifugation with a filter tube and gel pieces were eluted in Tris-HCl, pH8.5, for 24 hr at RT using a shaker (**Figure 3.3-2**). Eluted cDNA libraries were taken for QC and their concentration was normalized before proceeding to sequencing. Sequencing was carried out using NextSeq 500 Mid v2 Kit, 150 cycles, and the NextSeq 500 System (Illumina, San Diego CA) at High Impact Research Building, University of Malaya.

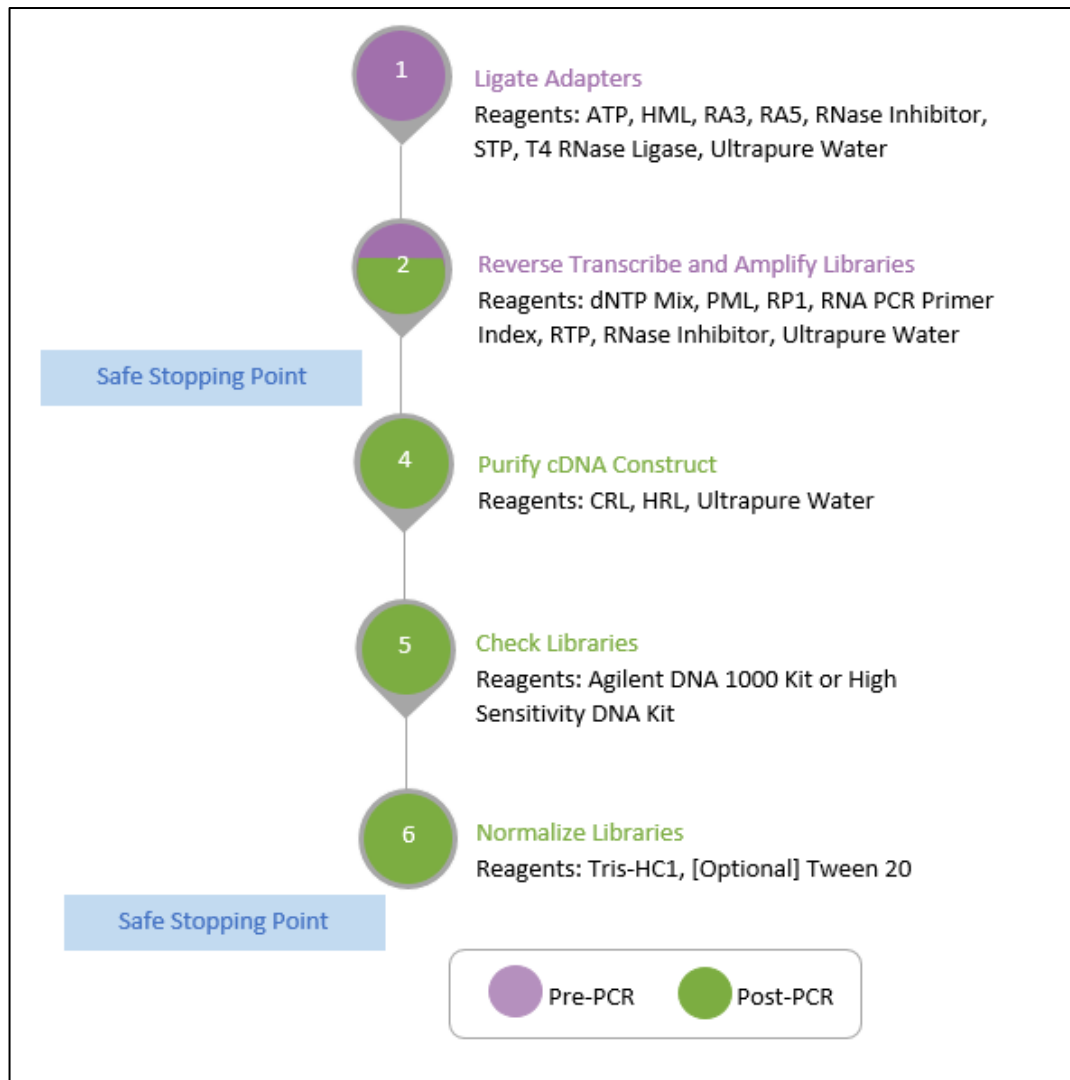


Figure 3.3-1: Truseq Small RNA Library preparation workflow. Briefly, total RNA was ligated with adapters, reverse transcribed and amplified. Amplified cDNA libraries were purified according to size using 6% native PAGE. The libraries were eluted in Tris-HCl, pH8.5, for 24 hr at RT using a shaker. Eluted cDNA libraries were taken for QC and their concentration was normalized before proceeding to sequencing.

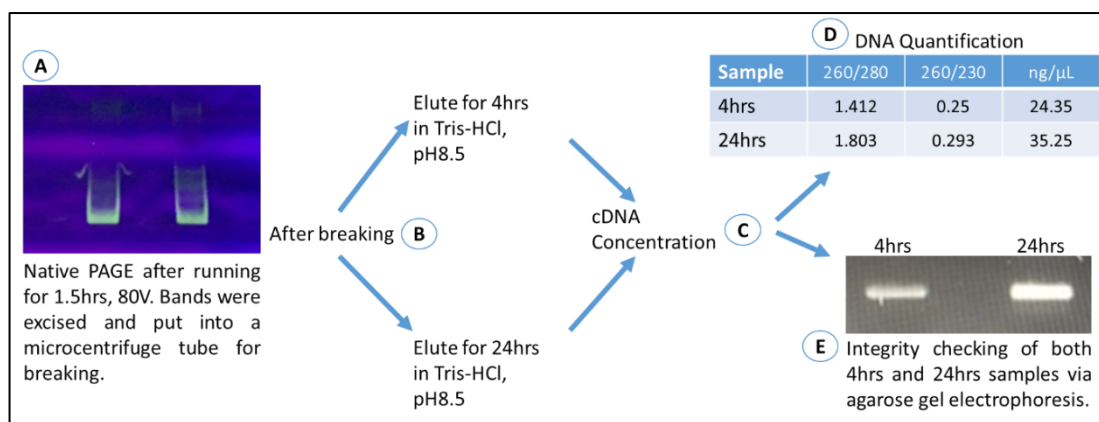


Figure 3.3-2: Optimization of DNA elution for NGS library prep. (A) Bands from 6% native PAGE were excised and put into a filter tube for breaking via centrifugation at 20 000 x *g*. **(B)** After breaking, DNA was eluted for either 4 hrs or 24 hrs in Tris-HCl, pH8.5. **(C)** DNA was quantified to obtain DNA concentration. **(D)** In the 4hrs sample, the cDNA concentration after native PAGE purification was 24.35ng/ml, the 260/280 ratio was 1.412 and the 260/230 ratio was 1.803. In the 24hrs sample, the cDNA concentration was 35.25ng/ml, the 260/280 ratio was 1.803 and the 260/230 ratio was 0.293. All parameters measured were higher in the 24hrs sample when compared to those of the 4hrs sample. **(E)** Agarose gel electrophoresis observed a significantly brighter band in the 24hrs sample whilst the band of the 4hrs sample was slightly blurry. This indicated that the cDNA in the 24hrs were higher in concentration and had better integrity, thus implying that eluting the gel containing the cDNA library for 24hrs yielded more cDNA with better integrity.

3.4. Primary and Secondary Data Analysis of Whole-Genome Small RNA Next-Generation Sequencing

Sequencing data processing involved three main analyses: primary, secondary and tertiary. Primary analysis was performed by the NextSeq 500 System during sequencing where hardware generated data and machine statistics were analysed together with sequence reads their quality scores.

Secondary analysis was performed using the CAP-miRSeq workflow (**Figure 3.4-1**) (175, 232). Raw reads were subjected to QC before and after sequencing adapters and indices were trimmed off using Cutadapt. In the QC of small RNA sequencing, five main modules were assessed: basic statistics, per base sequence quality, per sequence quality scores, per base N content and sequence length distribution.

The basic statistics module generated simple composition statistics for the file analysed, such as the total sequences, filtered sequences, sequence length and G-C content. Per base sequence quality represented an overview of the range of quality values across all bases at each position in the FastQ file. Per sequence quality score assessed the quality values of a subset of the sequences and determined its quality values compared to the universal data. It is often the case that a subset of sequences will have universally poor quality, often because they were poorly imaged (on the edge of the field of view etc), however these should represent only a small percentage of the total sequences. Per base N content determined whether a sequencer was unable to make a base call with sufficient confidence, in which case the base call will be substituted with an N rather than a conventional base call. This module plotted out the percentage of base calls at each position for which an N was called. Lastly, some high throughput sequencers generated sequence fragments of uniform length, but others can contain reads of wildly varying lengths. Even within uniform length

libraries some pipelines will trim sequences to remove poor quality base calls from the end. Therefore, sequence length distribution analysis generated a graph that visualized the distribution of fragment sizes in the input file.

Altogether, these modules contribute to overall QC of small RNA sequencing and allow proper assessment of base and sequence quality prior to subsequent mapping or sequence alignment to the reference genome. Trimmed reads that passed QC were mapped to the human reference genome and human miRBase Database (v.22). After mapping, known and novel miRNAs were identified and classified accordingly using miRDeep2. Subsequently, known mature miRNAs were analysed using EdgeR to identify differentially expressed miRNAs in hVSMCs and exosomes during replicative senescence.

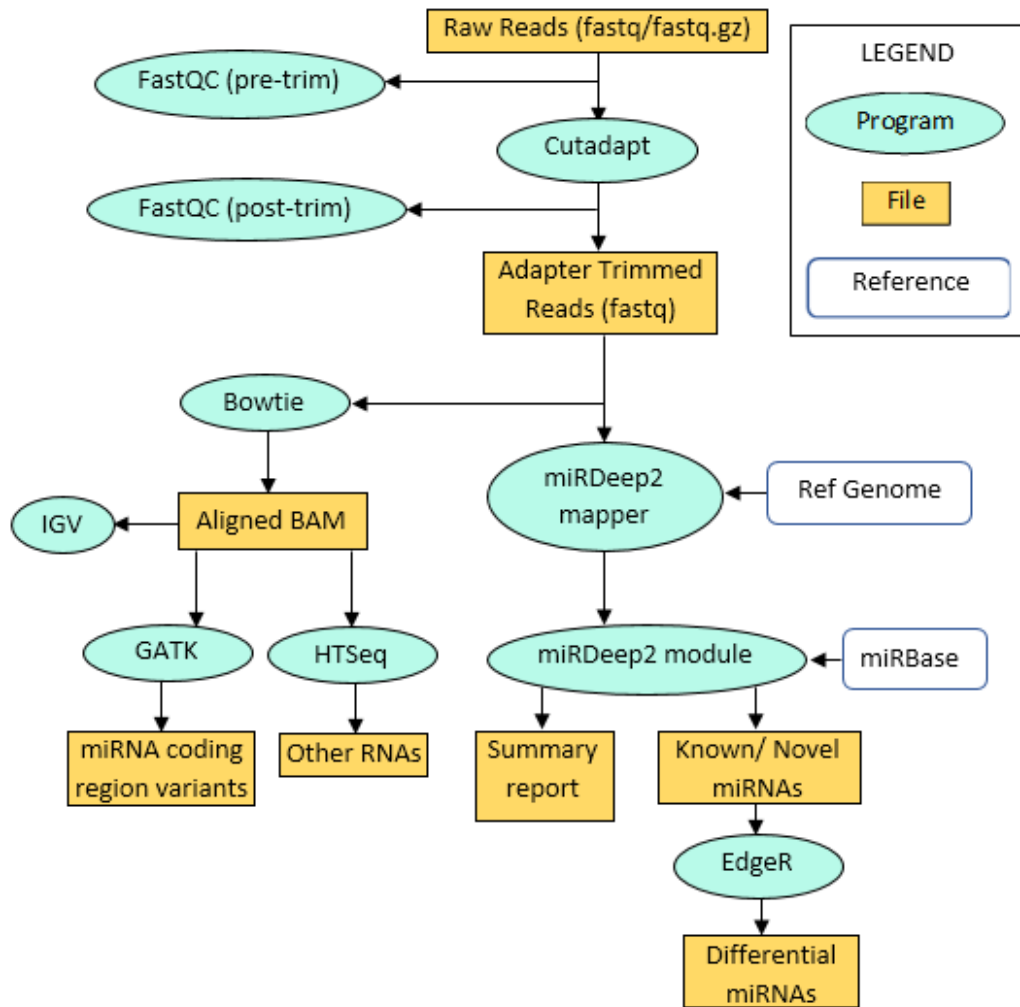


Figure 3.4-1: Secondary analysis using the CAP-miRSeq workflow adapted from Sun *et al.* (2014). Raw reads underwent pre-trimming and post-trimming QC to ensure extra primer and indices were trimmed off. The trimmed reads were then mapped to the Homo sapiens genome and miRNA database (miRBase). Mapped reads were categorized in novel and known mature mRNAs. Mature miRNAs were subjected to differential expression analysis using EdgeR.

3.5. miRNA Target Prediction and Pathway Analyses

Data were categorized into four groups: upregulated intracellular miRNAs, downregulated intracellular miRNAs, upregulated exosomal miRNAs and downregulated exosomal miRNAs. Tertiary analyses, including mature miRNA differential expression, miRNA target prediction and pathway and gene ontology analyses were performed. Mature miRNA differential expression was analysed using edgeR (Bioconductor). MiRNA target prediction was performed using miRWalk (261). MiRWalk was developed based on information produced with TarPmiR, a prediction tool which applied a random-forest-based approach for miRNA-mRNA target prediction (75). MiRWalk also used multiple databases, including: NCBI Homo sapiens, miRBase, TargetScan, miRDB and miRTarBase (5, 50, 110, 141, 152). As an additional advantage, miRWalk provided records of miRNA-mRNA interactions which had been experimental validated. Although the interactions were not explicitly validated on hVSMCs, they allowed the data analysis to proceed with higher confidence in data integrity.

Pathway analyses were performed using Kyoto Encyclopedia of Genes and Genomes (KEGG) Pathway and Reactome pathway databases (126–128). Gene ontology categorization was performed using PANTHER Classification System (275). Related pathways were mapped separately for each group using KEGG. Input was used by mapping the miRNA target genes predicted from miRWalk. Pathways irrelevant to the interest of the study were then filtered out.

Pathway and GO enrichment analyses were performed using gProfiler with the cut-off value based on false discovery rate (FDR) < 0.05. GO terms were then sorted according to descending fold enrichment and the top 10 GO terms were selected for data visualization. The bar graph for GO Enrichment Analysis of each group were then generated using Microsoft Excel. Similarly, pathway enrichment was performed using the KEGG and REACTOME pathway databases .

Target genes involved in selected GO terms and KEGG pathways were mapped onto the interaction network. Visualization of miRNA-mRNA interaction network was constructed using Cytoscape 3.8.0 (251). Human database used for miRNA-target interaction network mapping was obtained from miRNet (80). Protein-protein interaction (PPI) network was generated using STRING database with a cut-off of $p < 0.05$ for term analysis (265).

3.6. Validation of Differentially Expressed miRNAs in Human Vascular Smooth Muscle Cells

3.6.1. *Materials*

All kits and molecular-grade chemicals were purchased from Qiagen, Germany. Purchased kits included miScript II RT Kit, miScript Catalogue Primer Assays and miScript Custom Primer Assays and miScript SYBR Green PCR Kit. Purchased chemicals included molecular grade nuclease-free water.

3.6.2. *Total RNA Reverse Transcription Targeting Matured miRNAs*

Quality control of total RNA of all samples were performed as described in 3.3.2 and 3.3.3. Reverse transcription of mature miRNAs into cDNA libraries was carried out according to the manufacturer's protocol using miScript II RT Kit (Qiagen, Germany). In brief, template RNA was added to a reverse-transcription master mix consisting 1x miScript HiSpec Buffer, 1x miScript Nucleics Mix, miScript Reverse Transcriptase Mix and RNase-free water. The reactions were incubated at 37°C for 1 hr and then at 95°C for 5 min to inactivate the miScript Reverse Transcriptase Mix. Reactions were then put on ice for subsequent mature miRNA quantification for at -20°C for long term storage.

3.6.3. Primer Design and Validation for Differentially Expressed miRNA Validation

Primers used for validation consisted of miScript Catalogue Primer Assays and miScript Custom Primer Assays (Qiagen, Germany). Primers were validated using absolute quantification methods described in 3.1.9 with slight modifications. The qPCR was run using miScript SYBR Green PCR Kit (Qiagen, Germany) and cDNA of mature miRNA samples synthesized from 3.6.2. was used. Cycling conditions involved PCR Initial activation step at 95°C for 15 min, followed by 3-step cycling of denaturation at 94°C for 15 sec, annealing at 55°C for 30 sec and extension at 70°C for 30 sec, for 40 cycles. Primer efficiency assessment was performed as described in 3.1.9. albeit without gel electrophoresis due to small product size.

Table 5: Primer assays for differentially expressed miRNA validation.

Gene	Target sequence	Catalogue number	Primer Assay
<i>hsa-miR-146b-5p</i>	UGAGAACUGAAUCCAUAGGCU	MS00003542	Catalogue
<i>hsa-miR-664a-3p</i>	UAUUCAUUUUAUCCCCAGCCUACA	MS00014819	Catalogue
<i>hsa-miR-155-5p</i>	UUAAUGCUGAAUCGUGAUAGGGGU	MS00031486	Catalogue
<i>hsa-miR-20a-5p</i>	UAAAGUGCUUAUAGUGCAGGUAG	MS00003199	Catalogue
<i>hsa-miR-664a-5p</i>	ACUGGCUAGGGAAAAUGAUUGGAU	MS00014826	Catalogue
<i>hsa-miR-664b-3p</i>	UUCAUUUGCCUCCCAGCCUACA	MS00037877	Catalogue
<i>RNU6-6P RNA</i>	N/A	MS00033740	Catalogue
<i>hsa-miR-16-5p</i>	UAGCAGCACGUAAAUAUUGGCG	MS00031493	Catalogue
<i>hsa-miR-4485-3p</i>	UAACGGCCGCGGUACCCUAA	MSC0076558	Custom
<i>hsa-miR-12136</i>	GAAAAAGUCAUGGAGGCC	MSC0076559	Custom
<i>hsa-miR-10527-5p</i>	AAAGCAAUGUUGGGUGAACGGC	MSC0076560	Custom

3.6.4. miRNA Differential Expression Validation

Relative quantification method of real-time PCR was performed using miScript SYBR Green PCR Kit (Qiagen, Germany). The cDNA template was used at a final concentration of 1ng/μl.

The pseudogene RNU6-6P RNA and *hsa-miR16-5p* were used as reference genes. Cycling conditions involved PCR Initial activation step at 95°C for 15 min, followed by 3-step cycling of denaturation at 94°C for 15 sec, annealing at 55°C for 30 sec and extension at 70°C for 30 sec, for 40 cycles. Delta (Δ) Ct values were used to calculate the fold change of the relative expression of each gene as described in **0** using EcoStudy software (Illumina, San Diego CA).

3.7. Statistical Analysis

All tests and assays were performed with minimal three technical and biological replicates. All statistical analyses were performed on Graphpad Prism. Paired t-test was used for significance analysis followed by Tukey's post hoc test and false-discovery rate (FDR) adjusted *p*-value. A value of *p* < 0.05 was considered statistically significant.

Chapter 4. Results

4.1. Characterization of Replicative Senescence in Human Vascular Smooth Muscle Cells

4.1.1. Human Vascular Smooth Muscle Cell Morphology during Senescence

Proliferative hVSMCs cells grew into a hill-and-valley topography on the surface of the culture flask with a regular fibroblastic, spindle-like and bipolar appearance. When confluent, the cells packed closely with each other and grew in a uni-directional manner. On the other hand, senescent hVSMCs adopted an irregular, amorphous, fibroblastic and multipolar morphology. Cells appeared enlarged with big nucleus, multiple nucleoli and heavy cellular granulation. Flattened topography was observed instead of hill-and-valley topography. When confluent, cells did not grow directionally and did not have the 'fibrous' look like that observed in young and proliferative hVSMCs (**Figure 4.1-1 A and B**).

4.1.2. Senescence-associated β -galactosidase Activities in Human Vascular Smooth Muscle Cells during Senescence

SA β -galactosidase activities were detected at pH 6.0 in old and non-proliferative hVSMCs indicating presence of cellular senescence. The activity of SA β -galactosidases were represented as blue grains, which were abundantly observed in the old samples while little to no stain was observed in the young samples (**Figure 4.1-1 C and D**).

4.1.3. Gene Expression in Human Vascular Smooth Muscle Cells during Senescence

Gene expression was represented as expression ratios, or fold-change, in the form of $2^{-\Delta(\Delta C_t)}$ values. Differential expression levels were determined based on the relative fold change of the gene expression of the old samples compared to that of the young samples. Values for fold change calculation were first normalized against the Ct values of the reference gene *36B4*, which was consistently expressed in both samples. Young samples were used as the reference samples, which was normalized to 1. Meanwhile, the unknown (old) sample might have values of more than, less than, or equal to 1. Values greater than 1 indicated an upregulation in gene expression and values lesser than 1 (but greater than 0) indicated downregulation in the expression of the gene being analysed. From **Figure 4.1-2**, the expression of senescence marker genes *CDKN2A*, *CDKN1B* and *CDKN1A* encoding p16^{INK4 α} , p27^{Kip1} and p21^{Cip1} were 5.09, 5.03 and 5.13 fold higher in old samples, respectively, when compared to those of young samples ($p < 0.05$, $n=3$).

4.1.4. Relative Telomere Length of Human Vascular Smooth Muscle Cells during Senescence

Relative telomere length measurement was used to verify replicative senescence (**Figure 4.1-3**). The T/S ratios for young against reference samples and old against reference samples were 0.846 and 0.648 respectively. The T/S ratio of the old sample was significantly lower than that of the young sample, indicating relatively shorter total telomere length and confirming replicative cellular senescence of hVSMCs in the old samples ($p < 0.05$, $n=3-4$). The T/S ratio comparison was made between young and old samples on the basis of how the qPCR assays were designed and executed by the original report (43). As the experiment relied on a reference sample (or a control), the data analysis only allowed direct comparison of

either the young or old sample to the control and not the young and old samples to each other, accounting for the relative, and not absolute, measurement of the telomere length. Nevertheless, data showed relatively shorter telomere length in old samples, which was further consolidated by senescent hVSMC morphology, increased SA β -galactosidase activity and increased SA gene expression.

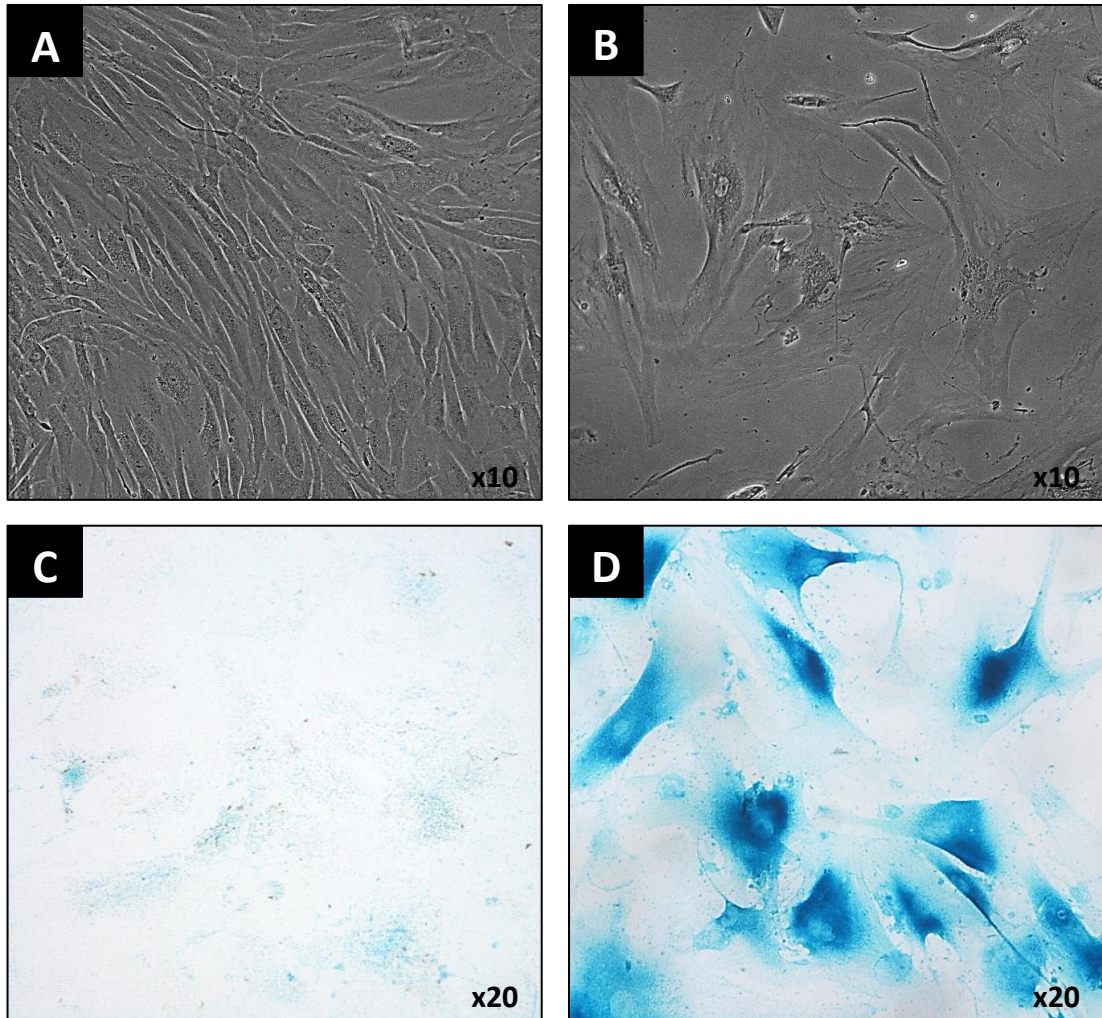


Figure 4.1-1: A qualitative comparison between proliferating and senescent hVSMCs in terms of morphology and SA β -galactosidase activities under a bright field microscope. (A) Young hVSMCs were relatively small in size and possess a regular fibroblastic bipolar shape. When confluent, they grew into a hill-and-valley topography on the culture flask. (B) Old hVSMCs were enlarged with enlarged nucleus, enlarged multiple nucleoli and irregular fibroblastic multipolar shape. Cells exhibited a flattened topography and were also heavily granulated as a result of increased lysosomal mass and damaged protein degradation system leading to protein build up. Senescence-associated β -galactosidase activity was observed in (D) old cells and not in young cells (C) via specific staining at pH6.0, confirming cellular senescence of old hVSMCs.

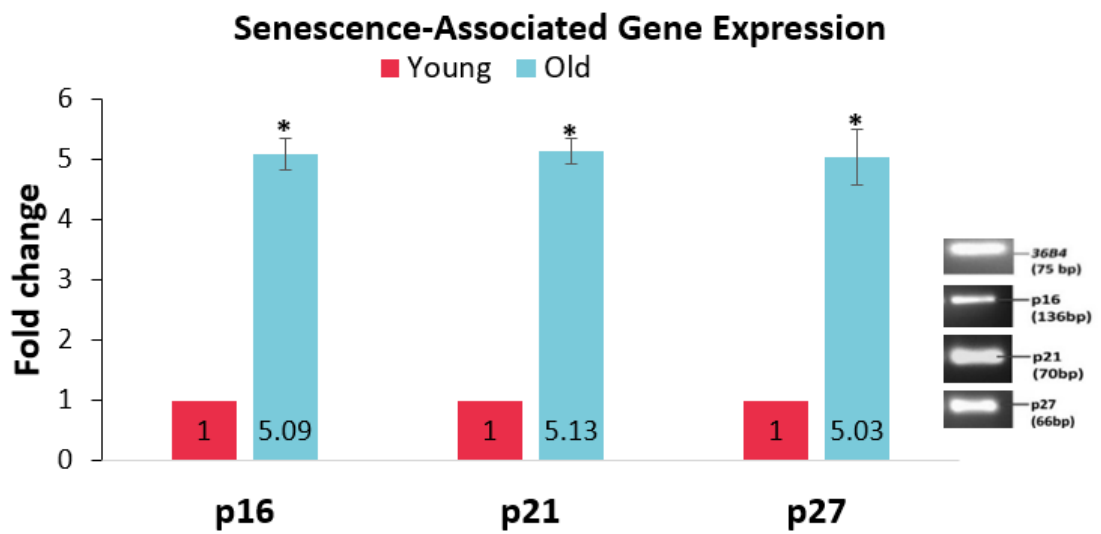


Figure 4.1-2: Relative fold change of the expression of the senescence-associated genes *CDKN2A*, *CDKN1A* and *CDKN1B* encoding p16^{INK4α}, p21^{Cip1} and p27^{Kip1} in old samples showed a significant upregulated expression by 5.09, 5.13 and 5.03 fold compared to young samples respectively (n=3 **p* < 0.05).

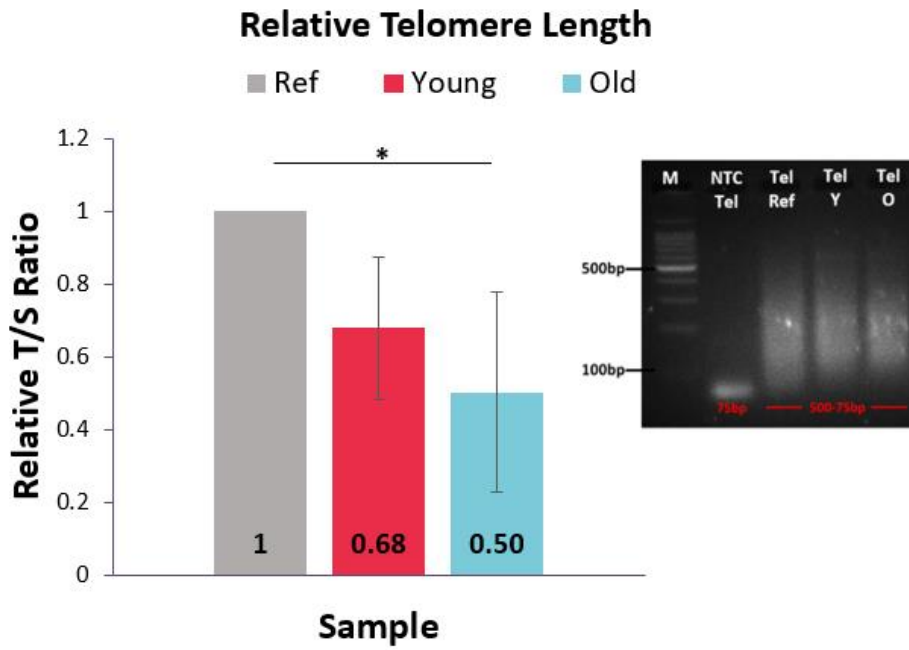


Figure 4.1-3: Relative telomere length of young and old samples. T/S Ratio of the old sample (0.50) was significantly lower than that of the young (0.68), when compared to the reference ($n=3$, $*p < 0.05$), confirming replicative senescence in old samples.

4.2. Characterization of Exosomes Isolated from Human Vascular Smooth Muscle Cell Conditioned Media

4.2.1. Scanning Electron Microscopy

In the SEM sample, the average diameter of the vesicles was $136.6\text{nm} \pm 37.6\text{nm}$ ($n=60$) with minimum and maximum measurements being 79nm and 238.5nm (**Figure 4.2-1 A**). Vesicle morphology could not be observed with high resolutions due to the limitations within the SEM.

4.2.2. Transmission Electron Microscopy

In TEM images, clearer resolution could be achieved (**Figure 4.2-1 B and C**). Exosome-like vesicles in the young sample had an average diameter of $140.8\text{nm} \pm 31\text{nm}$ ($n=28$). In the old sample, the average diameter was $154\text{nm} \pm 32.6\text{nm}$ ($n=49$). There was no significant difference between the average size of the exosomes of the young and old samples ($p > 0.05$). However, exosomes from the young sample were more sparse while those in the old samples were more clustered. These qualitative results from the SEM and TEM indicated the presence of exosome-like vesicles in the samples.

4.2.3. Immunoblotting

Immunoblotting against the protein TSG101 resulted in visible bands in both young and old samples, from intracellular and extracellular sources (**Figure 4.2-2**). In both intracellular and extracellular samples, young sample showed much more intense band than old samples. There was very low expression of TSG101 in old intracellular samples while a significantly higher level of TSG101 expression in the old extracellular sample was observed. The bands representing TSG101 in intracellular samples were of smaller size ($\sim 50\text{kDa}$) than that of the extracellular samples ($\sim 75\text{kDa}$). This observation was consistent in all samples.

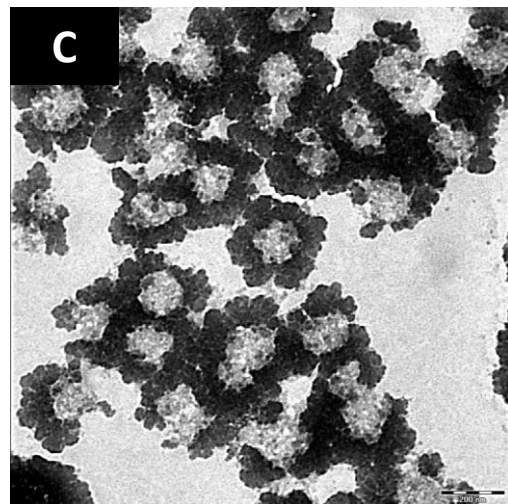
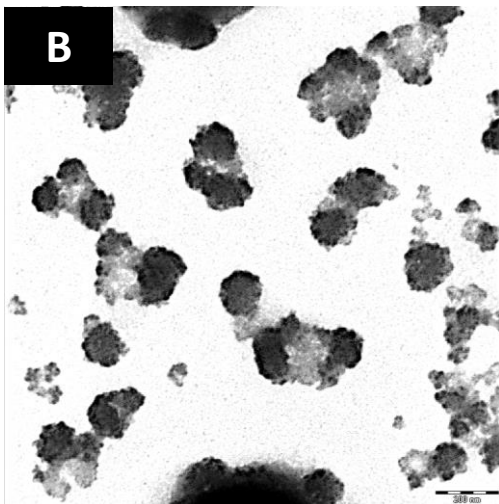
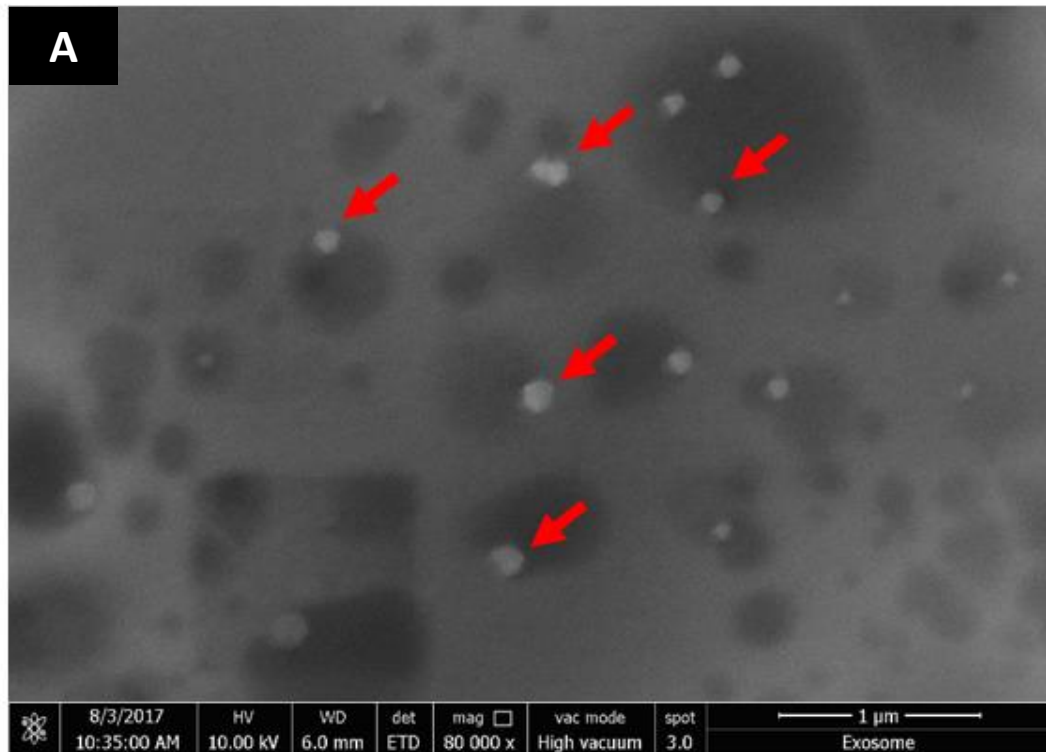


Figure 4.2-1: Ultrastructure of exosomes from scanning electron microscope and transmission electron microscope. (A) SEM image of old hVSMC sample with an average diameter of $136.6\text{nm} \pm 37.6\text{nm}$ ($n=60$) with minimum and maximum measurements being 79nm and 238.5nm . TEM image of **(B)** young sample with an average diameter of $140.8\text{nm} \pm 31\text{nm}$ ($n=28$) and **(C)** old sample with an average diameter of $154\text{nm} \pm 32.6\text{nm}$ ($n=49$). The exosomes from the young sample were more sparse while those in the old samples were more clustered. The black patches surrounding the vesicles represent the negative stain which stained the background black.

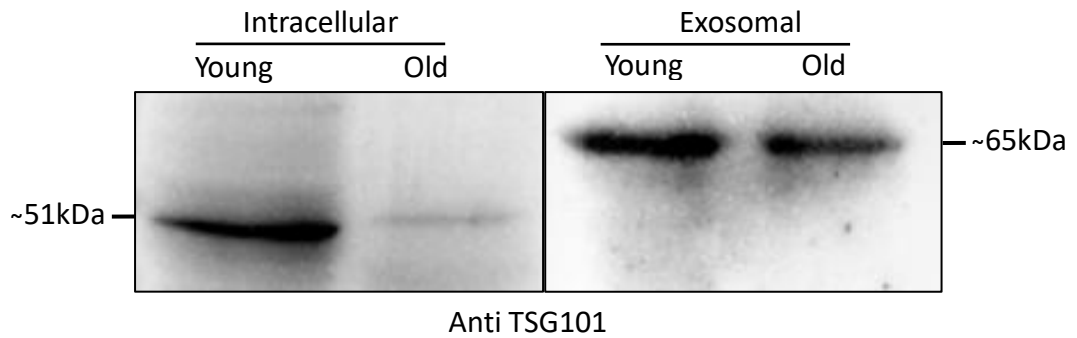


Figure 4.2-2: Immunoblotting via Western Blot against the protein TSG101. In both intracellular and extracellular samples, young sample showed much more intense band than old samples. There was almost no expression of TSG101 in old intracellular samples whilst there was a higher level of TSG101 expression in the old extracellular sample. Although clear bands were observed, the size of the protein in intracellular samples were larger than that of the extracellular samples (n=3).

4.3. Optimization of Small RNA Library Prep prior to Sequencing

Optimization of the library prep was performed in order to ensure successful amplification of the cDNA libraries. In particular, the native PAGE density, electrophoresis running voltage and cDNA elution time were optimized. Firstly, different percentages (6%, 12% and 20%) of native PAGE were casted and the gels were run at 40V for 4 hrs, 80V for 1.5 hrs and 145V for 1 hr. The DNA ladder did not separate in the 12% and 20% native PAGE, indicating that the gel was too dense. While the DNA ladder separated decently in the 6% native PAGE run at 145V for 1 hr, the resolution of the bands was not clear, suggesting that the voltage used was too high. Finally, the DNA ladder separated nicely with clear bands in the 6% native PAGE run at 80V for 1.5 hrs, indicating optimal gel percentage, running voltage and time (**Figure 4.3-1**).

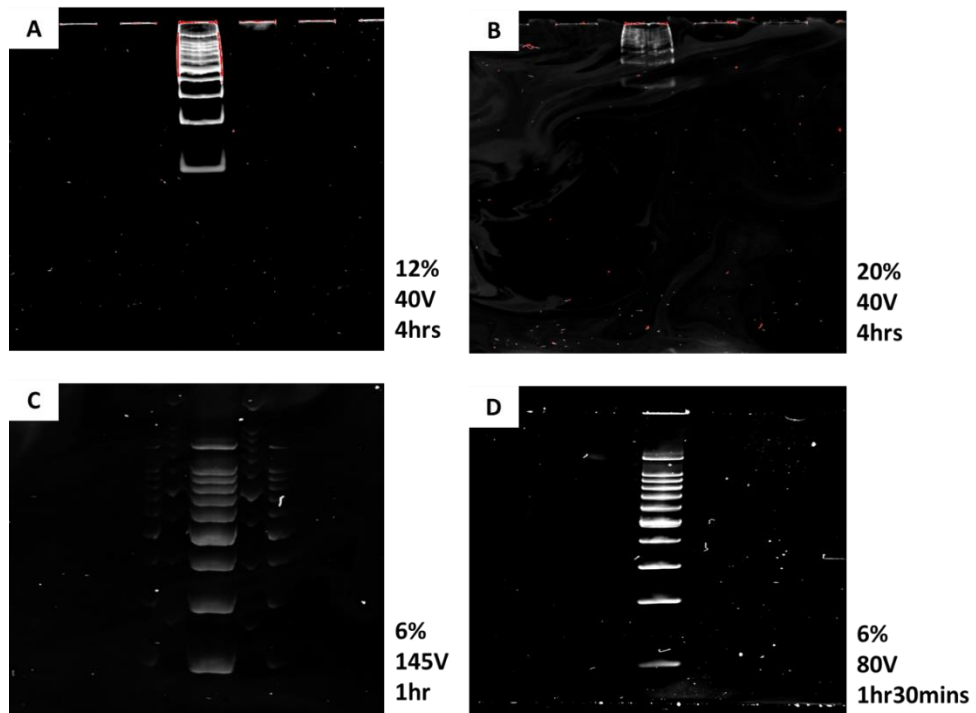


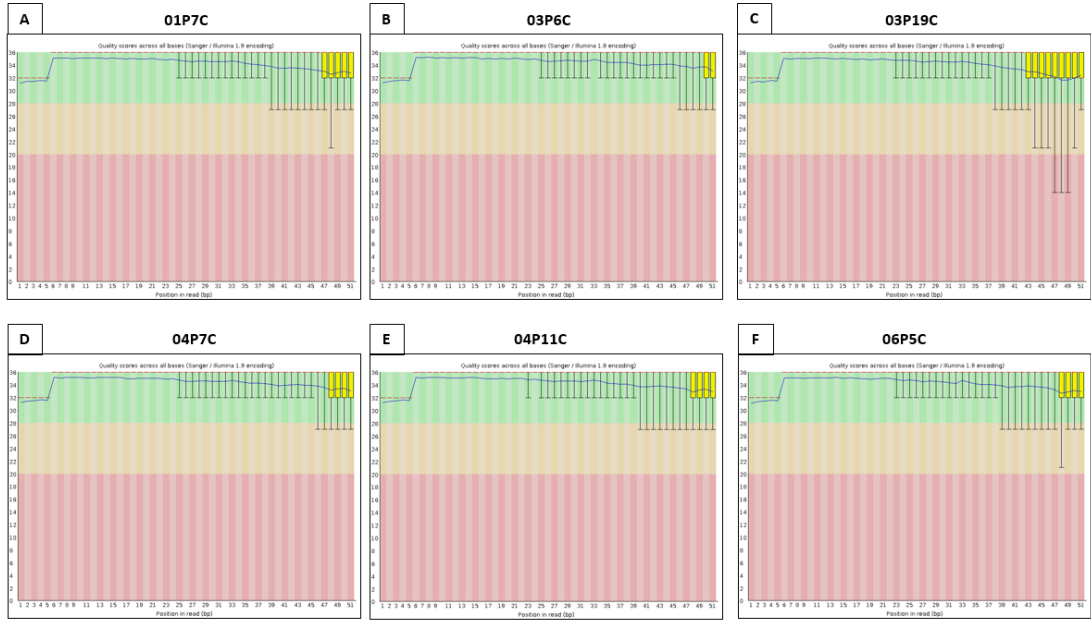
Figure 4.3-1: Optimization of native PAGE for NGS library prep. From **A.** and **B.** the DNA ladder was not separated properly, indicating that the PAGE percentage of 12% -20% was too high. **C.** The DNA ladder, albeit decent separation, did not have a clear resolution, suggesting that the voltage used was too high (145V), leading to rapid migration thus low resolutions of the bands. **D.** presented a nicely separated DNA ladder and clear resolution of the bands, implicating that the gel percentage (6%), voltage (80V) and running time (1hr30mins) was optimal.

4.4. Primary and Secondary Data Analysis of Whole-Genome Small RNA Next-Generation Sequencing

Post-sequencing data consisted of 127,457,682 million reads, of which 110,405,465 reads were sent for alignment after pre and post-QC trimming. A total of 36,238,440 reads were successfully aligned to obtain 21,637 precursor miRNA reads and 21,108,016 mature miRNA reads. After filtration of all known miRNAs with equal or more than 5x coverage, a total of 3,806 mature miRNAs were detected (Appendix **Table 12**).

All samples passed the basic statistics test pre- and post-trimming. Data are presented below for the analysis of the modules testing per base sequence quality, per sequence quality scores, per base N content and sequence length distribution post-trimming. As shown in **Figure 4.4-1**, per base sequence quality QC showed all samples had sequence quality in the upper range (green). It is normal for the quality to drop at the longer sequences as these would not be included in downstream analyses. In per sequence quality scores, all samples achieved an average of 35 Phred scores, indicating that all samples had high quality sequences as shown in **Figure 4.4-2**. In **Figure 4.4-3** showing per base N content, no failed base call was detected, represented by 0% of N base across all samples. Finally, sequence length distribution for all samples was represented in **Figure 4.4-4**. While sequence length distribution was rather consistent in samples **A – F**, sample **C** showed a more irregular distribution with lesser 18-26 bp sequences and higher 30+ bp sequences. This was later revealed in subsequent mapping that sample **C** consisted more of other small RNA species, which will be elaborated below. Meanwhile, exosomal miRNAs represented in **Figure 4.4-4 G – L** had highly variable distribution of sequence length, which also required subsequent mapping to determine the cause to this inconsistency. Overall, sample QC post-trimming showed that all bases and sequences were qualified for subsequent mapping, which is sequence alignment to the reference genome.

Per base sequence quality – Intracellular miRNAs



Per base sequence quality – Exosomal miRNAs

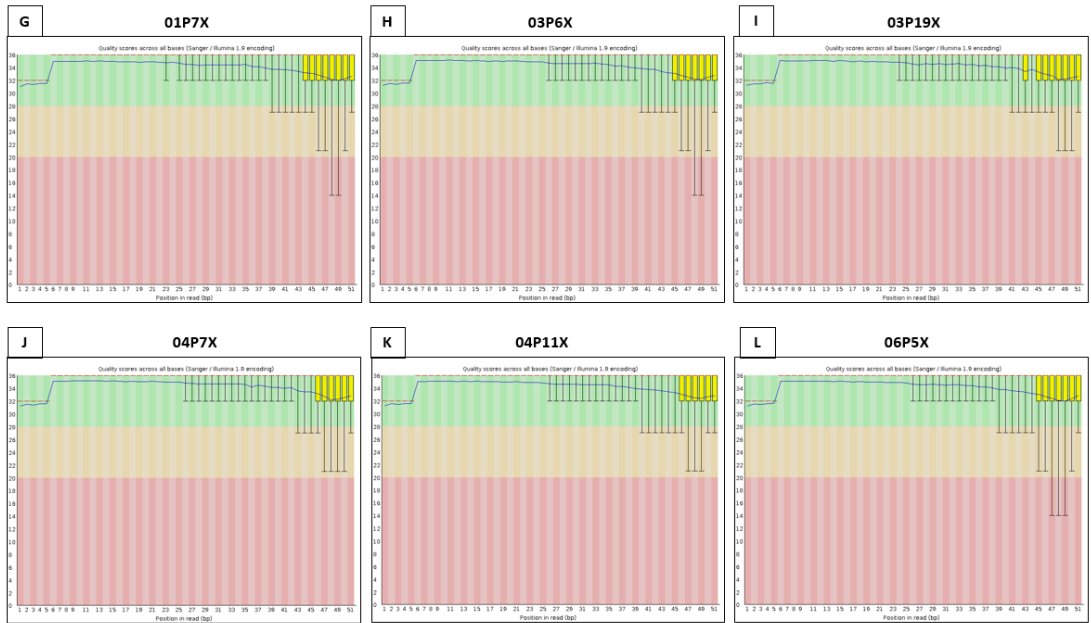
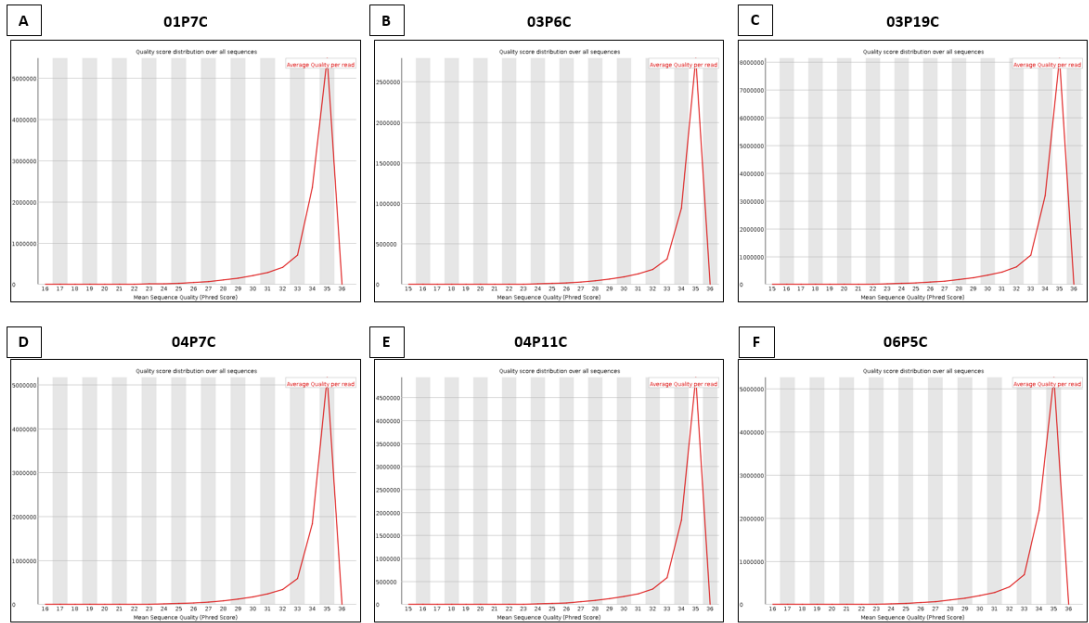


Figure 4.4-1: Per base sequence quality of intracellular and exosomal miRNAs post-trimming.

Per sequence quality scores— Intracellular miRNAs



Per sequence quality scores – Exosomal miRNAs

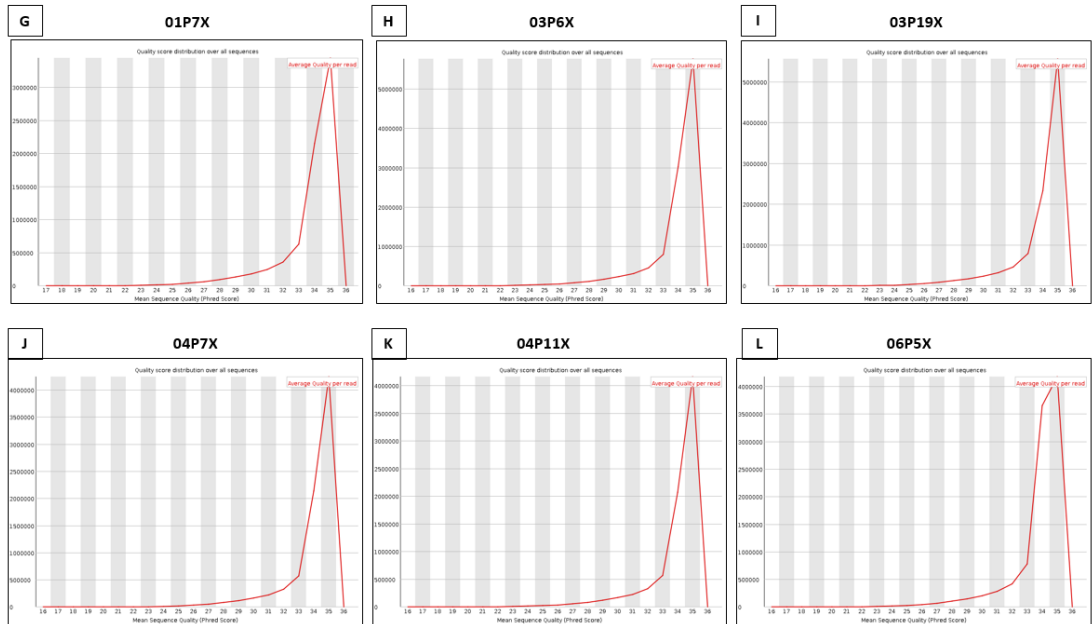
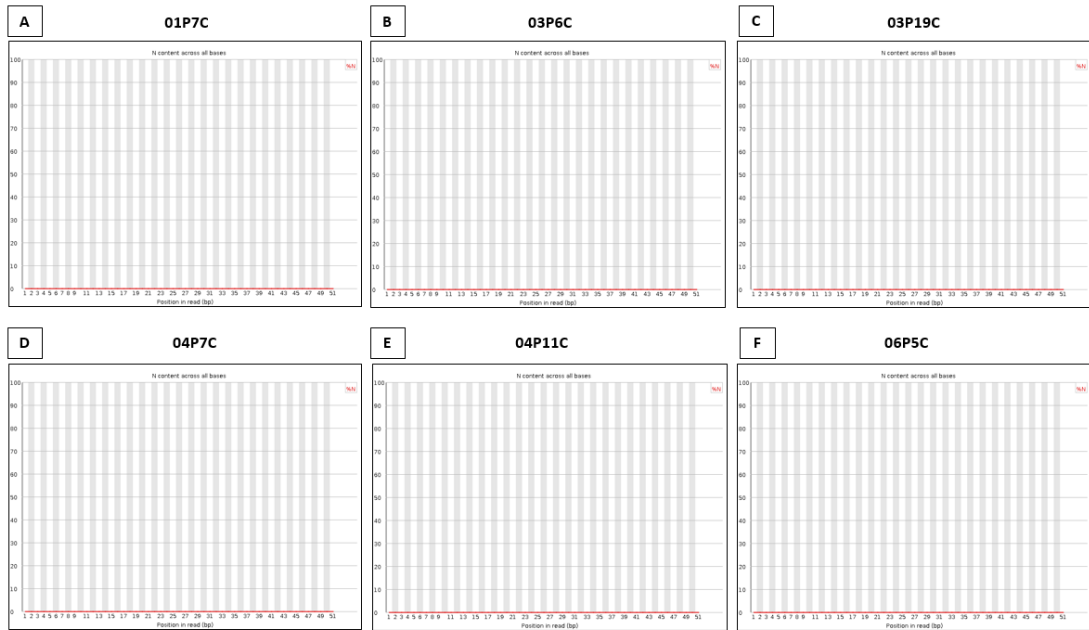


Figure 4.4-2: Per sequence quality scores of intracellular and exosomal miRNAs post-trimming.

Per base N content– Intracellular miRNAs



Per base N content – Exosomal miRNAs

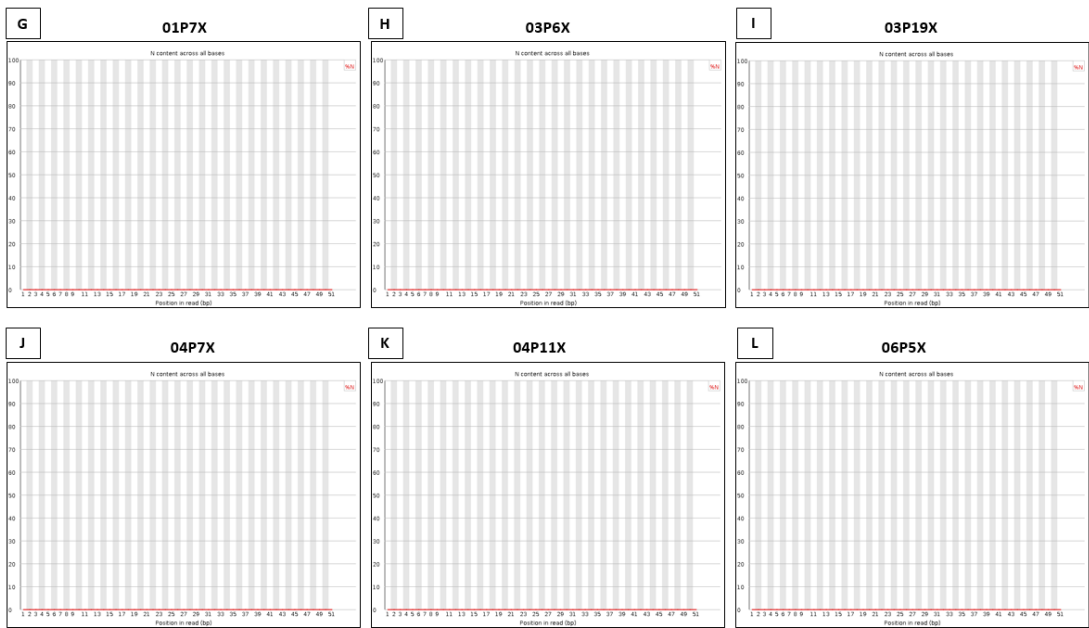
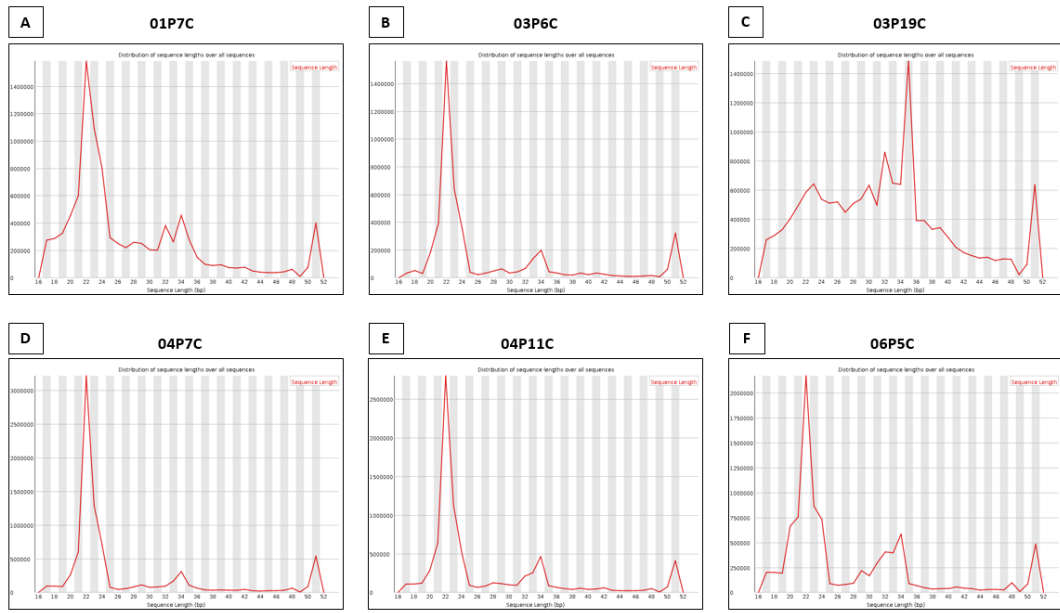


Figure 4.4-3: Per base N content of intracellular and exosomal miRNAs post-trimming.

Sequence length distribution – Intracellular miRNAs



Sequence length distribution – Exosomal miRNAs

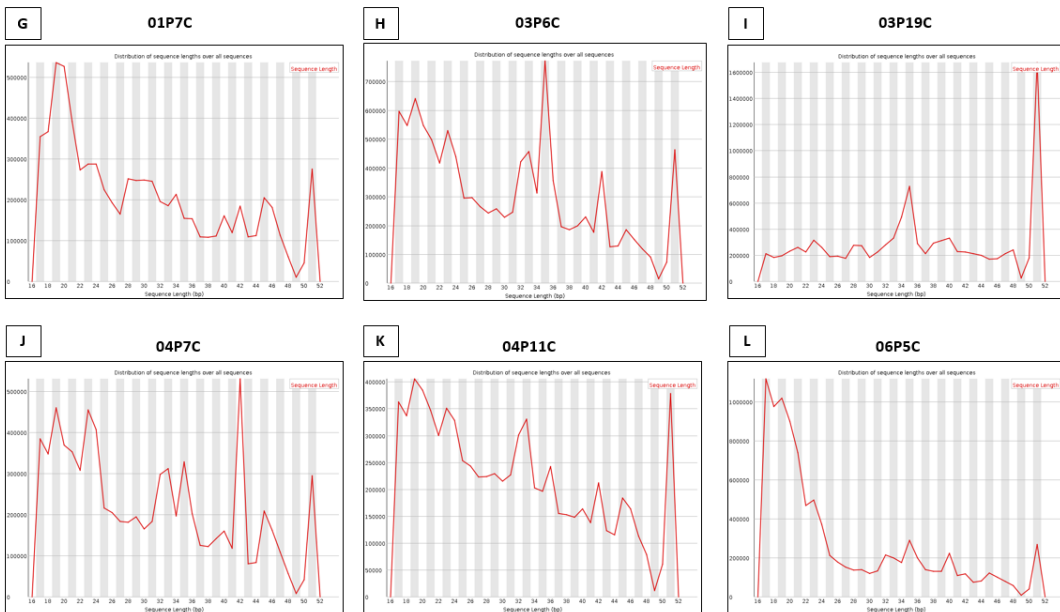


Figure 4.4-4: Sequence length distribution of intracellular and exosomal miRNAs post-trimming.

Sequences aligned to the reference genome consisted of miRNAs as well as mRNAs and other types of RNA, such as: ribosomal RNA (rRNA), mitochondrial tRNA, mitochondrial rRNA, long intervening/intergenic non-coding RNA (lincRNA), small nuclear RNA (snRNA) and small nucleolar RNA (snoRNA). Intracellular RNA quantification yielded consistent miRNA profiles in young samples, whereas more irregular profiles were observed in old samples. Exosomal RNA quantification obtained irregular profiles with a smaller proportion of miRNAs compared to that of intracellular samples (**Figure 4.4-5&Figure 4.4-6**).

Data were normalized and data distribution was analysed for both intracellular and exosomal samples. From the box and whiskers plots, the interquartile range as well as the median (Q2) were consistent across young and old intracellular samples (**Figure 4.4-7 A**). On the other hand, interquartile range was different between young and old exosomal samples. However, their median were consistent in all exosomal samples (**Figure 4.4-7 B**). Consistent median values across all samples indicated good data distribution therefore allowed downstream comparison of data between young and old samples from both intracellular and exosomal origins.

Principal component analysis was also performed to assess data distribution. For intracellular mapped transcripts, X and Y axis showed principal component 1 and principal component 5 that explained 69.1% and 3.3% of the total variance, respectively (**Figure 4.4-7 C**). For exosomal transcripts, X and Y axis showed principal component 1 and principal component 3 that explained 60.2% and 9.3% of the total variance, respectively. Prediction ellipses were such that with probability 0.95, a new observation from the same group would fall inside the ellipse (n=6) (**Figure 4.4-7 D**).



Figure 4.4-5: RNA profiling of intracellular hVSMCs. RNA content was similar in young samples while that of old samples was more irregular, especially for intracellular miRNA content. Old samples also contained larger portions of protein-coding mRNAs and miscRNAs than those in young samples.



Figure 4.4-6: RNA profiling of hVSMC-derived exosomes. Exosomal RNA content in all samples were not similar between young and old samples as well as between each other within the same condition. MiRNAs occupied a smaller portion compared to those in intracellular samples. Protein-coding mRNAs and miscRNAs constitute the largest portions of the exosomal RNA content. There was also a significant portion of identified lincRNA transcripts, which was bigger than the miRNA portion in most samples.

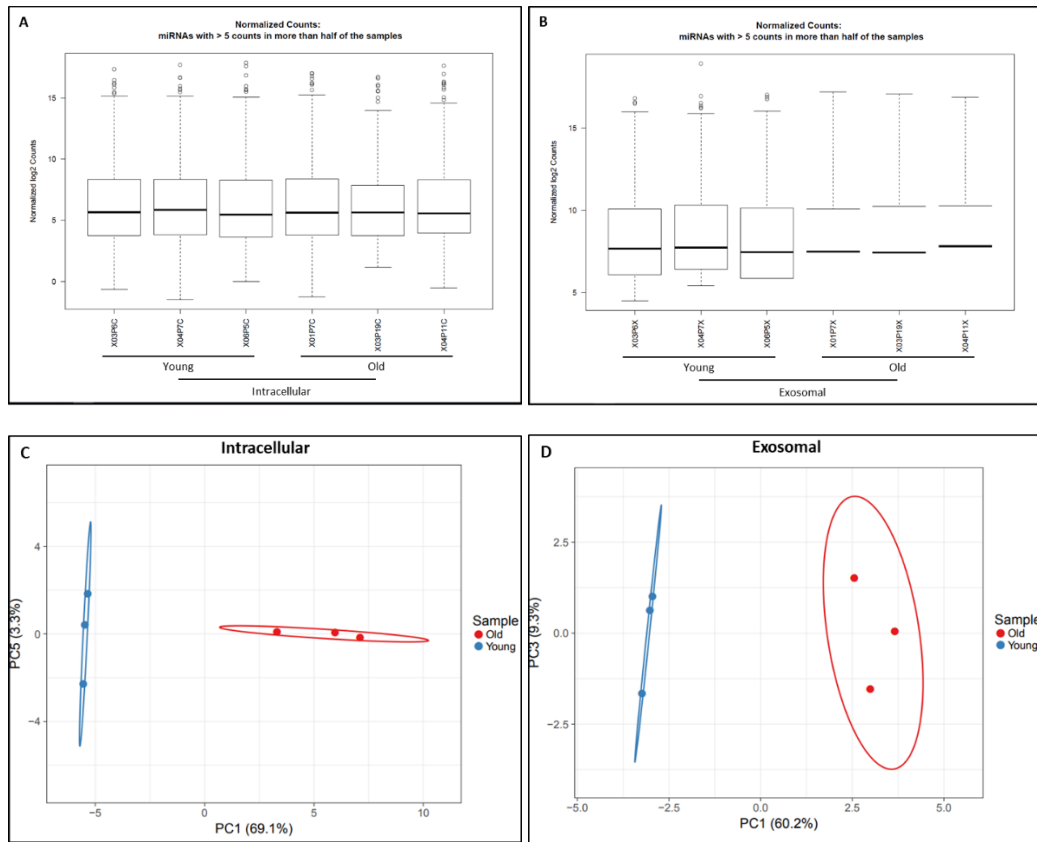


Figure 4.4-7: Data distribution analyses. Box and whiskers plots representing data distribution of (A) intracellular and (B) exosomal miRNAs. In the box and whiskers plots, the middle line (Q2) represents the median. Relatively similar medians across all samples indicates good data distribution and therefore is suitable for data comparison between young and old samples. Principal component analysis was performed to assess data distribution. (C) For intracellular mapped transcripts, X and Y axis show principal component 1 and principal component 5 that explain 69.1% and 3.3% of the total variance, respectively. (D) For exosomal transcripts, X and Y axis show principal component 1 and principal component 3 that explain 60.2% and 9.3% of the total variance, respectively. Prediction ellipses are such that with probability 0.95, a new observation from the same group will fall inside the ellipse ($n=6$).

4.5. Intracellular and Exosomal miRNAs in Human Vascular Smooth Muscle Cells during Replicative Senescence

4.5.1. Differential Expression Analysis and Validation of Intracellular and Exosomal miRNAs in Senescent Human Vascular Smooth Muscle Cells

Differential expression analysis yielded 54 dysregulated miRNAs in senescent hVSMCs. Thirty miRNAs were upregulated while 24 miRNAs were downregulated. In senescent hVSMC-derived exosomes, 19 dysregulated miRNAs were discovered, of which 8 were upregulated and 11 were downregulated ($p < 0.05$) (**Figure 4.5-1** & **Figure 4.5-2**). After FDR adjustment, the dysregulated miRNAs were narrowed down to 8 miRNAs, of which 6 were upregulated and 2 were downregulated. In senescent hVSMC-derived exosomes, 2 miRNAs were downregulated while one was upregulated after FDR adjustment ($q < 0.05$). The FDR-adjusted miRNAs were represented as volcano plots with red circles representing the miRNAs that had passed the stringent QC for both intracellular (**Figure 4.5-3**) and exosomal miRNAs (**Figure 4.5-4**). Subsequently, the name of the mature miRNAs together with their fold change values (logFC), p value (PValue), FDR-adjusted p value (FDR) and differential expression remarks (Expression) were presented in **Table 6** & **Table 7**. In particular, the intracellular miRNAs *hsa-miR-4485-3p*, *hsa-miR-12136*, *hsa-miR-664a-3p*, *hsa-miR-664a-5p*, *hsa-miR-10527-5p* and *hsa-miR-664b-3p* were upregulated by 6.47, 4.42, 2.64, 2.25, 2.75 and 2.65 fold, respectively. Conversely, intracellular miRNAs *hsa-miR-155-5p* and *hsa-miR-20a-5p* were downregulated by -2.27 and -2.22 fold, respectively. Similarly, exosomal miRNA *hsa-miR-7704* was upregulated by 4.30 fold while exosomal miRNA *hsa-miR-155-5p* and *hsa-miR-146b-5p* were downregulated by -4.03 and -2.21 fold, respectively. Ultimately, the structure of both the 3p and 5p species of the miRNAs of interest was visualized using miRDeep2 (**Figure 4.5-5**).

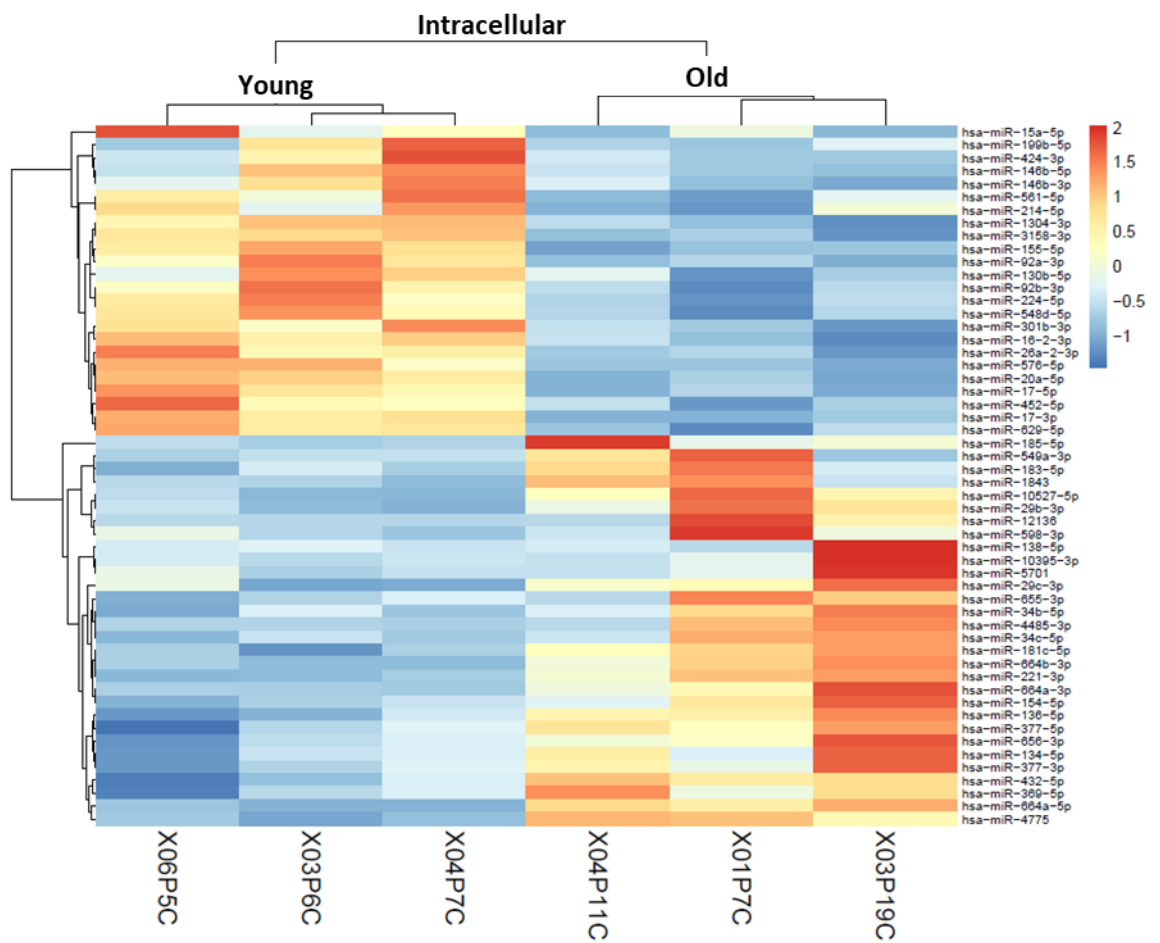


Figure 4.5-1: Heat map representing significant differentially expressed intracellular miRNAs of hVSMCs ($n=3$, $p < 0.05$). The red spectrum indicates upregulated miRNAs and the blue spectrum indicated downregulates miRNAs in hVSMC samples.

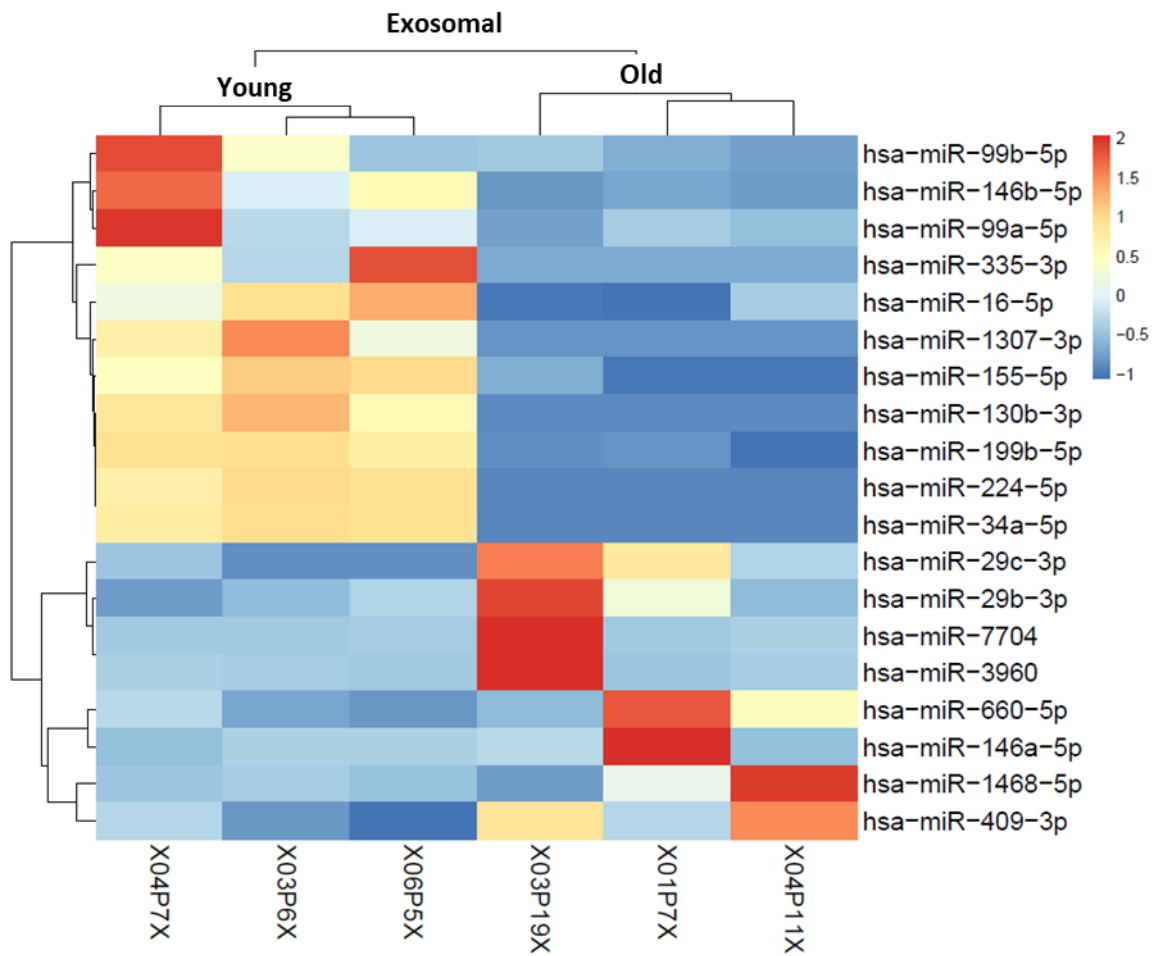


Figure 4.5-2: Heat map representing significant differentially expressed exosomal miRNAs in hVSMC-derived exosomes ($n=3, p < 0.05$). The red spectrum indicates upregulated miRNAs and the blue spectrum indicates downregulated miRNAs in hVSMC-derived exosomal samples.

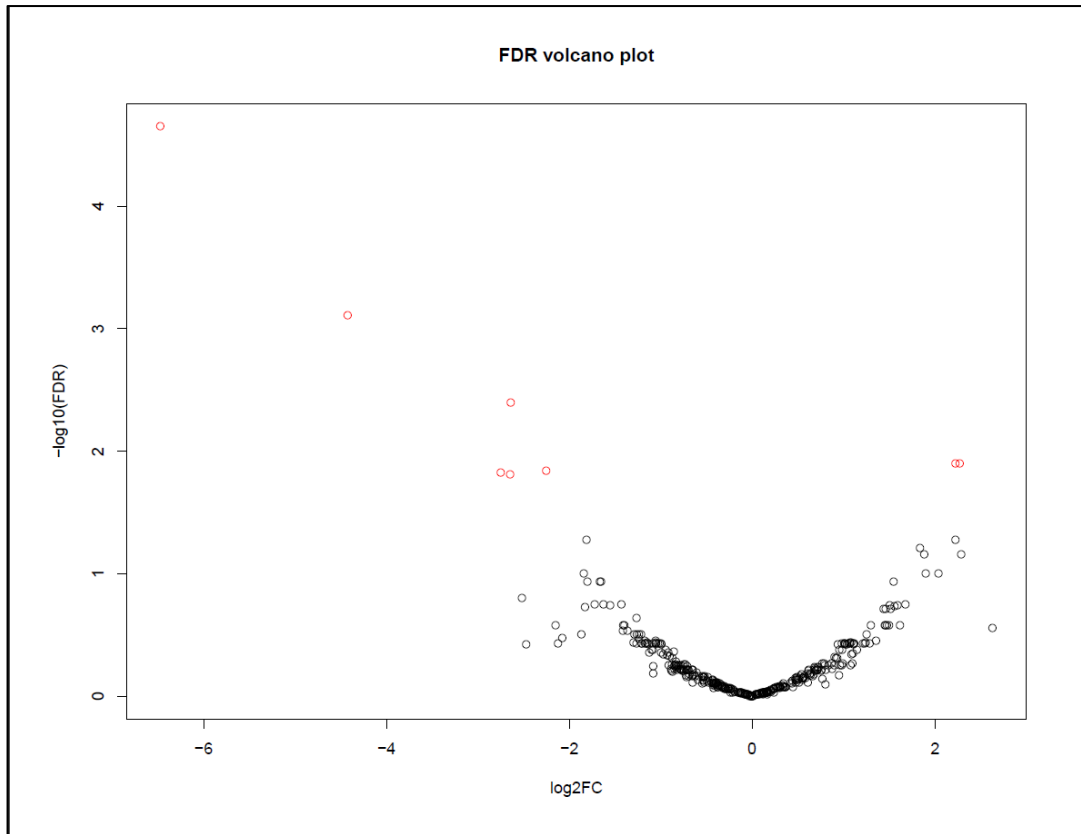


Figure 4.5-3: Differential expression of young compared to old intracellular miRNAs. Red circles represent significant differentially expressed miRNAs with FDR-adjusted p values ($\text{FDR} < 0.05$, $n=3$). Differentially expressed miRNAs were *hsa-miR-155-5p*, *hsa-miR-20a-5p*, *hsa-miR-664a-3p*, *hsa-miR-664a-5p*, *hsa-miR-664b-3p*, *hsa-miR-10527-5p*, *hsa-miR-12136* and *hsa-miR-4485-3p*.

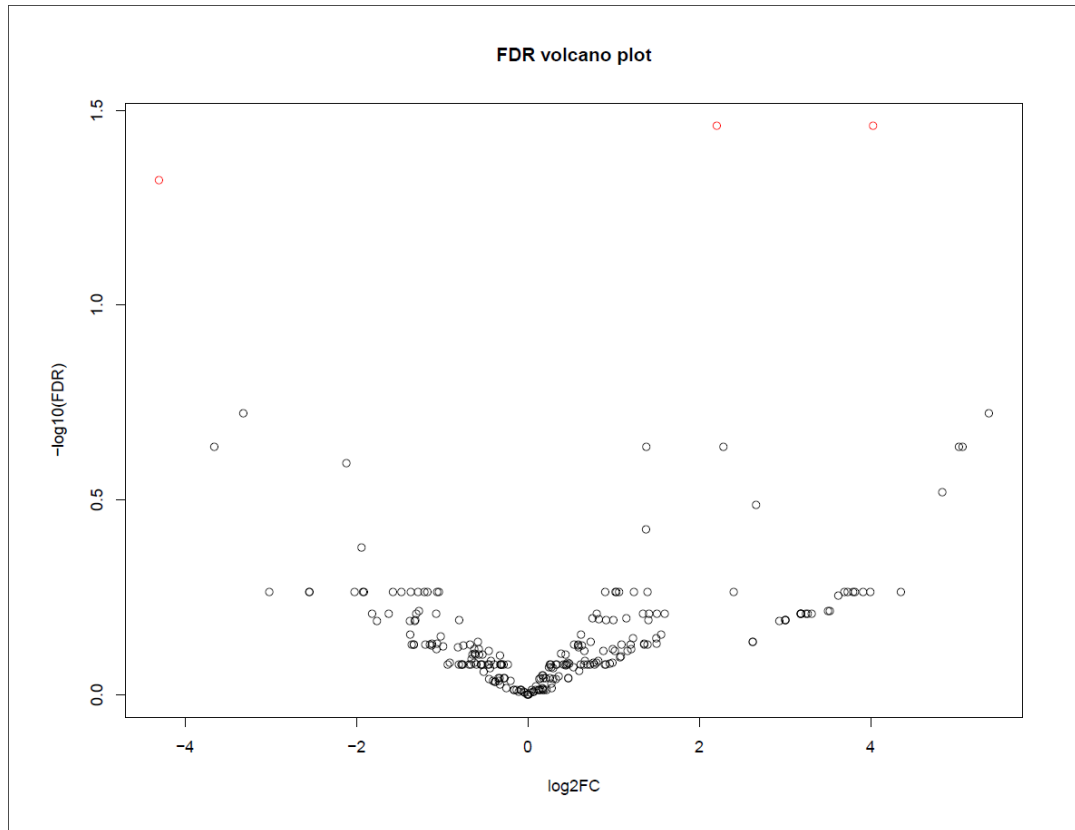


Figure 4.5-4: Differential expression of young compared to old exosomal miRNAs. Red circles represent significant differentially expressed miRNAs with FDR-adjusted p values ($\text{FDR} < 0.05$, $n=3$). Differentially expressed miRNAs were *hsa-miR-146b-5p*, *hsa-miR-155-5p*, and *hsa-miR-7704*.

Table 6: Dysregulated miRNAs in senescent hVSMCs.

Mature miRNA	logFC	PValue	FDR	Expression
hsa-miR-155-5p	-2.270907	0.000152	0.012561	Down
hsa-miR-20a-5p	-2.223714	0.000167	0.012561	Down
hsa-miR-4485-3p	6.47284	5.95E-08	2.24E-05	Up
hsa-miR-12136	4.42413	4.11E-06	0.000776	Up
hsa-miR-664a-3p	2.63899	3.21E-05	0.004033	Up
hsa-miR-664a-5p	2.25357	0.00023	0.014483	Up
hsa-miR-10527-5p	2.74949	0.000277	0.014929	Up
hsa-miR-664b-3p	2.64739	0.000328	0.015462	Up

Table 7: Dysregulated miRNAs in exosomes derived from senescent hVSMCs.

Mature miRNA	logFC	PValue	FDR	Expression
hsa-miR-155-5p	-4.027492	0.000146	0.034709	Down
hsa-miR-146b-5p	-2.206939	0.000292	0.034718	Down
hsa-miR-7704	4.30286	0.000602	0.047758	Up

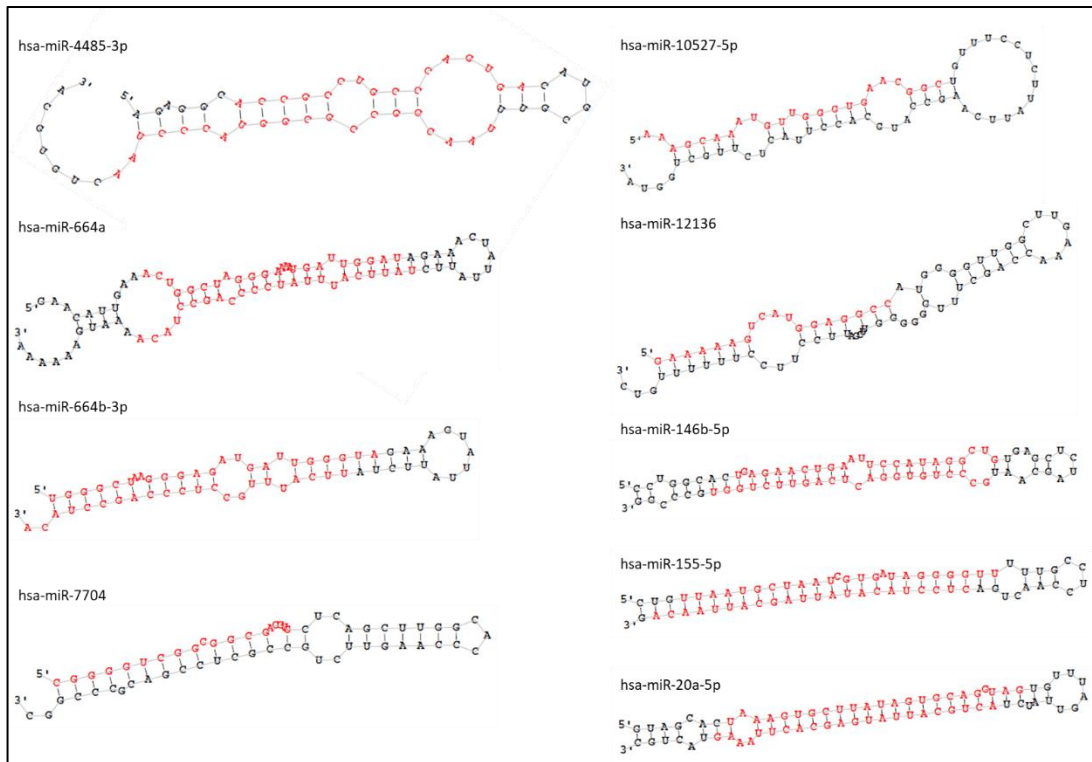


Figure 4.5-5: Structure of differentially expressed miRNAs generated by miRDeep2.

4.5.2. Validation of Differentially Expressed miRNAs in Senescent Human Vascular Smooth Muscle Cells and Exosomes

Gene expression was represented as expression ratios, or fold-change, in the form of $2^{-\Delta(\Delta C_t)}$ values. Differential expression levels were determined based on the relative fold change of the gene expression of the old samples compared to that of the young samples. Values for fold change calculation were first normalized against the Ct values of the reference gene *RNU6*. From **Figure 4.5-6**, average fold change of intracellular *hsa-miR-664a-3p*, *hsa-miR-10527-5p*, *hsa-miR-12136* and *hsa-miR-4485-3p* was 2.83 ± 0.82 , 13.52 ± 0.61 , 36.00 ± 0.63 and 49.83 ± 0.61 fold higher in old samples, respectively, when compared to those of young samples ($p < 0.05$, $n=3$). Higher fold change in old samples indicated upregulation of these miRNAs in replicative senescent hVSMCs. In **Figure 4.5-7**, the average fold change of intracellular *hsa-miR-155-5p* and *hsa-miR-20a-5p* was 0.18 and 0.63, respectively, indicating the downregulation of these miRNAs in senescent hVSMCs. The data were represented as $\log_2(\text{fold change})$ values, which were -2.50 ± 0.52 and -0.66 ± 0.62 for *hsa-miR-155-5p* and *hsa-miR20a-5p* respectively ($p < 0.05$, $n=3$).

Figure 4.5-8 represented the exosomal expression of *hsa-miR-146b-5p* and *hsa-miR-155-5p* with the average fold change of 0.51 and 0.09, respectively, indicating downregulation of *hsa-miR-146b-5p* and *hsa-miR-155-5p* in senescent hVSMC-derived exosomes ($p < 0.05$, $n=3$). Similarly, data were presented as $\log_2(\text{fold change})$ values for better visualization, which were -1.43 ± 0.37 and -3.11 ± 0.46 for *hsa-miR-146b-5p* and *hsa-miR-155-5p* respectively. Expression validation for *hsa-miR-7704* was not applicable as no suitable primer could be designed due to high G-C content of the sequences, which was not compatible with the miScript qPCR detection system (Qiagen, Germany).

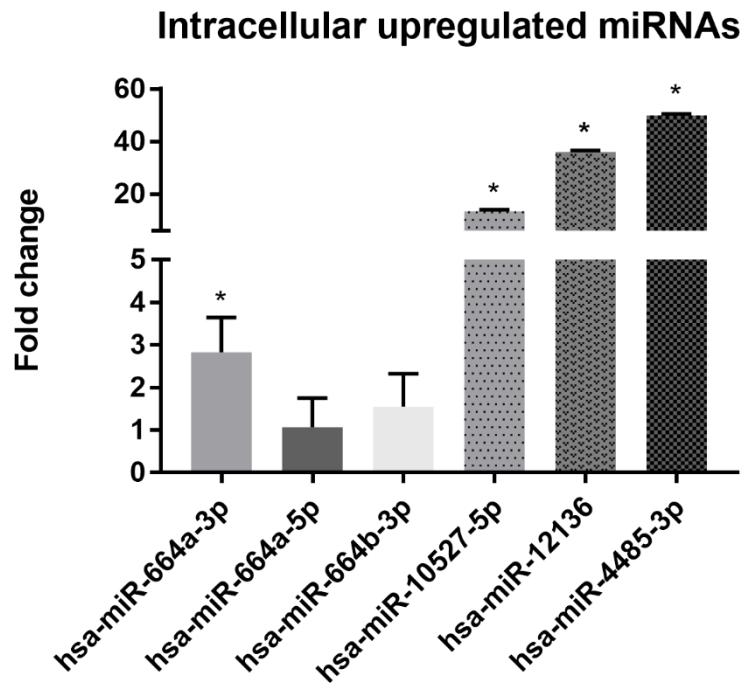


Figure 4.5-6: Validation of upregulated intracellular miRNAs in senescent hVSMCs. Average fold change of intracellular *hsa-miR-664a-3p*, *hsa-miR-10527-5p*, *hsa-miR-12136* and *hsa-miR-4485-3p* were 2.83 ± 0.82 , 13.52 ± 0.61 , 36.00 ± 0.63 and 49.83 ± 0.61 fold higher in old samples, respectively, when compared to those of young samples ($p < 0.05$, $n=3$). Higher fold change in old samples indicated upregulation of these miRNAs in replicative senescent hVSMCs.

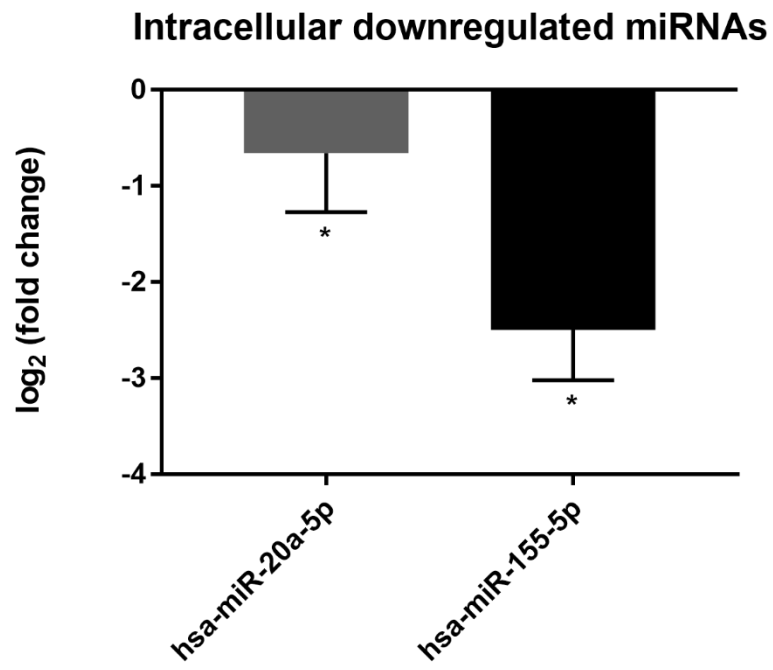


Figure 4.5-7: Validation of downregulated intracellular miRNAs in senescent hVSMCs. Average fold change of intracellular *hsa-miR-155-5p* and *hsa-miR-20a-5p* were 0.18 and 0.63, respectively, indicating the downregulation of these miRNAs in senescent hVSMCs. The data was represented as $\log_2(\text{fold change})$ values, which were -2.50 ± 0.52 and -0.66 ± 0.62 for *hsa-miR-155-5p* and *hsa-miR20a-5p* respectively ($p < 0.05$, $n=3$).

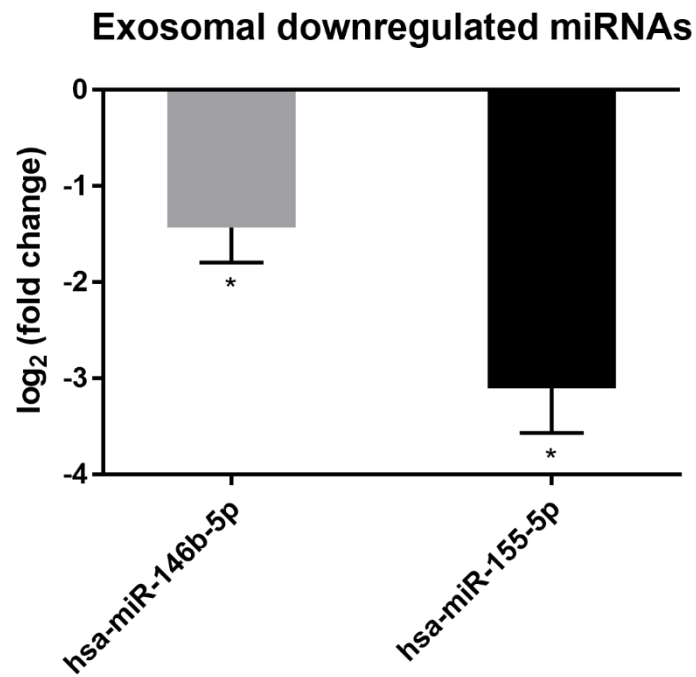


Figure 4.5-8: Validation of downregulated exosomal miRNAs in senescent hVSMC-derived exosomes. Expression of *hsa-miR-146b-5p* and *hsa-miR-155-5p* with the average fold change of 0.51 and 0.09, respectively, indicating downregulation of *hsa-miR-146b-5p* and *hsa-miR-155-5p* in senescent hVSMC-derived exosomes ($p < 0.05$, $n=3$). Data were presented as $\log_2(\text{fold change})$ values, which were -1.43 ± 0.37 and -3.11 ± 0.46 for *hsa-miR-146b-5p* and *hsa-miR-155-5p* respectively.

4.5.3. Predicted Target Genes of Differentially Expressed miRNAs

Target prediction of all differentially expressed miRNAs was performed using miRWalk. Target genes acquired from this database were experimentally validated and reported in published articles (**Appendix Table 13**). In intracellular samples, only 4 out of 6 miRNAs were successfully mapped to the miRNA-target interaction database. In a respective manner, validated target genes acquired for upregulated miRNAs *hsa-miR-664a-3p*, *hsa-miR-664a-5p*, *hsa-miR-664b-3p* and *hsa-miR-4485-3p* were 58, 97, 124 and 4. For downregulated *hsa-miR-20a-5p* and *hsa-miR-155-5p*, a number of 772 and 333 validated target genes were found, respectively. However, both validated and unvalidated target genes for *hsa-miR-12136* and *hsa-miR-10527-5p* were not found. On the other hand, in exosomal samples, upregulated *hsa-miR-7704* acquired 46 validated target genes. Meanwhile, downregulated *hsa-miR-146b-5p* and *hsa-miR-155-5p* had 62 and 333 validated target genes, respectively.

Although an extensive list of target genes was acquired, the depth of information remained superficial and the data was only considered as preliminary and the parameters obtained were insufficient to extrapolate or conclude which target genes were worth further investigation. In order to narrow down potential biological significant target genes, the preliminary lists of target genes were used as input for the following analyses, such as gene ontology categorization, pathway enrichment analysis and regulatory interaction network generation. As such, important predicted target genes obtained after GO and KEGG enrichment analyses were presented in **Table 8** below.

Table 8: Highlight of target genes filtered from GO and KEGG enrichment analyses.

Intracellular Upregulated miRNAs							
hsa-miR-4485-3p	DUSP8	hsa-miR-155-5p	ATP6V1C1	hsa-miR-155-5p	MAN1A2	hsa-miR-155-5p	SSH2
hsa-miR-664a-3p	CACNA2D3	hsa-miR-155-5p	BCL6	hsa-miR-155-5p	MTAP	hsa-miR-155-5p	STAG2
hsa-miR-664a-3p	HSPA1B	hsa-miR-155-5p	CAB39L	hsa-miR-155-5p	MYB	hsa-miR-155-5p	STIM1
hsa-miR-664a-3p	MAPK8	hsa-miR-155-5p	CASP3	hsa-miR-155-5p	NCKAP1	hsa-miR-155-5p	TJP1
hsa-miR-664a-3p	PPM1A	hsa-miR-155-5p	CBL	hsa-miR-155-5p	NFKB1	hsa-miR-155-5p	TRAM1
hsa-miR-664a-5p	CTSS	hsa-miR-155-5p	CCND1	hsa-miR-155-5p	NOTCH2	hsa-miR-155-5p	UBE2D3
hsa-miR-664a-5p	EFNA1	hsa-miR-155-5p	CCR9	hsa-miR-155-5p	NUP155	hsa-miR-155-5p	UBE2G1
hsa-miR-664a-5p	STK4	hsa-miR-155-5p	CD36	hsa-miR-155-5p	PATJ	hsa-miR-155-5p	UBQLN1
hsa-miR-664a-5p	UBE2N	hsa-miR-155-5p	CDK2	hsa-miR-155-5p	PDK1	hsa-miR-155-5p	UBQLN2
hsa-miR-664b-3p	CALM1	hsa-miR-155-5p	CDKN1B	hsa-miR-155-5p	PIK3CA	hsa-miR-155-5p	VANGL1
hsa-miR-664b-3p	CAMKK2	hsa-miR-155-5p	CDKN2A	hsa-miR-155-5p	PIK3R1	hsa-miR-155-5p	VAV2
hsa-miR-664b-3p	MAP3K7	hsa-miR-155-5p	CHD8	hsa-miR-155-5p	PPP2R2A	hsa-miR-155-5p	VCAM1
hsa-miR-664b-3p	MAP3K7	hsa-miR-155-5p	CYFIP1	hsa-miR-155-5p	PSEN1	hsa-miR-155-5p	WWC1
hsa-miR-664b-3p	MAPK14	hsa-miR-155-5p	DIAPH3	hsa-miR-155-5p	RAB2A	hsa-miR-20a-5p	ABI2
hsa-miR-664b-3p	PPP2R1B	hsa-miR-155-5p	DOCK1	hsa-miR-155-5p	RAC1	hsa-miR-20a-5p	ABL2
Intracellular Downregulated miRNAs		hsa-miR-155-5p	DOCK4	hsa-miR-155-5p	RAD23B	hsa-miR-20a-5p	ACER2
hsa-miR-155-5p	ABCC4	hsa-miR-155-5p	EDEM3	hsa-miR-155-5p	RAPGEF2	hsa-miR-20a-5p	ACVR1B
hsa-miR-155-5p	AGTR1	hsa-miR-155-5p	ERBIN	hsa-miR-155-5p	RPTOR	hsa-miR-20a-5p	ARHGAP35
hsa-miR-155-5p	ANTXR1	hsa-miR-155-5p	FADD	hsa-miR-155-5p	SEC24B	hsa-miR-20a-5p	ARHGEF7
hsa-miR-155-5p	APAF1	hsa-miR-155-5p	FLNB	hsa-miR-155-5p	SEL1L	hsa-miR-20a-5p	ARPC2
hsa-miR-155-5p	APC	hsa-miR-155-5p	GANAB	hsa-miR-155-5p	SIRT1	hsa-miR-20a-5p	ATG16L1
hsa-miR-155-5p	ASNS	hsa-miR-155-5p	GNA13	hsa-miR-155-5p	SMAD1	hsa-miR-20a-5p	ATP2B1
		hsa-miR-155-5p	HHIP	hsa-miR-155-5p	SMAD2	hsa-miR-20a-5p	BAMBI
		hsa-miR-155-5p	INPP5D	hsa-miR-155-5p	SMAD3	hsa-miR-20a-5p	BCL2
		hsa-miR-155-5p	ITGB4	hsa-miR-155-5p	SOCS1	hsa-miR-20a-5p	BCL2L11
		hsa-miR-155-5p	KMT5A	hsa-miR-155-5p	SP1	hsa-miR-20a-5p	BMP8B
		hsa-miR-155-5p	LPL	hsa-miR-155-5p	SRSF1	hsa-miR-20a-5p	BMPR2

hsa-miR-20a-5p	CASP2	hsa-miR-20a-5p	F2RL3	hsa-miR-20a-5p	MAP2K3	hsa-miR-20a-5p	PFKP
hsa-miR-20a-5p	CAV1	hsa-miR-20a-5p	F3	hsa-miR-20a-5p	MAP3K12	hsa-miR-20a-5p	PHLPP2
hsa-miR-20a-5p	CCL5	hsa-miR-20a-5p	FLNA	hsa-miR-20a-5p	MAP3K14	hsa-miR-20a-5p	PIP4K2A
hsa-miR-20a-5p	CCNB1	hsa-miR-20a-5p	FRMD6	hsa-miR-20a-5p	MAP3K2	hsa-miR-20a-5p	PPP1R12B
hsa-miR-20a-5p	CERS2	hsa-miR-20a-5p	GAB1	hsa-miR-20a-5p	MAP3K3	hsa-miR-20a-5p	PPP2R1A
hsa-miR-20a-5p	CFL2	hsa-miR-20a-5p	GABBR1	hsa-miR-20a-5p	MAP3K5	hsa-miR-20a-5p	PPP3R1
hsa-miR-20a-5p	CNOT4	hsa-miR-20a-5p	GNAS	hsa-miR-20a-5p	MAPK1	hsa-miR-20a-5p	PRKACB
hsa-miR-20a-5p	CNOT6L	hsa-miR-20a-5p	GNB5	hsa-miR-20a-5p	MAPK9	hsa-miR-20a-5p	PRKCB
hsa-miR-20a-5p	CPT1A	hsa-miR-20a-5p	GPAM	hsa-miR-20a-5p	MAPKAPK5	hsa-miR-20a-5p	PRKG1
hsa-miR-20a-5p	CREB1	hsa-miR-20a-5p	GRK3	hsa-miR-20a-5p	MAVS	hsa-miR-20a-5p	PTEN
hsa-miR-20a-5p	CRK	hsa-miR-20a-5p	HSPA8	hsa-miR-20a-5p	MCL1	hsa-miR-20a-5p	PTGES3
hsa-miR-20a-5p	CSNK1A1	hsa-miR-20a-5p	IFNAR1	hsa-miR-20a-5p	MDM2	hsa-miR-20a-5p	RAN
hsa-miR-20a-5p	CYCS	hsa-miR-20a-5p	IL17RC	hsa-miR-20a-5p	MFN1	hsa-miR-20a-5p	RB1CC1
hsa-miR-20a-5p	CYLD	hsa-miR-20a-5p	IRAK4	hsa-miR-20a-5p	MKNK2	hsa-miR-20a-5p	RBL1
hsa-miR-20a-5p	DNAJC10	hsa-miR-20a-5p	ITCH	hsa-miR-20a-5p	MYC	hsa-miR-20a-5p	RBL2
hsa-miR-20a-5p	DNM1L	hsa-miR-20a-5p	ITGA2	hsa-miR-20a-5p	MYH9	hsa-miR-20a-5p	RGMB
hsa-miR-20a-5p	DNMT1	hsa-miR-20a-5p	ITGB1	hsa-miR-20a-5p	MYLK3	hsa-miR-20a-5p	RPL14
hsa-miR-20a-5p	DUSP2	hsa-miR-20a-5p	ITGB8	hsa-miR-20a-5p	NBL1	hsa-miR-20a-5p	RPL17
hsa-miR-20a-5p	E2F2	hsa-miR-20a-5p	JAK1	hsa-miR-20a-5p	NCOR2	hsa-miR-20a-5p	RPL21
hsa-miR-20a-5p	E2F3	hsa-miR-20a-5p	KMT2B	hsa-miR-20a-5p	NUP188	hsa-miR-20a-5p	RPL31
hsa-miR-20a-5p	E2F5	hsa-miR-20a-5p	LAMC1	hsa-miR-20a-5p	OCRL	hsa-miR-20a-5p	RPS27
hsa-miR-20a-5p	EGLN3	hsa-miR-20a-5p	LDHB	hsa-miR-20a-5p	ORAI2	hsa-miR-20a-5p	RPS6KA5
hsa-miR-20a-5p	EIF2S1	hsa-miR-20a-5p	LIMK1	hsa-miR-20a-5p	PAFAH1B1	hsa-miR-20a-5p	RRAGD
hsa-miR-20a-5p	ELK4	hsa-miR-20a-5p	LPAR2	hsa-miR-20a-5p	PDHB	hsa-miR-20a-5p	RRM2
hsa-miR-20a-5p	ELOC	hsa-miR-20a-5p	MAD1L1	hsa-miR-20a-5p	PDPK1	hsa-miR-20a-5p	RUNX1
hsa-miR-20a-5p	EREG	hsa-miR-20a-5p	MAGOHB	hsa-miR-20a-5p	PFKFB2	hsa-miR-20a-5p	SCD
hsa-miR-20a-5p	F2R	hsa-miR-20a-5p	MAN1C1			hsa-miR-20a-5p	SESN1

hsa-miR-20a-5p	SESN2	hsa-miR-20a-5p	XIAP	hsa-miR-7704	ORAI1	hsa-miR-146b-5p	PDGFRA
hsa-miR-20a-5p	SESN3	hsa-miR-20a-5p	YOD1	hsa-miR-7704	ORAI2	hsa-miR-146b-5p	PMAIP1
hsa-miR-20a-5p	SGMS1	hsa-miR-20a-5p	YWHAZ	hsa-miR-7704	OXTR	hsa-miR-146b-5p	RHOA
hsa-miR-20a-5p	SIRPA	hsa-miR-20a-5p	ZMAT3	hsa-miR-7704	P2RX1	hsa-miR-146b-5p	SFRP1
hsa-miR-20a-5p	SMAD4	Exosomal Upregulated miRNAs		hsa-miR-7704	P2RX3	hsa-miR-146b-5p	TLR4
hsa-miR-20a-5p	SMAD5	hsa-miR-7704	ADRA1A	hsa-miR-7704	P2RX6	hsa-miR-146b-5p	TRAF6
hsa-miR-20a-5p	SOC5	hsa-miR-7704	CACNA1A	hsa-miR-7704	PDGFRA	hsa-miR-146b-5p	ZNRF3
hsa-miR-20a-5p	SOD2	hsa-miR-7704	CACNA1C	hsa-miR-7704	PHKA2	hsa-miR-155-5p	AGTR1
hsa-miR-20a-5p	SPOPL	hsa-miR-7704	CACNA1E	hsa-miR-7704	PLCD3	hsa-miR-155-5p	APAF1
hsa-miR-20a-5p	SQSTM1	hsa-miR-7704	CACNA1H	hsa-miR-7704	PLCD4	hsa-miR-155-5p	APC
hsa-miR-20a-5p	STAT3	hsa-miR-7704	CAMK1D	hsa-miR-7704	PLCE1	hsa-miR-155-5p	ATP6V1C1
hsa-miR-20a-5p	STX4	hsa-miR-7704	CHRM2	hsa-miR-7704	PPIF	hsa-miR-155-5p	BCL6
hsa-miR-20a-5p	TBL1XR1	hsa-miR-7704	CHRM3	hsa-miR-7704	PRKCB	hsa-miR-155-5p	CAB39L
hsa-miR-20a-5p	TCF7L2	hsa-miR-7704	EGFR	hsa-miR-7704	SLC8A2	hsa-miR-155-5p	CASP3
hsa-miR-20a-5p	TGFBR1	hsa-miR-7704	GNAL	hsa-miR-7704	TACR3	hsa-miR-155-5p	CBL
hsa-miR-20a-5p	THBS1	hsa-miR-7704	GRIN1	hsa-miR-7704	TBXA2R	hsa-miR-155-5p	CCND1
hsa-miR-20a-5p	THEM4	hsa-miR-7704	GRIN2C	hsa-miR-7704	TNNC2	hsa-miR-155-5p	CD36
hsa-miR-20a-5p	TNFRSF10B	hsa-miR-7704	GRIN2D	hsa-miR-7704	TPCN1	hsa-miR-155-5p	CDK2
hsa-miR-20a-5p	TP53	hsa-miR-7704	GRM5	hsa-miR-7704	TPCN2	hsa-miR-155-5p	CDKN1B
hsa-miR-20a-5p	TRAF3IP2	hsa-miR-7704	HTR4	Exosomal Downregulated miRNAs		hsa-miR-155-5p	CDKN2A
hsa-miR-20a-5p	TXNIP	hsa-miR-7704	HTR6	hsa-miR-146b-5p	AKT3	hsa-miR-155-5p	CHD8
hsa-miR-20a-5p	ULK1	hsa-miR-7704	ITPKC	hsa-miR-146b-5p	CASR	hsa-miR-155-5p	CLTC
hsa-miR-20a-5p	VDAC1	hsa-miR-7704	ITPR2	hsa-miR-146b-5p	CDKN1A	hsa-miR-155-5p	CYFIP1
hsa-miR-20a-5p	VEGFA	hsa-miR-7704	MCOLN1	hsa-miR-146b-5p	EGFR	hsa-miR-155-5p	DIAPH3
hsa-miR-20a-5p	WASL	hsa-miR-7704	MCOLN2	hsa-miR-146b-5p	KIT	hsa-miR-155-5p	DOCK1
hsa-miR-20a-5p	WEE1	hsa-miR-7704	NOS1	hsa-miR-146b-5p	MYLK	hsa-miR-155-5p	DOCK4
hsa-miR-20a-5p		hsa-miR-7704	NTSR1	hsa-miR-146b-5p	PARD6B	hsa-miR-155-5p	EDEM3

hsa-miR-155-5p	ERBIN	hsa-miR-155-5p	NCKAP1	hsa-miR-155-5p	RPTOR	hsa-miR-155-5p	TJP1
hsa-miR-155-5p	FADD	hsa-miR-155-5p	NFKB1	hsa-miR-155-5p	SEC24B	hsa-miR-155-5p	TRAM1
hsa-miR-155-5p	GANAB	hsa-miR-155-5p	PDK1	hsa-miR-155-5p	SEL1L	hsa-miR-155-5p	UBE2D3
hsa-miR-155-5p	GNA13	hsa-miR-155-5p	PIK3CA	hsa-miR-155-5p	SIRT1	hsa-miR-155-5p	UBE2G1
hsa-miR-155-5p	HHIP	hsa-miR-155-5p	PIK3R1	hsa-miR-155-5p	SMAD1	hsa-miR-155-5p	UBQLN1
hsa-miR-155-5p	INPP5D	hsa-miR-155-5p	PPP2R2A	hsa-miR-155-5p	SMAD2	hsa-miR-155-5p	UBQLN2
hsa-miR-155-5p	ITGB4	hsa-miR-155-5p	PSEN1	hsa-miR-155-5p	SMAD3	hsa-miR-155-5p	VANGL1
hsa-miR-155-5p	LPL	hsa-miR-155-5p	RAB2A	hsa-miR-155-5p	SOCS1	hsa-miR-155-5p	VAV2
hsa-miR-155-5p	MAN1A2	hsa-miR-155-5p	RAC1	hsa-miR-155-5p	SP1	hsa-miR-155-5p	VCAM1
hsa-miR-155-5p	MTAP	hsa-miR-155-5p	RAD23B	hsa-miR-155-5p	SSH2	hsa-miR-155-5p	WWC1
hsa-miR-155-5p	MYB	hsa-miR-155-5p	RAPGEF2	hsa-miR-155-5p	STAG2		

4.5.4. Gene Ontology Categorization of Predicted Target Genes of Differentially Expressed miRNAs

Genes from each of the 4 groups were used as input for gene ontology (GO) Enrichment Analysis to obtain their enriched GO terms within each category of biological process (BP), molecular function (MF) and cellular component (CC). Data were selectively chosen for graphs to assist in visualization. More extensive GO Enrichment data was included in **Appendix section 8.4**.

In intracellular upregulated miRNA target genes, the terms “regulation of protein export from nucleus (GO:0046825)”, “positive regulation of nucleocytoplasmic transport (GO:0046824)”, “stress-activated protein kinase signaling cascade (GO:0031098)”, “regulation of nucleocytoplasmic transport (GO:0046822)” and “positive regulation of intracellular protein transport (GO:0090316)” were most highly enriched. These results indicated the function of target genes mostly focused on intracellular transport of proteins and stress-activated signaling cascades (**Figure 4.5-9**). In intracellular downregulated miRNA target genes, the most highly enriched terms included “SMAD protein complex assembly (GO:0007183)”, “stress-induced premature senescence (GO:0090400)”, “‘de novo’ pyrimidine nucleobase biosynthetic process (GO:0006207)”, “positive regulation of Arp2/3 complex-mediated actin nucleation (GO:2000601)”, “positive regulation of ER-associated ubiquitin-dependent protein catabolic process (GO:1903071)” and “regulation of vascular associated smooth muscle cell apoptotic process (GO:1905459)”. Together with other enriched terms, target genes of the downregulated miRNAs were highly involved in signaling cascades of distinct pathways such as the SMAD, PI3K, MAPK, UPP and apoptotic pathways (**Figure 4.5-10**).

Enrichment analysis for the group of exosomal upregulated miRNAs did not yield significant results therefore could not be reported. However, target genes were still categorized into

BP, MF and CC accordingly. Target genes were involved in a variety of cellular processes and catalytic activities, particularly localizing at membrane and extracellular regions (**Figure 4.5-11**). On the other hand, from the exosomal downregulated miRNA target genes, most enriched terms were “negative regulation of interleukin-23 production (GO:0032707)”, “negative regulation of cardiac muscle tissue regeneration (GO:1905179)”, “SMAD protein complex assembly (GO:0007183)”, “positive regulation of Arp2/3 complex-mediated actin nucleation (GO:2000601)” and “positive regulation of vascular endothelial cell proliferation (GO:1905564)”. These results suggested that target genes might participate in the regulatory pathways of multiple cell types (**Figure 4.5-12**).

Lastly, as *hsa-miR-155-5p* was downregulated in both intracellular and exosomal senescent samples, a separate GO Enrichment analysis for *hsa-miR-155-5p* was performed for further inspection. Among the most enriched terms for biological processes were “organelle organization”, “anatomical structure morphogenesis”, negative regulation of transcription by RNA polymerase II” and “cell cycle arrest”. Most enriched molecular functions were “enzyme binding”, “protein binding” and transcription factor binding”, at the cellular components of “intracellular membrane-bounded organelles”, “cytoplasm” and “nucleoplasm”. Overall, the gene ontology categorization of preliminary predicted target genes suggested association to various pathways, regulating intracellular transport, cell cycle, cellular senescence as well as cell survival and escape from apoptosis.

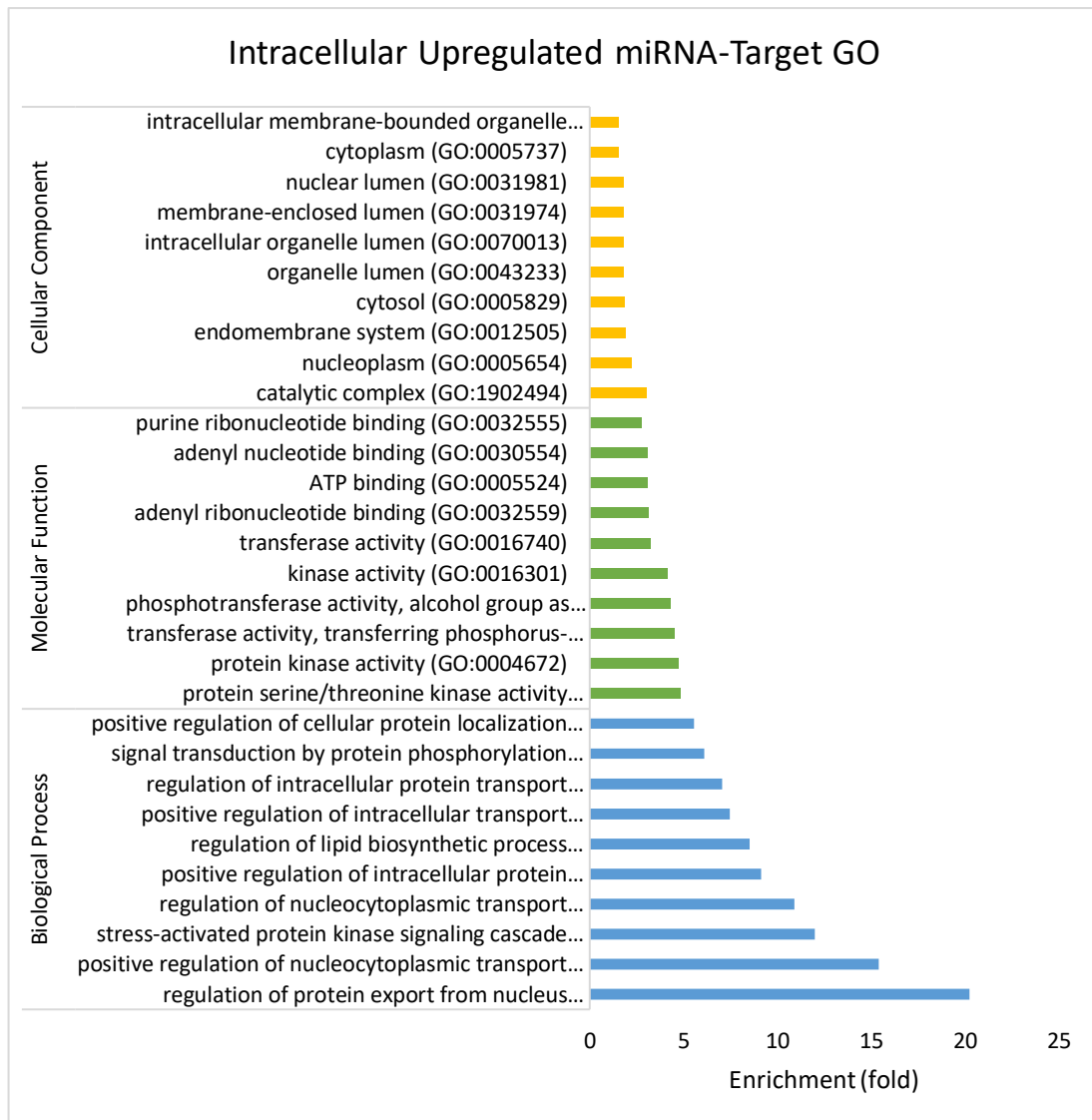


Figure 4.5-9: GO Enrichment Analysis of target genes of intracellular upregulated miRNAs. Top 10 most enriched terms were chosen for target genes of *hsa-miR-664a-3p*, *hsa-miR-664a-5p*, *hsa-miR-664b-3p* and *hsa-miR-4485-3p*. The terms “regulation of protein export from nucleus”, “positive regulation of nucleocytoplasmic transport”, “stress-activated protein kinase signaling cascade”, “regulation of nucleocytoplasmic transport” and “positive regulation of intracellular protein transport” were most highly enriched. Term enrichment highlighted association of target genes with the regulation of cellular metabolism and stress response.

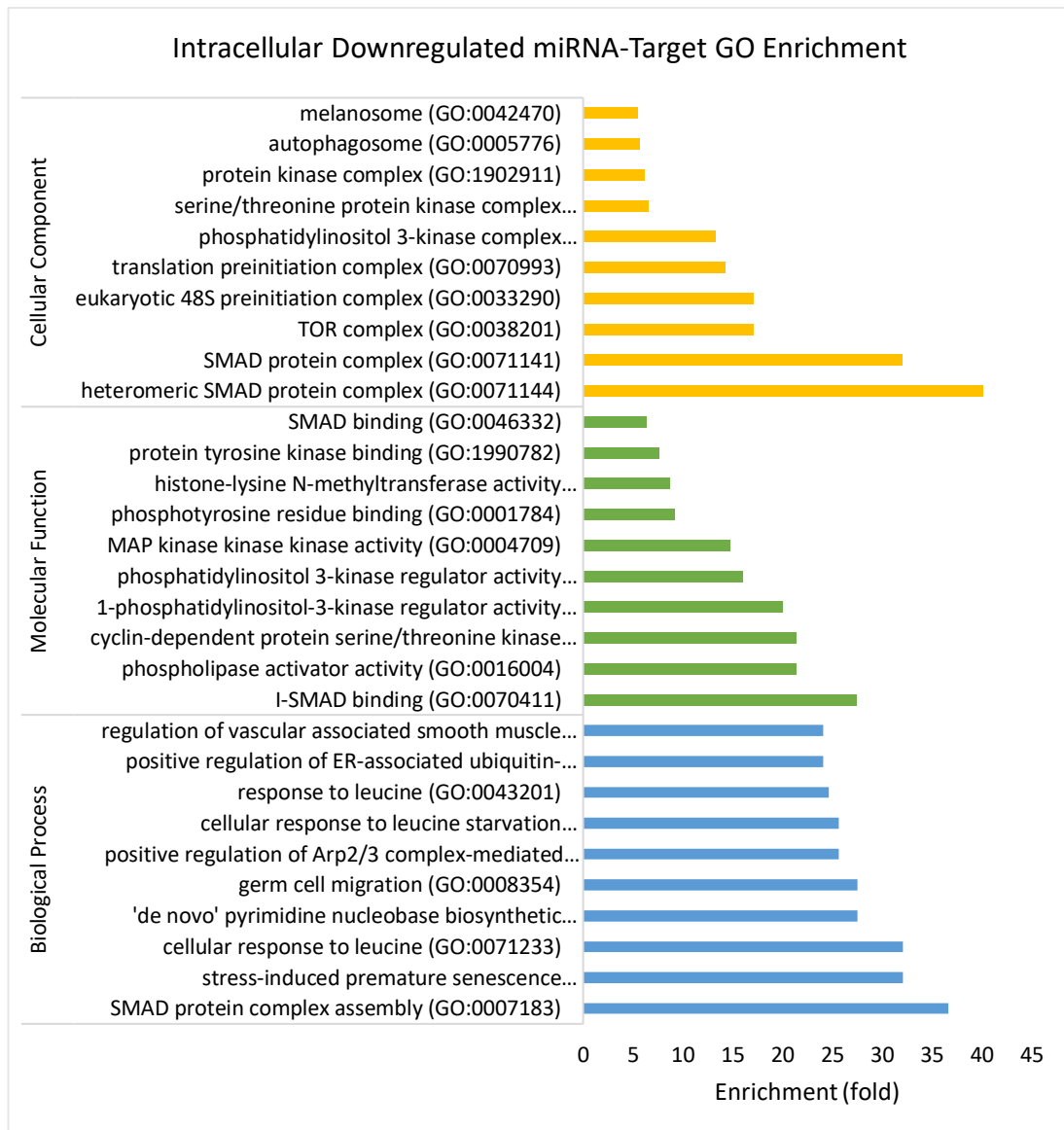


Figure 4.5-10: GO Enrichment Analysis of target genes of intracellular downregulated miRNAs. Top 10 most enriched terms were chosen for target genes of *hsa-miR-20a-5p* and *hsa-miR-155-5p*. The most highly enriched terms included “SMAD protein complex assembly”, “positive regulation of Arp2/3 complex-mediated actin nucleation”, “positive regulation of ER-associated ubiquitin-dependent protein catabolic process” and “regulation of vascular associated smooth muscle cell apoptotic process”. Together with other enriched terms, target genes of the downregulated miRNAs were highly involved in signaling cascades of major pathways such as the PI3K/Akt/mTOR, Smad/TGF- β , MAPK and unfolded protein response signaling pathways.

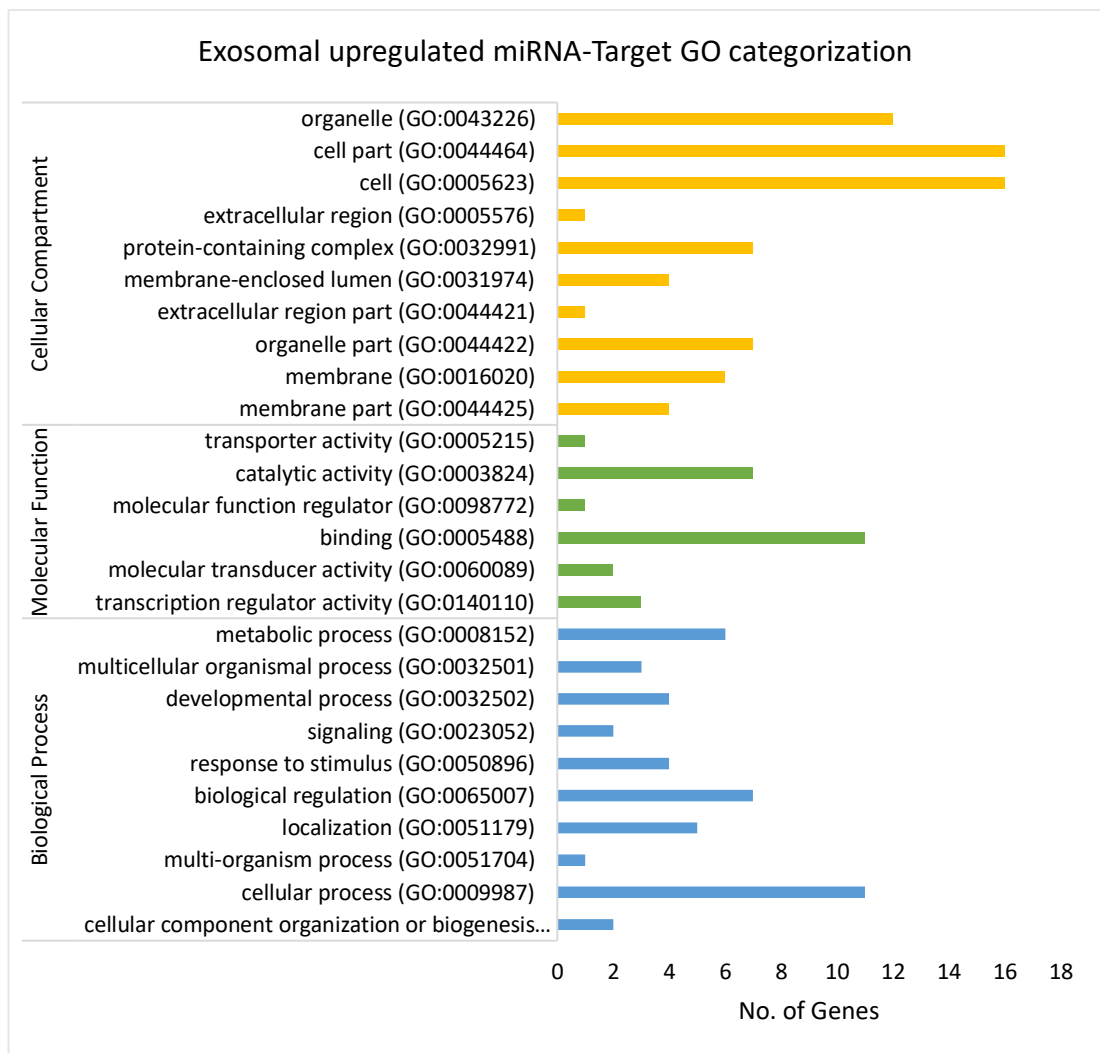


Figure 4.5-11: GO Categorization of target genes of upregulated exosomal *hsa-miR-7704*. Categorized target genes participated main in cellular metabolism and signal transduction, localizing at the extracellular and membranal regions of the cells.

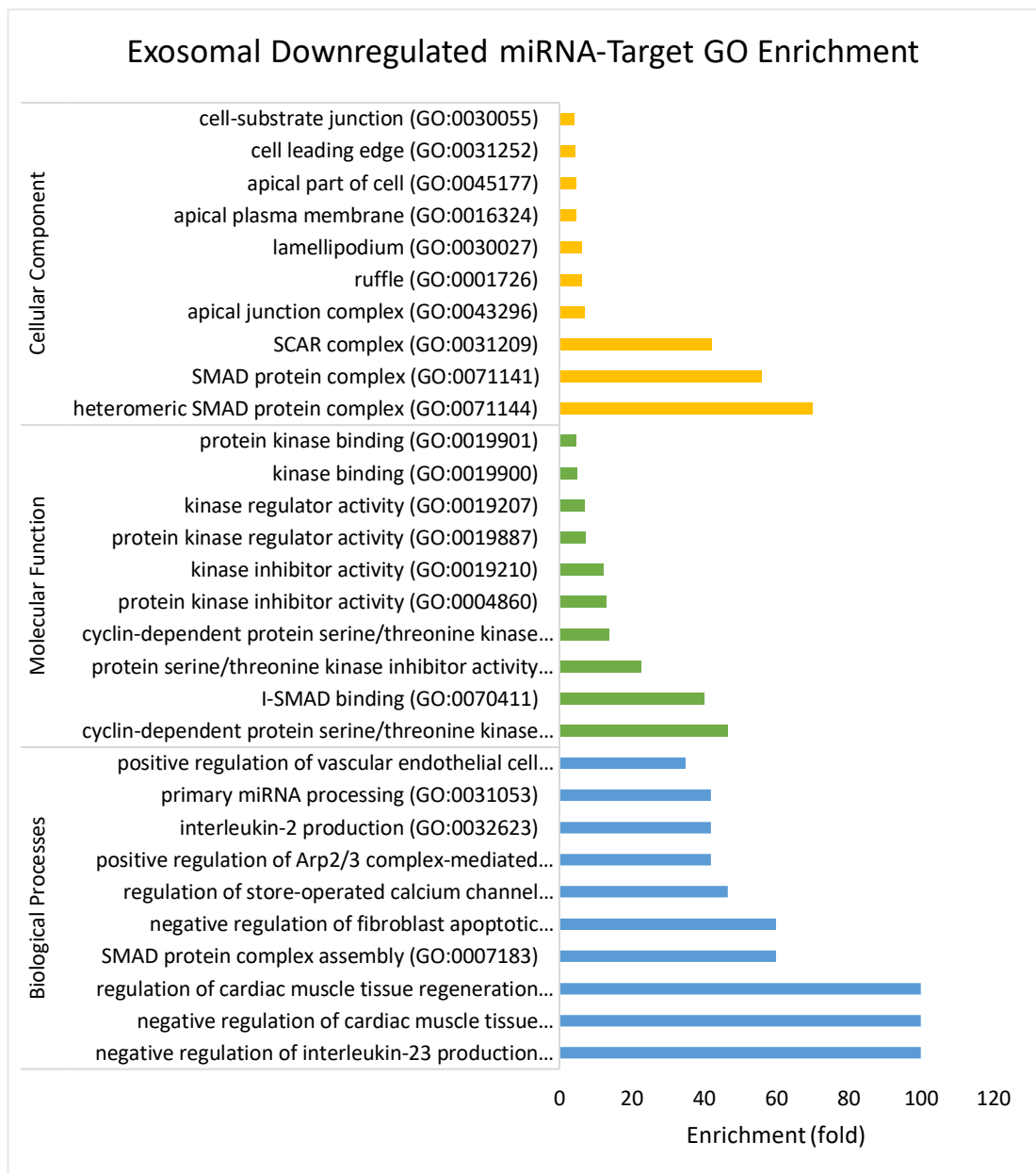


Figure 4.5-12: GO Enrichment Analysis of gene targets of exosomal downregulated miRNAs. Top 10 most enriched terms were chosen for target genes of *hsa-miR-146b-5p* and *hsa-miR-155-5p*. The most enriched terms were “negative regulation of interleukin-23 production”, “negative regulation of cardiac muscle tissue regeneration”, “SMAD protein complex assembly”, “positive regulation of Arp2/3 complex-mediated actin nucleation” and “positive regulation of vascular endothelial cell proliferation”. These results suggested that target genes might participate in the regulatory pathways of both VSMCs and endothelial cells.

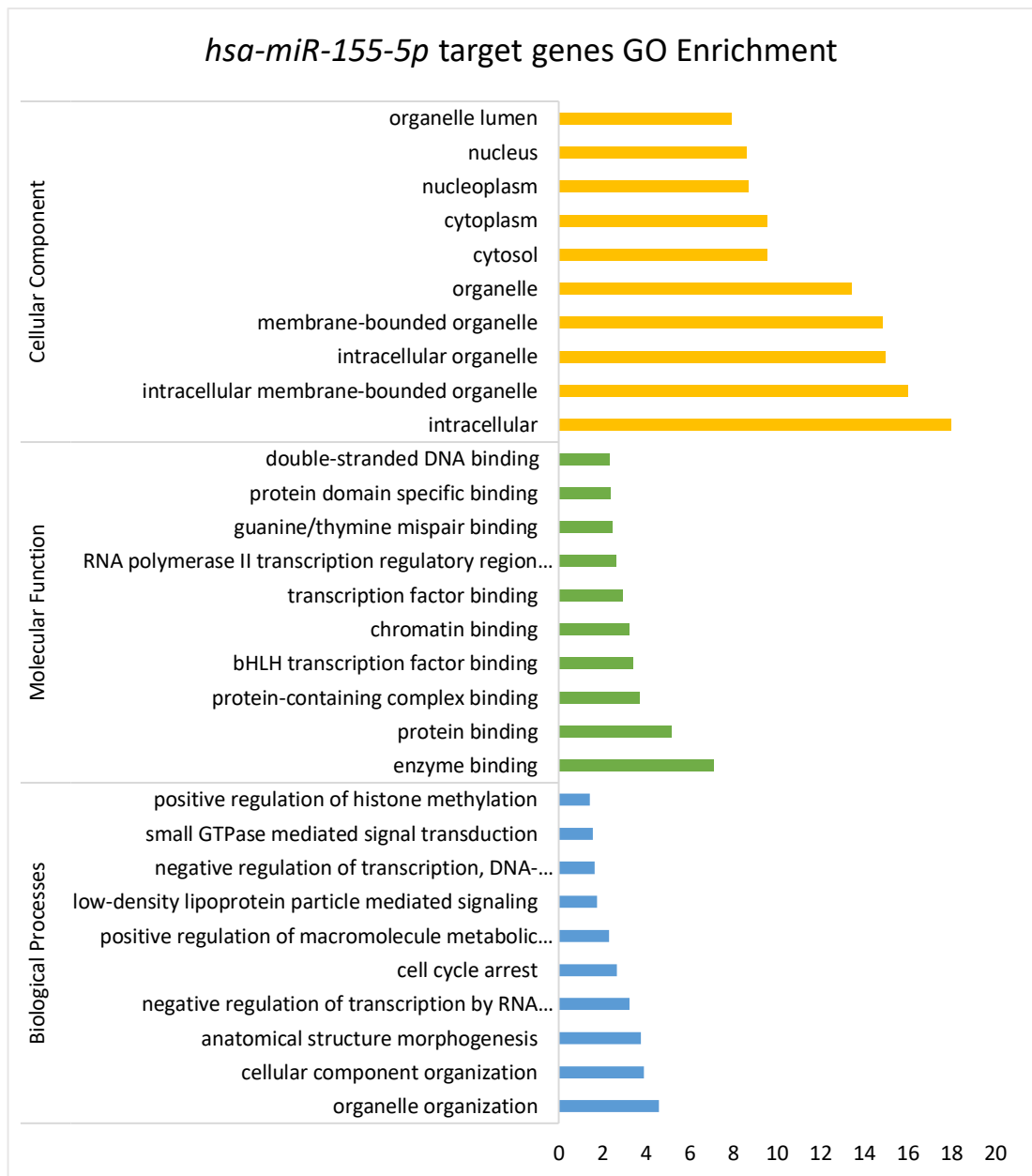
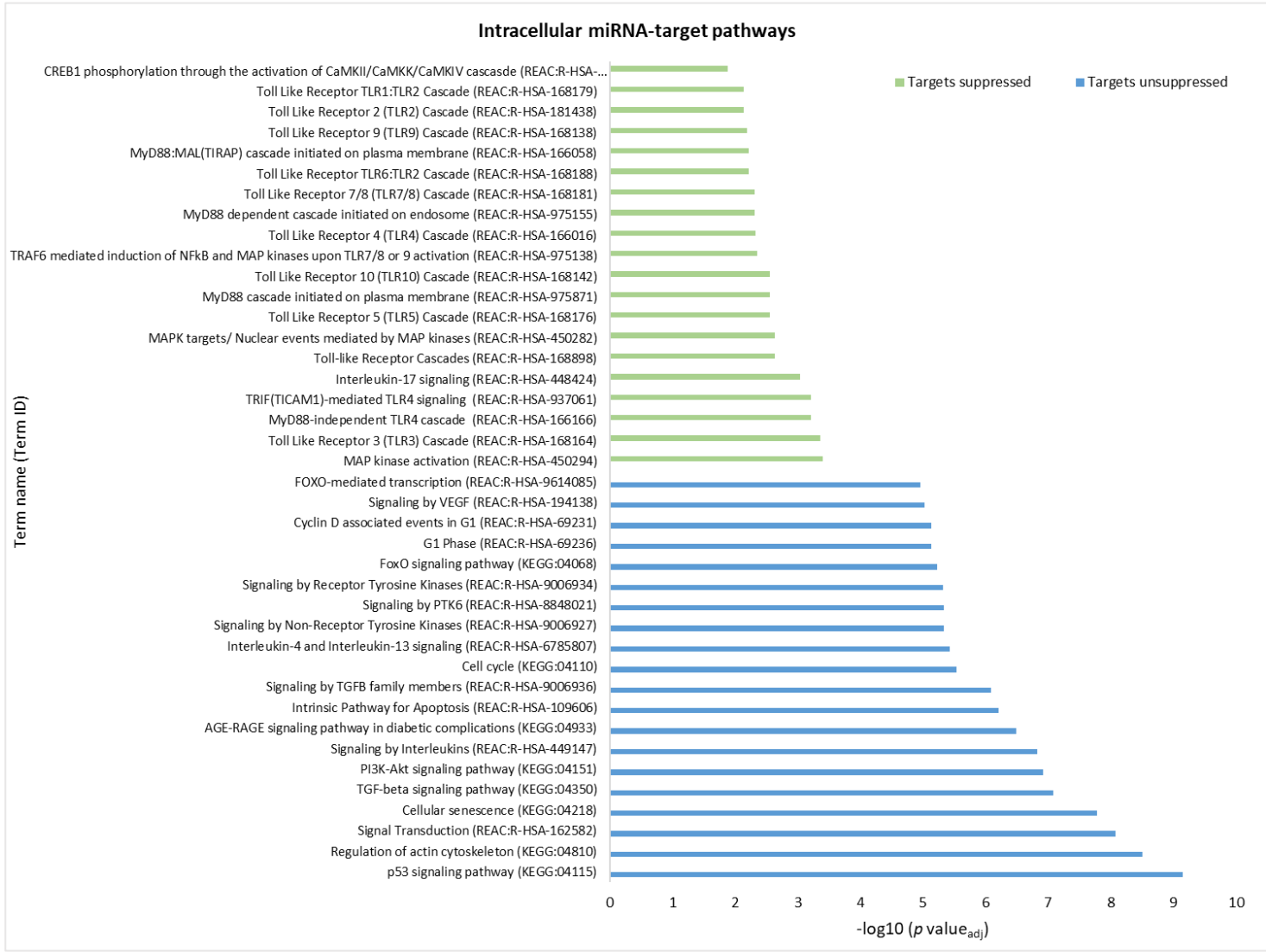


Figure 4.5-13: GO Enrichment analysis of the target genes of *hsa-miR-155-5p*. GO terms that were significantly enriched involved in the cytoskeletal arrangements within the cell, negative regulation of transcription activities and cell cycle arrest. Only top 10 GO terms for each category were selected for graph presentation.

4.5.5. Pathway Analysis of Predicted Targets of Differentially Expressed miRNAs

Pathway analysis from KEGG and Reactome database showed enriched terms in all groups. In intracellular samples, Toll-like receptor signaling cascades, MAPK and interleukin 17 (IL-17) signaling pathways were enriched as a result of gene expression suppression by upregulated miRNAs. Meanwhile, unsuppressed genes due to downregulated miRNAs led to higher enrichment of multiple pathways regulating cell cycle progression, cellular senescence, interleukin 4 (IL-4), interleukin 13 (IL-13) and PI3K/TGF- β signaling pathways (**Figure 4.5-14**).

For exosomal upregulated miRNA targets, calcium signaling pathway was the only enriched pathway. However, unsuppressed genes due to downregulated exosomal miRNAs resulted in enrichment of various key signaling pathways, including cellular senescence, PI3K/Akt/TGF- β , ErbB, p53 signaling pathways, VEGF signaling and actin cytoskeleton regulating pathways (**Figure 4.5-15**).



(next page)

Figure 4.5-14: Most enriched pathways associated with target genes of intracellular miRNAs. Both target genes suppressed by upregulated miRNAs (green) and targets unsuppressed due to downregulated miRNAs (blue) in intracellular samples were presented. Intracellular suppressed target genes were associated with the Toll-like receptor and MAPK signaling cascades while unsuppressed target genes were associated with a wider range of pathways, including cellular senescence, cell cycle, TGF- β , PI3K/Akt/FOXO and apoptotic signaling pathways.

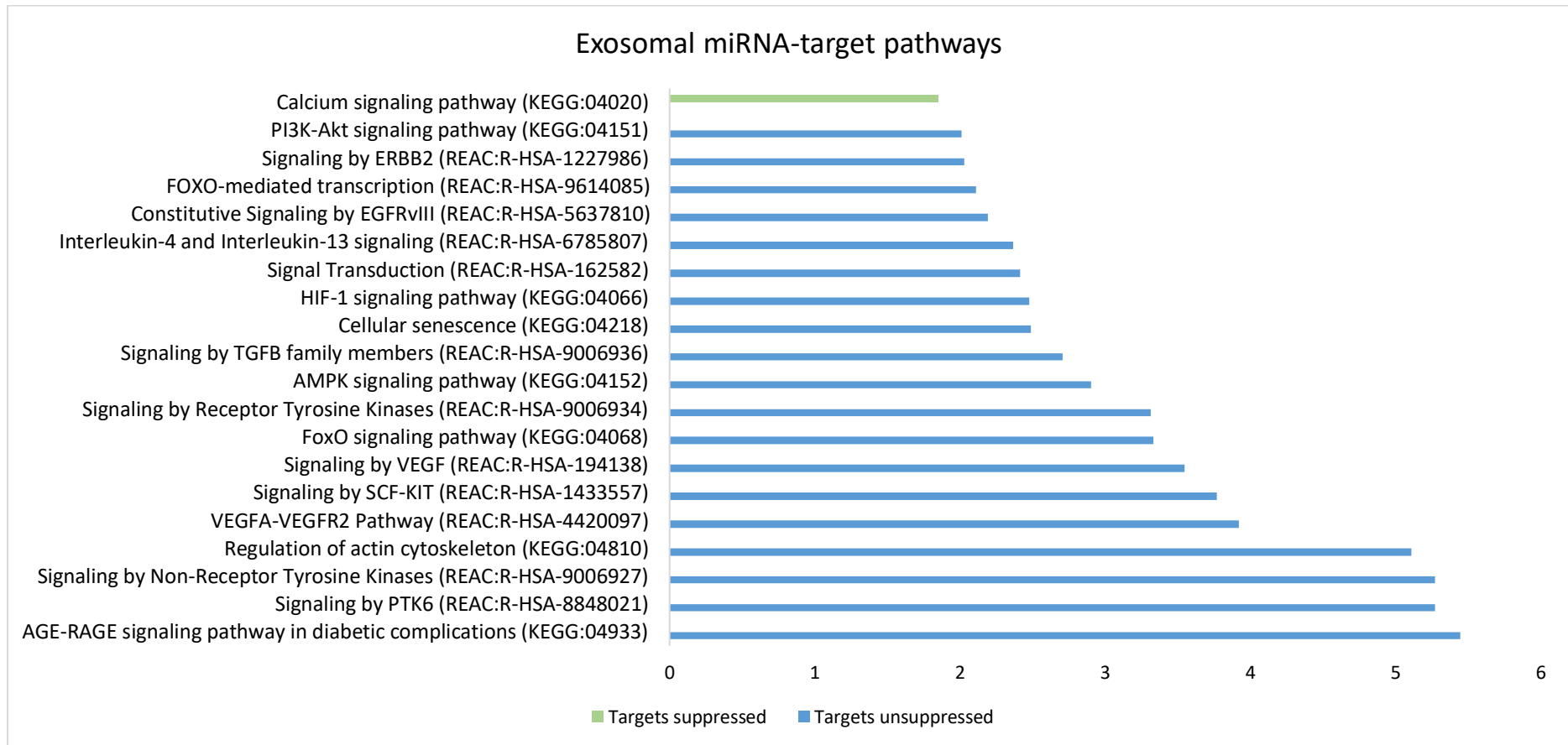


Figure 4.5-15: Most enriched pathways associated with target genes of exosomal miRNAs. The target genes suppressed by upregulated miRNAs (green) were associated with the calcium signaling pathway while target genes unsuppressed due to downregulated miRNAs (blue) were associated with the enrichment of various key signaling pathways, including cellular senescence, PI3K/Akt/TGF- β , VEGF and actin cytoskeleton regulating signaling pathways.

4.5.6. Regulatory Interaction Network of Differentially Expressed miRNAs and Their Target Genes

4.5.6.1. MiRNA-target Gene Interaction Networks

The miRNA-target gene interaction networks were constructed based on the KEGG and GO enrichment analyses. Only validated target genes that participated in the significantly enriched pathways were used to map the miRNA-RNA interaction network ($p < 0.05$). Among the validated target genes, those that were found to be more commonly involved in all the enriched pathways were highlighted for further investigation.

As such, in the intracellular downregulated miRNA-mRNA network, the target genes PIK3R1, RAC1, PIK3CA, CDKN1B, MAPK1, CDKN1A and TP53 shared the highest number of associated enriched pathways (**Figure 4.5-16**). These genes were found to participate in pathways regulating cell cycle, cellular senescence, TGF- β signaling, PI3K/Akt signaling and actin cytoskeleton. Meanwhile, in the intracellular upregulated miRNA-mRNA network, the target genes MAPK8, RPS6KA5, CREB1, MAP3K7, PPP2R1B and MAPK14 shared the highest number of associated enriched pathways (**Figure 4.5-17**). These genes were involved in MAP kinase activation and Toll-like receptor (TLR) signaling cascades, such as TLR3 cascade, MyD88-independent TLR4 cascade and TRIF-mediated TLR4 signaling.

In the exosomal downregulated miRNA-RNA network, the target genes AKT3, RHOA, EGFR, PIK3CA, PIK3R1, CDKN1B, RAC1 and CCND1 shared the highest number of associated enriched pathways (**Figure 4.5-18**). These genes were highly involved in VEGFA-VEGFR2 signaling pathway, cellular senescence, signaling by protein tyrosin kinase 6 (PTK6), interleukin signaling and cell cycle regulation. Lastly, in the exosomal upregulated miRNA-mRNA network, despite the interaction with validated target genes, only one gene, NTSR1, was involved in the enriched calcium signaling pathway pathway (**Figure 4.5-19**).

Nevertheless, the limited records and annotations associated with the exosomal upregulated hsa-miR-7704 provided opportunities for novel discovery of its intercellular regulation.

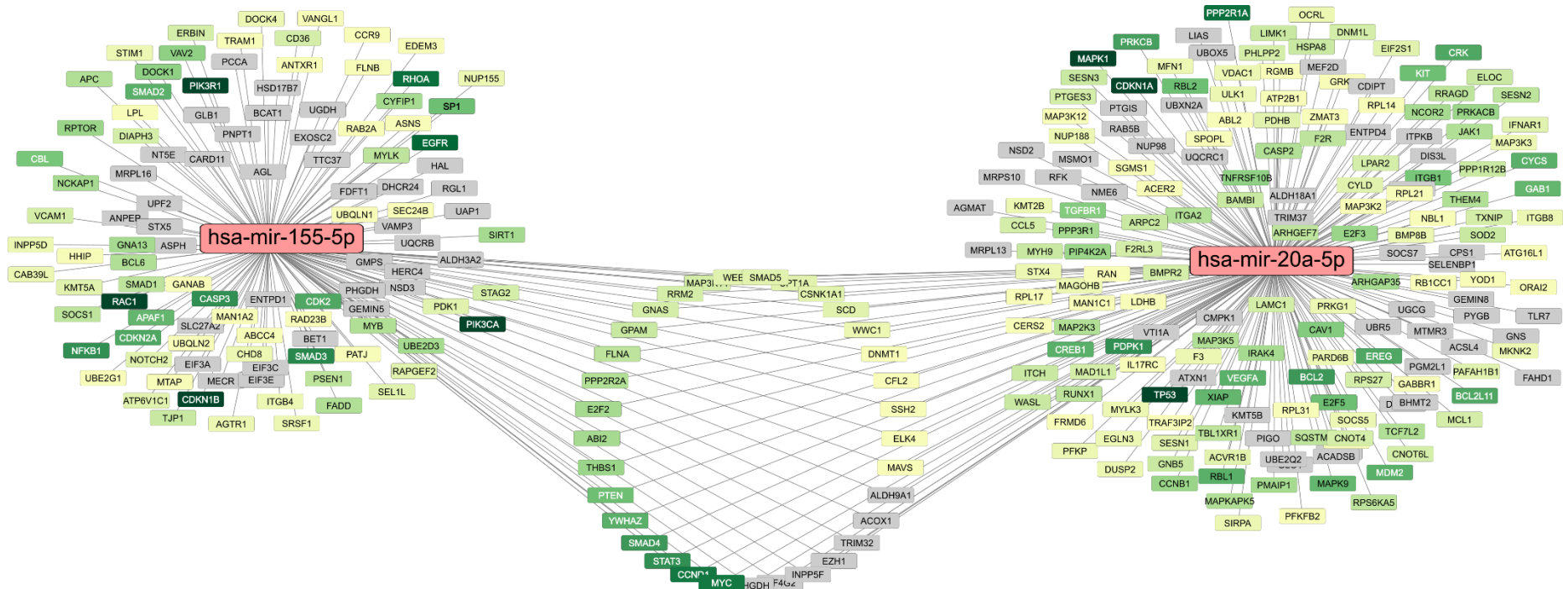


Figure 4.5-16: miRNA-mRNA target interaction network of downregulated intracellular *miR-155-5p* and *miR-20a-5p*. Target genes associated with a higher number of enriched pathways were colored in darker shades of green. Grey target genes belonged to the validated miRNA target genes but did not participate in enriched pathways. The genes PIK3R1, RAC1, PIK3CA, CDKN1B, MAPK1, CDKN1A and TP53 shared the highest number of associated enriched pathways.

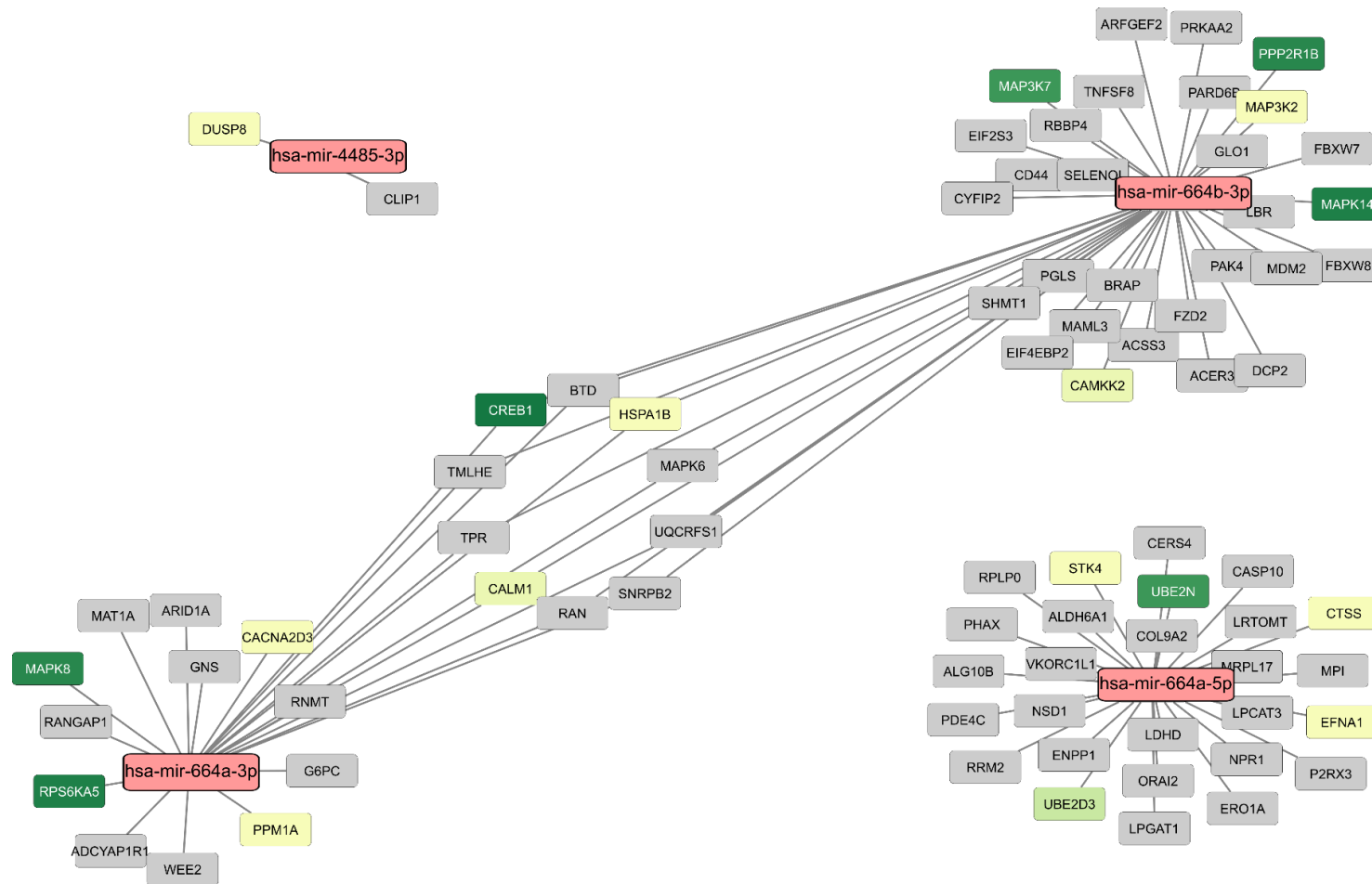


Figure 4.5-17: miRNA-RNA target interaction network of upregulated intracellular miRNAs. Target genes associated with a higher number of enriched pathways were colored in darker shades of green. Grey target genes belonged to the validated miRNA target genes but did not participate in enriched pathways. The genes MAPK8, RPS6KA5, CREB1, MAP3K7, PPP2R1B and MAPK14 shared the highest number of associated enriched pathways.

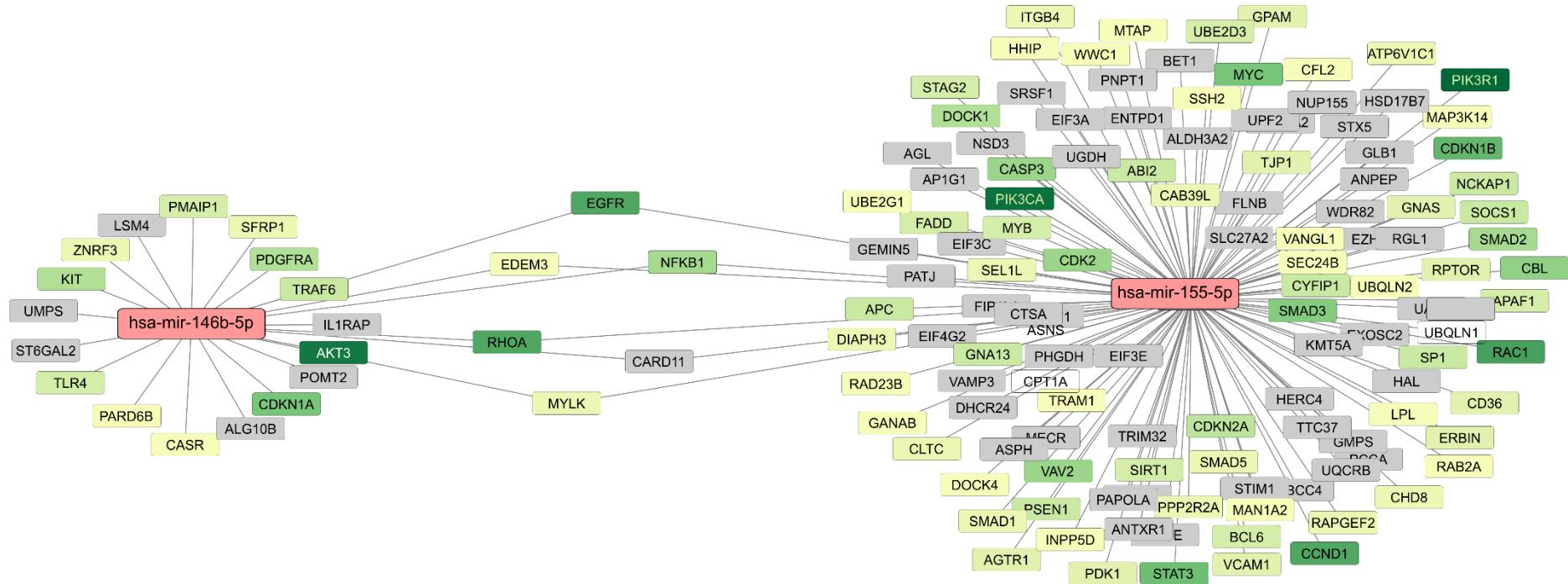


Figure 4.5-18: miRNA-RNA target interaction network of downregulated exosomal miRNAs. Target genes associated with a higher number of enriched pathways were colored in darker shades of green. Grey target genes belonged to the validated miRNA target genes but did not participate in enriched pathways. The genes AKT3, RHOA, EGFR, PIK3CA, PIK3R1, CDKN1B, RAC1 and CCND1 shared the highest number of associated enriched pathways.

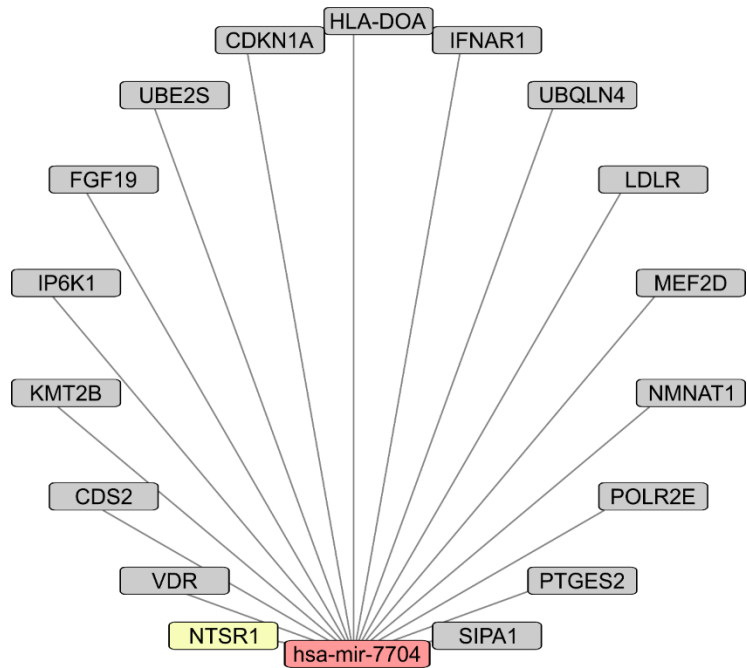


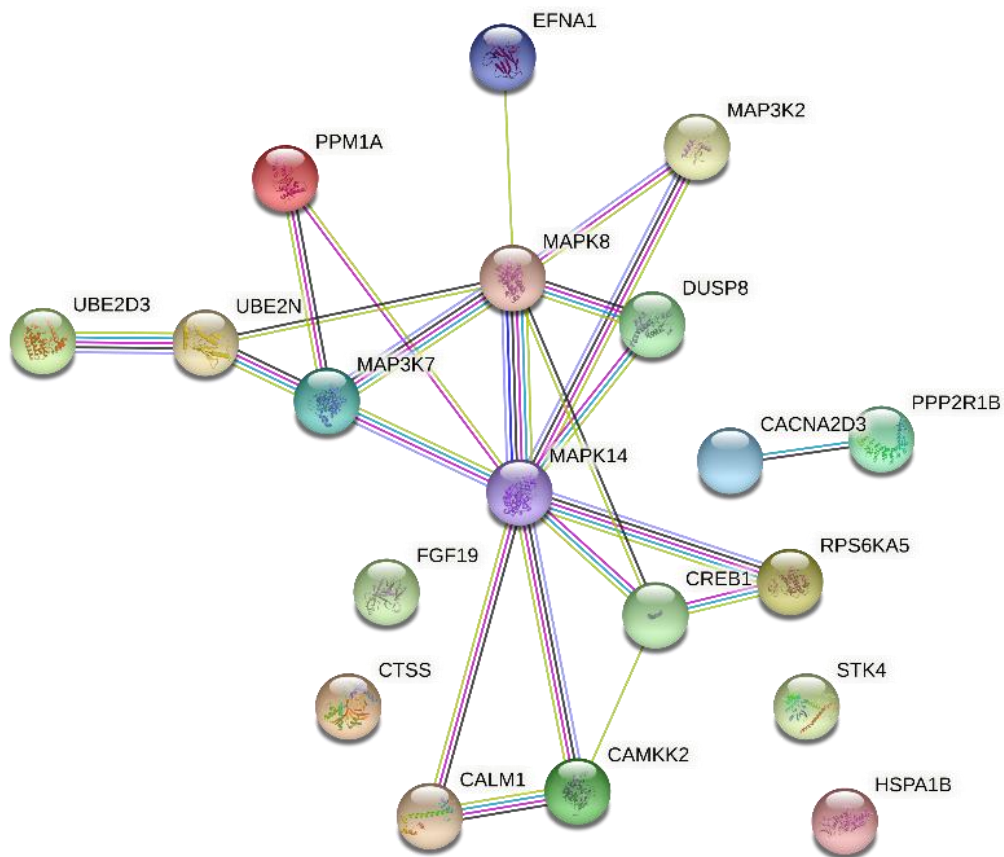
Figure 4.5-19: miRNA-RNA target interaction network of upregulated exosomal *hsa-miR-7704*. *Hsa-miR-7704* was not well-characterized. Despite the interaction with validated target genes, only one gene, *NTSR1*, was involved in an enriched pathway.

4.5.6.2. Protein-protein Interaction Network

Protein-protein interaction (PPI) networks were generated in order to visualize the genes biological functions and their association with each other if they were to be translated and expressed. In **Figure 4.5-20**, PPI network of significantly enriched target genes of intracellular upregulated miRNAs was analysed. Their activity was most strongly linked to cellular 'stress response', 'serine/threonine-protein kinase', 'protein phosphatase', 'biological rhythms' and 'magnesium' based on their annotations.

Meanwhile, PPI network of significantly enriched target genes of intracellular downregulated miRNAs showed regulation of cellular senescence and survival. Majority of protein (in red) were associated with promotion of cell survival, thus might play a role in senescent hVSMC acquired resistance to apoptosis (**Figure 4.5-21**).

Lastly, PPI network of significantly enriched target genes of exosomal downregulated miRNAs also showed association with cell survival. Proteins (in red) were found to regulate cellular senescence, with active PI3K/Akt signaling that promoted cell survival, which might also contribute to senescent hVSMC acquired resistance to apoptosis (**Figure 4.5-22**).



Nodes:

Network nodes represent proteins

splice isoforms or post-translational modifications are collapsed, i.e. each node represents all the proteins produced by a single, protein-coding gene locus.

Node Color

-  *colored nodes: query proteins and first shell of interactors*
-  *white nodes: second shell of interactors*

Node Content

-  *empty nodes: proteins of unknown 3D structure*
-  *filled nodes: some 3D structure is known or predicted*

Edges:

Edges represent protein-protein associations

associations are meant to be specific and meaningful, i.e. proteins jointly contribute to a shared function; this does not necessarily mean they are physically binding each other.

Known Interactions

-  *from curated databases*
-  *experimentally determined*

Predicted Interactions

-  *gene neighborhood*
-  *gene fusions*
-  *gene co-occurrence*

Others

-  *textmining*
-  *co-expression*
-  *protein homology*

Figure 4.5-20: PPI network of significantly enriched target genes of intracellular upregulated miRNAs. Although the proteins were not tightly connected to each other, their activity was most strongly linked to cellular ‘stress response’ based on their annotations.

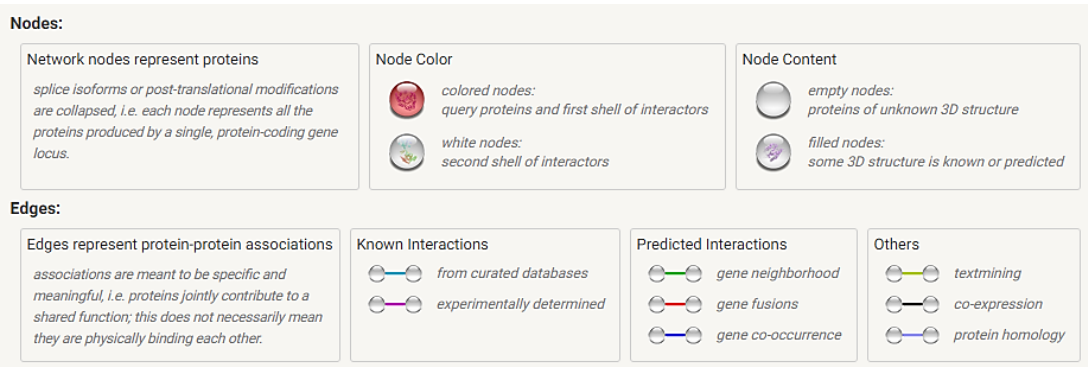
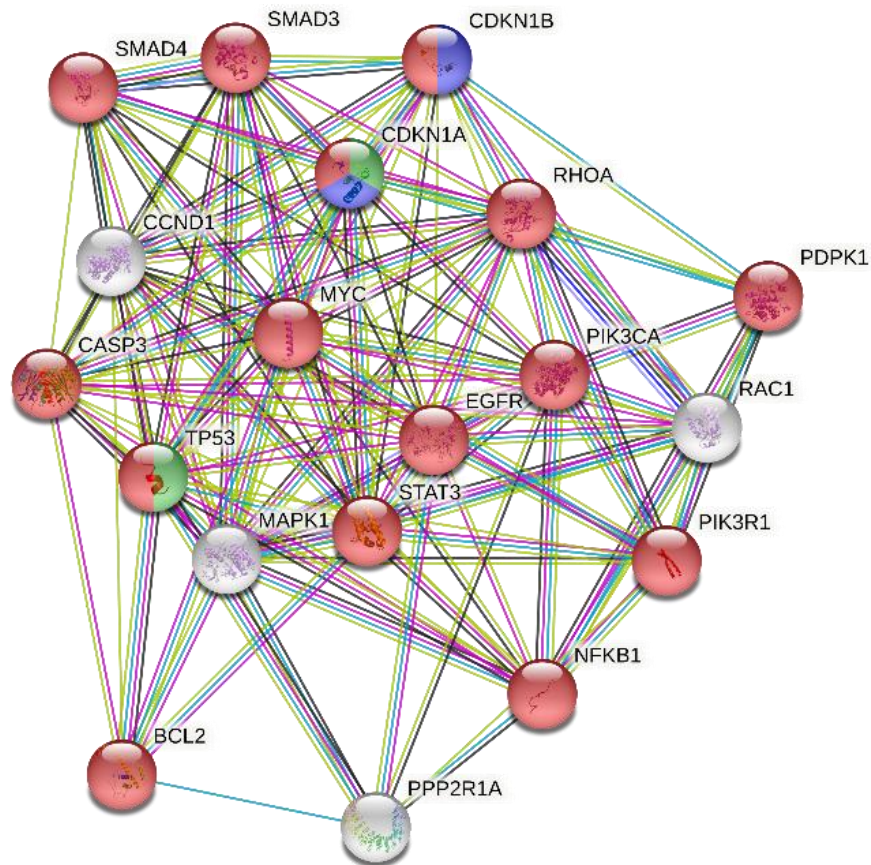


Figure 4.5-21: PPI network of significantly enriched target genes of intracellular downregulated miRNAs. Majority of protein (in red) were associated with promotion of cell survival, thus might play a role in senescent hVSMC acquired resistance to apoptosis.

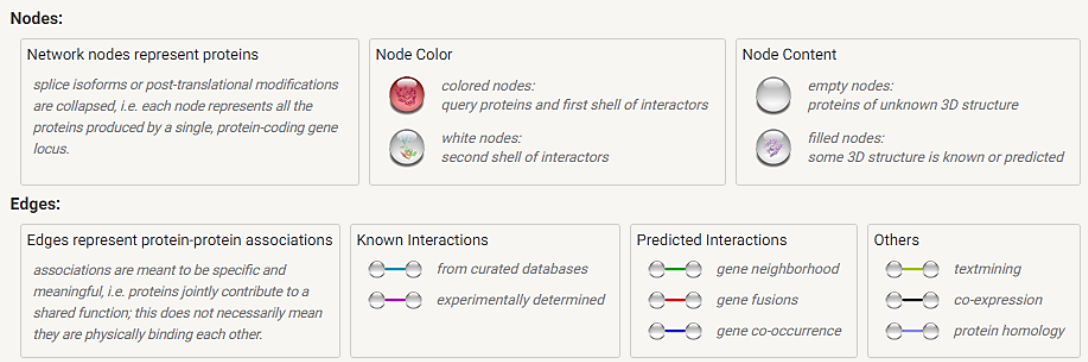
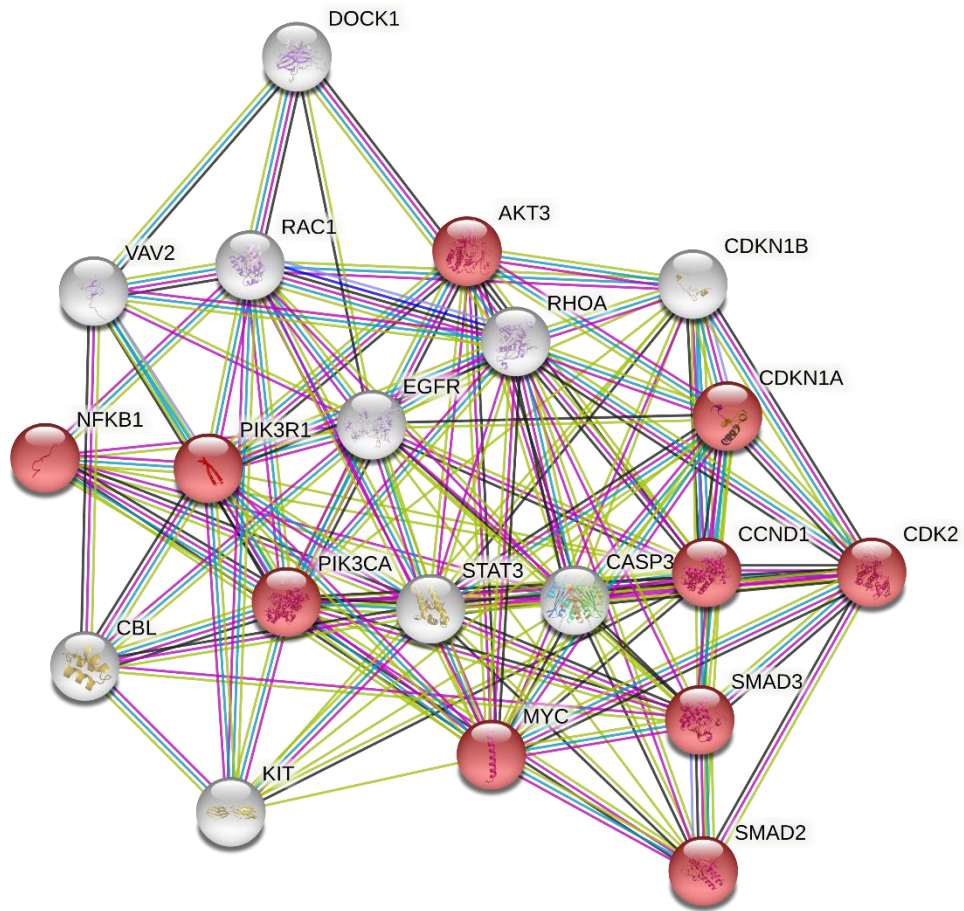


Figure 4.5-22: PPI network of significantly enriched target genes of exosomal downregulated miRNAs. Proteins (in red) were found to regulate cellular senescence, with active PI3K/Akt signaling that promoted cell survival, which might also contribute to senescent hVSMC acquired resistance to apoptosis.

Chapter 5. Discussion

5.1. Human Vascular Smooth Muscle Cells Replicative Senescence Characterization

In order to study hVSMC miRNA signaling during replicative senescence, characterization of hVSMCs undergoing replicative senescence was an essential prerequisite. Cellular senescence could be qualitatively assessed via hVSMC morphological changes as well as positive senescence-associated (SA) β -galactosidase staining at pH6.0. However, in order to distinguish between stress-induced and replicative senescence, quantitative analyses were required whereby SA gene or protein expression levels would be quantified. At the time, gene expression analysis using real-time polymerase chain reaction (qPCR) was the most accurate, time-efficient and cost-effective method to examine SA gene expression. Another reliable quantitative method to distinguish between replicative and stress-induced senescence was relative telomere length measurement(43). A combination of qualitative morphological changes and increased SA β -galactosidase activity, coupled with quantitative SA gene expression level and relative telomere length measurement were sufficient to confirm replicative senescence within hVSMCs.

In congruent with literature, increased SA β -gal activity in the old sample signified the increase in lysosomal mass of old hVSMCs(143). Under the light microscope, increased cellular granulation in the old sample might have been due to a defect in the protein degradation system of the aging hVSMCs (**Figure 4.1-1, B.**). Protein degradation can take place via autophagy or the ubiquitin-proteasome pathway (UPP). Autophagy allows for non-specific, bulk elimination of proteins and organelles while the UPP facilitates specific proteolytic degradation (70).

In aging cells, there is a general downregulation of proteins which facilitate autophagy, most importantly autophagy-related (ATG) proteins, leading to reduced autophagic activities (63). In fact, ATG protein knock-out studies have witnessed an increase in lysosomal mass, accumulation of inclusion bodies, protein aggregates and disorganized mitochondria, similar to that of cellular senescence (238). Interestingly, an increase in autophagy activities was proposed to be one of the forces driving mitotic cells into senescence (324). On the other hand, ubiquitin-proteasome pathway (UPP) is a fast and specific pathway of protein degradation via protein ubiquitination (104). In aging cells, however, the UPP becomes impaired, mainly due to a decline in proteasomal activities (106). It is well-recognized that the impairment of the 26S proteasome assembly is the major cause of the UPP dysfunction in the replicative senescence (285). Together, these two failing mechanisms result in the appearance of 'dirty' cells full of inclusion bodies, protein aggregates and dysfunctional organelles observed as heavy granulation under the microscope. Accumulation of these macromolecules also resulted in cell enlargement and altered cell integrity, partly constituting to the irregular appearance of the once-uniform cell population.

Enlargement of the nucleus was observed in senescent cells (**Figure 4.1-1, B**). During cellular senescence, alterations of the genome and ribosomal biogenesis occur, both of which take place within the nucleus, at the nucleoplasm and nucleolus respectively. In the nucleus, polyploidy is considered to be one of the biomarkers of cellular senescence (290). Polyploidy of senescence cells have been manifested with enlarged and abnormally shaped nucleus, altered nuclear membrane-related proteins (88) and the accumulation of senescence related protein inside the nucleus (68). Meanwhile, the nucleolus houses ribosomal biogenesis, one of the most energy-consuming machineries of a cell (100). Cellular senescence, however, is associated with a decrease in ribosomal biogenetic activities thus a decline in ribosomal translational activities and the cell's growth capacity (31). Nevertheless, there is an increase

in protein deposits in the nucleolus due to rearrangement of protein nucleolar localization during senescence (56).

Conclusively, these qualitative observations confirmed the cells in the old sample had undergone cellular senescence. Nonetheless, in order to distinguish between replicative and SIPS, gene expression of senescence markers and telomere length analyses were substantial.

The most evident quantitative validation was the significant increase in the expression of the genes *CDKN2A*, *CDKN1A* and *CDKN1B* encoding the proteins p16^{INK4α}, p21^{Cip1} and p27^{Kip1} respectively, which participate in the p16^{INK4α} and pRb pathways (267). Increased p21^{Cip1} levels inhibit CDK1/CDK2 complexes hence cell cycle inhibition of G1 to S and G2 to M phase transitions (243). On the other hand, increased expression of p27^{Kip1} inhibits CDK4 and CDK2, allowing pRb activation which halts cell cycle progression from G1 to S phase (224). P16^{INK4α} acts to inhibit CDK4 and CDK6, which hampered the phosphorylation of retinoblastoma proteins (pRb) (249). These combined expressions confirmed hVSMCs in the old samples were senescent (**Figure 5.1-1**).

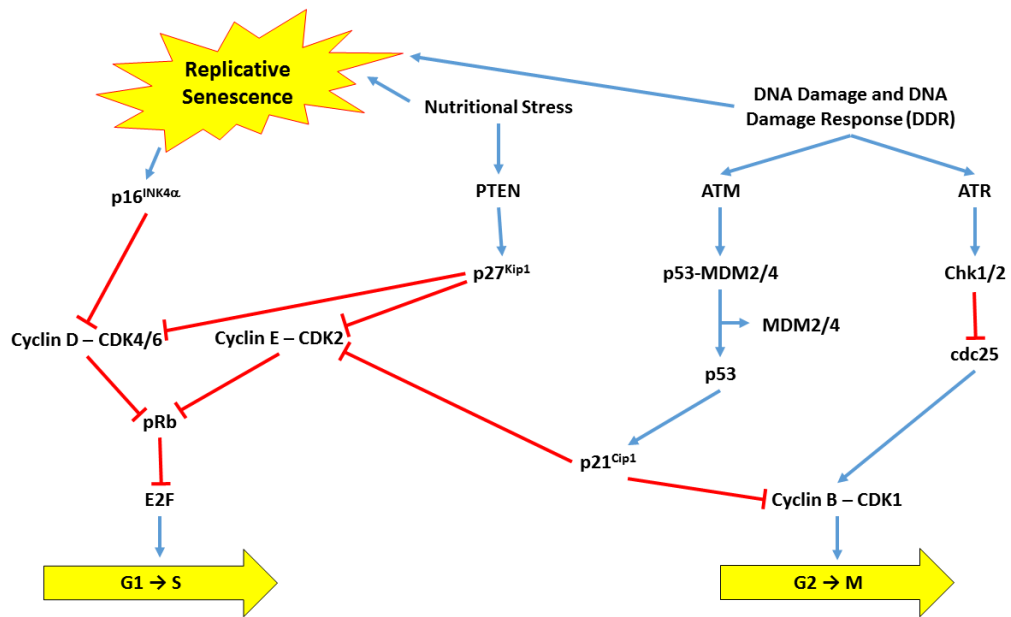


Figure 5.1-1: A simplified diagram of senescence-associated signaling pathways. Major cross-talks between the pathways to induce and maintain senescence and halt cell cycle progression, primarily at the G1/S and G2/M checkpoints, via the three main effector proteins p16^{INK4a}, p27^{Kip1} and p21^{Cip1}, all of which act to inhibit the CDK complexes that drive cell cycle progression.

Telomeres tandem repeats – TTAGGG – are followed by 3' G-rich single-stranded overhangs which are highly important for telomere maintenance and regulation. The telomeres are thought to fold themselves into two types of loop: The T loop and the D loop. The telomere DNA folds back to itself to form the T loop and the 3' G-rich overhang associates with the double-stranded telomere DNA to form a triple-stranded D loop (211).

The conserved telomeric sequences are not replicated by DNA polymerase and thus becomes shorter over time. When the short telomeric capping is recognized, DNA damage response mechanisms and cell cycle arrest are initiated in a similar fashion to that of double stranded breaks (DSB) (109). The point of cell cycle arrest due to cellular response to telomere shortening, or telomere attrition, is referred to as the Hayflick limit (208, 297).

In our data, shortened telomere length due to replicative exhaustion was detected in the old samples. Together with the gene expression data, replicative senescence was confirmed in the old hVSMC samples, validating the replicative senescence characterization method.

5.2. Human VSMC-Derived Exosome Isolation and Characterization

Isolation and characterization of exosomes secreted by the hVSMCs were other important requirements prior to miRNA expression profiling of hVSMCs. Different methods were available for exosome isolation, such as direct ultracentrifugation, column-binding isolation and isolation based on density gradient. Isolation based on density gradient involved the use of a 60% sucrose cushion that would preserve the exosome structure after centrifuge as compared to direct ultracentrifugation without the sucrose cushion. Although not as time-efficient as the column-binding isolation, exosomal isolation via ultracentrifugation with sucrose cushion was much more cost-effective.

Characterization of exosomes was followed using qualitative and semi-quantitative methods such as scanning and transmission electron microscopy to make sure the vesicles isolated were within the expected diameter range. Immunoblotting against exosomal markers, such as TSG-101, was also carried out to confirm the vesicles viewed under the microscopes were exosomes.

Despite being a valuable target for cell signalling studies, exosome isolation and characterization are big challenges for researchers. There is no 'gold standard' for exosome isolation, especially from conditioned medium. Furthermore, exosome isolation are more often collected from cancer cell lines with a large amount of conditioned medium, while primary cell conditioned media volume is limited due to limited cell growth and proliferation. Additionally, there is no specific marker to differentiate between exosomes and microvesicles(227). Under the electron microscope, it is not possible to differentiate between exosomes and microvesicles, as some microvesicles can be 100nm in size. Therefore, the most efficient isolation of exosomes relies primarily on gradient ultracentrifugation and size exclusion methods(184). Further inspection of exosomal sub-

population and heterogeneity would be meaningful in the development of a more efficient isolation method and improvement in exosome characterization(199).

5.2.1. Differences in Proliferative and Senescent hVSMC-Derived Exosomes

From the immunoblotting data, the intensity of the bands in young and old extracellular samples was quite similar (**Figure 4.2-2**). However, in terms of the source of the exosomes, there was at least twice the number of cells in the young sample compared to that in the old sample. With the difference in cell number taken into consideration, there was an increase in exosome release in the old sample, suggesting elevated exosomal release in senescent hVSMCs.

There were two unexpected significant differences in exosomes between young and old samples: exosomal clustering and TSG101 protein size. Although exosome clustering had been observed in other studies(77, 307, 341), there has been no report regarding differences in the level of exosomal clustering between proliferative and senescent VSMC-derived exosomes. Therefore, this observation posed as an interesting research question whose answer may contribute to elucidate the unidentified mechanisms of exosomal signaling and their specific behaviour as VSMC-derived exosomes. For instance, recently, Nakase *et al.* (2017) reported a novel signalling mechanism in exosome via inducing receptor clustering, which activated the receptors and contributed to endocytic uptake of the exosomes(199).

Another surprising observation was the larger size of the TSG101 protein in extracellular samples compared to that from intracellular samples. This observation has not been reported in any literature and posed as another interesting research question, which focuses on the mechanism in which exosomes were packaged inside the cell as well as any potential post-translational modification (PTM) of the protein TSG101. Based on the molecular weight (MW) differences between intracellular and exosomal TSG-101 (approximately 20kDa), the

predicted PTM was either ubiquitination or ISGylation. In previous reports, the PTMs of exosome-related proteins (including TSG-101) were associated with ubiquitination and ISGylation that promoted degradation and inhibited exosome release (191, 286). As opposed to previous reports, the TSG-101 with higher MW was found in exosomes that were already released into the conditioned media, which indicated that the PTM of exosomal TSG-101 does not always impair exosome secretion and may be necessary for exosome biogenesis and secretion. One possible explanation could be the difference in sample source, where exosomes were isolated from conditioned media, as opposed to exosomes isolated from serum and plasma samples in other studies. Similarly, difference in TSG-101 MW between exosomes isolated from conditioned media and serum was observed in our lab. Further study is required to determine the type of PTMs in exosomal TSG-101 as well as its biological significance in young and senescent hVSMCs during replicative senescence.

Altogether, the differences observed in these experiments provided evidence for further investigation of exosomes secreted by hVSMCs and their structural and compositional differences in proliferating and senescent conditions.

5.3. Genome-wide Small RNA Landscape in Young and Old Human Vascular Smooth Muscle Cells and Their Exosomes during Replicative Senescence

5.3.1. Highly Variable RNA Profiles in Human Vascular Smooth Muscle Cells during Replicative Senescence

After the necessary characterizations, whole-genome next-generation sequencing (NGS) was the preferred method to acquire a high-resolution overview of the miRNA landscape within hVSMCs and hVSMC-derived exosomes. This untargeted NGS method allows for unbiased detection of miRNA expression as well as enables the discovery of novel miRNAs. Accurate sequencing of small RNAs required specifications different from those for genomic or messenger RNA sequencing. Therefore, the sequencing platform was carefully chosen to maximize data output which would be able to detect miRNAs that might be expressed in low abundance.

At first glance, there was a significant difference in the RNA quantification profiles of young and old hVSMC samples (**Figure 4.4-5**). The highly variable RNA profiles in old samples indicated abnormal RNA expression levels in senescent hVSMCs. As our study used primary hVSMC cultures, hVSMC heterogeneity could account for the difference of RNA expression profiles between young and old samples, as well as the difference between the profiles of one old hVSMC sample to another. Differences in RNA expression profiles of senescent hVSMCs could also influence the outcome of distinct cellular fates. For instance, single-cell transcriptome analysis by Chen *et al.* (2020) reported the existence of different cell fates within a heterogeneous population of replicative senescent mouse embryonic fibroblasts (48). Similarly, the varying RNA profiles in old samples could be the the playout of heteroneous senescent hVSMCs influencing multiple different cell fates, such as further promoting cellular senescence, inhibiting cell proliferation as well as enforcing cell survival, all of which will be further discussed below.

Altered RNA expression profiles during senescence could also be a result of reduced RNA decay during senescence. It has been reported that RNA turnover rate was greatly reduced during cellular senescence, which reduced mitochondrial activity in a negative-feedback-loop manner. Reduced RNA turnover led to RNA accumulation and the cell's altered gene expression in order to stabilize accumulated RNA and maintain the senescence phenotype (194).

Regardless of what could be accountable for the variability, the observation of highly variable RNA profiles might have shed light on our partial understand of the progression towards cellular senescence in hVSMCs. Over the years, many studies have reported the altered expression of the transcriptome of cells undergoing cellular senescence. Casella *et al.* (2019) reported altered RNA expression levels in different cell types, including human diploid fibroblasts (WI-38, IMR-90) and endothelial cells (HUVEC, HAEC) upon induced cellular senescence as well as replicative senescence. The study found a common set of 50 upregulated RNAs and 18 downregulated RNAs in all cell types, including protein-coding mRNAs as well as non-coding RNAs. The study found significant sushi repeat-containing protein X-lined (SRPX) mRNA upregulation and decreased expression of multiple histone-encoding mRNAs. Interestingly, our data (discussed later on in section 5.6) also reflected association to histone methylation, which has been reported in vasculopathology related to VSMCs (298). More importantly, the study highlighted that the senescence profile of each cell type was more dependent on the cell of origin rather than the method of senescence induction. This implied that different cell types may progress into senescence differently and the dynamic progression of a specific cell type towards senescence is worth further exploration (41).

In another narrative, Hudgins *et al.* (2018) reported that senescence biomarkers were deemed to be age- and tissue-specific in mice (111). In their study, senescence-associated

genes that were usually more associated with *in vitro* studies were also differentially expressed in age- and tissue-specific samples. In light of this observation, one may deduce that in addition to commonly expressed senescence biomarkers, identifying the specificity-determining genes in different cells or tissue would elucidate the dynamics of their unique progression into cellular senescence mentioned above.

Altogether, hVSMC heterogeneity as well as reduced RNA decay during replicative senescence could be accountable for the highly variable RNA profiles observed in old samples. In the age of senolytic drug development where current studies focus on establishing a panel of commonly expressed biomarkers of cellular senescence, it is imperative that senescence biomarkers are age-, cell type- and tissue-specific. Therefore, this variability might greatly contribute to their cell type-specific gene expression profile, thus allowing biomarker discovery and elucidating hVSMC dynamic progression into cellular senescence.

5.3.2. RNA Profiles of Human Vascular Smooth Muscle Cell-Derived Exosomes

Exosomal RNA profiles were highly different from those of intracellular origins. Additionally, their profiles were irregular even between themselves, regardless of young or old samples. In order to have an unbiased sequencing profile of exosomal RNA content, the samples were not enriched prior to sequencing so the results obtained reflected the natural RNA content as closely as possible. Our results corresponded with previously described observations that there were discrepancies between the composition of cellular and exosomal RNAs (**Figure 4.4-5 & Figure 4.4-6**) (61, 122, 185). In exosomes, the small RNA components such as miRNAs, snRNAs and snoRNAs were much smaller in proportion with protein-coding mRNAs and lincRNAs, which agreed with other studies (221).

While miRNAs belong to the most well-known class of small RNAs, the proportion of exosomal miRNAs in the pie charts in **Figure 4.4-6** were significantly smaller than that of intracellular miRNAs, suggesting that exosomal miRNA loading and export was a tightly regulated active process. This observation also aligned with other published studies (18, 23, 122). Despite the high irregularity in all samples, the miRNA portion in young samples were slightly larger than that of old samples. It is possible to hypothesize that the miRNA sorting and loading mechanism was less active in senescent hVSMCs.

The most striking feature of the exosomal RNA profiles was the large proportion of mRNAs and miscellaneous RNAs (miscRNA). Apart from the ongoing interest in exosomal miRNAs as biomarkers and signaling molecules, exosomal mRNAs have also been proposed as biomarkers (225, 311). Lasser *et al.* (2017) demonstrated an interesting existence of two sub-populations of exosomes separated by density, which were termed HD and LD. The sub-population HD reportedly contain a higher percentage of reads that mapped to mRNA transcripts (149). While exosomes from our study was isolated using the sucrose cushion, a form of gradient isolation method, sub-populations based on density was not distinguished prior to total RNA isolation. Therefore, the difference in mRNA content between samples could have been attributed to the differences within the sub-populations of exosomes. Additionally, reports have shown that there were cellular mRNAs transcribed in the host cells solely for exporting to recipient cells (168).

On the other hand, miscRNAs constitute the other large portion of the exosomal RNA profiles. MiscRNAs represent non-coding small RNA fragments that could not be classified. The large proportion of miscRNAs in all samples inversely correlated to the degree of our current understanding of exosomes and their content.

Overall, exosomal RNA content is largely dependent on the intra- and extracellular microenvironment of the host cell and differences between exosomal and cellular RNA

contents suggests an active and specific loading mechanism within the host cell, which is currently still poorly understood and requires more research. As exosome content might be cell-type specific, deeper study on hVSMC-derived exosomes is needed in order to elucidate and characterize them in a more focused light.

5.3.3. Other Non-coding RNA classes and Their Association with Cellular Senescence in Vascular-Related Diseases

Apart from the expected miRNA and mRNA mapped transcripts, the sequencing data were also mapped to other different RNA classes. In intracellular samples, snoRNAs occupied the second to third largest portion of total RNA content. On the other hand, exosomal samples consisted a significant amount of lincRNAs, similar to the portion of miRNAs.

SnoRNA is a class of small RNAs that have been reported to have implications in cellular senescence, most often related to the ribosome biogenesis pathways (21, 178, 272). There are two main classes of snoRNAs: the box C/D snoRNAs and the box H/ACA snoRNAs. The box C/D snoRNAs Snord123 and Snord1a were identified as regulators of altered rRNA methylation in B cells thus related to age-related immune decline in mice (21). In regards to replicative senescence, snoRNAs have been found to interact with telomerase RNA, a core component of the telomerase enzyme . A conserved box H/ACA snoRNA domain has been discovered at the 3' termini of telomerase RNAs. This domain allowed regulatory actions of snoRNAs on telomerase RNA particularly on their localization within the nucleus (272). However, further functional outcome of telomerase RNA regulation by snoRNA relating to cellular senescence is still unclear.

Disregarding cellular senescence, snoRNAs have been sparingly reported to associate with vascular diseases and pathological conditions. For instance, a study involving the scanning of 5244 participants reported single-nucleotide polymorphisms (SNPs) within the snoRNA

cluster were significantly associated with heart failure, and that the expression of these snoRNAs were highly vessel-specific. *In vitro* functional study of these snoRNAs suggested their involvement in methylation through canonical mechanisms (92). In another study, SNORD113.2 and SNORD114.1 levels were found elevated in patients with peripheral artery disease and were strongly linked to platelet activation in blood plasma (204).

Overall, the studies on snoRNAs and their association with cellular senescence has been mostly as an implication of other diseases such as cancer and immune-related diseases. While studies correlating snoRNAs to vascular diseases were scarce, they did not involve snoRNA regulation of cellular senescence. Meanwhile, the prominent exosomal lincRNA portion of exosome samples proved to have more association with cellular senescence regulation in vascular-related diseases.

LincRNAs belong to the long non-coding RNA (lncRNA) family. However, lincRNA sequences do not overlap protein-coding genes (226). Although an abundant of lncRNA and lincRNA transcripts have been identified, not as many have been functionally characterized. Nevertheless, emerging evidence of lncRNA regulation of cellular senescence have been reported (3, 4, 321, 69, 155, 200, 226, 305, 309, 309, 310). The studies looked into the effects of lncRNA on well-known senescence-related genes such as *p21* and *p53*.

LincRNA-p21 is another lincRNA that has been frequently reported to involve in age-related heart diseases (3, 305, 321). *LincRNA-p21* was identified as a reciprocal regulator of *p53* that regulated pro-senescence pathways. Additionally, *LincRNA-p21* interacted with β -catenin which participated in the Wnt/ β -catenin signaling pathway to promote cellular senescence. A study by Xie *et al.* proposed the use of *lincRNA-p21* as a therapeutic target as modulation of its expression levels might result in cardioprotective effects on cancer patients receiving doxorubicin treatment, of which cardiotoxicity was a well-known side-effect (309).

In another study, a novel lincRNA, *Linc-ASEN*, was found to suppress *p21* in a multi-level manner, thus prevents cellular senescence. *Linc-ASEN* interacted with up-frameshift 1 (UPF1) and form a complex, which recruited polycomb repressive complex 1 (PRC1) and PRC2 to inhibit p53 binding and activation of *p21* gene transcription. Posttranscriptionally, the *Linc-ASEN-UPF1* complex repressed *p21* translation by enhancing *p21* mRNA degradation (155).

Following that, another lincRNA, SENELOC, was reported to suppress senescence via both p53-dependent and -independent mechanisms. Here, SENELOC promoted p53 degradation, which led to decreased *p21* transactivation. SENELOC alternatively intervened with *miR-3175* regulation of the histone deacetylase HDAC5 to prevent its turnover, which also contributed to p21 repression (310).

Altogether, the existing literature has allowed us to conclude that, when compared to intracellular snoRNAs, exosomal lincRNAs may play a more significant role in regulating cellular senescence in hVSMCs and may serve as worthy targets for further in-depth study of their biological and functional significance in cardiovascular exosomal signaling research.

5.3.4. Overcoming Limitations and disadvantages of Irregular RNA Profiles in Senescent hVSMCs and hVSMC-derived exosomes

Due to the high irregularity of RNA profile of old and exosomal samples, appropriate algorithmic tests and adjustments were needed to assess data distribution, normalize data sets to reduce data redundancy and increase data integrity and ensure data suitability for group comparison as well as further downstream analyses.

Box and whiskers plots provided a simple and effective overview of the data distribution across all samples, qualifying data for the subsequent differential expression analysis (**Figure 4.4-7**). At the same time, the gene expression PCA plot provided a map of the distances between young and old samples from which variation of RNA-seq data could be inferred. In

both intracellular and exosomal sample groups, while the genes in young samples did not vary too far from the total number of transcripts detected (3.3-9.3%), old samples constituted to most of the variation within the entire gene set (60.2-69.1%). The PCA plots showing distinguishable data variation between young and old samples thus further indicating that differential expression analysis could be performed.

The discovery of differentially expressed miRNAs between two conditions is one of the main purposes for high-throughput sequencing. While gene detection was in the form of fluorescent signals in microarrays, more modern digital gene expression data such as those obtained from NGS registered the gene detection as a count. Therefore, it is imperative that the methods used for NGS data analysis could perform multiple testing procedures on the count-based expression data and process information acquired in all observations to improve statistical inference. The chosen CAP-miRSeq workflow implemented edgeR, using empirical Bayes analysis of gene expression data (175, 233). Empirical Bayes estimation and tests performed were based on the negative binomial distribution model (263).

EdgeR assumes that the variance of gene counts depends on two dispersion parameters, namely the negative binomial dispersion and the quasi-likelihood dispersion. The negative binomial dispersion was estimated by fitting a mean-dispersion trend across all genes whereas the quasi-likelihood dispersion was estimated by Bayesian shrinkage approach (234). The differential expression statistical tests were conducted based on either the likelihood ratio tests or the quasi-likelihood F-tests (49, 175).

The negative binomial regression model belong to the generalized linear model (GLM) class, which provides ease of implementation and interpretation, by assuming the link function is a linear combination of covariates. However, the linearity assumption is not always appropriate and nonlinear models for linking the phenotype to gene expression in RNA-Seq data may be important. Therefore, continuous efforts are still carried out to improve

differentially expressed gene identification and statistical inference, especially from small sample sizes (230, 283). In RNA-seq differential expression data analysis, EdgeR is widely used thanks to the shrinkage estimators, which can improve differential expression test stability in a large range of RNA-seq data.

5.4. Differentially Expressed Intracellular miRNAs in Human Vascular Smooth Muscle Cells during Replicative Senescence

After differential expression analysis using edgeR, data were categorized into 4 groups: upregulated intracellular miRNAs, downregulated intracellular miRNAs, upregulated exosomal miRNAs and downregulated exosomal miRNAs. Tertiary analyses such as differential expression analysis, pathway analysis and gene ontology enrichment (GO) analysis were performed to discover dysregulated miRNAs expressed and obtain an overview of their potential roles in the mapped signaling pathways. As such, the data would shed light on potential function of the dysregulated miRNAs and their mechanism of action during replicative senescence of hVSMCs. The discussion of dysregulated miRNAs will focus on intracellular upregulated miRNAs from section **5.4.1 - 5.4.2** and downregulated intracellular miRNAs from section **5.4.3 - 5.4.6**.

5.4.1. Upregulation of Intracellular hsa-miR-664a-3p, hsa-miR-664a-5p, hsa-miR-664b-3p and hsa-miR-4485-3p and the Negative Regulation of Cellular Phosphate Metabolism, Subcellular Localization and Transport

As miRNAs exert gene silencing effects on protein coding mRNAs, an increased expression of miRNAs will further suppress their target genes. In pathological conditions, there may exist a feedback loop mechanism that would enhance the transcription of these upregulated miRNAs. This mechanism might be linked to the suppression of the pathways associated with the upregulated miRNA target genes. GO enrichment analysis of upregulated miRNAs *miR-664a-3p*, *miR-664a-5p*, *miR-664b-3p* and *miR-4485-3p* target genes resulted in the enrichment of biological processes such as phosphorus metabolism processes, subcellular protein localization and intracellular transport (**Figure 4.5-9**).

It is generally established that aging is associated with attenuated stress response(124, 213). Upregulation of differentially expressed intracellular *miR-664a-3p*, *miR-664a-5p*, *miR-664b-3p* and *miR-4485-3p* suppressed stress-activated protein kinase signaling cascades in senescent hVSMCs, which might have contributed to reduced stress responsiveness of senescent cells(217). Mitogen-activated protein kinase (MAPK) cascade was one of the significantly enriched biological processes associated with the upregulated miRNA targets. Targets might have regulate these biological processes by participating in MAP kinase activity, protein serine/threonine kinase activity and transferase activity, which transfers phosphorus-containing groups (**Table 15**). All the interactions were reported to be enriched at the catalytic complexes, which were located at the cytosol, intracellular membrane-bounded organelles and nucleus (**Appendix Table 16**) . The results were agreeable with existing findings as the MAPK cascade is a signaling pathway that spans from the cellular membrane, through the cytoplasm and ultimately delivering the signal to the nucleus for subsequent gene transcription(300).

In senescent hVSMCs, miRNA targets were also highly involved in positive regulation of phosphorus metabolic processes, including those involved in protein phosphorylation (**Appendix Table 14**). Protein phosphorylation is a reversible post-translational modification of proteins in which an amino acid residue is phosphorylated by a protein kinase via the covalent addition of a phosphate group. The phosphorylation of a protein may activate, deactivate or modify its function, therefore essentially acts as an 'on/off switch' of protein function(54). Suppression of phosphorylation-related genes by miRNAs might result in decreasing phosphorylating activities, thus disrupting the balance of intracellular protein function.

Furthermore, protein phosphorylation plays a major role in cell cycle regulation. In particular, cell cycle exit and entry into cellular senescence are specifically regulated by appropriate

sequences of protein phosphorylation(241). One of the key factors driving cellular senescence, p53, is activated upon phosphorylation, which resulted in the transactivation of *p21*(312). On the other hand, the protein pRb, a principle regulator of the cell cycle and cellular senescence, becomes deactivated upon phosphorylation (267). Additionally, *p16^{INK4α}*, a negative regulator of pRb and well-known marker of cellular senescence, is reported to have multiple sites for phosphorylation, each influencing *p16^{INK4α}* function differently(89). Lastly, inhibition of the cyclin-dependent kinases prevents phosphorylation of their respective targets thus arresting the cell cycle and initiate cellular senescence.

Another major phosphorylative process is the oxidative phosphorylation to synthesize adenosine triphosphate (ATP) at the mitochondrial inner membrane. Mitochondria are well-known power-house of the cell where ATP is produced and supplied to fuel other cellular processes. Mitochondrial dysfunction is a feature of cellular senescence, whereby mitochondrial mass increases, mitochondrial membrane potential decreases and the antioxidant defense mechanism declines. The degenerating mitochondrial functions give rise to reactive oxygen species (ROS) production and increase oxidative stress within the cell (59). Also during senescence, ATP levels are altered and AMP:ATP ratio has been reported to increase in senescent cells, accompanied by enhanced levels and activity of AMP-activated protein kinase (AMPK) (293). Additionally, ATP binding was interfered due to the enhanced suppression of upregulated miRNAs. The binding of ATP to other molecules provides energy for molecular functions to take place and interruption of ATP binding may lead to failed initiation of a range of different cellular processes.

Apart from affecting cellular metabolism, upregulated *miR-664a-3p*, *miR-664a-5p*, *miR-664b-3p* and *miR-4485-3p* also suppressed targets which were involved in protein subcellular localization and intracellular transport. Protein localization is the accumulation of a protein at a given site, which determines the environments in which proteins operate. Protein

function is influenced by their subcellular localization, which controls the access and availability of their interacting molecules (246). Protein subcellular localization is facilitated by protein trafficking thus is highly dependent on intracellular transport, especially processes involved in nucleus import and export. Our results also indicated most negative regulation of protein localization and intracellular transport occurred between the nucleus and cytoplasm, especially at the sites of nucleoplasm and nuclear lumen (**Figure 4.5-9**).

Changes in the protein trafficking machinery can have detrimental effects on protein transport, resulting in modification of cellular morphology and physiology. Protein mislocalization may occur due to mutations, altered expression of cargo proteins or transport receptors and/or deregulation of the trafficking machinery components (114). For instance, defects in the nucleoporin NUP155 were found in patients with familial atrial fibrillation. The defects resulted in decreased nuclear envelope permeability, which affected the nuclear import and export of Hsp70 protein and mRNA, respectively (333). Alteration in protein trafficking and localization may also affect communication via intercellular protein transfer between cells as reported by Biran *et al.* (26). Similarly, Bernard *et al.* reported unexpected participation of molecular transport proteins upon the induction of senescence (9).

It is well-aware that senescent cells generate cues to attract immune cells and signal them for immune clearance (256). Perhaps increased suppression by the identified upregulated *miR-664a-3p*, *miR-664a-5p*, *miR-664b-3p* and *miR-4485-3p* have contributed in altering hVSMC metabolic processes, protein trafficking and localization to transform their intercellular signaling profile into one that would recruit and initiate immune clearance.

5.4.2. Upregulation of Intracellular hsa-miR-664a-3p, hsa-miR-664a-5p, hsa-miR-664b-3p and hsa-miR-4485-3p in the Regulation of Toll-like receptor and MAPK Signaling Pathways in hVSMCs during Replicative Senescence

Upon pathway enrichment analysis using the databases from KEGG and Reactome, the Toll-like receptor (TLR) signaling pathway was found to be greatly enriched in which miRNA targets were found to participate. TLRs belong to a class of pattern-recognition receptors (PRRs), which belong to the innate immune system, and are expressed in multiple immune cells as well as non-immune cells, including hVSMCs (136, 317). The TLR pathway is among the first line of defense against invading pathogens and mainly occurs via MyD88- or TRIF-dependent signaling pathways, both of which result in inflammation, immune cell regulation, survival and proliferation (231). In VSMCs, TLR signaling have been found to associate with the proinflammatory phenotype, vascular calcification and the development of atherosclerotic lesions (154, 188, 231).

On the other hand, mitogen-activated phosphate kinase (MAPK) signaling cascade is a well-known pathway which has been the focus of many studies and is involved in mediating cellular proliferation and growth (15, 300). Functional changes within the cascade have been associated with many different human diseases, including those affecting cardiovascular health (137, 139, 236).

Most evidences reported increased TLR signaling in proliferative VSMCs, whereas senescent hVSMCs were non-proliferative. However, increased signaling of TLR4 in particular and aberrant MAPK activities have been reported in senescent cells (14, 82, 257, 281). Our results suggested that TLR downstream signaling was dampened in replicative senescent hVSMCs and its downstream activation of MAPK was also negatively affected by the increased expression of miRNAs. Perhaps increased target gene suppression might be the

counteracting mechanism against uncontrolled pro-inflammatory signaling. However, experimental validation needs to be carried out to ascertain this hypothesis.

Although *miR-664a-3p*, *miR-664a-5p*, *miR-664b-3p* and *miR-4485-3p* target genes were found to participate mostly in the TLR and MAPK signaling pathways, most target genes were downstream of the pathway and further inspection using the PPI network (**Figure 4.5-20**) indicated that these target genes were significantly related to each other in a different context where 'stress response' was the strongest link. Therefore, it is appropriate to interpret that *miR-664a-3p*, *miR-664a-5p*, *miR-664b-3p* and *miR-4485-3p* target gene suppression were geared toward dampening stress response within hVSMCs rather than complete inhibition of the TLR and MAPK signaling pathways, at the same time not excluding the possibility of *miR-664a-3p*, *miR-664a-5p*, *miR-664b-3p* and *miR-4485-3p* antagonistic regulation of these pathways.

5.4.3. Downregulation of Intracellular *hsa-miR-155-5p* and *hsa-miR-20a-5p* Promoted Cytoskeletal Reorganization and Cell Cycle Arrest

Based on the enrichment analyses, downregulation of *miR-155-5p* and *miR-20a-5p* were highly associated with hVSMC phenotypic switching including structural and molecular changes (**Appendix Table 23**).

Unsuppressed target genes were found to associate with actin nucleation and polymerization, which were known to involve in cytoskeletal remodeling. As synthetic VSMCs have been concurrently described as migratory, dedifferentiated VSMCs can migrate from the tunica media to the tunica intima, leading to a decline in vascular tone regulating abilities (169, 325). Actin and microtubule polymerization has also been reported in VSMC migration in the events of vascular remodeling, injury response and vascular diseases (36, 266). Actin lies within the central regulatory network of cytoskeletal remodeling and is an integral factor

in the formation of focal adhesion, which was a term enriched by decreased expression of *miR-155-5p* and *miR-20a-5p* in senescent hVSMCs. Focal adhesion has been suggested to play a major role in age-related VSMC changes and arterial stiffness (73).

The polymerization of G-actin to F-actin has been reported to disrupt the dynamic actomyosin interactions within VSMCs with strong association to cell stiffness (115, 197). Actin nucleation enrichment has been linked to the promotion of G-actin polymerization, F-actin stress fibre formation and VSMC migration (121). Overall, changes in actin polymerization and depolymerization associated with focal adhesions have been suggested to be master inducers of VSMC stiffness in aging (146).

Downregulation of intracellular miRNAs also affected the molecular control of cell cycle-related regulatory molecules, such as cyclin-dependent protein serine/threonine kinases, which are important factors in cell cycle arrest and senescence induction. hVSMCs were predominantly at the G1/S phase checkpoint with enriched negative regulation of G1/S transition of the mitotic cell cycle. This negative enrichment indicated halted cell cycle progression thus consequently prevents DNA replication and subsequent mitosis. More importantly, exit of the cell cycle at the G1/S phase has been linked to entry into senescence (**Figure 4.5-10**). Negative regulation of VSMC proliferation was enriched by unsuppressed miRNA target genes, which was expected of senescent hVSMCs (**Table 17**). After extensive enrichment analyses, the genes *CDKN1A* and *CDKN1B* showed to be the most significantly active after escaping *miR-155-5p* and *miR-20a-5p* suppression. *CDKN1A* and *CDKN1B* encode for the proteins p21 and p27 respectively, both have been described to participate in senescence-inducing pathways described in **2.2.3.3**. Furthermore, positive regulation of translation was also enriched, with particular enrichment at the 48S preinitiation complex (**Figure 4.5-10 & Table 18**).

Interestingly, unsuppressed target genes due to low levels of *miR-155-5p* and *miR-20a-5p* highly enriched the negative regulation of VSMC differentiation during phenotypic switching. Earlier, it was explained that the dedifferentiation of contractile into synthetic VSMC was a reversible process. It seemed that senescent hVSMCs molecular changes gravitated towards promoting the synthetic hVSMCs while suppressing their reversibility back into the contractile phenotype. Nevertheless, this observation remains to be experimentally tested before any concrete conclusion can be drawn.

Altogether, downregulation of *miR-155-5p* and *miR-20a-5p* was significantly associated with central pathways influencing hVSMC morphological change as observed in **Figure 4.1-1** as well as molecular changes. While actin nucleation/polymerization/depolymerization gave clues towards hVSMC cytoskeletal reorganization, genes encoding the proteins p21 and p27 were proven as important players in the field of cellular senescence, which agreed with our initial knowledge of hVSMC behaviour during replicative senescence.

5.4.4. Downregulation of Intracellular hsa-miR-155-5p and hsa-miR-20a-5p Dampened hVSMC Stress Response during Replicative Senescence

Downregulation of intracellular *miR-155-5p* and *miR-20a-5p* resulted in both negative and positive regulation of the MAPK cascade, with the negative regulation of the cascade being predominantly more enriched. The targets mainly associated with the regulation of stress-activated and p38 MAPK cascades in particular.

There was an interesting observation that both upregulated and downregulated miRNAs contributed to the negative regulation of the stress-activated MAPK signaling cascade. Cellular stress response is an integral adaptive mechanism of cells upon intrinsic or extrinsic changes and declining stress response has been reported to associate with aging (91). Given the study focuses on hVSMCs, the main contractile unit of the blood vessels, which are

constantly under exposure to a variety of vascular stresses (i.e. shear stress, stretch, oxidative stress), proper stress response is crucial for the maintenance of vascular tone and vascular compliance. VSMCs can initiate vascular remodeling in response to environmental stressors and a decline in stress response may reduce the cell's adaptive capacity and impair vascular function (329).

Another MAPK cascade involved with downregulated miRNA targets was the p38 MAPKs, which are members of the MAPK family that are activated by a variety of environmental stresses and inflammatory cytokines, making it essential for normal immune and inflammatory response (140). In cardiovascular research, p38 has been mostly reported in conditions affecting the heart, as well as before and after ischemic events (62). Activation of p38 has been linked with subsequent cell death and inhibition of p38 has been suggested to be cardioprotective (158, 167, 247). In VSMCs, p38 has been reported to exert both proliferative and anti-proliferative effects on VSMCs upon its activation, depending on the context of activation (8, 308). Furthermore, p38 can also induce VSMC apoptosis, growth and migration (85, 145, 268). Therefore, the outcome of p38 MAPK regulation of the downregulated *miR-155-5p* and *miR-20a-5p* target genes in this particular observation remains uncertain without further study. Overall, downregulation of *miR-155-5p* and *miR-20a-5p* was suggested to contribute to the decline in stress response of senescent hVSMCs.

5.4.5. Downregulation of Intracellular hsa-miR-155-5p and hsa-miR-20a-5p Promoted TGF- β Accumulation but Inhibited TGF- β signaling Pathway in hVSMCs during Replicative Senescence

The transforming growth factor-beta (TGF- β) superfamily signaling plays a critical role in the regulation of cell growth, differentiation and development. Signaling is initiated with oligomerization of serine/threonine receptor kinases and phosphorylation of the

cytoplasmic signaling molecules Smad2 and Smad3 for the TGF- β /activin pathway, or Smad1/5/9 for the bone morphogenetic protein (BMP) pathway (107, 244). Meanwhile, the I-Smads 6 and 7 antagonize the activation of receptor-regulated Smads (R-Smads) and are induced by both TGF- β and BMP signaling as part of a negative feedback loop (187).

In hVSMCs, unsuppressed target genes from downregulated *miR-155-5p* and *miR-20a-5p* participated in the upregulation of inhibitory Smad (I-Smad) binding, which resulted in negative regulation of the TGF- β signaling pathway. Concurrently, GO terms for 'TGF- β production' were positively enriched (**Appendix Table 23, Figure 4.5-12**). TGF- β pathway was also enriched in the pathway analysis (**Figure 4.5-14**). Accumulation of TGF- β during cellular senescence has been reported in many cell types (276). Although TGF- β signaling was inhibited by the co-expressing I-Smads, increased levels of TGF- β could also participate in other Smad-independent pathways, such as promoting cell cycle arrest through interactions with cell cycle regulators or increasing DNA damage through ROS production, all of which would promote cellular senescence (322, 335).

In conclusion, downregulation of *miR-155-5p* and *miR-20a-5p* might have contributed to the promotion TGF- β accumulation while inhibiting the TGF- β /Smad-dependent signaling pathway in hVSMCs during replicative senescence.

5.4.6. Downregulation of intracellular hsa-miR-155-5p and hsa-miR-20a-5p activated PI3K/Akt signaling in human vascular smooth muscle cells during replicative senescence

The serine/threonine kinase Akt (also known as protein kinase B or PKB) has a critical role in regulating diverse cellular functions including metabolism, growth, proliferation, survival, transcription and protein synthesis. The Akt signaling cascade is activated by stimuli that induce production of phosphatidylinositol (3,4,5) trisphosphates (PIP3) by phosphoinositide

3-kinase (PI3K) (103). PI3K and Akt activation occur upstream of the mechanistic target of rapamycin (mTOR) pathway. mTOR is an atypical serine/threonine kinase that is present in two distinct complexes: mTOR complex 1 (mTORC1) and mTOR complex 2 (mTORC2). While mTORC1 is a master growth regulator, mTORC2 promotes cellular survival by activating Akt, regulates cytoskeletal dynamics and controls ion transport and growth (148).

In hVSMCs, activated Akt has been reported to phosphorylate the Forkhead transcription factor, FOXO3a, causing it to deactivate and unable to initiate the transcription of radical scavenger genes, resulting in increase ROS levels and oxidative stress within the cell (280, 313).

The results showed enrichment in the positive regulation of PI3K and Akt signaling (**Table 17**). This finding was particularly exciting as earlier studies by Tan *et al.* has demonstrated significantly activated PI3K/Akt/mTOR signaling in hVSMCs under going replicative senescence on a protein expression level (270). The study also showed that activated PI3K/Akt/mTOR signaling associated with increase in oxidative stress and decrease in telomerase activities, both of which were involved in the aging of hVSMCs. Our study has found that this finding with the downregulation of *miR-155-5p* and *miR-20a-5p* during replicative senescence as the contributing factor to the hyper-activation of the PI3K/Akt/mTOR signaling pathway in hVSMCs, which complemented the earlier reports. Overall, downregulation of *miR-155-5p* and *miR-20a-5p* resulted in the positive regulation of PI3K and Akt in replicative senescent hVSMCs, which might contribute to the activation of PI3K/Akt/mTOR signaling pathway to enhance oxidative stress and promote survival of senescent hVSMCs.

5.5. Differentially Expressed Exosomal miRNAs in Human Vascular Smooth Muscle Cell-Derived Exosomes during Replicative Senescence

In senescent hVSMC-derived exosomes, *hsa-miR-7704* was up regulated while *hsa-miR-155-5p* and *hsa-miR-146b-5p* were downregulated (**Table 7**). Although differentially expressed miRNAs may not directly mediate cellular changes, dysregulated exosomal miRNA levels inferred changes to the communicating message that hVSMCs were sending out to their outer environment and neighbouring cells. Therefore, it is important to investigate the change in the signaling message and identify discrepancies in the exosomal communication between proliferating and senescent hVSMCs.

5.5.1. The Potential of Exosomal *hsa-miR-7704* in hVSMC-derived Exosomes during Replicative Senescence

Although found to be significantly upregulated in the exosomes of senescent hVSMCs (**Figure 4.5-2**), *miR-7704* could not be validated using qPCR as no suitable primer could be designed for the chosen miScript qPCR technology from Qiagen (Germany) as the G-C content was too high. Additionally, *miR-7704* was a newly annotated miRNA that only yielded two published articles when searched through PubMed database of the United States National Library of Medicine, both of which were in the field of cancer research (252, 342).

As a newly annotated miRNA, *miR-7704* target genes that were experimentally validated were also scarce. However, GO categorization of *miR-7704* target genes suggested possible association of *miR-7704* in extracellular processes and signaling (**Figure 4.5-11**). This was an interesting observation, given the rise of *miR-7704* levels in exosomes, which were vesicles that could facilitate extracellular signaling. *miR-7704* target genes participated in several different molecular functions, such as transcription regulator and signal transduction activities (**Appendix Table 20-Table 22**). Therefore, increased levels of exosomal *miR-7704*

may suppress or interfere with the recipient cell transcription and signal transduction processes related to the calcium signaling pathway near membrane or extracellular regions of the recipient cell (**Figure 4.5-15**). Certainly, further study is required to validate this hypothesis, which may add to our understanding of cell signaling via the exosomal axis.

5.5.2. Downregulation of Exosomal miRNAs *hsa-miR-155-5p* and *hsa-miR-146b-5p* as an Intercellular Signal to Mitigate hVSMC Proliferation and Proinflammatory Signaling

In senescent hVSMC-derived exosomes, *miR-155-5p* and *miR-146b-5p* were downregulated (**Table 7**). GO and pathway enrichment analyses have shown that downregulated miRNA target genes were involved in the regulation of VSMC contraction and proliferation, as well as negative regulation of the cell cycle (**Appendix Table 23**). PPI pathway analysis also showed that the majority of the significantly associated proteins were involved in the regulation of cellular senescence (**Figure 4.5-22**). Upregulation of *miR-155-5p* has been found to negatively regulate the contractile phenotype of VSMC (215). Additionally, upregulated expression of *miR-155-5p* and *miR-146b-5p* has been found to promote VSMC proliferation and migration (292, 330). In atherosclerotic plaques, there was increase expression of *miR-155-5p* while reducing *miR-155-5p* expression resulted in inhibited VSMC proliferation and migration (320, 330).

Data also showed enrichment in interleukin-1 β (IL-1 β) and interleukin-6 (IL-6) production (**Appendix Table 23**). In senescent VSMCs, IL-1 β and IL-6 have been reported to be commonly expressed and secreted in an elevated manner (82). IL-1 β is known as a cytokine that is synthesized and secreted by VSMCs to promote VSMC proliferation and inflammation, which may contribute to neointimal hyperplasia and lesion progression in atherosclerosis (74, 78). On the other hand, IL-6 is a cytokine synthesized by VSMCs and is elevated in the arterial wall in atherosclerosis and restenosis after angioplasty (327). Overexpression of IL-6 has been linked to apoptosis of contractile VSMCs and growth and proliferation of synthetic VSMCs

(12, 116). In addition to inducing cellular senescence, IL-1 β and IL-6 have also been found to mediate VSMC osteoblastic transition, with enhanced VSMC migration and cytoskeletal reorganization (93, 296).

Increased levels of *miR-155-5p* expression has been linked to IL-6 production in VSMCs and expression of *miR-155-5p* has been found to be induced by the activation of the NF- κ B pathway, which is related to inflammatory signaling within hVSMCs (215, 222, 315). On the other hand, no reports of *hsa-miR-146b-5p* relating to VSMC inflammation has been published, although *miR-146b-5p* has been reported as a negative regulator of IL-1 β in human airway SMCs, whose observation agreed with our results (57).

Our enrichment analyses observed discrepancies between the pathways regulated by *miR-155-5p* and *miR-146b-5p*. Based on both the RNA-Seq differential expression and qPCR validation data (**Figure 4.5-2** & **Figure 4.5-8**), *miR-155-5p* downregulation was much more significant compared to that of *miR-146b-5p*. As such, it is interpreted that the pathways associated with *miR-155-5p* target genes would be more affected by its changes in expression levels. Accordingly, data suggested that the downregulation of exosomal *miR-155-5p* and *miR-146b-5p* posed as an intercellular message from senescent hVSMCs to avoid additional proliferative and pro-inflammatory signaling in recipient cells.

5.6. Significant Downregulation of *hsa-miR-155-5p* Expression in Senescent hVSMCs and Their Exosomes

Both RNA-seq and qPCR data reported a significant decrease in intracellular and exosomal *miR-155-5p* expression in senescent hVSMCs and exosomes. GO enrichment analysis was carried out separately to assess *miR-155-5p* target genes association and found that *miR-155-5p* target genes were highly involved in “anatomical structural morphogenesis”, “negative regulation of transcription” and “cell cycle arrest” (**Figure 4.5-13**). These GO terms were associated with the target genes. Reduced levels of endogenous *miR-155-5p* will fail to suppress the target genes, which would enhance their biological function, therefore augmenting the associated enriched GO terms for above biological processes.

As mentioned in **5.4.3**, senescent hVSMCs dysregulated miRNAs promoted cytoskeletal changes and interfered with cell cycle progression at the G1/S phase. In addition to interacting with cyclin-dependent protein serine/threonine kinases described above, *miR-155-5p* target genes might also participate in histone methylation and negative regulation of RNA polymerase II (RNA Pol II). Histone methylation is a reversible post-translational modification process that acts as the “on/off switch” of gene transcription (86). Many studies have revealed that histone methylation was involved in a variety of vascular diseases, such as atherosclerotic and endothelial dysfunction, with prominent association to VSMCs (298).

One interesting correlation between the diminishing levels of *miR-155-5p* found in this study and other published studies was the relationship between *miR-155-5p* expression and Kruppel-like factor 5 (KLF5). KLF5 is a zinc-finger-containing transcription factor that plays an important role in cardiovascular remodelling by mediating VSMC proliferation and migration (253). KLF5 was found to induce *miR-155-5p* expression in VSMCs, whose exosomal transfer from VSMCs to ECs induced endothelial injury and promoted atherosclerosis (340). More recently, *miR-155-5p* was reported to associate with VSMC proliferation and apoptosis in

patients with abdominal aortic aneurysm (337). In addition, another recent study reported by a different group that downregulation of KLF5 levels could induce cellular senescence (172). Downstream signaling of KLF5 have been reported to involve in the inhibition of p21 in VSMCs (99). As mentioned earlier, downregulated intracellular miRNAs were also associated with unsuppressed target gene *CDKN1A* encoding the protein p21. These data suggested the potential existence of a KLF5/*miR-155-5p*/p21 signaling axis.

Altogether, these findings suggested that reduced *miR-155-5p* levels in senescent VSMCs might be due to reduced KLF5 levels and *miR-155-5p* expression might be a prominent marker to distinguish between VSMC proliferative and non-proliferative states. Additionally, downregulation of *miR-155-5p* could contribute to altered cellular architecture in replicative senescence, which might contribute to arterial stiffness. In conclusion, *miR-155-5p* deemed to be a worthy target for extensive study to investigate its full biological function in VSMCs in particular and vascular diseases as a whole.

5.7. Senescent hVSMCs Trying to Escape Death?

Although the fate of senescent cells are generally immune clearance or cell death, senescent cells have been reported to be resistant towards apoptotic signals (256), which was also reflected in our results. There was a high consensus in our data that senescent hVSMCs were resistant to apoptosis. In *in vitro* cell culture, although senescent hVSMCs stopped proliferating, they could survive for at least one month with regular media replenishment. GO and pathway enriched terms were highly associated with the regulation of apoptosis (**Table 14, Table 17** and **Table 23**).

Apoptosis is a gene-controlled form of programmed cell death whose activation mechanisms include intrinsic and extrinsic pathways (66). The mitochondria are involved in the intrinsic apoptotic pathway (159). Mitochondrial dysfunction is related to increased redox stress and is a feature in senescent cells which may mediate apoptosis dysregulation (259). Senescent hVSMCs showed declined stress response, which could nullify cellular apoptotic response to stress stimuli and promote survival (117).

Downregulation of intracellular *miR-155-5p* and *miR-20a-5p* were significantly associated to survival-promoting genes with unsuppressed expression of the anti-apoptotic BCL2 proteins (**Figure 4.5-21**), which are often overexpressed in senescent cells (291, 323). In addition, the activation of PI3K/Akt/mTOR pathway has been known to promote cell survival (10, 190, 318). Activated Akt can inhibit the pro-apoptotic protein Bad that initiates the Bax-Bak dependent mitochondrial pathway of apoptosis or FOXO3a and GSK3 involved in transcription of pro-apoptotic genes and degradation of BCL2 proteins (10, 67).

In VSMCs, the activation of the TGF- β /Smad3 signaling pathway has been found to promote VSMC proliferation and neointimal formation (279). Conversely, inhibition of TGF- β signaling has been linked to acquired resistance to apoptosis due to the loss of TGF- β receptors in low-

proliferating VSMCs (174). Our data suggested an increase in TGF- β production with decrease in TGF- β Smad-dependent signaling due to inhibitory actions of I-Smads. Therefore, the negative regulation of TGF- β might be contributing to senescent hVSMC resistance to apoptosis.

Much less is known about apoptotic signals between hVSMCs and neighbouring communication via the exosomal signaling axis. However, based on our data, senescent hVSMCs were no longer secreting miRNAs that promoted proliferative and pro-inflammatory signals. This could be interpreted as senescent hVSMCs attempting to attenuate local immune-attracting signals to evade clearance by immune cells.

Altogether, data suggested that senescent hVSMCs grew resistant to apoptosis by inhibiting pro-apoptotic signals, altering cellular stress response and evading from immune clearance. Although lowered proliferative and inflammatory signals might alleviate progression of vascular dysfunction, such as endothelial dysfunction and atherosclerosis, prolonged survival of senescent hVSMCs may pose as a negative regulator in their local environment, as they may influence neighbouring cells to transform into senescence-associated secretory phenotype (SASP), which may lead to overall vascular dysfunction (82).

Chapter 6. Limitations, Conclusion and Future Work

6.1. Limitations

Some potential limitations of the study include small sample size, individual variation and technological limitations. As the study focused on the non-targeted whole-genome sequencing of small RNAs, a higher number of biological replicates would greatly affect the budget for sequencing. As opposed to targeted sequencing, non-targeted sequencing requires higher (by 10-fold) data output as well as sequence reads per sample. Additionally, as the study focused on replicative senescence, the sample collection period was prolonged, which contributed to the decision to have a small sample size. When the sequencing data was analysed for differential expression, individual variation might have contributed to false positive or false negative discovery of differentially expressed miRNAs. As mentioned, miRNAs have been found to be tissue- and cell- specific and the signature miRNA profiles could vary from one individual to another. However, miRNA profiles must be screened in a larger cohort in order to ascertain this postulation. Finally, miRNA sequencing technology still requires tremendous advancement due to their small size and high G-C content. The upregulated exosomal *hsa-miR-7704* could not be validated using the chosen qPCR technology at the time due to its high G-C content, which made it impossible to design a primer for the miRNA in question. Regrettably, the potential for investigating the biological significance of exosomal *hsa-miR-7704* was hampered as its expression could not be experimentally validated.

Despite aforementioned limitations, stringent QC and filtering increased data integrity and confidence. Evidently, consistent miRNA profiles in young samples suggest that the issue of individual genetic variation was overcome and replicative senescence was mainly accountable for the differentially expressed miRNAs. On the other hand, continuous

advancement of small RNA sequencing technology has been promising, potentially facilitating the amplification of high G-C sequences such as exosomal *hsa-miR-7704* via simple qPCR experiments.

6.2. Conclusion

In summary, hVSMCs undergoing replicative senescence had altered morphology with elevated expression of SA β -gal, specifically detectable at pH6.0. Senescent marker genes encoding the proteins p16^{INK4 α} , p21^{Cip1} and p27^{Kip1} were highly expressed in senescent hVSMCs, accompanied by shortened telomere length, confirming replicative senescence. Exosomes secreted by young and senescent hVSMCs appeared to be different, suggesting changes in exosomal membrane composition as well as post-translational protein modifications in the exosome biogenesis pathway during replicative senescence. There was a significant amount of snoRNA and lincRNA content apart from miRNAs in the exosomes. In overview, exosomal RNA profiles, including snoRNAs and lincRNAs, remained to be further explored.

During hVSMC replicative senescence, differentially expressed miRNAs were involved in the regulation of cellular metabolism, intracellular transport, ATP interactions, cytoskeletal reorganization, stress response, cell cycle arrest, cellular senescence, ROS production and intercellular signaling. Senescent hVSMC intracellular and exosomal signaling might regulate cellular processes that promote cell survival. At the same time, anti-proliferative and anti-inflammatory exosomal signaling suggested an attempt to evade immune clearance. Significant loss of *hsa-miR-155-5p* might have contributed to the senescence phenotype and hVSMC resistance to apoptosis (**Figure 6.2-1**). Additionally, distinct miRNA levels in senescent hVSMC-derived exosomes also suggested that miRNAs were loaded in a selective and specific manner prior to exosome release.

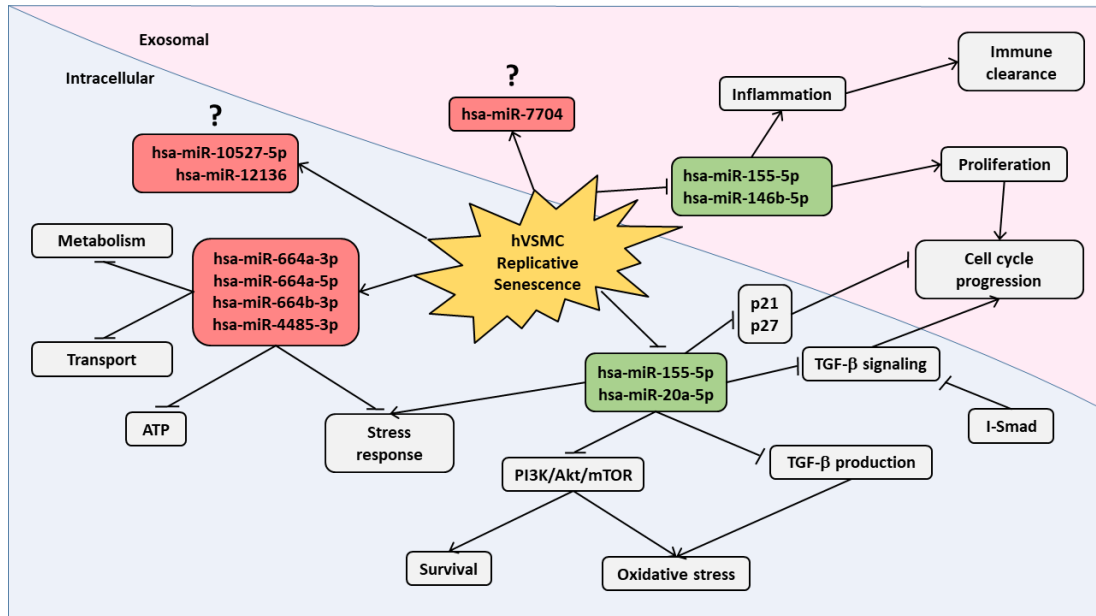


Figure 6.2-1: Schematic diagram of miRNA intracellular and exosomal regulation of hVSMC during replicative senescence. The miRNAs in red boxes were upregulated while miRNAs in green boxes were downregulated during hVSMC replicative senescence. Differentially expressed miRNAs were involved in the regulation of cellular metabolism, intracellular transport, ATP interactions, cytoskeletal reorganization, stress response, cell cycle arrest, cellular senescence, ROS production and intercellular signaling.

Overall, changes in miRNA signaling in senescent hVSMCs reflected association with early vascular aging. This study was the first to profile intracellular and exosomal miRNAs of hVSMCs during replicative senescence. Novel observations from the study include exosomal clustering and TSG-101 post-translational modifications, which require further studies to elucidate their biological significance. Lastly, intracellular and exosomal *hsa-miR-155-5p* downregulation indicated a potential cell-type-specific biomarker of hVSMC during replicative senescence. In conclusion, our findings suggested replicative senescence manifested through cell cycle arrest, increased oxidative stress, cytoskeletal reorganization and reduced inflammation, which appeared to contribute to the development of early vascular aging. Early vascular aging might be a contributing risk factor for hypertension and other vascular diseases.

6.3. Future work

The initial phase of our study was achieved and also gave rise to many more interesting research questions to be addressed. There is a wide range of downstream experimental studies that could be considered for the data and results that have been uncovered. Future work may focus on further characterizing of hVSMC-derived exosomes, the dysregulated intracellular miRNAs or exosomal miRNAs in senescent hVSMCs, or further bioinformatics and data mining on other RNA species as well as discovered novel mature miRNAs.

6.3.1. Direct Interactions and Functional Studies Derived from the Profiling of the miRNA Landscape within hVSMCs and Exosomes during Replicative Senescence

6.3.1.1. Expression Validation and Functional Study on Upregulated Exosomal hsa-miR-7704 in Senescent hVSMCs

First and foremost, the exosomal miRNA *hsa-miR-7704* should be validated using a primer design method that would complement a more advanced technology, such as the locked nucleic acid (LNA) technology. Depending on the significance of exosomal *miR-7704*, we can proceed to target interaction experiment to assess the mode of binding of exosomal *miR-7704* to target genes. Additionally, exosomes from senescent hVSMCs can also be isolated and used to treat young hVSMCs to look for phenotypic transitions or changes. Senescent hVSMCs can also be co-cultured with ECs to further study of intercellular communication and how senescent exosomal signaling would affect endothelial changes which may lead to endothelial dysfunction in vascular diseases.

6.3.1.2. *Novel biological significance of upregulated intracellular hsa-miR-10527-5p, hsa-miR-12136 and hsa-miR-4485-3p in human vascular smooth muscle cells during replicative senescence*

There was a complete lack of reports on the expression of *miR-10527-5p* and *miR-12136* in hVSMCs and their interaction with target genes still remains a mystery. These miRNAs, including *miR-4485-3p*, were still poorly characterized, yet their expression was significantly elevated in replicative senescent hVSMCs. Therefore, elucidating their biological significance in senescent hVSMCs could prove to be extremely meaningful.

For the upregulated intracellular *hsa-miR-10527-5p*, *hsa-miR-12136* and *hsa-miR-4485-3p*, target genes could be predicted using computational predictions based on the miRNA conserved seed sequences, target mRNA 3' UTR, coding region (CDS) or 5' UTR sequences and free energy binding index to determine the stability of binding. Computational predictions can then be followed with experimental validation of miRNA-target interaction study using the luciferase assay to determine direct/indirect binding. Subsequently, senescent hVSMCs can be transfected with miRNA mimic or inhibitors to observe changes in target gene expression in order to assess the biological significance of that particular miRNA expression within senescent hVSMCs. Other functional studies could also be performed as appropriate.

6.3.1.3. *Investigating up-and downstream signaling of hsa-miR-155-5p*

Results obtained have highly suggested the importance of *miR-155-5p* expression in the entry of proliferative hVSMCs into senescence. Further elucidation of *miR-155-5p* signalling pathway is, therefore, encouraged to discover upstream factors that would influence *miR-155-5p* expression as well as downstream targets that would promote cellular proliferation upon their inhibition. Additionally, *miR-155-5p* could also be a therapeutic target whose expression levels could be manipulated as an "on/off" switch for hVSMC proliferation.

6.3.2. Long Intergenic Non-coding RNA Profiling in Young and Senescent hVSMC-Derived Exosomes

Apart from the miRNA discovered, our data also contained reads from other RNA classes, particularly snoRNAs and lincRNAs in hVSMC-derived exosomes. Analysing differential expression of these RNAs using the CAP-miRSeq workflow could potentially discover interesting differences in the expression of snoRNA and lincRNA in replicative senescent hVSMCs. In particular, lincRNA has been shown to be promising targets of study in recent reports and further exploration of these RNAs may yield fruitful results that would contribute to our understanding of hVSMC senescence.

6.3.3. Exosome Composition of Senescent hVSMCs and Uptake by Recipient Cells

Qualitative analyses of exosomes secreted by hVSMCs observed interesting differences between proliferative and senescent hVSMC-derived exosomes. Proteomic studies and comparison between these two conditions would yield promising results not only of the exosomal composition but also potential post-translational modifications of exosomal proteins during vesicle formation or loading.

6.3.4. Linking Differentially Expressed miRNAs from Replicative Senescent hVSMCs to Arterial Stiffness and Hypertension

In order to link differentially expressed miRNAs from replicative senescent hVSMCs to arterial stiffness, the second phase of the study, which is to perform functional studies and validation of the biological significance of the identified miRNAs and their target genes. These studies can be coupled with *in vitro* or *ex vivo* culture of hVSMCs from patients with arterial stiffness or animal models induced with arterial stiffness. As early vascular aging and arterial stiffness are major events that contribute to the early development of hypertension, identifying a

panel of biomarkers for these conditions will greatly increase the chances of establishing a method to accurately diagnose the early development of hypertension.

Subsequently, in order to extrapolate the association between differentially expressed miRNAs from replicative senescent hVSMCs to hypertension, the last phase of the study can be performed, which involved clinical screening and comparison between healthy and early hypertensive subjects using a panel of the differentially expressed miRNAs combined with functionally validated mRNA targets obtainable through the second phase. Ultimately, study should be tailored to be suitable for downstream transition into translational, bench-to-bedside research, as the original aim was to develop a panel of diagnostic biomarkers that could be implemented in routine clinical settings.

Chapter 7. References

1. **Ab Majid NL, Omar MA, Khoo YY, Mahadir Naidu B, Ling Miaw Yn J, Rodzlan Hasani WS, Mat Rifin H, Abd Hamid HA, Robert Lourdes TG, Mohd Yusoff MF.** Prevalence, Awareness, Treatment and Control of hypertension in the Malaysian population: findings from the National Health and Morbidity Survey 2006–2015. *J Hum Hypertens* 32, 2018. doi: 10.1038/s41371-018-0082-x.
2. **Abdelfattah AM, Park C, Choi MY.** Update on non-canonical microRNAs. *Biomol Concepts* 5: 275–287, 2014. doi: 10.1515/bmc-2014-0012.
3. **Abdelmohsen K, Gorospe M.** Noncoding RNA control of cellular senescence. *Wiley Interdiscip Rev RNA* 6, 2015. doi: 10.1002/wrna.1297.
4. **Abdelmohsen K, Panda A, Kang M-J, Xu J, Selimyan R, Yoon J-H, Martindale JL, De S, Wood WH, Becker KG, Gorospe M.** SAL-RNAs: Senescence-associated long non-coding RNAs. *Aging Cell* 12, 2013.
5. **Agarwal V, Bell GW, Nam JW, Bartel DP.** Predicting effective microRNA target sites in mammalian mRNAs. *Elife* 4, 2015. doi: 10.7554/eLife.05005.
6. **Agrawal N, Dasaradhi PVN, Mohammed A, Malhotra P, Bhatnagar RK, Mukherjee SK.** RNA Interference: Biology, Mechanism, and Applications. *Microbiol Mol Biol Rev* 67: 657–685, 2003. doi: 10.1128/MMBR.67.4.657-685.2003.
7. **Aird KM, Zhang R.** ATM in senescence. *Oncotarget* 6: 14729–14730, 2015.
8. **Alanazi AZ, Clark MA.** Angiotensin III induces p38 Mitogen-activated protein kinase leading to proliferation of vascular smooth muscle cells. *Pharmacol Reports* 72, 2020. doi: 10.1007/s43440-019-00035-8.
9. **Ali N, Venkateswaran G, Garcia E, Landry T, McColl H, Sergi C, Persad A, Abuetaab Y, Eisenstat DD, Persad S.** Osteosarcoma progression is associated with increased nuclear levels and transcriptional activity of activated β -catenin. *Genes and Cancer* 10: 63–79, 2019. doi: 10.18632/oncoscience.191.
10. **Allard D, Figg N, Bennett MR, Littlewood TD.** Akt regulates the survival of vascular smooth muscle cells via inhibition of FoxO3a and GSK3. *J Biol Chem* 283, 2008. doi: 10.1074/jbc.M710098200.
11. **Ambros V, Bartel B, Bartel DP, Burge CB, Carrington JC, Chen X, Dreyfuss G, Eddy SR, Griffiths-Jones S, Marshall M, Matzke M, Ruvkun G, Tuschl T.** A uniform system for microRNA annotation. *Rna* 9: 277–279, 2003. doi: 10.1261/rna.2183803.
12. **An Z, Qiao F, Lu Q, Ma Y, Liu Y, Lu F, Xu Z.** Interleukin-6 downregulated vascular smooth muscle cell contractile proteins via ATG4B-mediated autophagy in thoracic aortic dissection. *Heart Vessels* 32, 2017. doi: 10.1007/s00380-017-1054-8.
13. **Andrade JM, Pobre V, Silva IJ, Domingues S, Arraiano CM.** The Role of 3'-5' Exoribonucleases in RNA Degradation. .
14. **Anerillas C, Abdelmohsen K, Gorospe M.** Regulation of senescence traits by MAPKs. *GeroScience* 42: 2020.
15. **Anjum R, Blenis J.** The RSK family of kinases: Emerging roles in cellular signalling. *Nat. Rev. Mol. Cell Biol.* 9: 2008.

16. **Babst M.** MVB vesicle formation: ESCRT-dependent, ESCRT-independent and everything in between. *Curr Opin Cell Biol* 23: 452–457, 2011. doi: 10.1016/j.ceb.2011.04.008.
17. **Badi I, Burba I, Ruggeri C, Zeni F, Bertolotti M, Scopece A, Pompilio G, Raucci A.** MicroRNA-34a Induces Vascular Smooth Muscle Cells Senescence by SIRT1 Downregulation and Promotes the Expression of Age-Associated Pro-inflammatory Secretary Factors. *Journals Gerontol - Ser A Biol Sci Med Sci* 70: 1304–1311, 2015. doi: 10.1093/gerona/glu180.
18. **Baglio SR, Rooijers K, Koppers-Lalic D, Verweij FJ, Pérez Lanzón M, Zini N, Naaijkens B, Perut F, Niessen HWM, Baldini N, Pegtel DM.** Human bone marrow- and adipose-mesenchymal stem cells secrete exosomes enriched in distinctive miRNA and tRNA species. *Stem Cell Res Ther* 6, 2015. doi: 10.1186/s13287-015-0116-z.
19. **Bail S, Swerdel M, Liu H, Jiao X, Goff LA, Hart RP, Kiledjian M.** Differential regulation of microRNA stability. *RNA* 16: 1032–1039, 2010. doi: 10.1261/rna.1851510.
20. **Basquin J, Roudko V V, Rode M, Basquin C, Séraphin B, Conti E.** Architecture of the nuclease module of the yeast ccr4-Not complex: The not1-caf1-ccr4 interaction. *Mol Cell* 48: 207–218, 2012. doi: 10.1016/j.molcel.2012.08.014.
21. **Baudier RL, Czarny-Ratajczak M, Eastwood JR, Zvezdaryk KJ, Norton EB.** Transcriptomic analyses reveal senescent and SnoRNA changes in B cells with age irrespective of vaccine-stimulation in mice. [Online]. *J Immunol* 196: 198.7 LP-198.7, 2016. http://www.jimmunol.org/content/196/1_Supplement/198.7.abstract.
22. **Beaumont J, López B, Ravassa S, Hermida N, José GS, Gallego I, Valencia F, Gómez-Doblas JJ, De Teresa E, Díez J, González A.** MicroRNA-19b is a potential biomarker of increased myocardial collagen cross-linking in patients with aortic stenosis and heart failure. *Sci Rep* 7, 2017. doi: 10.1038/srep40696.
23. **Bellingham SA, Coleman BM, Hill AF.** Small RNA deep sequencing reveals a distinct miRNA signature released in exosomes from prion-infected neuronal cells. *Nucleic Acids Res* 40, 2012. doi: 10.1093/nar/gks832.
24. **Ben-Porath I, Weinberg RA.** The signals and pathways activating cellular senescence. *Int. J. Biochem. Cell Biol.* 37: 961–976, 2005.
25. **Bhaskaran M, Mohan M.** MicroRNAs: History, Biogenesis, and Their Evolving Role in Animal Development and Disease. *Vet Pathol* 51: 759–774, 2014. doi: 10.1177/0300985813502820.
26. **Biran A, Perelmutter M, Gal H, G.A. Burton D, Ovadya Y, Vadai E, Geiger T, Krizhanovsky V.** Senescent cells communicate via intercellular protein transfer. *Genes Dev* 29, 2014. doi: 10.1101/gad.259341.115.
27. **Blackburn EH.** Switching and signaling at the telomere. *Cell* 106: 661–673, 2001. doi: 10.1016/S0092-8674(01)00492-5.
28. **Blackburn EH, Gall JG.** A tandemly repeated sequence at the termini of the extrachromosomal ribosomal RNA genes in Tetrahymena. *J Mol Biol* 120: 33–53, 1978. doi: 10.1016/0022-2836(78)90294-2.
29. **Blagosklonny M V.** Cell cycle arrest is not senescence. *Aging (Albany NY)* 3: 94–101,

2011. doi: 100281 [pii].
30. **Bloch A.** Cardiovascular risks of hypertension. *Internist Prax* 62: 136–143, 2020.
 31. **Boisvert F, Koningsbruggen S Van, Navascués J, Lamond AI, van Koningsbruggen S.** The multifunctional nucleolus. [Online]. *Nat Rev Mol Cell Biol* 8: 574–585, 2007. <http://www.ncbi.nlm.nih.gov/pubmed/17519961>.
 32. **Boyer M, Baggett A, Scalia R, Eguchi S, Rizzo V.** Characterization of exosomes isolated from cultured vascular endothelial and smooth muscle cells. *FASEB J* 31: e837.7, 2017. doi: 10.1096/fasebj.31.1_supplement.837.7.
 33. **Bratic A, Larsson N.** Review series The role of mitochondria in aging. *J Clin Invest* 123: 951–957, 2013. doi: 10.1172/JCI64125.Mitochondrial.
 34. **Braun JE, Huntzinger E, Fauser M, Izaurralde E.** GW182 proteins directly recruit cytoplasmic deadenylase complexes to miRNA targets. *Mol Cell* 44: 120–133, 2011. doi: 10.1016/j.molcel.2011.09.007.
 35. **Brookes S, Rowe J, Gutierrez Del Arroyo A, Bond J, Peters G.** Contribution of p16(INK4a) to replicative senescence of human fibroblasts. *Exp Cell Res* 298: 549–559, 2004. doi: 10.1016/j.yexcr.2004.04.035\rS0014482704002551 [pii].
 36. **Cai Y, Nagel DJ, Zhou Q, Cygnar KD, Zhao H, Li F, Pi X, Knight PA, Yan C.** Role of cAMP-phosphodiesterase 1C signaling in regulating growth factor receptor stability, vascular smooth muscle cell growth, migration, and neointimal hyperplasia. *Circ Res* 116: 1120–1132, 2015. doi: 10.1161/CIRCRESAHA.116.304408.
 37. **Campbell GR, Chamley-Campbell JH.** Smooth muscle phenotypic modulation: Role in atherogenesis. *Med Hypotheses* 7: 729–735, 1981. doi: 10.1016/0306-9877(81)90084-0.
 38. **Campisi J.** The biology of replicative senescence. *Eur J Cancer* 33: 703–709, 1997. doi: 10.1016/S0959-8049(96)00058-5.
 39. **Campisi J, d’Adda di Fagagna F.** Cellular senescence: when bad things happen to good cells. *Nat Rev Mol Cell Biol* 8: 729–740, 2007.
 40. **Carrel A.** On The Permanent Life Of Tissues Outside Of The Organism. *J Exp Med* 15: 516–528, 1912. doi: 10.1084/jem.15.5.516.
 41. **Casella G, Munk R, Kim KM, Piao Y, De S, Abdelmohsen K, Gorospe M.** Transcriptome signature of cellular senescence. *Nucleic Acids Res* 47, 2019. doi: 10.1093/nar/gkz555.
 42. **Catalanotto C, Cogoni C, Zardo G.** MicroRNA in control of gene expression: An overview of nuclear functions. *Int J Mol Sci* 7: 1712, 2016. doi: 10.3390/ijms17101712.
 43. **Cawthon RM.** Telomere measurement by quantitative PCR. *Nucleic Acids Res* 30: e47, 2002. doi: 10.1093/nar/30.10.e47.
 44. **Cecelja M, Chowienczyk P.** Dissociation of aortic pulse wave velocity with risk factors for cardiovascular disease other than hypertension: A systematic review. *Hypertension* 54: 1328–1336, 2009. doi: 10.1161/HYPERTENSIONAHA.109.137653.
 45. **Chandek C, Mooi WJ.** Oncogene-induced Cellular Senescence. *Adv Anat Pathol* 17: 42–48, 2010. doi: 10.1097/PAP.0b013e3181c66f4e.

46. **Chang TC, Wentzel EA, Kent OA, Ramachandran K, Mullendore M, Lee KH, Feldmann G, Yamakuchi M, Ferlito M, Lowenstein CJ, Arking DEE, Beer MA, Maitra A, Mendell JT.** Transactivation of miR-34a by p53 Broadly Influences Gene Expression and Promotes Apoptosis. *Mol Cell* 26: 745–752, 2007. doi: 10.1016/j.molcel.2007.05.010.
47. **Chekulaeva M, Mathys H, Zipprich JT, Attig J, Colic M, Parker R, Filipowicz W.** MiRNA repression involves GW182-mediated recruitment of CCR4-NOT through conserved W-containing motifs. *Nat Struct Mol Biol* 18: 1218–1226, 2011. doi: 10.1038/nsmb.2166.
48. **Chen W, Wang X, Wei G, Huang Y, Shi Y, Li D, Qiu S, Zhou B, Cao J, Chen M, Qin P, Jin W, Ni T.** Single-Cell Transcriptome Analysis Reveals Six Subpopulations Reflecting Distinct Cellular Fates in Senescent Mouse Embryonic Fibroblasts. *Front Genet* 11, 2020. doi: 10.3389/fgene.2020.00867.
49. **Chen Y, Lun ATL, Smyth GK.** Differential Expression Analysis of Complex RNA-seq Experiments Using edgeR. In: *Statistical Analysis of Next Generation Sequencing Data*. 2014.
50. **Chen Y, Wang X.** MiRDB: An online database for prediction of functional microRNA targets. *Nucleic Acids Res* 48, 2020. doi: 10.1093/nar/gkz757.
51. **Cheng Y, Liu X, Yang J, Lin Y, Xu DZ, Lu Q, Deitch EA, Huo Y, Delphin ES, Zhang C.** MicroRNA-145, a novel smooth muscle cell phenotypic marker and modulator, controls vascular neointimal lesion formation. *Circ Res* 105: 158–166, 2009. doi: 10.1161/CIRCRESAHA.109.197517.
52. **Chu CY, Rana TM.** Translation repression in human cells by MicroRNA-induced gene silencing requires RCK/p54. *PLoS Biol* 4: 1122–1136, 2006. doi: 10.1371/journal.pbio.0040210.
53. **Clancy S (2008) DD& RM for MDI.** DNA Damage & Repair: Mechanisms for Maintaining DNA Integrity. *Nat Educ* 1: 103, 2008. doi: 10.1038/nrm2351.pdf.
54. **Cohen P.** The origins of protein phosphorylation. *Nat Cell Biol* 4: E127–E130, 2002. doi: 10.1038/ncb0502-e127.
55. **Collier SR, Landram MJ.** Treatment of prehypertension: Lifestyle and/or medication. *Vasc. Health Risk Manag.* 8: 613–619, 2012.
56. **Comai L.** The nucleolus: A paradigm for cell proliferation and aging. *Brazilian J Med Biol Res* 32: 1473–1478, 1999.
57. **Comer BS, Camoretti-Mercado B, Kogut PC, Halayko AJ, Solway J, Gerthoffer WT.** MicroRNA-146a and microRNA-146b expression and anti-inflammatory function in human airway smooth muscle. *Am J Physiol - Lung Cell Mol Physiol* 307, 2014. doi: 10.1152/ajplung.00174.2014.
58. **Coppé J-P, Desprez P-Y, Krtolica A, Campisi J.** The Senescence-Associated Secretory Phenotype: The Dark Side of Tumor Suppression. *Annu Rev Pathol Mech Dis* 5: 99–118, 2010. doi: 10.1146/annurev-pathol-121808-102144.
59. **Correia-Melo C, Passos JF.** Mitochondria: Are they causal players in cellular senescence? *Biochim Biophys Acta - Bioenerg* 1847: 1373–1379, 2015. doi: 10.1016/j.bbabi.2015.05.017.

60. **Creemers EE, Tijssen AJ, Pinto YM.** Circulating MicroRNAs. *Circ Res* 110: 483–495, 2012. doi: 10.1161/CIRCRESAHA.111.247452.
61. **Crescitelli R, Lässer C, Szabó TG, Kittel A, Eldh M, Dianzani I, Buzás EI, Lötvall J.** Distinct RNA profiles in subpopulations of extracellular vesicles: Apoptotic bodies, microvesicles and exosomes. *J Extracell Vesicles* 2, 2013. doi: 10.3402/jev.v2i0.20677.
62. **Cuenda A, Rousseau S.** p38 MAP-Kinases pathway regulation, function and role in human diseases. *Biochim. Biophys. Acta - Mol. Cell Res.* 1773: 2007.
63. **Cuervo AM.** Autophagy and aging: keeping that old broom working. *Trends Genet.* 24: 604–612, 2008.
64. **Cui R-R, Li S-J, Liu L-J, Yi L, Liang Q-H, Zhu X, Liu G-Y, Liu Y, Wu S-S, Liao X-B, Yuan L-Q, Mao D-A, Liao E-Y.** MicroRNA-204 regulates vascular smooth muscle cell calcification in vitro and in vivo. *Cardiovasc Res* 96: 320–329, 2012. doi: 10.1093/cvr/cvs258.
65. **d’Adda di Fagagna F.** Living on a break: cellular senescence as a DNA-damage response. *Nat Rev Cancer* 8: 512–522, 2008.
66. **D’Arcy MS.** Cell death: a review of the major forms of apoptosis, necrosis and autophagy. *Cell Biol. Int.* 43: 2019.
67. **Datta SR, Dudek H, Xu T, Masters S, Haian F, Gotoh Y, Greenberg ME.** Akt phosphorylation of BAD couples survival signals to the cell- intrinsic death machinery. *Cell* 91, 1997. doi: 10.1016/S0092-8674(00)80405-5.
68. **De Cecco M, Jeyapalan J, Zhao X, Tamamori-Adachi M, Sedivy JM.** Nuclear protein accumulation in cellular senescence and organismal aging revealed with a novel single-cell resolution fluorescence microscopy assay. *Aging (Albany NY)* 3: 955–967, 2011.
69. **Degirmenci U, Lei S.** Role of lncRNAs in cellular aging. *Front. Endocrinol. (Lausanne).* 7: 2016.
70. **Deschênes-Simard X, Lessard F, Gaumont-Leclerc MF, Bardeesy N, Ferbeyre G.** Cellular senescence and protein degradation: Breaking down cancer. *Cell Cycle* 13 Landes Bioscience: 1840–1858, 2014.
71. **Desvignes T, Batzel P, Berezikov E, Eilbeck K, Eppig JT, McAndrews MS, Singer A, Postlethwait JH.** miRNA Nomenclature: A View Incorporating Genetic Origins, Biosynthetic Pathways, and Sequence Variants. *Trends Genet* 31: 613–626, 2015. doi: 10.1016/j.tig.2015.09.002.
72. **Dimri GP, Lee X, Basile G, Acosta M, Scott G, Roskelley C, Medrano EE, Linskens M, Rubelj I, Pereira-Smith O.** A biomarker that identifies senescent human cells in culture and in aging skin in vivo. *Proc. Natl. Acad. Sci. U. S. A.* 92: 9363–9367, 1995.
73. **Dinardo CL, Venturini G, Zhou EH, Watanabe IS, Campos LCG, Dariolli R, da Motta-Leal-Filho JM, Carvalho VM, Cardozo KHM, Krieger JE, Alencar AM, Pereira AC.** Variation of mechanical properties and quantitative proteomics of VSMC along the arterial tree. *Am J Physiol Circ Physiol* 306: H505–H516, 2014. doi: 10.1152/ajpheart.00655.2013.
74. **Dinarello CA.** Biologic basis for interleukin-1 in disease. *Blood* 87: 1996.

75. **Ding J, Li X, Hu H.** TarPmiR: A new approach for microRNA target site prediction. *Bioinformatics* 32, 2016. doi: 10.1093/bioinformatics/btw318.
76. **Dupont A, Corseaux D, Dekeyzer O, Drobecq H, Guihot AL, Susen S, Vincentelli A, Amouyel P, Jude B, Pinet F.** The proteome and secretome of human arterial smooth muscle cells. *Proteomics* 5: 585–596, 2005. doi: 10.1002/pmic.200400965.
77. **Edgar JR, Manna PT, Nishimura S, Banting G, Robinson MS.** Tetherin is an exosomal tether. *Elife* 5, 2016. doi: 10.7554/eLife.17180.
78. **Eun SY, Ko YS, Park SW, Chang KC, Kim HJ.** IL-1 β enhances vascular smooth muscle cell proliferation and migration via P2Y2 receptor-mediated RAGE expression and HMGB1 release. *Vascul Pharmacol* 72, 2015. doi: 10.1016/j.vph.2015.04.013.
79. **Fabian MR, Cieplak MK, Frank F, Morita M, Green J, Srikumar T, Nagar B, Yamamoto T, Raught B, Duchaine TF, Sonenberg N.** MiRNA-mediated deadenylation is orchestrated by GW182 through two conserved motifs that interact with CCR4-NOT. *Nat Struct Mol Biol* 18: 1211–1217, 2011. doi: 10.1038/nsmb.2149.
80. **Fan Y, Siklenka K, Arora SK, Ribeiro P, Kimmins S, Xia J.** miRNet - dissecting miRNA-target interactions and functional associations through network-based visual analysis. *Nucleic Acids Res* 44, 2016. doi: 10.1093/nar/gkw288.
81. **Fisher SA.** Vascular smooth muscle phenotypic diversity and function. *Physiol Genomics* 42A: 169–187, 2010. doi: 10.1152/physiolgenomics.00111.2010.
82. **Gardner SE, Humphry M, Bennett MR, Clarke MCH.** Senescent vascular smooth muscle cells drive inflammation through an interleukin-1 α -dependent senescence-associated secretory phenotype. *Atherosclerosis* 244, 2016. doi: 10.1016/j.atherosclerosis.2015.10.065.
83. **Ghebre YT, Yakubov E, Wong WT, Krishnamurthy P.** Vascular Aging: Implications for Cardiovascular Disease and Therapy. *Transl Med* 6: 183, 2016. doi: 10.4172/2161-1025.1000183.
84. **Gomez D, Owens GK.** Smooth muscle cell phenotypic switching in atherosclerosis. *Cardiovasc Res* 95: 156–164, 2012. doi: 10.1093/cvr/cvs115.
85. **Graf K, Xi XP, Yang D, Fleck E, Hsueh WA, Law RE.** Mitogen-activated protein kinase activation is involved in platelet-derived growth factor-directed migration by vascular smooth muscle cells. *Hypertension* 29, 1997. doi: 10.1161/01.hyp.29.1.334.
86. **Greer EL, Shi Y.** Histone methylation: A dynamic mark in health, disease and inheritance. *Nat. Rev. Genet.* 13: 2012.
87. **Gregory RI, Yan KP, Amuthan G, Chendrimada T, Doratotaj B, Cooch N, Shiekhattar R.** The Microprocessor complex mediates the genesis of microRNAs. *Nature* 432: 235–240, 2004. doi: 10.1038/nature03120.
88. **Gruenbaum Y, Margalit A, Goldman RD, Shumaker DK, Wilson KL.** The nuclear lamina comes of age. *Nat Rev Mol Cell Biol* 6: 21–31, 2005.
89. **Gump J, Stokoe D, McCormick F.** Phosphorylation of p16INK4A correlates with Cdk4 association. *J Biol Chem* 278, 2003. doi: 10.1074/jbc.C200622200.
90. **Ha M, Kim VN.** Regulation of microRNA biogenesis. *Nat Rev Mol Cell Biol* 15: 509–524, 2014. doi: 10.1038/nrm3838.

91. **Haigis MC, Yankner BA.** The Aging Stress Response. *Mol. Cell* 40: 2010.
92. **Håkansson KEJ, Goossens EAC, Trompet S, Van Ingen E, De Vries MR, Van Der Kwast RVCT, Ripa RS, Kastrup J, Hohensinner PJ, Kaun C, Wojta J, Böhringer S, Le Cessie S, Jukema JW, Quax PHA, Yael Nossent A.** Genetic associations and regulation of expression indicate an independent role for 14q32 snoRNAs in human cardiovascular disease. *Cardiovasc Res* 115, 2019. doi: 10.1093/cvr/cvy309.
93. **Han L, Zhang Y, Zhang M, Guo L, Wang J, Zeng F, Xu D, Yin Z, Xu Y, Wang D, Zhou H.** Interleukin-1 β -Induced Senescence Promotes Osteoblastic Transition of Vascular Smooth Muscle Cells. *Kidney Blood Press Res* 45, 2020. doi: 10.1159/000504298.
94. **Hannon GJ, Beach D.** p15INK4B is a potential effector of TGF-beta-induced cell cycle arrest. *Nature* 371: 257–261, 1994.
95. **Harding C, Heuser J, Stahl P.** Endocytosis and intracellular processing of transferrin and colloidal gold-transferrin in rat reticulocytes: demonstration of a pathway for receptor shedding. *Eur J Cell Biol* 35: 256–263, 1984.
96. **Hayflick L.** The Cell Biology of Aging. *J Invest Dermatol* 73: 8–14, 1979. doi: 10.1111/1523-1747.ep12532752.
97. **Hayflick L.** The illusion of cell immortality. *Br J Cancer* 83: 841–846, 2000. doi: 10.1054/bjoc.2000.1296.
98. **Hayflick L, Moorhead PS.** The serial cultivation of human diploid cell strains. *Exp Cell Res* 25: 585–621, 1961. doi: 10.1016/0014-4827(61)90192-6.
99. **He M, Han M, Zheng B, Shu Y-N, Wen J-K.** Angiotensin II Stimulates KLF5 Phosphorylation and its Interaction with c-Jun Leading to Suppression of p21 Expression in Vascular Smooth Muscle Cells. *J Biochem* 146: 683–691, 2009. doi: 10.1093/jb/mvp115.
100. **Hein N, Sanij E, Quin J, M. K, Ganley A, D. R.** The Nucleolus and Ribosomal Genes in Aging and Senescence. In: *Senescence*, p. 171–208.
101. **Helin K, Wu CL, Fattaey AR, Lees JA, Dynlacht BD, Ngwu C, Harlow E.** Heterodimerization of the transcription factors E2F-1 and DP-1 leads to cooperative trans-activation. *Genes Dev* 7: 1850–1861, 1993.
102. **Hergenreider E, Heydt S, Tréguer K, Boettger T, Horrevoets AJG, Zeiher AM, Scheffer MP, Frangakis AS, Yin X, Mayr M, Braun T, Urbich C, Boon RA, Dimmeler S.** Atheroprotective communication between endothelial cells and smooth muscle cells through miRNAs. *Nat Cell Biol* 14: 249–256, 2012. doi: 10.1038/ncb2441.
103. **Hers I, Vincent EE, Tavaré JM.** Akt signalling in health and disease. *Cell Signal* 23: 1515–1527, 2011. doi: 10.1016/j.cellsig.2011.05.004.
104. **Hershko a, Ciechanover A.** The ubiquitin system. *Annu Rev Biochem* 67: 425–479, 1998. doi: 10.1146/annurev.biochem.67.1.425.
105. **Hessvik NP, Llorente A.** Current knowledge on exosome biogenesis and release. *Cell Mol Life Sci* 75: 193–208, 2018. doi: 10.1007/s00018-017-2595-9.
106. **Hoppe T.** Life and destruction: ubiquitin-mediated proteolysis in aging and longevity [Online]. *F1000 Biol Rep* 2: 79, 2010. <http://www.ncbi.nlm.nih.gov/pubmed/21151840%5Cnhttp://f1000.com/prime/reports/b/2/79/pdf>.

107. **Horbelt D, Denkis A, Knaus P.** A portrait of Transforming Growth Factor β superfamily signalling: Background matters. *Int J Biochem Cell Biol* 44: 469–474, 2012. doi: 10.1016/j.biocel.2011.12.013.
108. **Houghton D, Jones TW, Cassidy S, Siervo M, MacGowan GA, Trenell MI, Jakovljevic DG.** The effect of age on the relationship between cardiac and vascular function. *Mech Ageing Dev* 153: 1–6, 2015. doi: 10.1016/j.mad.2015.11.001.
109. **Hovest MG, Bruggenolte N, Hosseini KS, Krieg T, Herrmann G.** Senescence of human fibroblasts after psoralen photoactivation is mediated by ATR kinase and persistent DNA damage foci at telomeres [Online]. *Mol Biol Cell* 17: 1758–1767, 2006.
http://www.ncbi.nlm.nih.gov/entrez/query.fcgi?cmd=Retrieve&db=PubMed&dopt=Citation&list_uids=16436511%5CnD:%5CEigene.
110. **Huang HY, Lin YCD, Li J, Huang KY, Shrestha S, Hong HC, Tang Y, Chen YG, Jin CN, Yu Y, Xu JT, Li YM, Cai XX, Zhou ZY, Chen XH, Pei YY, Hu L, Su JJ, Cui SD, Wang F, Xie YY, Ding SY, Luo MF, Chou CH, Chang NW, Chen KW, Cheng YH, Wan XH, Hsu WL, Lee TY, Wei FX, Huang H Da.** MiRTarBase 2020: Updates to the experimentally validated microRNA-target interaction database. *Nucleic Acids Res* 48, 2020. doi: 10.1093/nar/gkz896.
111. **Hudgins AD, Tazearslan C, Tare A, Zhu Y, Huffman D, Suh Y.** Age- and tissue-specific expression of senescence biomarkers in mice. *Front Genet* 9, 2018. doi: 10.3389/fgene.2018.00059.
112. **Huertas P, Aguilera A.** Cotranscriptionally Formed DNA:RNA Hybrids Mediate Transcription Elongation Impairment and Transcription-Associated Recombination. *Mol Cell* 12: 711–721, 2003. doi: 10.1016/j.molcel.2003.08.010.
113. **Huertas P, Aguilera A.** Cotranscriptionally Formed DNA:RNA Hybrids Mediate Transcription Elongation Impairment and Transcription-Associated Recombination. *Mol Cell* 12: 711–721, 2003. doi: 10.1016/j.molcel.2003.08.010.
114. **Hung MC, Link W.** Protein localization in disease and therapy. *J Cell Sci* 124, 2011. doi: 10.1242/jcs.089110.
115. **Huveneers S, Daemen MJAP, Hordijk PL.** Between Rho(k) and a Hard Place. *Circ Res* 116: 895–908, 2015. doi: 10.1161/CIRCRESAHA.116.305720.
116. **Ikeda U, Ikeda M, Oohara T, Oguchi A, Kamitani T, Tsuruya Y, Kano S.** Interleukin 6 stimulates growth of vascular smooth muscle cells in a PDGF-dependent manner. *Am J Physiol - Hear Circ Physiol* 260, 1991. doi: 10.1152/ajpheart.1991.260.5.h1713.
117. **Iurlaro R, Muñoz-Pinedo C.** Cell death induced by endoplasmic reticulum stress. *FEBS J.*: 2016.
118. **Iyemere VP, Proudfoot D, Weissberg PL, Shanahan CM.** Vascular smooth muscle cell phenotypic plasticity and the regulation of vascular calcification. *J Intern Med* 260: 192–210, 2006. doi: 10.1111/j.1365-2796.2006.01692.x.
119. **Janas MM, Wang B, Harris AS, Aguiar M, Shaffer JM, Subrahmanyam YVBK, Behlke MA, Wucherpfennig KW, Gygi SP, Gagnon E, Novina CD.** Alternative RISC assembly: Binding and repression of microRNA-mRNA duplexes by human Ago proteins. *RNA* 18: 2041–2055, 2012. doi: 10.1261/rna.035675.112.
120. **Janas T, Janas MM, Sapoń K, Janas T.** Mechanisms of RNA loading into exosomes.

FEBS Lett 589: 1391–1398, 2015. doi: 10.1016/j.febslet.2015.04.036.

121. **Janjanam J, Kumar Chandaka G, Kotla S, Rao GN.** PLC β 3 mediates cortactin interaction with WAVE2 in MCP1-induced actin polymerization and cell migration. *Mol Biol Cell* 26: 4589–4606, 2015. doi: 10.1091/mbc.E15-08-0570.
122. **Jenjaroenpun P, Kremenska Y, Nair VM, Kremenskoy M, Joseph B, Kurochkin I V.** Characterization of RNA in exosomes secreted by human breast cancer cell lines using next-generation sequencing. *PeerJ* 2013, 2013. doi: 10.7717/peerj.201.
123. **Ji L, Chen X.** Regulation of small RNA stability: methylation and beyond. *Cell Res* 22: 624–636, 2012. doi: 10.1038/cr.2012.36 [doi].
124. **Jurivich DA, Qiu L, Welk JF.** Attenuated stress responses in young and old human lymphocytes. In: *Mechanisms of Ageing and Development*. 1997.
125. **Kaess BM, Rong J, Larson MG, Hamburg NM, Vita JA, Levy D, Benjamin EJ, Vasan RS, Mitchell GF.** Aortic stiffness, blood pressure progression, and incident hypertension. *JAMA - J Am Med Assoc* 308, 2012. doi: 10.1001/2012.jama.10503.
126. **Kanehisa M.** KEGG: Kyoto Encyclopedia of Genes and Genomes. *Nucleic Acids Res* 28: 27–30, 2000. doi: 10.1093/nar/28.1.27.
127. **Kanehisa M.** Toward understanding the origin and evolution of cellular organisms. *Protein Sci* 28: 1947–1951, 2019. doi: 10.1002/pro.3715.
128. **Kanehisa M, Sato Y, Furumichi M, Morishima K, Tanabe M.** New approach for understanding genome variations in KEGG. *Nucleic Acids Res* 47: D590–D595, 2019. doi: 10.1093/nar/gky962.
129. **Kapustin AN, Chatrou MLL, Drozdov I, Zheng Y, Davidson SM, Soong D, Furmanik M, Sanchis P, De Rosales RTM, Alvarez-Hernandez D, Shroff R, Yin X, Muller K, Skepper JN, Mayr M, Reutelingsperger CP, Chester A, Bertazzo S, Schurgers LJ, Shanahan CM.** Vascular smooth muscle cell calcification is mediated by regulated exosome secretion. *Circ Res* 116: 1312–1323, 2015. doi: 10.1161/CIRCRESAHA.116.305012.
130. **Kapustin AN, Schoppet M, Schurgers LJ, Reynolds JL, McNair R, Heiss A, Jahnchen-Dechent W, Hackeng TM, Schlieper G, Harrison P, Shanahan CM.** Prothrombin Loading of Vascular Smooth Muscle Cell-Derived Exosomes Regulates Coagulation and Calcification. *Arterioscler Thromb Vasc Biol* 37: e22–e32, 2017. doi: 10.1161/ATVBAHA.116.308886.
131. **Kapustin AN, Shanahan CM.** Osteocalcin: A novel vascular metabolic and osteoinductive factor? *Arterioscler Thromb Vasc Biol* 31: 2169–2171, 2011. doi: 10.1161/ATVBAHA.111.233601.
132. **Kapustin AN, Shanahan CM.** Calcium Regulation of Vascular Smooth Muscle Cell-Derived Matrix Vesicles. *Trends Cardiovasc Med* 22: 133–137, 2012. doi: 10.1016/j.tcm.2012.07.009.
133. **Kapustin AN, Shanahan CM.** Emerging roles for vascular smooth muscle cell exosomes in calcification and coagulation. *J Physiol* 594: 2905–2914, 2016. doi: 10.1113/JP271340.
134. **Karakas M, Schulte C, Appelbaum S, Ojeda F, Lackner KJ, Münzel T, Schnabel RB, Blankenberg S, Zeller T.** Circulating microRNAs strongly predict cardiovascular death

- in patients with coronary artery disease-results from the large AtheroGene study. *Eur Heart J* 38: 516–523, 2017. doi: 10.1093/eurheartj/ehw250.
135. **Karanjawala ZE, Grawunder U, Hsieh CL, Lieber MR.** The nonhomologous DNA end joining pathway is important for chromosome stability in primary fibroblasts. *Curr Biol* 9: 1501–1504, 1999.
 136. **Kawasaki T, Kawai T.** Toll-like receptor signaling pathways. *Front. Immunol.* 5: 2014.
 137. **Kim EK, Choi EJ.** Pathological roles of MAPK signaling pathways in human diseases. *Biochim. Biophys. Acta - Mol. Basis Dis.* 1802: 2010.
 138. **Kim Y-K, Kim B, Kim VN.** Re-evaluation of the roles of DROSHA , Exportin 5 , and DICER in microRNA biogenesis. *Proc Natl Acad Sci* 113: E1881--E1889, 2016. doi: 10.1073/pnas.1602532113.
 139. **Kojonazarov B, Novoyatleva T, Boehm M, Happe C, Sibinska Z, Tian X, Sajjad A, Luitel H, Kriechling P, Posern G, Evans SM, Grimminger F, Ghofrani HA, Weissmann N, Bogaard HJ, Seeger W, Schermuly RT.** P38 mapk inhibition improves heart function in pressure-loaded right ventricular hypertrophy. *Am J Respir Cell Mol Biol* 57, 2017. doi: 10.1165/rcmb.2016-0374OC.
 140. **Kostenko S.** Physiological roles of mitogen-activated-protein-kinase-activated p38-regulated/activated protein kinase. *World J Biol Chem* 2, 2011. doi: 10.4331/wjbc.v2.i5.73.
 141. **Kozomara A, Birgaoanu M, Griffiths-Jones S.** MiRBase: From microRNA sequences to function. *Nucleic Acids Res* 47, 2019. doi: 10.1093/nar/gky1141.
 142. **Kozomara A, Griffiths-Jones S.** MiRBase: Annotating high confidence microRNAs using deep sequencing data. *Nucleic Acids Res* 42, 2014. doi: 10.1093/nar/gkt1181.
 143. **Kurz DJ, Decary S, Hong Y, Erusalimsky JD.** Senescence-associated (beta)-galactosidase reflects an increase in lysosomal mass during replicative ageing of human endothelial cells. *J Cell Sci* 113 (Pt 2: 3613–3622, 2000.
 144. **Kuzuoğlu-Öztürk D, Bhandari D, Huntzinger E, Fauser M, Helms S, Izaurralde E.** miRISC and the CCR4–NOT complex silence mRNA targets independently of 43S ribosomal scanning. *EMBO J* 35: 1186–1203, 2016. doi: 10.15252/embj.201592901.
 145. **Kyaw M, Yoshizumi M, Tsuchiya K, Kirima K, Tamaki T.** Antioxidants inhibit JNK and p38 MAPK activation but not ERK 1/2 activation by angiotensin II in rat aortic smooth muscle cells. *Hypertens Res* 24, 2001. doi: 10.1291/hypres.24.251.
 146. **Lacolley P, Regnault V, Avolio AP.** Smooth muscle cell and arterial aging: basic and clinical aspects. *Cardiovasc Res* 114: 513–528, 2018. doi: 10.1093/cvr/cvy009.
 147. **Lacolley P, Regnault V, Segers P, Laurent S.** Vascular Smooth Muscle Cells and Arterial Stiffening: Relevance in Development, Aging, and Disease. *Physiol Rev* 97: 1555–1617, 2017. doi: 10.1152/physrev.00003.2017.
 148. **Laplante M, Sabatini DM.** mTOR Signaling in Growth Control and Disease. *Cell* 149: 274–293, 2012. doi: 10.1016/j.cell.2012.03.017.
 149. **Lässer C, Shelke GV, Yeri A, Kim DK, Crescitelli R, Raimondo S, Sjöstrand M, Gho YS, Van Keuren Jensen K, Lötvall J.** Two distinct extracellular RNA signatures released by a single cell type identified by microarray and next-generation sequencing. *RNA Biol* 14, 2017. doi: 10.1080/15476286.2016.1249092.

150. **Latronico MVG, Catalucci D, Condorelli G.** Emerging Role of MicroRNAs in Cardiovascular Biology. *Circ Res* 101: 1225–1236, 2007. doi: 10.1161/CIRCRESAHA.107.163147.
151. **Laurent S, Boutouyrie P.** Arterial Stiffness and Hypertension in the Elderly. *Front Cardiovasc Med* 7: 202, 2020. doi: 10.3389/fcvm.2020.544302.
152. **Law WD, Warren RL, McCallion AS.** Establishment of an eHAP1 human haploid cell line hybrid reference genome assembled from short and long reads. *Genomics* 112, 2020. doi: 10.1016/j.ygeno.2020.01.009.
153. **Lee BY, Han J a., Im JS, Morrone A, Johung K, Goodwin EC, Kleijer WJ, DiMaio D, Hwang ES.** Senescence-associated β -galactosidase is lysosomal β -galactosidase. *Aging Cell* 5: 187–195, 2006. doi: 10.1111/j.1474-9726.2006.00199.x.
154. **Lee GL, Yeh CC, Wu JY, Lin HC, Wang YF, Kuo YY, Hsieh YT, Hsu YJ, Kuo CC.** TLR2 promotes vascular smooth muscle cell chondrogenic differentiation and consequent calcification via the concerted actions of osteoprotegerin suppression and IL-6-Mediated RANKL induction. *Arterioscler Thromb Vasc Biol* 39, 2019. doi: 10.1161/ATVBAHA.118.311874.
155. **Lee HC, Kang D, Han N, Lee Y, Hwang HJ, Lee SB, You JS, Min BS, Park HJ, Ko YG, Gorospe M, Lee JS.** A novel long noncoding RNA Linc-ASEN represses cellular senescence through multileveled reduction of p21 expression. *Cell Death Differ* 27, 2020. doi: 10.1038/s41418-019-0467-6.
156. **Lee RC, Feinbaum RL, Ambros V.** The *C. elegans* heterochronic gene *lin-4* encodes small RNAs with antisense complementarity to *lin-14*. *Cell* 75: 843–854, 1993. doi: 10.1016/0092-8674(93)90529-Y.
157. **Lee Y, Ahn C, Han J, Choi H, Kim J, Yim J, Lee J, Provost P, Rådmark O, Kim S, Kim VN.** The nuclear RNase III Drosha initiates microRNA processing. *Nature* 425: 415–419, 2003. doi: 10.1038/nature01957.
158. **Li Z, Jing YM, Kerr I, Chakravarty S, Dugar S, Schreiner G, Protter AA.** Selective inhibition of p38 α MAPK improves cardiac function and reduces myocardial apoptosis in rat model of myocardial injury. *Am J Physiol - Hear Circ Physiol* 291, 2006. doi: 10.1152/ajpheart.00043.2006.
159. **Lin QS.** Mitochondria and apoptosis. *Acta Biochim Biophys Sin (Shanghai)* 31, 1999. doi: 10.1126/science.281.5381.1309.
160. **Lin X, He Y, Hou X, Zhang Z, Wang R, Wu Q.** Endothelial cells can regulate smooth muscle cells in contractile phenotype through the miR-206/ARF6&NCX1/exosome axis. *PLoS One* 11: e0152959, 2016. doi: 10.1371/journal.pone.0152959.
161. **Lin Y, Dent SYR, Wilson JH, Wells RD, Napierala M.** R loops stimulate genetic instability of CTG{middle dot}CAG repeats. *Proc Natl Acad Sci* 107: 692–697, 2010. doi: 10.1073/pnas.0909740107.
162. **Lindahl T.** Instability and decay of the primary structure of DNA. *Nature* 362: 709–715, 1993.
163. **Ling H, Kulasiri D, Samarasinghe S.** Robustness of G1/S checkpoint pathways in cell cycle regulation based on probability of DNA-damaged cells passing as healthy cells. *BioSystems* 101: 213–221, 2010.

164. **Liu D, O'Connor MS, Qin J, Songyang Z.** Telosome, a mammalian telomere-associated complex formed by multiple telomeric proteins. *J Biol Chem* 279: 51338–51342, 2004.
165. **Liu J, Xiao X, Shen Y, Chen L, Xu C, Zhao H, Wu Y, Zhang Q, Zhong J, Tang Z, Liu C, Zhao Q, Zheng Y, Cao R, Zu X.** MicroRNA-32 promotes calcification in vascular smooth muscle cells: Implications as a novel marker for coronary artery calcification. *PLoS One* 12: e0174138, 2017. doi: 10.1371/journal.pone.0174138.
166. **Liu N, Bezprozvannaya S, Williams AH, Qi X, Richardson JA, Bassel-Duby R, Olson EN.** microRNA-133a regulates cardiomyocyte proliferation and suppresses smooth muscle gene expression in the heart. *Genes Dev* 22: 3242–3254, 2008. doi: 10.1101/gad.1738708.
167. **Liu YH, Wang D, Rhaleb NE, Yang XP, Xu J, Sankey SS, Rudolph AE, Carretero OA.** Inhibition of p38 mitogen-activated protein kinase protects the heart against cardiac remodeling in mice with heart failure resulting from myocardial infarction. *J Card Fail* 11, 2005. doi: 10.1016/j.cardfail.2004.04.004.
168. **Lobb RJ, van Amerongen R, Wiegmans A, Ham S, Larsen JE, Möller A.** Exosomes derived from mesenchymal non-small cell lung cancer cells promote chemoresistance. *Int J Cancer* 141, 2017. doi: 10.1002/ijc.30752.
169. **Louis SF, Zahradka P.** Vascular smooth muscle cell motility: From migration to invasion. [Online]. *Exp Clin Cardiol* 15: e75-85, 2010. <http://www.ncbi.nlm.nih.gov/pubmed/21264073>.
170. **Louvet L, Metzinger L, Büchel J, Steppan S, Massy ZA.** Magnesium attenuates phosphate-induced deregulation of a MicroRNA signature and prevents modulation of smad1 and osterix during the course of vascular calcification. *Biomed Res Int* 2016: e7419524, 2016. doi: 10.1155/2016/7419524.
171. **Lu W, Zhang Y, Liu D, Songyang Z, Wan M.** Telomeres-structure, function, and regulation. *Exp. Cell Res.* 319: 133–141, 2013.
172. **Ma D, Zheng B, Liu HL, Zhao YB, Liu X, Zhang XH, Li Q, Shi WB, Suzuki T, Wen JK.** Klf5 down-regulation induces vascular senescence through eIF5a depletion and mitochondrial fission. *PLoS Biol* 18: e3000808, 2020. doi: 10.1371/JOURNAL.PBIO.3000808.
173. **Mathivanan S, Simpson RJ.** ExoCarta: A compendium of exosomal proteins and RNA. *Proteomics* 9: 4997–5000, 2009. doi: 10.1002/pmic.200900351.
174. **McCaffrey TA, Du B, Fu C, Bray PJ, Sanborn TA, Deutsch E, Tarazona N, Shaknovitch A, Newman G, Patterson C, Bush HL.** The expression of TGF- β receptors in human atherosclerosis: Evidence for acquired resistance to apoptosis due to receptor imbalance. *J Mol Cell Cardiol* 31, 1999. doi: 10.1006/jmcc.1999.0999.
175. **McCarthy DJ, Chen Y, Smyth GK.** Differential expression analysis of multifactor RNA-Seq experiments with respect to biological variation. *Nucleic Acids Res* 40: 4288–4297, 2012. doi: 10.1093/nar/gks042.
176. **McClintock B.** The Stability of Broken Ends of Chromosomes in Zea Mays. *Genetics* 26: 234–282, 1941. doi: 10.1038/378739a0.
177. **McEniery CM, McDonnell BJ, So A, Aitken S, Bolton CE, Munnery M, Hickson SS, Yasmin, Maki-Petaja KM, Cockcroft JR, Dixon AK, Wilkinson IB.** Aortic calcification

is associated with aortic stiffness and isolated systolic hypertension in healthy individuals. *Hypertension* 53: 524–531, 2009.

178. **McMahon M, Contreras A, Holm M, Uechi T, Forester CM, Pang X, Jackson C, Calvert ME, Chen B, Quigley DA, Luk JM, Kelley RK, Gordan JD, Gill RM, Blanchard SC, Ruggero D.** A single H/ACA small nucleolar RNA mediates tumor suppression downstream of oncogenic RAS. *Elife* 8, 2019. doi: 10.7554/eLife.48847.
179. **Meijer HA, Kong YW, Lu WT, Wilczynska A, Spriggs R V, Robinson SW, Godfrey JD, Willis AE, Bushell M.** Translational repression and eIF4A2 activity are critical for microRNA-mediated gene regulation. *Science (80-)* 340: 82–85, 2013. doi: 10.1126/science.1231197.
180. **Meijer HA, Schmidt T, Gillen SL, Langlais C, Jukes-Jones R, de Moor CH, Cain K, Wilczynska A, Bushell M.** DEAD-box helicase eIF4A2 inhibits CNOT7 deadenylation activity. *Nucleic Acids Res* 47: 8224–8238, 2019. doi: 10.1093/nar/gkz509.
181. **Meister G.** Argonaute proteins: functional insights and emerging roles. *Nat Rev Genet* 14: 447–459, 2013. doi: 10.1038/nrg3462.
182. **Meister G, Landthaler M, Patkaniowska A, Dorsett Y, Teng G, Tuschl T.** Human Argonaute2 mediates RNA cleavage targeted by miRNAs and siRNAs. *Mol Cell* 15: 185–197, 2004. doi: 10.1016/j.molcel.2004.07.007.
183. **Mercier N, El Hadri K, Osborne-Pellegrin M, Nehme J, Perret C, Labat C, Regnault V, Lamazière JMD, Challande P, Lacolley P, Fève B.** Modifications of arterial phenotype in response to amine oxidase inhibition by semicarbazide. In: *Hypertension*. 2007, p. 234–241.
184. **Minamino T.** Vascular cell senescence and vascular aging. *J Mol Cell Cardiol* 36: 175–183, 2004. doi: 10.1016/j.yjmcc.2003.11.010.
185. **Miranda KC, Bond DT, Levin JZ, Adiconis X, Sivachenko A, Russ C, Brown D, Nusbaum C, Russo LM.** Massively parallel sequencing of human urinary exosome/microvesicle RNA reveals a predominance of non-coding RNA. *PLoS One* 9: 2014.
186. **Mitchell GF.** Arterial Stiffness and Hypertension. *Hypertension* 64: 210–214, 2014. doi: 10.1161/HYPERTENSIONAHA.114.03449.
187. **Miyazawa K, Miyazono K.** Regulation of TGF- β Family Signaling by Inhibitory Smads. *Cold Spring Harb Perspect Biol* 9: a022095, 2017. doi: 10.1101/cshperspect.a022095.
188. **Monaco C, Cole JE, Georgiou E.** The expression and functions of toll-like receptors in atherosclerosis. *Mediators Inflamm* 2010, 2010. doi: 10.1155/2010/393946.
189. **Montpetit AJ, Alhareeri AA, Montpetit M, Starkweather AR, Elmore LW, Filler K, Mohanraj L, Burton CW, Menzies VS, Lyon DE, Jackson-Cook CK.** Telomere Length. *Nurs Res* 63: 289–299, 2014. doi: 10.1097/NNR.0000000000000037.
190. **Morello F, Perino A, Hirsch E.** Phosphoinositide 3-kinase signalling in the vascular system. *Cardiovasc. Res.* 82: 2009.
191. **Moreno-Gonzalo O, Villarroya-Beltri C, Sanchez-Madrid F.** Post-Translational Modifications of Exosomal Proteins. *Front Immunol* 5: 383, 2014. doi: 10.3389/fimmu.2014.00383.
192. **Moyzis RK, Buckingham JM, Cram LS, Dani M, Deaven LL, Jones MD, Meyne J,**

- Ratliff RL, Wu JR.** A highly conserved repetitive DNA sequence, (TTAGGG)_n, present at the telomeres of human chromosomes. *Proc Natl Acad Sci U S A* 85: 6622–6626, 1988. doi: 10.1073/pnas.85.18.6622.
193. **Mukherjee K, Ghoshal B, Ghosh S, Chakrabarty Y, Shwetha S, Das S, Bhattacharyya SN.** Reversible HuR-microRNA binding controls extracellular export of miR-122 and augments stress response. *EMBO Rep* 17: 1184–1203, 2016. doi: 10.15252/embr.201541930.
194. **Mullani N, Porozhan Y, Costallat M, Batsché E, Goodhardt M, Cenci G, Mann C, Muchardt C.** Reduced RNA turnover as a driver of cellular senescence. .
195. **Muller HJ.** The remaking of chromosomes. *Collect Net* 8: 182–195, 1938.
196. **Muthukumaraswamy SD, Singh KD, Swettenham JB, Jones DK.** Visual gamma oscillations and evoked responses: Variability, repeatability and structural MRI correlates. *Neuroimage* 49: 3349–3357, 2010. doi: 10.1016/j.neuroimage.2009.11.045.
197. **Na S, Meininger GA, Humphrey JD.** A theoretical model for F-actin remodeling in vascular smooth muscle cells subjected to cyclic stretch. *J Theor Biol* 246: 87–99, 2007. doi: 10.1016/j.jtbi.2006.11.015.
198. **Nagarajan VK, Jones CI, Newbury SF, Green PJ.** XRN 5'→3' exoribonucleases: Structure, mechanisms and functions. *Biochim Biophys Acta - Gene Regul Mech* 1829: 590–603, 2013. doi: 10.1016/j.bbagr.2013.03.005.
199. **Nakase I, Ueno N, Katayama M, Noguchi K, Takatani-Nakase T, Kobayashi NB, Yoshida T, Fujii I, Futaki S.** Receptor clustering and activation by multivalent interaction through recognition peptides presented on exosomes. *Chem Commun* 53: 317–320, 2017. doi: 10.1039/C6CC06719K.
200. **Nie L, Zhang P, Wang Q, Zhou X, Wang Q.** lncRNA-Triggered Macrophage Inflammation Deteriorates Age-Related Diseases. *Mediators Inflamm.* 2019: 2019.
201. **Nilsson PM.** Early vascular aging (EVA): consequences and prevention. *Vasc. Health Risk Manag.* 4: 2008.
202. **Nilsson PM.** Early Vascular Aging in Hypertension. *Front Cardiovasc Med* 7, 2020. doi: 10.3389/fcvm.2020.00006.
203. **Nilsson PM, Lurbe E, Laurent S.** The early life origins of vascular ageing and cardiovascular risk: The EVA syndrome. *J. Hypertens.* 26: 2008.
204. **Nossent AY, Ektefaie N, Wojta J, Eichelberger B, Kopp C, Panzer S, Gremmel T.** Plasma levels of snoRNAs are associated with platelet activation in patients with peripheral artery disease. *Int J Mol Sci* 20, 2019. doi: 10.3390/ijms20235975.
205. **O'Rourke MF, Staessen JA, Vlachopoulos C, Duprez D, Plante G e. E.** Clinical applications of arterial stiffness; definitions and reference values. *Am J Hypertens* 15: 426–444, 2002. doi: 10.1016/S0895-7061(01)02319-6.
206. **O'Toole AS, Miller S, Haines N, Zink MC, Serra MJ.** Comprehensive thermodynamic analysis of 3' double-nucleotide overhangs neighboring Watson-Crick terminal base pairs. *Nucleic Acids Res* 34: 3338–3344, 2006. doi: 10.1093/nar/gkl428.
207. **Oh YS, Berkowitz DE, Cohen RA, Figueroa CA, Harrison DG, Humphrey JD, Larson DF, Leopold JA, Mecham RP, Ruiz-Opazo N, Santhanam L, Seta F, Shyy JYJ, Sun Z,**

- Tsao PS, Wagenseil JE, Galis ZS.** A special report on the NHLBI initiative to study cellular and molecular mechanisms of arterial stiffness and its association with hypertension. *Circ Res* 121, 2017. doi: 10.1161/CIRCRESAHA.117.311703.
208. **Olovnikov AM.** A theory of marginotomy. *J Theor Biol* 41: 181–190, 1973. doi: 10.1016/0022-5193(73)90198-7.
209. **Owens GK.** Regulation of differentiation of vascular smooth muscle cells. *Physiol Rev* 75: 487–517, 1995.
210. **Owens GK, Kumar MS, Wamhoff BR.** Molecular Regulation of Vascular Smooth Muscle Cell Differentiation in Development and Disease. *Physiol Rev* 84: 767–801, 2004. doi: 10.1152/physrev.00041.2003.
211. **Palm W, de Lange T.** How Shelterin Protects Mammalian Telomeres [Online]. *Annu Rev Genet* 42: 301–334, 2008. <http://www.annualreviews.org/doi/abs/10.1146/annurev.genet.41.110306.130350%5Cpapers2://publication/doi/10.1146/annurev.genet.41.110306.130350>.
212. **Panizo S, Naves-Diaz M, Carrillo-Lopez N, Martinez-Arias L, Fernandez-Martin JL, Ruiz-Torres MP, Cannata-Andia JB, Rodriguez I.** MicroRNAs 29b, 133b, and 211 Regulate Vascular Smooth Muscle Calcification Mediated by High Phosphorus. *J Am Soc Nephrol* 27: 824–834, 2016. doi: 10.1681/ASN.2014050520.
213. **Papaconstantinou J, Wang CZ, Zhang M, Yang S, Deford J, Bulavin D V., Ansari NH.** Attenuation of p38 α MAPK stress response signaling delays the in vivo aging of skeletal muscle myofibers and progenitor cells. *Aging (Albany NY)* 7, 2015. doi: 10.18632/aging.100802.
214. **Park JH, Shin C.** Non-canonical targets play an important role in microRNA stability control mechanisms. *BMB Rep* 50: 158–159, 2017. doi: 10.5483/BMBRep.2017.50.4.029.
215. **Park M, Choi S, Kim S, Kim J, Lee D-K, Park W, Kim T, Jung J, Hwang JY, Won M-H, Ryou S, Kang SG, Ha K-S, Kwon Y-G, Kim Y-M.** NF- κ B-responsive miR-155 induces functional impairment of vascular smooth muscle cells by downregulating soluble guanylyl cyclase. *Exp Mol Med* 51: 1–12, 2019. doi: 10.1038/s12276-019-0212-8.
216. **Park MS, Koff a.** Overview of the cell cycle. *Curr Protoc Cell Biol* Chapter 8: Unit 8.1, 2001.
217. **Park SC.** Nuclear barrier hypothesis of aging as mechanism for trade-off growth to survival. In: *Advances in Experimental Medicine and Biology*. 2011.
218. **Pasquinelli AE, Reinhart BJ, Slack F, Martindale MQ, Kuroda MI, Maller B, Hayward DC, Ball EE, Degan B, Müller P, Spring J, Srinivasan A, Fishman M, Finnerty J, Corbo J, Levine M, Leahy P, Davidson E, Ruvkun G.** Conservation of the sequence and temporal expression of let-7 heterochronic regulatory RNA. *Nature* 408: 86–89, 2000. doi: 10.1038/35040556.
219. **Patrushev LI, Kovalenko TF.** Functions of noncoding sequences in Mammalian genomes. *Biochemistry* 79: 1442–1469, 2014. doi: 10.1134/S0006297914130021.
220. **Payne RA, Wilkinson IB, Webb DJ.** Arterial stiffness and hypertension: Emerging concepts. *Hypertension* 55: 9–14, 2010.
221. **Pérez-Boza J, Lion M, Struman I.** Exploring the RNA landscape of endothelial

- exosomes. *RNA* 24, 2018. doi: 10.1261/rna.064352.117.
222. **Pessi T, Viiri LE, Raitoharju E, Astola N, Seppälä I, Waldenberger M, Lounatmaa K, Davies AH, Lehtimäki T, Karhunen PJ, Monaco C.** Interleukin-6 and microRNA profiles induced by oral bacteria in human atheroma derived and healthy smooth muscle cells. *Springerplus* 4: 206, 2015. doi: 10.1186/s40064-015-0993-8.
223. **Polyak K, Lee MH, Erdjument-Bromage H, Koff A, Roberts JM, Tempst P, Massagué J.** Cloning of p27Kip1, a cyclin-dependent kinase inhibitor and a potential mediator of extracellular antimitogenic signals. *Cell* 78, 1994. doi: 10.1016/0092-8674(94)90572-X.
224. **Prasad SB, Yadav SS, Das M, Modi A, Kumari S, Pandey LK, Singh S, Pradhan S, Narayan G.** PI3K/AKT pathway-mediated regulation of p27Kip1 is associated with cell cycle arrest and apoptosis in cervical cancer. *Cell Oncol* 38: 215–225, 2015. doi: 10.1007/s13402-015-0224-x.
225. **Provencio M, Rodríguez M, Cantos B, Sabín P, Quero C, García-Arroyo FR, Rueda A, Maximiano C, Rodríguez-Abreu D, Sánchez A, Silva J, García V.** mRNA in exosomes as a liquid biopsy in non-Hodgkin Lymphoma: A multicentric study by the Spanish lymphoma oncology group. *Oncotarget* 8, 2017. doi: 10.18632/oncotarget.16435.
226. **Ransohoff JD, Wei Y, Khavari PA.** The functions and unique features of long intergenic non-coding RNA. *Nat. Rev. Mol. Cell Biol.* 19: 2018.
227. **Raposo G, Stoorvogel W.** Extracellular vesicles: Exosomes, microvesicles, and friends. *J Cell Biol* 200: 373–383, 2013. doi: 10.1083/jcb.201211138.
228. **Reddy JP, Li Y.** Oncogene-induced senescence and its role in tumor suppression. *J Mammary Gland Biol Neoplasia* 16: 247–256, 2011.
229. **Reinhart BJ, Slack FJ, Basson M, Pasquienelli AE, Bettlinger JC, Rougvie AE, Horvitz HR, Ruvkun G.** The 21-nucleotide let-7 RNA regulates developmental timing in *Caenorhabditis elegans*. *Nature* 403: 901–906, 2000. doi: 10.1038/35002607.
230. **Ren X, Kuan PF.** Negative binomial additive model for RNA-Seq data analysis. *BMC Bioinformatics* 21, 2020. doi: 10.1186/s12859-020-3506-x.
231. **Reuven EM, Fink A, Shai Y.** Regulation of innate immune responses by transmembrane interactions: Lessons from the TLR family. *Biochim. Biophys. Acta - Biomembr.* 1838: 2014.
232. **Robinson MD, McCarthy DJ, Smyth GK.** edgeR: A Bioconductor package for differential expression analysis of digital gene expression data. *Bioinformatics* 26, 2009. doi: 10.1093/bioinformatics/btp616.
233. **Robinson MD, McCarthy DJ, Smyth GK.** edgeR: a Bioconductor package for differential expression analysis of digital gene expression data. *Bioinformatics* 26: 139–140, 2010. doi: 10.1093/bioinformatics/btp616.
234. **Robinson MD, Smyth GK.** Moderated statistical tests for assessing differences in tag abundance. *Bioinformatics* 23, 2007. doi: 10.1093/bioinformatics/btm453.
235. **Rodier F, Campisi J.** Four faces of cellular senescence. *J Cell Biol* 192: 547–556, 2011. doi: 10.1083/jcb.201009094.
236. **Rose BA, Force T, Wang Y.** Mitogen-activated protein kinase signaling in the heart: Angels versus demons in a heart-breaking tale. *Physiol. Rev.* 90: 2010.

237. **Roy S, Kaur M, Agarwal C, Tecklenburg M, Sclafani R a, Agarwal R.** P21 and P27 Induction By Silibinin Is Essential for Its Cell Cycle Arrest Effect in Prostate Carcinoma Cells. *Mol Cancer Ther* 6: 2696–2707, 2007. doi: 10.1158/1535-7163.MCT-07-0104.
238. **Rubinsztein DC, Mariño G, Kroemer G.** Autophagy and aging. *Cell* 146: 682–695, 2011.
239. **Ruby JG, Jan CH, Bartel DP.** Intronic microRNA precursors that bypass Drosha processing. *Nature* 448: 83–86, 2007. doi: 10.1038/nature05983.
240. **Salvi P, Scalise F, Rovina M, Moretti F, Salvi L, Grillo A, Gao L, Baldi C, Faini A, Furlanis G, Sorropago A, Millasseau SC, Sorropago G, Carretta R, Avolio AP, Parati G.** Noninvasive Estimation of Aortic Stiffness Through Different Approaches. *Hypertension* 74: 117–129, 2019. doi: 10.1161/HYPERTENSIONAHA.119.12853.
241. **Sandhu C.** Phosphorylation of cell cycle proteins at senescence. *Protien Phosphorylation Aging Age-related Dis* 16: 15–34, 2004. doi: 10.1016/S1566-3124(04)16002-1.
242. **Santangelo L, Giurato G, Cicchini C, Montaldo C, Mancone C, Tarallo R, Battistelli C, Alonzi T, Weisz A, Tripodi M.** The RNA-Binding Protein SYNCRIP Is a Component of the Hepatocyte Exosomal Machinery Controlling MicroRNA Sorting. *Cell Rep* 17: 799–808, 2016. doi: 10.1016/j.celrep.2016.09.031.
243. **Satyanarayana A, Hilton MB, Kaldis P.** p21 Inhibits Cdk1 in the Absence of Cdk2 to Maintain the G1/S Phase DNA Damage Checkpoint. *Mol Biol Cell* 19: 65–77, 2008.
244. **Schmierer B, Hill CS.** TGF β –SMAD signal transduction: molecular specificity and functional flexibility. *Nat Rev Mol Cell Biol* 8: 970–982, 2007. doi: 10.1038/nrm2297.
245. **Schulte C, Molz S, Appelbaum S, Karakas M, Ojeda F, Lau DM, Hartmann T, Lackner KJ, Westermann D, Schnabel RB, Blankenberg S, Zeller T.** MiRNA-197 and miRNA-223 predict cardiovascular death in a cohort of patients with symptomatic coronary artery disease. *PLoS One* 10: e0145930, 2015. doi: 10.1371/journal.pone.0145930.
246. **Scott MS, Calafell SJ, Thomas DY, Hallett MT.** Refining Protein Subcellular Localization. *PLoS Comput Biol* 1: e66, 2005. doi: 10.1371/journal.pcbi.0010066.
247. **See F, Thomas W, Way K, Tzanidis A, Kompa A, Lewis D, Itescu S, Krum H.** P38 mitogen-activated protein kinase inhibition improves cardiac function and attenuates left ventricular remodeling following myocardial infarction in the rat. *J Am Coll Cardiol* 44, 2004. doi: 10.1016/j.jacc.2004.07.038.
248. **Seok H, Ham J, Jang E-S, Chi SW.** MicroRNA Target Recognition: Insights from Transcriptome-Wide Non-Canonical Interactions. *Mol Cells* 39: 375–381, 2016. doi: 10.14348/molcells.2016.0013.
249. **Serrano M, Hannon GJ, Beach D.** A new regulatory motif in cell-cycle control causing specific inhibition of cyclin D/CDK4. *Nature* 366: 704–707, 1993.
250. **Shan Z, Qin S, Li W, Wu W, Yang J, Chu M, Li X, Huo Y, Schaer GL, Wang S, Zhang C.** An endocrine genetic signal between blood cells and vascular smooth muscle cells: Role of microRNA-223 in smooth muscle function and atherogenesis. *J Am Coll Cardiol* 65: 2526–2537, 2015. doi: 10.1016/j.jacc.2015.03.570.
251. **Shannon P.** Cytoscape: A Software Environment for Integrated Models of

- Biomolecular Interaction Networks. *Genome Res* 13: 2498–2504, 2003. doi: 10.1101/gr.1239303.
252. **Shen Z, Sun J, Shao J, Xu J.** Ultraviolet B irradiation enhances the secretion of exosomes by human primary melanocytes and changes their exosomal miRNA profile. *PLoS One* 15: e0237023, 2020. doi: 10.1371/journal.pone.0237023.
 253. **Shindo T, Manabe I, Fukushima Y, Tobe K, Aizawa K, Miyamoto S, Kawai-Kowase K, Moriyama N, Imai Y, Kawakami H, Nishimatsu H, Ishikawa T, Suzuki T, Morita H, Maemura K, Sata M, Hirata Y, Komukai M, Kagechika H, Kadowaki T, Kurabayashi M, Nagai R.** Krüppel-like zinc-finger transcription factor KLF5/BTEB2 is a target for angiotensin II signaling and an essential regulator of cardiovascular remodeling. *Nat Med* 8: 856–863, 2002. doi: 10.1038/nm738.
 254. **Slack FJ, Basson M, Liu Z, Ambros V, Horvitz HR, Ruvkun G.** The lin-41 RBCC gene acts in the *C. elegans* heterochronic pathway between the let-7 regulatory RNA and the LIN-29 transcription factor. *Mol Cell* 5: 659–669, 2000. doi: 10.1016/S1097-2765(00)80245-2.
 255. **Sohel MH.** Extracellular/Circulating MicroRNAs: Release Mechanisms, Functions and Challenges. *Achiev Life Sci* 10: 175–186, 2016. doi: 10.1016/j.als.2016.11.007.
 256. **Song P, An J, Zou M-H.** Immune Clearance of Senescent Cells to Combat Ageing and Chronic Diseases. *Cells* 9, 2020. doi: 10.3390/cells9030671.
 257. **Song Y, Shen H, Schenten D, Shan P, Lee PJ, Goldstein DR.** Aging enhances the basal production of IL-6 and CCL2 in vascular smooth muscle cells. *Arterioscler Thromb Vasc Biol* 32, 2012. doi: 10.1161/ATVBAHA.111.236349.
 258. **Sood P, Krek A, Zavolan M, Macino G, Rajewsky N.** Cell-type-specific signatures of microRNAs on target mRNA expression. *Proc Natl Acad Sci* 103: 2746–2751, 2006. doi: 10.1073/pnas.0511045103.
 259. **Soto-Gamez A, Quax WJ, Demaria M.** Regulation of Survival Networks in Senescent Cells: From Mechanisms to Interventions. *J. Mol. Biol.* 431: 2019.
 260. **Stewart AD, Jiang B, Millasseau SC, Ritter JM, Chowienczyk PJ.** Acute Reduction of Blood Pressure by Nitroglycerin Does Not Normalize Large Artery Stiffness in Essential Hypertension. *Hypertension* 48: 404–410, 2006. doi: 10.1161/01.HYP.0000237669.64066.c5.
 261. **Sticht C, De La Torre C, Parveen A, Gretz N.** Mirwalk: An online resource for prediction of microrna binding sites. *PLoS One* 13, 2018. doi: 10.1371/journal.pone.0206239.
 262. **Sun Z.** Aging, arterial stiffness, and hypertension. *Hypertension* 65: 252–256, 2015.
 263. **Sun Z, Evans J, Bhagwate A, Middha S, Bockol M, Yan H, Kocher J-P.** CAP-miRSeq: a comprehensive analysis pipeline for microRNA sequencing data. *BMC Genomics* 15: 423, 2014. doi: 10.1186/1471-2164-15-423.
 264. **Suram A, Herbig U.** The replicometer is broken: Telomeres activate cellular senescence in response to genotoxic stresses. .
 265. **Szklarczyk D, Gable AL, Lyon D, Junge A, Wyder S, Huerta-Cepas J, Simonovic M, Doncheva NT, Morris JH, Bork P, Jensen LJ, Mering C von.** STRING v11: protein–protein association networks with increased coverage, supporting functional

- discovery in genome-wide experimental datasets. *Nucleic Acids Res* 47: D607–D613, 2019. doi: 10.1093/nar/gky1131.
266. **Tahir H, Niculescu I, Bona-Casas C, Merks RMH, Hoekstra AG.** An in silico study on the role of smooth muscle cell migration in neointimal formation after coronary stenting. *J R Soc Interface* 12: 20150358, 2015. doi: 10.1098/rsif.2015.0358.
 267. **Takahashi A, Ohtani N, Hara E.** Irreversibility of cellular senescence: dual roles of p16INK4a/Rb-pathway in cell cycle control. *Cell Div* 2: 10, 2007. doi: 10.1186/1747-1028-2-10.
 268. **Takahashi E, Berk BC.** MAP kinases and vascular smooth muscle function. In: *Acta Physiologica Scandinavica*. 1998.
 269. **Tan J, Yang L, Liu C, Yan Z.** MicroRNA-26a targets MAPK6 to inhibit smooth muscle cell proliferation and vein graft neointimal hyperplasia. *Sci Rep* 7: 46602, 2017. doi: 10.1038/srep46602.
 270. **Tan P, Wang Y-J, Li S, Wang Y, He J-Y, Chen Y-Y, Deng H-Q, Huang W, Zhan J-K, Liu Y-S.** The PI3K/Akt/mTOR pathway regulates the replicative senescence of human VSMCs. *Mol Cell Biochem* 422: 1–10, 2016. doi: 10.1007/s11010-016-2796-9.
 271. **Tang Y, Yu S, Liu Y, Zhang J, Han L, Xu Z.** MicroRNA-124 controls human vascular smooth muscle cell phenotypic switch via Sp1. *Am J Physiol Circ Physiol* 313: H641–H649, 2017. doi: 10.1152/ajpheart.00660.2016.
 272. **Terns MP, Terns RM.** Small nucleolar RNAs: Versatile trans-acting molecules of ancient evolutionary origin. *Gene Expr.* 10: 2002.
 273. **Théry C, Amigorena S, Raposo G, Clayton A.** Isolation and characterization of exosomes from cell culture supernatants and biological fluids. *Curr Protoc Cell Biol* Chapter 3: Unit 3.22, 2006. doi: 10.1002/0471143030.cb0322s30.
 274. **Thomas C, Mackey MM, Diaz A a, Cox DP.** Hydroxyl radical is produced via the Fenton reaction in submitochondrial particles under oxidative stress: implications for diseases associated with iron accumulation. *Redox Rep* 14: 102–108, 2009. doi: 10.1179/135100009X392566.
 275. **Thomas PD.** PANTHER: A Library of Protein Families and Subfamilies Indexed by Function. *Genome Res* 13: 2129–2141, 2003. doi: 10.1101/gr.772403.
 276. **Tominaga K, Suzuki HI.** TGF- β signaling in cellular senescence and aging-related pathology. *Int. J. Mol. Sci.* 20: 2019.
 277. **Torella D, Iaconetti C, Catalucci D, Ellison GM, Leone A, Waring CD, Bochicchio A, Vicinanza C, Aquila I, Curcio A, Condorelli G, Indolfi C.** MicroRNA-133 controls vascular smooth muscle cell phenotypic switch in vitro and vascular remodeling in vivo. *Circ Res* 109: 880–893, 2011. doi: 10.1161/CIRCRESAHA.111.240150.
 278. **Toussaint O, Medrano E., von Zglinicki T.** Cellular and molecular mechanisms of stress-induced premature senescence (SIPS) of human diploid fibroblasts and melanocytes. *Exp Gerontol* 35: 927–945, 2000. doi: 10.1016/S0531-5565(00)00180-7.
 279. **Tsai S, Hollenbeck ST, Ryer EJ, Edlin R, Yamanouchi D, Kundi R, Wang C, Liu B, Kent KC.** TGF- β through Smad3 signaling stimulates vascular smooth muscle cell proliferation and neointimal formation. *Am J Physiol - Hear Circ Physiol* 297, 2009.

doi: 10.1152/ajpheart.91478.2007.

280. **Tucka J, Yu H, Gray K, Figg N, Maguire J, Lam B, Bennett M, Littlewood T.** Akt1 Regulates Vascular Smooth Muscle Cell Apoptosis Through FoxO3a and Apaf1 and Protects Against Arterial Remodeling and Atherosclerosis. *Arterioscler Thromb Vasc Biol* 34: 2421–2428, 2014. doi: 10.1161/ATVBAHA.114.304284.
281. **Uryga AK, Bennett MR.** Ageing induced vascular smooth muscle cell senescence in atherosclerosis. *J. Physiol.* 594: 2016.
282. **Valadi H, Ekström K, Bossios A, Sjöstrand M, Lee JJ, Lötvall JO.** Exosome-mediated transfer of mRNAs and microRNAs is a novel mechanism of genetic exchange between cells. *Nat Cell Biol* 9: 654–659, 2007. doi: 10.1038/ncb1596.
283. **Van den Berge K, Roux de Bézieux H, Street K, Saelens W, Cannoodt R, Saeys Y, Dudoit S, Clement L.** Trajectory-based differential expression analysis for single-cell sequencing data. *Nat Commun* 11, 2020. doi: 10.1038/s41467-020-14766-3.
284. **van Deursen JM.** The role of senescent cells in ageing. *Nature* 509: 439–446, 2014. doi: 10.1038/nature13193.
285. **Vernace VA, Schmidt-Glenewinkel T, Figueiredo-Pereira ME.** Aging and regulated protein degradation: Who has the UPPER hand? *Aging Cell* 6: 599–606, 2007.
286. **Villarroya-Beltri C, Baixauli F, Mittelbrunn M, Fernández-Delgado I, Torralba D, Moreno-Gonzalo O, Baldanta S, Enrich C, Guerra S, Sánchez-Madrid F.** ISGylation controls exosome secretion by promoting lysosomal degradation of MVB proteins. *Nat Commun* 7: 13588, 2016. doi: 10.1038/ncomms13588.
287. **Villarroya-Beltri C, Gutiérrez-Vázquez C, Sánchez-Cabo F, Pérez-Hernández D, Vázquez J, Martín-Cofreces N, Martínez-Herrera DJ, Pascual-Montano A, Mittelbrunn M, Sánchez-Madrid F.** Sumoylated hnRNPA2B1 controls the sorting of miRNAs into exosomes through binding to specific motifs. *Nat Commun* 4: 2980, 2013. doi: 10.1038/ncomms3980.
288. **Vlachopoulos C, Xaplanteris P, Aboyans V, Brodmann M, Cífková R, Cosentino F, De Carlo M, Gallino A, Landmesser U, Laurent S, Lekakis J, Mikhailidis DP, Naka KK, Protogerou AD, Rizzoni D, Schmidt-Trucksäss A, Van Bortel L, Weber T, Yamashina A, Zimlichman R, Boutouyrie P, Cockcroft J, O'Rourke M, Park JB, Schillaci G, Sillesen H, Townsend RR.** The role of vascular biomarkers for primary and secondary prevention. A position paper from the European Society of Cardiology Working Group on peripheral circulation. *Atherosclerosis* 241: 507–532, 2015. doi: 10.1016/j.atherosclerosis.2015.05.007.
289. **Wagenseil JE, Mecham RP.** Elastin in large artery stiffness and hypertension. *J Cardiovasc Transl Res* 5: 264–273, 2012.
290. **Wagner M, Hampel B, Bernhard D, Hala M, Zwerschke W, Jansen-Dürr P.** Replicative senescence of human endothelial cells in vitro involves G1 arrest, polyploidization and senescence-associated apoptosis. *Exp Gerontol* 36: 1327–1347, 2001. doi: 10.1016/S0531-5565(01)00105-X.
291. **Wang E.** Senescent human fibroblasts resist programmed cell death, and failure to suppress bcl2 is involved. *Cancer Res* 55: 5585, 1995.
292. **Wang H, Jiang M, Xu Z, Huang H, Gong P, Zhu H, Ruan C.** miR-146b-5p promotes VSMC proliferation and migration. [Online]. *Int J Clin Exp Pathol* 8: 12901–7, 2015.

<http://www.ncbi.nlm.nih.gov/pubmed/26722482>.

293. **Wang W, Yang X, López de Silanes I, Carling D, Gorospe M.** Increased AMP:ATP Ratio and AMP-activated Protein Kinase Activity during Cellular Senescence Linked to Reduced HuR Function. *J Biol Chem* 278: 27016–27023, 2003. doi: 10.1074/jbc.M300318200.
294. **Wang X.** Composition of seed sequence is a major determinant of microRNA targeting patterns. *Bioinformatics* 30: 1377–1383, 2014. doi: 10.1093/bioinformatics/btu045.
295. **Wang Y-S, Wang H-YJ, Liao Y-C, Tsai P-C, Chen K-C, Cheng H-Y, Lin R-T, Juo S-HH.** MicroRNA-195 regulates vascular smooth muscle cell phenotype and prevents neointimal formation. *Cardiovasc Res* 95: 517–526, 2012. doi: 10.1093/cvr/cvs223.
296. **Wang Z, Newman WH.** Smooth muscle cell migration stimulated by interleukin 6 is associated with cytoskeletal reorganization. *J Surg Res* 111, 2003. doi: 10.1016/S0022-4804(03)00087-8.
297. **Watson JD.** Origin of concatemeric T7 DNA. *Nat New Biol* 239: 197–201, 1972. doi: 10.1038/newbio239197a0.
298. **Wei X, Yi X, Zhu XH, Jiang DS.** Histone methylation and vascular biology. *Clin. Epigenetics* 12: 2020.
299. **Wei Y, Li L, Wang D, Zhang CY, Zen K.** Importin 8 regulates the transport of mature microRNAs into the cell nucleus. *J Biol Chem* 289: 10270–10275, 2014. doi: 10.1074/jbc.C113.541417.
300. **Wei Z, Liu HT.** MAPK signal pathways in the regulation of cell proliferation in mammalian cells. *Cell Res.* 12: 2002.
301. **Weston A, Sommerville J.** Xp54 and related (DDX6-like) RNA helicases: Roles in messenger RNP assembly, translation regulation and RNA degradation. *Nucleic Acids Res* 34: 3082–3094, 2006. doi: 10.1093/nar/gkl409.
302. **Wilczynska A, Bushell M.** The complexity of miRNA-mediated repression. *Cell Death Differ* 22: 22–33, 2015. doi: 10.1038/cdd.2014.112.
303. **Wilkinson IB, Mäki-Petäjä KM, Mitchell GF.** Uses of Arterial Stiffness in Clinical Practice. *Arterioscler. Thromb. Vasc. Biol.:* 2020.
304. **World Health Organization.** Hypertension [Online]. 2019. <https://www.who.int/news-room/fact-sheets/detail/hypertension>.
305. **Wu G, Cai J, Han Y, Chen J, Huang ZP, Chen C, Cai Y, Huang H, Yang Y, Liu Y, Xu Z, He D, Zhang X, Hu X, Pinello L, Zhong D, He F, Yuan GC, Wang DZ, Zeng C.** LincRNA-p21 regulates neointima formation, vascular smooth muscle cell proliferation, apoptosis, and atherosclerosis by enhancing p53 activity. *Circulation* 130, 2014. doi: 10.1161/CIRCULATIONAHA.114.011675.
306. **Wu M, Rementer C, Giachelli CM.** Vascular calcification: an update on mechanisms and challenges in treatment. *Calcif Tissue Int* 93: 365–373, 2013. doi: 10.1007/s00223-013-9712-z.
307. **Wu Y, Deng W, Klinke II DJ.** Exosomes: improved methods to characterize their morphology, RNA content, and surface protein biomarkers. *Analyst* 140: 6631–6642, 2015. doi: 10.1039/C5AN00688K.

308. **Wu Y, Zhou J, Wang H, Wu Y, Gao Q, Wang L, Zhao Q, Liu P, Gao S, Wen W, Zhang W, Liu Y, Yuan Z.** The activation of p38 MAPK limits the abnormal proliferation of vascular smooth muscle cells induced by high sodium concentrations. *Int J Mol Med* 37, 2016. doi: 10.3892/ijmm.2015.2394.
309. **Xie Z, Xia W, Hou M.** Long intergenic non-coding RNA-p21 mediates cardiac senescence via the Wnt/ β -catenin signaling pathway in doxorubicin-induced cardiotoxicity. *Mol Med Rep* 17, 2018. doi: 10.3892/mmr.2017.8169.
310. **Xu CL, Sang B, Liu GZ, Li JM, Zhang XD, Liu LX, Thorne RF, Wu M.** SENELOC, a long non-coding RNA suppresses senescence via p53-dependent and independent mechanisms. *Nucleic Acids Res* 48, 2020. doi: 10.1093/nar/gkaa063.
311. **Xu JF, Wang YP, Zhang SJ, Chen Y, Gu HF, Dou XF, Xia B, Bi Q, Fan SW.** Exosomes containing differential expression of microRNA and mRNA in osteosarcoma that can predict response to chemotherapy. *Oncotarget* 8, 2017. doi: 10.18632/oncotarget.18373.
312. **Xu Y.** Regulation of p53 responses by post-translational modifications. [Online]. *Cell Death Differ* 10: 400–403, 2003. <http://www.ncbi.nlm.nih.gov/pubmed/12719715>.
313. **Xu Y, Li N, Xiang R, Sun P.** Emerging roles of the p38 MAPK and PI3K/AKT/mTOR pathways in oncogene-induced senescence. *Trends Biochem Sci* 39: 268–276, 2014. doi: 10.1016/j.tibs.2014.04.004.
314. **Yamakoshi K, Takahashi A, Hirota F, Nakayama R, Ishimaru N, Kubo Y, Mann DJ, Ohmura M, Hirao A, Saya H, Arase S, Hayashi Y, Nakao K, Matsumoto M, Ohtani N, Hara E.** Real-time in vivo imaging of p16Ink4a reveals cross talk with p53. *J Cell Biol* 186: 393–407, 2009. doi: 10.1083/jcb.200904105.
315. **Yang D, Sun C, Zhang J, Lin S, Zhao L, Wang L, Lin R, Lv J, Xin S.** Proliferation of vascular smooth muscle cells under inflammation is regulated by NF- κ B p65/microRNA-17/RB pathway activation. *Int J Mol Med* 41, 2018. doi: 10.3892/ijmm.2017.3212.
316. **Yang F, Chen Q, He S, Yang M, Maguire EM, An W, Afzal TA, Luong LA, Zhang L, Xiao Q.** miR-22 Is a Novel Mediator of Vascular Smooth Muscle Cell Phenotypic Modulation and Neointima Formation. *Circulation* 137: 1824–1841, 2018. doi: 10.1161/CIRCULATIONAHA.117.027799.
317. **Yang X, Coriolan D, Murthy V, Schultz K, Golenbock DT, Beasley D.** Proinflammatory phenotype of vascular smooth muscle cells: Role of efficient Toll-like receptor 4 signaling. *Am J Physiol - Hear Circ Physiol* 289, 2005. doi: 10.1152/ajpheart.00143.2005.
318. **Ye G, Fu Q, Jiang L, Li Z.** Vascular smooth muscle cells activate PI3K/Akt pathway to attenuate myocardial ischemia/reperfusion-induced apoptosis and autophagy by secreting bFGF. *Biomed Pharmacother* 107, 2018. doi: 10.1016/j.biopha.2018.05.113.
319. **Yi R, Qin Y, Macara IG, Cullen BR.** Exportin-5 mediates the nuclear export of pre-microRNAs and short hairpin RNAs. *Genes Dev* 17: 3011–3016, 2003. doi: 10.1101/gad.1158803.
320. **Yin X, Xu C, Xu Q, Lang D.** Docosahexaenoic acid inhibits vascular smooth muscle cell migration and proliferation by decreasing microRNA-155 expression levels. *Mol*

Med Rep 22: 3396–3404, 2020. doi: 10.3892/mmr.2020.11404.

321. **Yoon JH, Abdelmohsen K, Srikantan S, Yang X, Martindale JL, De S, Huarte M, Zhan M, Becker KG, Gorospe M.** LincRNA-p21 Suppresses Target mRNA Translation. *Mol Cell* 47, 2012. doi: 10.1016/j.molcel.2012.06.027.
322. **Yoon YS, Lee JH, Hwang SC, Choi KS, Yoon G.** TGF β 1 induces prolonged mitochondrial ROS generation through decreased complex IV activity with senescent arrest in Mv1Lu cells. *Oncogene* 24: 1895–1903, 2005. doi: 10.1038/sj.onc.1208262.
323. **Yosef R, Pilpel N, Tokarsky-Amiel R, Biran A, Ovadya Y, Cohen S, Vadai E, Dassa L, Shahar E, Condiotti R, Ben-Porath I, Krizhanovsky V.** Directed elimination of senescent cells by inhibition of BCL-W and BCL-XL. *Nat Commun* 7, 2016. doi: 10.1038/ncomms11190.
324. **Young ARJ, Narita M, Ferreira M, Kirschner K, Sadaie M, Darot JFJ, Tavar?? S, Arakawa S, Shimizu S, Watt FM, Narita M.** Autophagy mediates the mitotic senescence transition. *Genes Dev* 23: 798–803, 2009.
325. **Yu B, Wong MM, Potter CMF, Simpson RML, Karamariti E, Zhang Z, Zeng L, Warren D, Hu Y, Wang W, Xu Q.** Vascular Stem/Progenitor Cell Migration Induced by Smooth Muscle Cell-Derived Chemokine (C-C Motif) Ligand 2 and Chemokine (C-X-C motif) Ligand 1 Contributes to Neointima Formation. *Stem Cells* 34: 2368–2380, 2016. doi: 10.1002/stem.2410.
326. **Yu Z, Hecht NB.** The DNA/RNA-binding protein, translin, binds microRNA122a and increases its in vivo stability. *J Androl* 29: 572–579, 2008. doi: 10.2164/jandrol.108.005090.
327. **Yudkin JS, Kumari M, Humphries SE, Mohamed-Ali V.** Inflammation, obesity, stress and coronary heart disease: Is interleukin-6 the link? *Atherosclerosis* 148: 2000.
328. **Zampetaki A, Willeit P, Tilling L, Drozdov I, Prokopi M, Renard JM, Mayr A, Weger S, Schett G, Shah A, Boulanger CM, Willeit J, Chowienczyk PJ, Kiechl S, Mayr M.** Prospective study on circulating microRNAs and risk of myocardial infarction. *J Am Coll Cardiol* 60: 290–299, 2012. doi: 10.1016/j.jacc.2012.03.056.
329. **Zappe M, Feldner A, Arnold C, Sticht C, Hecker M, Korff T.** NFAT5 isoform C controls biomechanical stress responses of vascular smooth muscle cells. *Front Physiol* 9, 2018. doi: 10.3389/fphys.2018.01190.
330. **Zhang J, Fei Z, Xiaoling Y, Xiang L, Guofeng Z.** MicroRNA-155 modulates the proliferation of vascular smooth muscle cells by targeting endothelial nitric oxide synthase. *Int J Mol Med* 35: 1708–1714, 2015. doi: 10.3892/ijmm.2015.2181.
331. **Zhang J, Li S, Li L, Li M, Guo C, Yao J, Mi S.** Exosome and Exosomal MicroRNA: Trafficking, Sorting, and Function. *Genomics Proteomics Bioinformatics* 13: 17–24, 2015. doi: 10.1016/j.gpb.2015.02.001.
332. **Zhang J, Wang L, Fu W, Wang C, Guo D, Jiang J, Wang Y.** Smooth muscle cell phenotypic diversity between dissected and unaffected thoracic aortic media. [Online]. *J Cardiovasc Surg (Torino)* 54: 511–21, 2013. <http://www.ncbi.nlm.nih.gov/pubmed/23594508>.
333. **Zhang X, Chen S, Yoo S, Chakrabarti S, Zhang T, Ke T, Oberti C, Yong SL, Fang F, Li L, de la Fuente R, Wang L, Chen Q, Wang QK.** Mutation in Nuclear Pore Component

- NUP155 Leads to Atrial Fibrillation and Early Sudden Cardiac Death. *Cell* 135, 2008. doi: 10.1016/j.cell.2008.10.022.
334. **Zhang Y.** RNA-induced Silencing Complex (RISC). In: *Encyclopedia of Systems Biology*, edited by Dubitzky W, Wolkenhauer O, Cho K-H, Yokota H. Springer New York, p. 1876–1876.
335. **Zhang Y, Alexander PB, Wang X-F.** TGF- β Family Signaling in the Control of Cell Proliferation and Survival. *Cold Spring Harb Perspect Biol* 9: a022145, 2017. doi: 10.1101/cshperspect.a022145.
336. **Zhang Y, Xie B, Sun L, Chen W, Jiang S-L, Liu W, Bian F, Tian H, Li R-K.** Phenotypic switching of vascular smooth muscle cells in the ‘normal region’ of aorta from atherosclerosis patients is regulated by miR-145. *J Cell Mol Med* 20: 1049–1061, 2016. doi: 10.1111/jcmm.12825.
337. **Zhao L, Ouyang Y, Bai Y, Gong J, Liao H.** miR-155-5p inhibits the viability of vascular smooth muscle cell via targeting FOS and ZIC3 to promote aneurysm formation. *Eur J Pharmacol* 853: 145–152, 2019. doi: 10.1016/j.ejphar.2019.03.030.
338. **Zhao W, Zheng XL, Peng DQ, Zhao SP.** Myocyte Enhancer Factor 2A Regulates Hydrogen Peroxide-Induced Senescence of Vascular Smooth Muscle Cells Via microRNA-143. *J Cell Physiol* 230: 2202–2211, 2015. doi: 10.1002/jcp.24948.
339. **Zhao Y, Li Y, Luo P, Gao Y, Yang J, Lao KH, Wang G, Cockerill G, Hu Y, Xu Q, Li T, Zeng L.** XBP1 splicing triggers miR-150 transfer from smooth muscle cells to endothelial cells via extracellular vesicles. *Sci Rep* 6: e28627, 2016. doi: 10.1038/srep28627.
340. **Zheng B, Yin W-N na, Suzuki T, Zhang X-H hua, Zhang Y, Song L-L li, Jin L-S shuang, Zhan H, Zhang H, Li J-S shui, Wen J-K kun.** Exosome-Mediated miR-155 Transfer from Smooth Muscle Cells to Endothelial Cells Induces Endothelial Injury and Promotes Atherosclerosis. *Mol Ther* 25: 1279–1294, 2017. doi: 10.1016/j.ymthe.2017.03.031.
341. **Zheng T, Pu J, Chen Y, Mao Y, Guo Z, Pan H, Zhang L, Zhang H, Sun B, Zhang B.** Plasma exosomes spread and cluster around β -amyloid plaques in an animal model of Alzheimer’s disease. .
342. **Zheng Y, Song A, Zhou Y, Zhong Y, Zhang W, Wang C, Ding X, Du Y, Zhang W, Li G, Wu H, Wu Y, Song X.** Identification of extracellular vesicles-transported miRNAs in Erlotinib-resistant head and neck squamous cell carcinoma. *J Cell Commun Signal* 14: 389–402, 2020. doi: 10.1007/s12079-020-00546-7.
343. **Zhou J, Li YS, Nguyen P, Wang KC, Weiss A, Kuo YC, Chiu JJ, Shyy JY, Chien S.** Regulation of vascular smooth muscle cell turnover by endothelial cell-secreted microRNA-126 role of shear stress. *Circ Res* 113: 40–51, 2013. doi: 10.1161/CIRCRESAHA.113.280883.

Chapter 8. Appendix

8.1. Cycling conditions and reaction setup for relative telomere length measurement

Table 9. Cycling conditions for Tel Assay.

Step	Temp (°C)	Time	Cycle
Initial Heat Activation	95	10 min	None
Denaturation	95	15 sec	
Annealing/ Extension	60	2 min	30
Melting Curve	60-95		None

Table 10. Reaction setup for 36B4 assay.

Components	10ul RXN (ul)	Final Conc
2xSYBR FAST MM	5	1x
10uM Primer F	0.3	300nM
10uM Primer R	0.5	500nM
PCR-grade dH2O	3.2	N/A
gDNA	1	
Total	10ul	

Table 11. Reaction setup for Tel Assay.

Components	10ul RXN (ul)	Final Conc
2xSYBR FAST MM	5	1x
10uM Primer F	0.27	270nM
10uM Primer R	0.9	900nM
PCR-grade dH2O	2.83	N/A
gDNA	1	
Total	10ul	

8.2. Sample summary

Table 12: Summary of sequenced reads of all samples.

Sample	Total Reads	Trimmed Reads	Reads sent to Aligner	Aligned Reads	Precursor miRNA Reads	Mature miRNA Reads	Known miRNA with $\geq 5x$ coverage
03P6C	4,924,608	4,525,030	4654736	3724810	2844	2988132	528
03P6X	13,537,285	12,958,433	11109960	1396307	410	37503	186
04P7C	9,471,967	8,814,867	8726065	6843025	4912	5722413	604
04P7X	9,711,338	9,350,993	8015520	921642	158	34475	146
06P5C	10,432,939	9,834,979	9463280	5724745	2177	4504369	562
06P5X	13,168,855	12,829,966	9962104	2194131	171	16392	116
01P7C	11,266,822	10,761,913	9914147	4439284	2979	2552389	500
01P7X	8,579,597	8,233,284	7413359	826997	44	5213	70
03P19C	15,585,311	14,801,322	14524922	2868489	4364	327301	342
03P19X	12,628,241	10,714,777	10253705	317729	484	5325	75
04P11C	9,085,040	8,580,974	8455775	6086056	3026	4905795	581
04P11X	9,065,679	8,594,624	7911892	895225	68	8709	96
Total	127,457,682	120,001,162	110,405,465	36,238,440	21,637	21,108,016	3,806

8.3. Target genes of Differentially Expressed miRNAs

Table 13: Validated target genes of differentially expressed miRNAs reported by miRWalk.

DE miRNA	Target genes
hsa-miR-146b-5p	SRPRB
hsa-miR-146b-5p	POMT2
hsa-miR-146b-5p	LSM4
hsa-miR-146b-5p	KCTD15
hsa-miR-146b-5p	ZNF260
hsa-miR-146b-5p	LIMD2
hsa-miR-146b-5p	NSL1
hsa-miR-146b-5p	AKT3
hsa-miR-146b-5p	AVL9
hsa-miR-146b-5p	FANCF
hsa-miR-146b-5p	TRAF6
hsa-miR-146b-5p	CENPU
hsa-miR-146b-5p	TLR4
hsa-miR-146b-5p	MICAL2
hsa-miR-146b-5p	WSB2
hsa-miR-146b-5p	EGFR
hsa-miR-146b-5p	TMEM167A
hsa-miR-146b-5p	GPM6B
hsa-miR-146b-5p	ALG10B
hsa-miR-146b-5p	CDC73
hsa-miR-146b-5p	ARL8A
hsa-miR-146b-5p	MYO6
hsa-miR-146b-5p	ZNF292
hsa-miR-146b-5p	MDN1
hsa-miR-146b-5p	SFRP1
hsa-miR-146b-5p	CCDC83
hsa-miR-146b-5p	CCDC6
hsa-miR-146b-5p	RUFY2
hsa-miR-146b-5p	MMP16
hsa-miR-146b-5p	DECR1
hsa-miR-146b-5p	CYBRD1
hsa-miR-146b-5p	MFSD6
hsa-miR-146b-5p	XPO4
hsa-miR-146b-5p	BRWD1
hsa-miR-146b-5p	TMPRSS5
hsa-miR-146b-5p	TMEM136
hsa-miR-146b-5p	PPP1R11
hsa-miR-146b-5p	RHOBTB3
hsa-miR-146b-5p	RAB2B
hsa-miR-146b-5p	MRPL10
hsa-miR-146b-5p	RHOA
hsa-miR-146b-5p	NOVA1
hsa-miR-146b-5p	PDGFRA
hsa-miR-146b-5p	KIT
hsa-miR-146b-5p	HNRNPD
hsa-miR-146b-5p	AKAP8
hsa-miR-146b-5p	ST6GAL2
hsa-miR-146b-5p	ZNF629
hsa-miR-146b-5p	COPA
hsa-miR-146b-5p	ZNRF3
hsa-miR-146b-5p	TLL1
hsa-miR-146b-5p	CARD11
hsa-miR-146b-5p	MKRN2
hsa-miR-146b-5p	CASR
hsa-miR-146b-5p	MYLK
hsa-miR-146b-5p	UMPS
hsa-miR-146b-5p	SERTAD2
hsa-miR-146b-5p	PMAIP1
hsa-miR-146b-5p	CYTIP
hsa-miR-146b-5p	CDKN1A
hsa-miR-146b-5p	PARD6B
hsa-miR-146b-5p	IL1RAP
hsa-miR-155-5p	SAP30L
hsa-miR-155-5p	GEMIN5
hsa-miR-155-5p	WNK1
hsa-miR-155-5p	ZNF384
hsa-miR-155-5p	CDKN1B
hsa-miR-155-5p	RAB2A
hsa-miR-155-5p	ANPEP
hsa-miR-155-5p	KCTD5
hsa-miR-155-5p	RAPH1
hsa-miR-155-5p	WDFY1
hsa-miR-155-5p	MFF
hsa-miR-155-5p	WWC1
hsa-miR-155-5p	CREBRF
hsa-miR-155-5p	CPEB4
hsa-miR-155-5p	DBN1
hsa-miR-155-5p	RREB1
hsa-miR-155-5p	AGTR1
hsa-miR-155-5p	GMPS
hsa-miR-155-5p	GEN1
hsa-miR-155-5p	PSEN1
hsa-miR-155-5p	SEL1L
hsa-miR-155-5p	TSHZ3
hsa-miR-155-5p	RBM42
hsa-miR-155-5p	CHD7
hsa-miR-155-5p	SRSF1
hsa-miR-155-5p	DHX40
hsa-miR-155-5p	CLTC
hsa-miR-155-5p	DCAF7
hsa-miR-155-5p	SMARCD2
hsa-miR-155-5p	GNA13
hsa-miR-155-5p	C17orf80
hsa-miR-155-5p	MARC1
hsa-miR-155-5p	KBTBD2
hsa-miR-155-5p	DPY19L1
hsa-miR-155-5p	TBC1D8B

hsa-miR-155-5p	STAG2	hsa-miR-155-5p	GAPVD1	hsa-miR-155-5p	EDEM3	hsa-miR-155-5p	SIRT1
hsa-miR-155-5p	MBNL3	hsa-miR-155-5p	CD3EAP	hsa-miR-155-5p	CDC73	hsa-miR-155-5p	HERC4
hsa-miR-155-5p	SOX6	hsa-miR-155-5p	QPCTL	hsa-miR-155-5p	DENND1B	hsa-miR-155-5p	CEP41
hsa-miR-155-5p	DCAF10	hsa-miR-155-5p	CARS	hsa-miR-155-5p	KIF14	hsa-miR-155-5p	MKLN1
hsa-miR-155-5p	UBQLN1	hsa-miR-155-5p	STIM1	hsa-miR-155-5p	NUCKS1	hsa-miR-155-5p	PODXL
hsa-miR-155-5p	UBE2G1	hsa-miR-155-5p	ARFIP2	hsa-miR-155-5p	SLC30A1	hsa-miR-155-5p	CDK5
hsa-miR-155-5p	NOLC1	hsa-miR-155-5p	KMT5A	hsa-miR-155-5p	OSBPL9	hsa-miR-155-5p	ZIC3
hsa-miR-155-5p	SH3PXD2A	hsa-miR-155-5p	EGFR	hsa-miR-155-5p	DHCR24	hsa-miR-155-5p	LDOC1
hsa-miR-155-5p	ADD3	hsa-miR-155-5p	NSUN5	hsa-miR-155-5p	TACSTD2	hsa-miR-155-5p	MMP16
hsa-miR-155-5p	RAB11FIP2	hsa-miR-155-5p	LAT2	hsa-miR-155-5p	PATJ	hsa-miR-155-5p	UQCRB
hsa-miR-155-5p	EIF3A	hsa-miR-155-5p	CD36	hsa-miR-155-5p	LRRC40	hsa-miR-155-5p	ATP6V1C1
hsa-miR-155-5p	DOCK1	hsa-miR-155-5p	DMTF1	hsa-miR-155-5p	RUNX2	hsa-miR-155-5p	EIF3E
hsa-miR-155-5p	TRAM1	hsa-miR-155-5p	BET1	hsa-miR-155-5p	MUT	hsa-miR-155-5p	TRPS1
hsa-miR-155-5p	PKIA	hsa-miR-155-5p	ASNS	hsa-miR-155-5p	FAM135A	hsa-miR-155-5p	FAM91A1
hsa-miR-155-5p	ACOT7	hsa-miR-155-5p	UPF2	hsa-miR-155-5p	CD109	hsa-miR-155-5p	PDLIM5
hsa-miR-155-5p	VAMP3	hsa-miR-155-5p	ARL5B	hsa-miR-155-5p	NT5E	hsa-miR-155-5p	NFKB1
hsa-miR-155-5p	AGTRAP	hsa-miR-155-5p	ZNF248	hsa-miR-155-5p	MMS22L	hsa-miR-155-5p	UBE2D3
hsa-miR-155-5p	CASP3	hsa-miR-155-5p	TTC37	hsa-miR-155-5p	NSD3	hsa-miR-155-5p	AIMP1
hsa-miR-155-5p	TRIO	hsa-miR-155-5p	PLEKHA5	hsa-miR-155-5p	PLEKHA2	hsa-miR-155-5p	SEC24B
hsa-miR-155-5p	OTULIN	hsa-miR-155-5p	GOLT1B	hsa-miR-155-5p	INTS4	hsa-miR-155-5p	PDK1
hsa-miR-155-5p	MYO10	hsa-miR-155-5p	BCAT1	hsa-miR-155-5p	PICALM	hsa-miR-155-5p	LNPK
hsa-miR-155-5p	GOLPH3	hsa-miR-155-5p	TWF1	hsa-miR-155-5p	CCDC82	hsa-miR-155-5p	HNRNPA3
hsa-miR-155-5p	NUP155	hsa-miR-155-5p	ARID2	hsa-miR-155-5p	DYNC2H1	hsa-miR-155-5p	NCKAP1
hsa-miR-155-5p	ARL15	hsa-miR-155-5p	TMBIM6	hsa-miR-155-5p	KDEL2	hsa-miR-155-5p	SLC39A10
hsa-miR-155-5p	MTREX	hsa-miR-155-5p	SLC11A2	hsa-miR-155-5p	CHTOP	hsa-miR-155-5p	SLC7A1
hsa-miR-155-5p	RAD23B	hsa-miR-155-5p	TFCP2	hsa-miR-155-5p	KCNN3	hsa-miR-155-5p	NAA16
hsa-miR-155-5p	STRBP	hsa-miR-155-5p	RGL1	hsa-miR-155-5p	MTRNR2L5	hsa-miR-155-5p	CAB39L

hsa-miR-155-5p	INTS6	hsa-miR-155-5p	ABCC4	hsa-miR-155-5p	MIA2	hsa-miR-155-5p	KIF22
hsa-miR-155-5p	VPS36	hsa-miR-155-5p	PCCA	hsa-miR-155-5p	VANGL1	hsa-miR-155-5p	BCL7C
hsa-miR-155-5p	ZNF260	hsa-miR-155-5p	TPP2	hsa-miR-155-5p	MAN1A2	hsa-miR-155-5p	LONP2
hsa-miR-155-5p	SUPT5H	hsa-miR-155-5p	KDELC1	hsa-miR-155-5p	PHGDH	hsa-miR-155-5p	ZSWIM6
hsa-miR-155-5p	LEMD3	hsa-miR-155-5p	DCUN1D2	hsa-miR-155-5p	NOTCH2	hsa-miR-155-5p	ERBIN
hsa-miR-155-5p	CCT2	hsa-miR-155-5p	CHD8	hsa-miR-155-5p	TMEM33	hsa-miR-155-5p	PIK3R1
hsa-miR-155-5p	GLIPR1	hsa-miR-155-5p	KANSL1	hsa-miR-155-5p	FIP1L1	hsa-miR-155-5p	TNPO1
hsa-miR-155-5p	CSR2	hsa-miR-155-5p	CUX1	hsa-miR-155-5p	MTAP	hsa-miR-155-5p	INPP5D
hsa-miR-155-5p	CEP83	hsa-miR-155-5p	SYPL1	hsa-miR-155-5p	CDKN2A	hsa-miR-155-5p	ARL8B
hsa-miR-155-5p	HAL	hsa-miR-155-5p	PNPLA8	hsa-miR-155-5p	ASPH	hsa-miR-155-5p	TBC1D14
hsa-miR-155-5p	APAF1	hsa-miR-155-5p	DOCK4	hsa-miR-155-5p	MYBL1	hsa-miR-155-5p	LCORL
hsa-miR-155-5p	APC	hsa-miR-155-5p	CALU	hsa-miR-155-5p	VCIPI1	hsa-miR-155-5p	KLHL5
hsa-miR-155-5p	PRRC1	hsa-miR-155-5p	PAPOLA	hsa-miR-155-5p	SMAD3	hsa-miR-155-5p	UGDH
hsa-miR-155-5p	FUBP1	hsa-miR-155-5p	RCOR1	hsa-miR-155-5p	RCN2	hsa-miR-155-5p	KDM1A
hsa-miR-155-5p	ZNF644	hsa-miR-155-5p	TNFAIP2	hsa-miR-155-5p	TSPAN3	hsa-miR-155-5p	LUZP1
hsa-miR-155-5p	AGL	hsa-miR-155-5p	CYFIP1	hsa-miR-155-5p	ZNF561	hsa-miR-155-5p	MECR
hsa-miR-155-5p	VCAM1	hsa-miR-155-5p	TJP1	hsa-miR-155-5p	SMARCA4	hsa-miR-155-5p	SSH2
hsa-miR-155-5p	CCND1	hsa-miR-155-5p	FAM98B	hsa-miR-155-5p	RETSAT	hsa-miR-155-5p	CPD
hsa-miR-155-5p	FADD	hsa-miR-155-5p	COPS3	hsa-miR-155-5p	CIAO1	hsa-miR-155-5p	ZNF207
hsa-miR-155-5p	CBL	hsa-miR-155-5p	ALDH3A2	hsa-miR-155-5p	CNNM3	hsa-miR-155-5p	FDFT1
hsa-miR-155-5p	TBRG1	hsa-miR-155-5p	AKAP10	hsa-miR-155-5p	LTN1	hsa-miR-155-5p	LPL
hsa-miR-155-5p	SP1	hsa-miR-155-5p	SPECC1	hsa-miR-155-5p	BACH1	hsa-miR-155-5p	SLC39A14
hsa-miR-155-5p	CDK2	hsa-miR-155-5p	MTRNR2L1	hsa-miR-155-5p	PAXB1	hsa-miR-155-5p	PPP2R2A
hsa-miR-155-5p	JARID2	hsa-miR-155-5p	TRAK1	hsa-miR-155-5p	HDHD5	hsa-miR-155-5p	SOCS1
hsa-miR-155-5p	DEK	hsa-miR-155-5p	CCR9	hsa-miR-155-5p	GNL3L	hsa-miR-155-5p	MARF1
hsa-miR-155-5p	MRS2	hsa-miR-155-5p	QRICH1	hsa-miR-155-5p	UBQLN2	hsa-miR-155-5p	RAB6A
hsa-miR-155-5p	DIAPH3	hsa-miR-155-5p	RHOA	hsa-miR-155-5p	EIF3C	hsa-miR-155-5p	TPD52

hsa-miR-155-5p	SLC12A4	hsa-miR-155-5p	TCF12	hsa-miR-155-5p	FLNB	hsa-miR-155-5p	BCL6
hsa-miR-155-5p	PDPR	hsa-miR-155-5p	ANXA2	hsa-miR-155-5p	EOGT	hsa-miR-20a-5p	NR3C1
hsa-miR-155-5p	GLG1	hsa-miR-155-5p	MYLK	hsa-miR-155-5p	ARL6IP5	hsa-miR-20a-5p	GRPEL2
hsa-miR-155-5p	CDH13	hsa-miR-155-5p	ZNF148	hsa-miR-155-5p	ZNF28	hsa-miR-20a-5p	CSNK1A1
hsa-miR-155-5p	UAP1	hsa-miR-155-5p	PLXND1	hsa-miR-155-5p	ASB6	hsa-miR-20a-5p	NCAPD2
hsa-miR-155-5p	HSD17B7	hsa-miR-155-5p	SHANK2	hsa-miR-155-5p	EXOSC2	hsa-miR-20a-5p	PHC1
hsa-miR-155-5p	XPR1	hsa-miR-155-5p	FEZ2	hsa-miR-155-5p	VAV2	hsa-miR-20a-5p	M6PR
hsa-miR-155-5p	JADE1	hsa-miR-155-5p	STRN	hsa-miR-155-5p	RAB6C	hsa-miR-20a-5p	KLRD1
hsa-miR-155-5p	HHIP	hsa-miR-155-5p	ATL2	hsa-miR-155-5p	RAB6D	hsa-miR-20a-5p	MAGOHB
hsa-miR-155-5p	SMAD1	hsa-miR-155-5p	MSH2	hsa-miR-155-5p	CCNT2	hsa-miR-20a-5p	PTPRO
hsa-miR-155-5p	ARFIP1	hsa-miR-155-5p	MSH6	hsa-miR-155-5p	RIF1	hsa-miR-20a-5p	WDR73
hsa-miR-155-5p	RAPGEF2	hsa-miR-155-5p	PSME4	hsa-miR-155-5p	HLA-DPA1	hsa-miR-20a-5p	SLC28A1
hsa-miR-155-5p	EHD1	hsa-miR-155-5p	PNPT1	hsa-miR-155-5p	CSE1L	hsa-miR-20a-5p	ABHD2
hsa-miR-155-5p	ITGB4	hsa-miR-155-5p	PELI1	hsa-miR-155-5p	AURKA	hsa-miR-20a-5p	AP3S2
hsa-miR-155-5p	RPTOR	hsa-miR-155-5p	SERTAD2	hsa-miR-155-5p	MTRNR2L3	hsa-miR-20a-5p	SEMA4B
hsa-miR-155-5p	TWSG1	hsa-miR-155-5p	MEIS1	hsa-miR-155-5p	TSPAN14	hsa-miR-20a-5p	CRTC3
hsa-miR-155-5p	CARD11	hsa-miR-155-5p	ANTXR1	hsa-miR-155-5p	GHITM	hsa-miR-20a-5p	RCCD1
hsa-miR-155-5p	RBAK	hsa-miR-155-5p	AAK1	hsa-miR-155-5p	IFIT5	hsa-miR-20a-5p	CAPN15
hsa-miR-155-5p	RAC1	hsa-miR-155-5p	PCYOX1	hsa-miR-155-5p	ENTPD1	hsa-miR-20a-5p	FAHD1
hsa-miR-155-5p	PHF14	hsa-miR-155-5p	MARCKS	hsa-miR-155-5p	TNKS1BP1	hsa-miR-20a-5p	ZNF598
hsa-miR-155-5p	OXNAD1	hsa-miR-155-5p	KPNA5	hsa-miR-155-5p	MRPL16	hsa-miR-20a-5p	ECI1
hsa-miR-155-5p	THRB	hsa-miR-155-5p	MYB	hsa-miR-155-5p	GANAB	hsa-miR-20a-5p	PDPK1
hsa-miR-155-5p	GLB1	hsa-miR-155-5p	DSG2	hsa-miR-155-5p	STX5	hsa-miR-20a-5p	FAM126B
hsa-miR-155-5p	MLH1	hsa-miR-155-5p	RPRD1A	hsa-miR-155-5p	RTN3	hsa-miR-20a-5p	BMPR2
hsa-miR-155-5p	RAD51	hsa-miR-155-5p	SMAD2	hsa-miR-155-5p	FNDC3B	hsa-miR-20a-5p	FAM117B
hsa-miR-155-5p	RPAP1	hsa-miR-155-5p	WDR82	hsa-miR-155-5p	PIK3CA	hsa-miR-20a-5p	ICA1L
hsa-miR-155-5p	SLC27A2	hsa-miR-155-5p	PDE12	hsa-miR-155-5p	YEATS2	hsa-miR-20a-5p	ABI2

hsa-miR-20a-5p	CREB1	hsa-miR-20a-5p	CHURC1	hsa-miR-20a-5p	KPNA2	hsa-miR-20a-5p	PHF6
hsa-miR-20a-5p	PLEKHM3	hsa-miR-20a-5p	EIF2S1	hsa-miR-20a-5p	PRKAR1A	hsa-miR-20a-5p	UEVLD
hsa-miR-20a-5p	CPS1	hsa-miR-20a-5p	ZFYVE26	hsa-miR-20a-5p	MIXL1	hsa-miR-20a-5p	LUZP2
hsa-miR-20a-5p	ARPC2	hsa-miR-20a-5p	SYNJ2BP	hsa-miR-20a-5p	ITPKB	hsa-miR-20a-5p	PRRG4
hsa-miR-20a-5p	KIAA1191	hsa-miR-20a-5p	TTC9	hsa-miR-20a-5p	SNAP47	hsa-miR-20a-5p	FBXO3
hsa-miR-20a-5p	FAF2	hsa-miR-20a-5p	DNAL1	hsa-miR-20a-5p	PCNX2	hsa-miR-20a-5p	FJX1
hsa-miR-20a-5p	ZNF454	hsa-miR-20a-5p	ELMSAN1	hsa-miR-20a-5p	TOMM20	hsa-miR-20a-5p	CRY2
hsa-miR-20a-5p	SQSTM1	hsa-miR-20a-5p	EFCAB11	hsa-miR-20a-5p	ARID4B	hsa-miR-20a-5p	ARHGAP1
hsa-miR-20a-5p	MAPK9	hsa-miR-20a-5p	RPS6KA5	hsa-miR-20a-5p	GPR137B	hsa-miR-20a-5p	PIGO
hsa-miR-20a-5p	SLC22A23	hsa-miR-20a-5p	CCDC88C	hsa-miR-20a-5p	CEP170	hsa-miR-20a-5p	MELK
hsa-miR-20a-5p	PLS1	hsa-miR-20a-5p	F2RL3	hsa-miR-20a-5p	ZBTB18	hsa-miR-20a-5p	ZBTB5
hsa-miR-20a-5p	U2SURP	hsa-miR-20a-5p	HAUS8	hsa-miR-20a-5p	KIF26B	hsa-miR-20a-5p	RFK
hsa-miR-20a-5p	FBXO31	hsa-miR-20a-5p	RFXANK	hsa-miR-20a-5p	TMEM196	hsa-miR-20a-5p	BICD2
hsa-miR-20a-5p	CDT1	hsa-miR-20a-5p	SUGP1	hsa-miR-20a-5p	ITGB8	hsa-miR-20a-5p	PTPDC1
hsa-miR-20a-5p	RNASEH1	hsa-miR-20a-5p	LPAR2	hsa-miR-20a-5p	SP4	hsa-miR-20a-5p	VPS53
hsa-miR-20a-5p	RRM2	hsa-miR-20a-5p	ZNF93	hsa-miR-20a-5p	CYCS	hsa-miR-20a-5p	FAM57A
hsa-miR-20a-5p	LAPTM4A	hsa-miR-20a-5p	ZNF681	hsa-miR-20a-5p	TAX1BP1	hsa-miR-20a-5p	CRK
hsa-miR-20a-5p	UBXN2A	hsa-miR-20a-5p	FXYD5	hsa-miR-20a-5p	FKBP14	hsa-miR-20a-5p	ANKFY1
hsa-miR-20a-5p	DNAJC27	hsa-miR-20a-5p	KMT2B	hsa-miR-20a-5p	POLM	hsa-miR-20a-5p	GBF1
hsa-miR-20a-5p	SLC35F6	hsa-miR-20a-5p	RUNX1	hsa-miR-20a-5p	PURB	hsa-miR-20a-5p	TRIM8
hsa-miR-20a-5p	MAPRE3	hsa-miR-20a-5p	TMEM100	hsa-miR-20a-5p	TSPAN6	hsa-miR-20a-5p	SLK
hsa-miR-20a-5p	NRBP1	hsa-miR-20a-5p	VEZF1	hsa-miR-20a-5p	RBM41	hsa-miR-20a-5p	MXI1
hsa-miR-20a-5p	CLIP4	hsa-miR-20a-5p	TRIM37	hsa-miR-20a-5p	ACSL4	hsa-miR-20a-5p	RBM20
hsa-miR-20a-5p	PCNX4	hsa-miR-20a-5p	USP32	hsa-miR-20a-5p	ZBTB33	hsa-miR-20a-5p	GPAM
hsa-miR-20a-5p	WDR89	hsa-miR-20a-5p	MAP3K3	hsa-miR-20a-5p	XIAP	hsa-miR-20a-5p	VTI1A
hsa-miR-20a-5p	ESR2	hsa-miR-20a-5p	CCDC47	hsa-miR-20a-5p	OCRL	hsa-miR-20a-5p	TCF7L2
hsa-miR-20a-5p	ZBTB25	hsa-miR-20a-5p	APOH	hsa-miR-20a-5p	ZNF280C	hsa-miR-20a-5p	FAM160B1

hsa-miR-20a-5p	INPP5F	hsa-miR-20a-5p	PPP6C	hsa-miR-20a-5p	EIF4H	hsa-miR-20a-5p	PRRG1
hsa-miR-20a-5p	IKZF5	hsa-miR-20a-5p	RTN2	hsa-miR-20a-5p	GTF2IRD2	hsa-miR-20a-5p	CXorf38
hsa-miR-20a-5p	ACADSB	hsa-miR-20a-5p	SLC1A5	hsa-miR-20a-5p	GTF2IRD2B	hsa-miR-20a-5p	LDHB
hsa-miR-20a-5p	ZRANB1	hsa-miR-20a-5p	ARHGAP35	hsa-miR-20a-5p	HIP1	hsa-miR-20a-5p	CAPRN2
hsa-miR-20a-5p	SLCO5A1	hsa-miR-20a-5p	KCNA7	hsa-miR-20a-5p	ANKIB1	hsa-miR-20a-5p	DENND5B
hsa-miR-20a-5p	ELOC	hsa-miR-20a-5p	TBC1D17	hsa-miR-20a-5p	GATAD1	hsa-miR-20a-5p	KIAA1551
hsa-miR-20a-5p	CAMTA1	hsa-miR-20a-5p	SPIB	hsa-miR-20a-5p	SAMD9L	hsa-miR-20a-5p	DNM1L
hsa-miR-20a-5p	LZIC	hsa-miR-20a-5p	NUP98	hsa-miR-20a-5p	VPS50	hsa-miR-20a-5p	IRAK4
hsa-miR-20a-5p	DRAXIN	hsa-miR-20a-5p	TMEM9B	hsa-miR-20a-5p	WDR37	hsa-miR-20a-5p	SENP1
hsa-miR-20a-5p	AGMAT	hsa-miR-20a-5p	NRIP3	hsa-miR-20a-5p	PFKP	hsa-miR-20a-5p	FMNL3
hsa-miR-20a-5p	DDI2	hsa-miR-20a-5p	WEE1	hsa-miR-20a-5p	PIP4K2A	hsa-miR-20a-5p	RACGAP1
hsa-miR-20a-5p	IRF2	hsa-miR-20a-5p	CTR9	hsa-miR-20a-5p	MASTL	hsa-miR-20a-5p	LIMA1
hsa-miR-20a-5p	CEP72	hsa-miR-20a-5p	EIF4G2	hsa-miR-20a-5p	WAC	hsa-miR-20a-5p	LAMC1
hsa-miR-20a-5p	MARCH6	hsa-miR-20a-5p	FICD	hsa-miR-20a-5p	BAMBI	hsa-miR-20a-5p	FAM129A
hsa-miR-20a-5p	ANKRD33B	hsa-miR-20a-5p	MAPKAPK5	hsa-miR-20a-5p	MTPAP	hsa-miR-20a-5p	TIMM17A
hsa-miR-20a-5p	ANKH	hsa-miR-20a-5p	FBXO21	hsa-miR-20a-5p	ARHGAP12	hsa-miR-20a-5p	PPP1R12B
hsa-miR-20a-5p	FBXL7	hsa-miR-20a-5p	CIT	hsa-miR-20a-5p	ITGB1	hsa-miR-20a-5p	PPP1R15B
hsa-miR-20a-5p	PTGER4	hsa-miR-20a-5p	RNF34	hsa-miR-20a-5p	MINK1	hsa-miR-20a-5p	DSTYK
hsa-miR-20a-5p	TMEM267	hsa-miR-20a-5p	MLXIP	hsa-miR-20a-5p	RABEP1	hsa-miR-20a-5p	ELK4
hsa-miR-20a-5p	PAIP1	hsa-miR-20a-5p	C12orf65	hsa-miR-20a-5p	TMEM167A	hsa-miR-20a-5p	YOD1
hsa-miR-20a-5p	ITGA2	hsa-miR-20a-5p	GTF2H3	hsa-miR-20a-5p	POLR3G	hsa-miR-20a-5p	PFKFB2
hsa-miR-20a-5p	TGFBR1	hsa-miR-20a-5p	NCOR2	hsa-miR-20a-5p	ZBED1	hsa-miR-20a-5p	LPGAT1
hsa-miR-20a-5p	ABCA1	hsa-miR-20a-5p	BRI3BP	hsa-miR-20a-5p	TLR7	hsa-miR-20a-5p	IPP
hsa-miR-20a-5p	UGCG	hsa-miR-20a-5p	RAN	hsa-miR-20a-5p	TRAPPC2	hsa-miR-20a-5p	EFCAB14
hsa-miR-20a-5p	PRPF4	hsa-miR-20a-5p	ULK1	hsa-miR-20a-5p	GEMIN8	hsa-miR-20a-5p	STIL
hsa-miR-20a-5p	TRIM32	hsa-miR-20a-5p	CRCP	hsa-miR-20a-5p	ACOT9	hsa-miR-20a-5p	CMPK1
hsa-miR-20a-5p	ZBTB6	hsa-miR-20a-5p	LIMK1	hsa-miR-20a-5p	KLHL15	hsa-miR-20a-5p	BTF3L4

hsa-miR-20a-5p	ZYG11A	hsa-miR-20a-5p	RPS27	hsa-miR-20a-5p	RBM12B	hsa-miR-20a-5p	SACS
hsa-miR-20a-5p	JAK1	hsa-miR-20a-5p	ATP8B2	hsa-miR-20a-5p	TMEM67	hsa-miR-20a-5p	RPL21
hsa-miR-20a-5p	LEPROT	hsa-miR-20a-5p	ADAR	hsa-miR-20a-5p	DPY19L4	hsa-miR-20a-5p	KATNAL1
hsa-miR-20a-5p	ANKRD13C	hsa-miR-20a-5p	PBXIP1	hsa-miR-20a-5p	TP53INP1	hsa-miR-20a-5p	HMGB1
hsa-miR-20a-5p	VEGFA	hsa-miR-20a-5p	SLC25A44	hsa-miR-20a-5p	YWHAZ	hsa-miR-20a-5p	N4BP2L2
hsa-miR-20a-5p	ENPP5	hsa-miR-20a-5p	MEF2D	hsa-miR-20a-5p	ZNF706	hsa-miR-20a-5p	RFC3
hsa-miR-20a-5p	TNFRSF21	hsa-miR-20a-5p	SGMS1	hsa-miR-20a-5p	UBR5	hsa-miR-20a-5p	NHLRC3
hsa-miR-20a-5p	LGSN	hsa-miR-20a-5p	A1CF	hsa-miR-20a-5p	KLF10	hsa-miR-20a-5p	AKAP11
hsa-miR-20a-5p	PTP4A1	hsa-miR-20a-5p	PRKG1	hsa-miR-20a-5p	OXR1	hsa-miR-20a-5p	KCNK6
hsa-miR-20a-5p	RNGTT	hsa-miR-20a-5p	TFAM	hsa-miR-20a-5p	SAMD12	hsa-miR-20a-5p	ZNF780A
hsa-miR-20a-5p	PNRC1	hsa-miR-20a-5p	SLC16A9	hsa-miR-20a-5p	MRPL13	hsa-miR-20a-5p	ZNF180
hsa-miR-20a-5p	RRAGD	hsa-miR-20a-5p	CCDC6	hsa-miR-20a-5p	ATAD2	hsa-miR-20a-5p	GNS
hsa-miR-20a-5p	FAXC	hsa-miR-20a-5p	REEP3	hsa-miR-20a-5p	MYC	hsa-miR-20a-5p	LLPH
hsa-miR-20a-5p	RAB11FIP1	hsa-miR-20a-5p	MYPN	hsa-miR-20a-5p	AFF1	hsa-miR-20a-5p	DYRK2
hsa-miR-20a-5p	GINS4	hsa-miR-20a-5p	RUFY2	hsa-miR-20a-5p	GPRIN3	hsa-miR-20a-5p	MDM2
hsa-miR-20a-5p	HOOK3	hsa-miR-20a-5p	VPS26A	hsa-miR-20a-5p	NPNT	hsa-miR-20a-5p	RAB3IP
hsa-miR-20a-5p	RB1CC1	hsa-miR-20a-5p	SAMD8	hsa-miR-20a-5p	FAM241A	hsa-miR-20a-5p	TBC1D15
hsa-miR-20a-5p	EMSY	hsa-miR-20a-5p	CNOT4	hsa-miR-20a-5p	ARSJ	hsa-miR-20a-5p	ATXN7L3B
hsa-miR-20a-5p	TSKU	hsa-miR-20a-5p	MKRN1	hsa-miR-20a-5p	QRFPR	hsa-miR-20a-5p	NAP1L1
hsa-miR-20a-5p	RAB30	hsa-miR-20a-5p	CASP2	hsa-miR-20a-5p	XIRP2	hsa-miR-20a-5p	ATP2B1
hsa-miR-20a-5p	MED17	hsa-miR-20a-5p	ZNF786	hsa-miR-20a-5p	METTL8	hsa-miR-20a-5p	NTN4
hsa-miR-20a-5p	KDM4D	hsa-miR-20a-5p	ZNF398	hsa-miR-20a-5p	CYBRD1	hsa-miR-20a-5p	ARL1
hsa-miR-20a-5p	SESN3	hsa-miR-20a-5p	INSIG1	hsa-miR-20a-5p	GPR155	hsa-miR-20a-5p	GNPTAB
hsa-miR-20a-5p	CEP57	hsa-miR-20a-5p	HMGB3	hsa-miR-20a-5p	DNAJC10	hsa-miR-20a-5p	SLC25A46
hsa-miR-20a-5p	TMEM123	hsa-miR-20a-5p	MECP2	hsa-miR-20a-5p	NABP1	hsa-miR-20a-5p	REEP5
hsa-miR-20a-5p	NPAT	hsa-miR-20a-5p	FLNA	hsa-miR-20a-5p	STK17B	hsa-miR-20a-5p	MCC
hsa-miR-20a-5p	ZC3H12C	hsa-miR-20a-5p	TMEM64	hsa-miR-20a-5p	ZDHHC20	hsa-miR-20a-5p	FEM1C

hsa-miR-20a-5p	CEP120	hsa-miR-20a-5p	BTN3A1	hsa-miR-20a-5p	HEXIM1	hsa-miR-20a-5p	THBS1
hsa-miR-20a-5p	VDAC1	hsa-miR-20a-5p	BTN3A3	hsa-miR-20a-5p	MAP3K14	hsa-miR-20a-5p	TP53
hsa-miR-20a-5p	SMAD5	hsa-miR-20a-5p	GABBR1	hsa-miR-20a-5p	PLEKHM1	hsa-miR-20a-5p	KDM6B
hsa-miR-20a-5p	ETF1	hsa-miR-20a-5p	TUBB	hsa-miR-20a-5p	SP2	hsa-miR-20a-5p	GID4
hsa-miR-20a-5p	PURA	hsa-miR-20a-5p	MICB	hsa-miR-20a-5p	CBX1	hsa-miR-20a-5p	MAP2K3
hsa-miR-20a-5p	PRKACB	hsa-miR-20a-5p	RGMB	hsa-miR-20a-5p	ZNF652	hsa-miR-20a-5p	WSB1
hsa-miR-20a-5p	SSX2IP	hsa-miR-20a-5p	KPNA6	hsa-miR-20a-5p	C7orf43	hsa-miR-20a-5p	TMEM97
hsa-miR-20a-5p	SH3GLB1	hsa-miR-20a-5p	TXLNA	hsa-miR-20a-5p	AGFG2	hsa-miR-20a-5p	KIAA0100
hsa-miR-20a-5p	FNBP1L	hsa-miR-20a-5p	RNF19B	hsa-miR-20a-5p	ORAI2	hsa-miR-20a-5p	NEK8
hsa-miR-20a-5p	F3	hsa-miR-20a-5p	ZMYM1	hsa-miR-20a-5p	CCDC71L	hsa-miR-20a-5p	FYCO1
hsa-miR-20a-5p	SLC30A7	hsa-miR-20a-5p	AGO4	hsa-miR-20a-5p	DNAJB9	hsa-miR-20a-5p	NME6
hsa-miR-20a-5p	USP28	hsa-miR-20a-5p	AGO1	hsa-miR-20a-5p	BMT2	hsa-miR-20a-5p	UQCRC1
hsa-miR-20a-5p	ARCN1	hsa-miR-20a-5p	AGO3	hsa-miR-20a-5p	CAV1	hsa-miR-20a-5p	BCL2L2
hsa-miR-20a-5p	HSPA8	hsa-miR-20a-5p	MTF1	hsa-miR-20a-5p	WASL	hsa-miR-20a-5p	EGLN3
hsa-miR-20a-5p	ACVR1B	hsa-miR-20a-5p	BMP8B	hsa-miR-20a-5p	ZNF800	hsa-miR-20a-5p	CFL2
hsa-miR-20a-5p	MAP3K12	hsa-miR-20a-5p	EXO5	hsa-miR-20a-5p	TMX3	hsa-miR-20a-5p	BRMS1L
hsa-miR-20a-5p	CBX5	hsa-miR-20a-5p	FOXJ3	hsa-miR-20a-5p	MKKNK2	hsa-miR-20a-5p	C14orf28
hsa-miR-20a-5p	ZNF385A	hsa-miR-20a-5p	CCDC30	hsa-miR-20a-5p	DAPK3	hsa-miR-20a-5p	L2HGDH
hsa-miR-20a-5p	GDF11	hsa-miR-20a-5p	YBX1	hsa-miR-20a-5p	CHAF1A	hsa-miR-20a-5p	NIN
hsa-miR-20a-5p	RAB5B	hsa-miR-20a-5p	KIF2C	hsa-miR-20a-5p	TNFAIP8L1	hsa-miR-20a-5p	FRMD6
hsa-miR-20a-5p	ANKRD52	hsa-miR-20a-5p	CKAP2	hsa-miR-20a-5p	DPP9	hsa-miR-20a-5p	DDHD1
hsa-miR-20a-5p	PTGES3	hsa-miR-20a-5p	TDRD3	hsa-miR-20a-5p	BTBD7	hsa-miR-20a-5p	ATG14
hsa-miR-20a-5p	SMIM13	hsa-miR-20a-5p	ARHGEF7	hsa-miR-20a-5p	ATG2B	hsa-miR-20a-5p	CCDC198
hsa-miR-20a-5p	ATXN1	hsa-miR-20a-5p	STAT3	hsa-miR-20a-5p	SLC12A6	hsa-miR-20a-5p	KCND3
hsa-miR-20a-5p	E2F3	hsa-miR-20a-5p	CAVIN1	hsa-miR-20a-5p	ZNF770	hsa-miR-20a-5p	CSDE1
hsa-miR-20a-5p	SOX4	hsa-miR-20a-5p	EZH1	hsa-miR-20a-5p	C15orf41	hsa-miR-20a-5p	SIKE1
hsa-miR-20a-5p	BTN3A2	hsa-miR-20a-5p	RUNDC1	hsa-miR-20a-5p	SPRED1	hsa-miR-20a-5p	PTGFRN

hsa-miR-20a-5p	FAM46C	hsa-miR-20a-5p	PEAK1	hsa-miR-20a-5p	TRAPPC10	hsa-miR-20a-5p	GTF2H2C
hsa-miR-20a-5p	TXNIP	hsa-miR-20a-5p	HMG20A	hsa-miR-20a-5p	MAPK1	hsa-miR-20a-5p	SERF1B
hsa-miR-20a-5p	RPRD2	hsa-miR-20a-5p	C15orf40	hsa-miR-20a-5p	ZNF280B	hsa-miR-20a-5p	SERF1A
hsa-miR-20a-5p	MCL1	hsa-miR-20a-5p	KMT5B	hsa-miR-20a-5p	ZNF70	hsa-miR-20a-5p	F2R
hsa-miR-20a-5p	CERS2	hsa-miR-20a-5p	CPT1A	hsa-miR-20a-5p	GRK3	hsa-miR-20a-5p	F2RL1
hsa-miR-20a-5p	SELENBP1	hsa-miR-20a-5p	MYO1F	hsa-miR-20a-5p	PHF8	hsa-miR-20a-5p	BHMT2
hsa-miR-20a-5p	POGZ	hsa-miR-20a-5p	ZNF426	hsa-miR-20a-5p	WNK3	hsa-miR-20a-5p	MSH3
hsa-miR-20a-5p	THEM4	hsa-miR-20a-5p	DNMT1	hsa-miR-20a-5p	PDZD11	hsa-miR-20a-5p	ATG16L1
hsa-miR-20a-5p	SLAIN2	hsa-miR-20a-5p	LDLR	hsa-miR-20a-5p	CHIC1	hsa-miR-20a-5p	ASB1
hsa-miR-20a-5p	OCIAD1	hsa-miR-20a-5p	ADGRE2	hsa-miR-20a-5p	RLIM	hsa-miR-20a-5p	SEPT2
hsa-miR-20a-5p	KIT	hsa-miR-20a-5p	PITPNA	hsa-miR-20a-5p	NFATC2IP	hsa-miR-20a-5p	IL17RC
hsa-miR-20a-5p	CLOCK	hsa-miR-20a-5p	TSR1	hsa-miR-20a-5p	CDIPT	hsa-miR-20a-5p	NSD2
hsa-miR-20a-5p	REST	hsa-miR-20a-5p	PAFAH1B1	hsa-miR-20a-5p	ZNF785	hsa-miR-20a-5p	ADD1
hsa-miR-20a-5p	ADGRL3	hsa-miR-20a-5p	TET3	hsa-miR-20a-5p	SRCAP	hsa-miR-20a-5p	LRPAP1
hsa-miR-20a-5p	EREG	hsa-miR-20a-5p	TGOLN2	hsa-miR-20a-5p	STX4	hsa-miR-20a-5p	KIAA0232
hsa-miR-20a-5p	CNOT6L	hsa-miR-20a-5p	ZNF514	hsa-miR-20a-5p	MYLK3	hsa-miR-20a-5p	TADA2B
hsa-miR-20a-5p	ZNF7	hsa-miR-20a-5p	DUSP2	hsa-miR-20a-5p	NETO2	hsa-miR-20a-5p	SORCS2
hsa-miR-20a-5p	NFIB	hsa-miR-20a-5p	TMEM127	hsa-miR-20a-5p	N4BP1	hsa-miR-20a-5p	WDR1
hsa-miR-20a-5p	ACER2	hsa-miR-20a-5p	REV1	hsa-miR-20a-5p	PAPD5	hsa-miR-20a-5p	ARAP2
hsa-miR-20a-5p	ELAVL2	hsa-miR-20a-5p	RPL31	hsa-miR-20a-5p	CYLD	hsa-miR-20a-5p	KLF3
hsa-miR-20a-5p	PLEKHO2	hsa-miR-20a-5p	GNAS	hsa-miR-20a-5p	CHD9	hsa-miR-20a-5p	LIAS
hsa-miR-20a-5p	DIS3L	hsa-miR-20a-5p	APP	hsa-miR-20a-5p	RBL2	hsa-miR-20a-5p	AKR7A2
hsa-miR-20a-5p	FEM1B	hsa-miR-20a-5p	USP16	hsa-miR-20a-5p	AKTIP	hsa-miR-20a-5p	NBL1
hsa-miR-20a-5p	PAQR5	hsa-miR-20a-5p	IFNAR1	hsa-miR-20a-5p	NUDT21	hsa-miR-20a-5p	USP48
hsa-miR-20a-5p	SEMA7A	hsa-miR-20a-5p	SON	hsa-miR-20a-5p	SREK1IP1	hsa-miR-20a-5p	HNRNPR
hsa-miR-20a-5p	SCAMP2	hsa-miR-20a-5p	SLC5A3	hsa-miR-20a-5p	SGTB	hsa-miR-20a-5p	E2F2
hsa-miR-20a-5p	UBE2Q2	hsa-miR-20a-5p	PKNOX1	hsa-miR-20a-5p	CCNB1	hsa-miR-20a-5p	RUNX3

hsa-miR-20a-5p	RSRP1	hsa-miR-20a-5p	RRN3	hsa-miR-20a-5p	SUCO	hsa-miR-20a-5p	ATG2A
hsa-miR-20a-5p	MAN1C1	hsa-miR-20a-5p	CCP110	hsa-miR-20a-5p	ZBTB37	hsa-miR-20a-5p	UNK
hsa-miR-20a-5p	SESN2	hsa-miR-20a-5p	ANKS4B	hsa-miR-20a-5p	ABL2	hsa-miR-20a-5p	ACOX1
hsa-miR-20a-5p	RAB42	hsa-miR-20a-5p	MOSMO	hsa-miR-20a-5p	MTMR3	hsa-miR-20a-5p	CCDC137
hsa-miR-20a-5p	NUFIP2	hsa-miR-20a-5p	DCTN5	hsa-miR-20a-5p	DUSP18	hsa-miR-20a-5p	FOXK2
hsa-miR-20a-5p	C17orf75	hsa-miR-20a-5p	PRKCB	hsa-miR-20a-5p	MYH9	hsa-miR-20a-5p	TMEM200C
hsa-miR-20a-5p	CCL5	hsa-miR-20a-5p	TNRC6A	hsa-miR-20a-5p	FOXRED2	hsa-miR-20a-5p	ANKRD12
hsa-miR-20a-5p	SOCS7	hsa-miR-20a-5p	DNAJB13	hsa-miR-20a-5p	TNRC6B	hsa-miR-20a-5p	RMND1
hsa-miR-20a-5p	STAC2	hsa-miR-20a-5p	PGM2L1	hsa-miR-20a-5p	SIRPA	hsa-miR-20a-5p	ARMT1
hsa-miR-20a-5p	ORMDL3	hsa-miR-20a-5p	E2F5	hsa-miR-20a-5p	UBOX5	hsa-miR-20a-5p	TMEM242
hsa-miR-20a-5p	WIPF2	hsa-miR-20a-5p	DYNC1LI2	hsa-miR-20a-5p	MAVS	hsa-miR-20a-5p	SOD2
hsa-miR-20a-5p	P3H4	hsa-miR-20a-5p	C16orf70	hsa-miR-20a-5p	PRNP	hsa-miR-20a-5p	QKI
hsa-miR-20a-5p	PPP1R3B	hsa-miR-20a-5p	SNTB2	hsa-miR-20a-5p	TMX4	hsa-miR-20a-5p	FGFR1OP
hsa-miR-20a-5p	MTMR9	hsa-miR-20a-5p	NFAT5	hsa-miR-20a-5p	PYGB	hsa-miR-20a-5p	C6orf120
hsa-miR-20a-5p	DLC1	hsa-miR-20a-5p	SF3B3	hsa-miR-20a-5p	PDRG1	hsa-miR-20a-5p	COX19
hsa-miR-20a-5p	PSD3	hsa-miR-20a-5p	CMTR2	hsa-miR-20a-5p	PLAGL2	hsa-miR-20a-5p	MAD1L1
hsa-miR-20a-5p	PIWIL2	hsa-miR-20a-5p	PHLPP2	hsa-miR-20a-5p	POFUT1	hsa-miR-20a-5p	FOXK1
hsa-miR-20a-5p	TNFRSF10B	hsa-miR-20a-5p	AP1G1	hsa-miR-20a-5p	ITCH	hsa-miR-20a-5p	RNF216
hsa-miR-20a-5p	ENTPD4	hsa-miR-20a-5p	DHODH	hsa-miR-20a-5p	ANKRD50	hsa-miR-20a-5p	ETV1
hsa-miR-20a-5p	DPYSL2	hsa-miR-20a-5p	LDHD	hsa-miR-20a-5p	MFSD8	hsa-miR-20a-5p	IQSEC1
hsa-miR-20a-5p	NUGGC	hsa-miR-20a-5p	KLHL36	hsa-miR-20a-5p	ABHD18	hsa-miR-20a-5p	NR2C2
hsa-miR-20a-5p	HMBOX1	hsa-miR-20a-5p	KIAA0513	hsa-miR-20a-5p	SLC7A11	hsa-miR-20a-5p	SH3BP5
hsa-miR-20a-5p	SARAF	hsa-miR-20a-5p	PEA15	hsa-miR-20a-5p	GAB1	hsa-miR-20a-5p	SLC4A7
hsa-miR-20a-5p	FUT10	hsa-miR-20a-5p	DCAF8	hsa-miR-20a-5p	OTUD4	hsa-miR-20a-5p	RPL14
hsa-miR-20a-5p	MAK16	hsa-miR-20a-5p	RGS5	hsa-miR-20a-5p	FHDC1	hsa-miR-20a-5p	HAUS2
hsa-miR-20a-5p	ZNF174	hsa-miR-20a-5p	ALDH9A1	hsa-miR-20a-5p	TMEM131L	hsa-miR-20a-5p	SERF2
hsa-miR-20a-5p	ZNF597	hsa-miR-20a-5p	PRRC2C	hsa-miR-20a-5p	MSMO1	hsa-miR-20a-5p	HYPK

hsa-miR-20a-5p	GABPB1	hsa-miR-20a-5p	HECA	hsa-miR-20a-5p	BCL2L11	hsa-miR-20a-5p	SLC25A28
hsa-miR-20a-5p	TMOD3	hsa-miR-20a-5p	RPL17	hsa-miR-20a-5p	POLR1B	hsa-miR-20a-5p	ENTPD7
hsa-miR-20a-5p	GNB5	hsa-miR-20a-5p	SMAD4	hsa-miR-20a-5p	SLC35F5	hsa-miR-20a-5p	SCD
hsa-miR-20a-5p	BNIP2	hsa-miR-20a-5p	TCF4	hsa-miR-20a-5p	PTPN4	hsa-miR-20a-5p	HIF1AN
hsa-miR-20a-5p	RORA	hsa-miR-20a-5p	ZNF532	hsa-miR-20a-5p	MAP3K2	hsa-miR-20a-5p	C2orf69
hsa-miR-20a-5p	USP3	hsa-miR-20a-5p	PMAIP1	hsa-miR-20a-5p	SPOPL	hsa-miR-20a-5p	BZW1
hsa-miR-20a-5p	CD47	hsa-miR-20a-5p	BCL2	hsa-miR-20a-5p	LYPD6	hsa-miR-20a-5p	SSRP1
hsa-miR-20a-5p	MORC1	hsa-miR-20a-5p	SPCS1	hsa-miR-20a-5p	FMNL2	hsa-miR-20a-5p	BSCL2
hsa-miR-20a-5p	LRRC58	hsa-miR-20a-5p	PXK	hsa-miR-20a-5p	CDKN1A	hsa-miR-20a-5p	ATL3
hsa-miR-20a-5p	POLQ	hsa-miR-20a-5p	PDHB	hsa-miR-20a-5p	GLO1	hsa-miR-20a-5p	SKIL
hsa-miR-20a-5p	PLXNA1	hsa-miR-20a-5p	CADM2	hsa-miR-20a-5p	KIF6	hsa-miR-20a-5p	EIF5A2
hsa-miR-20a-5p	ISY1	hsa-miR-20a-5p	C3orf38	hsa-miR-20a-5p	MRPS10	hsa-miR-20a-5p	TBL1XR1
hsa-miR-20a-5p	GPATCH11	hsa-miR-20a-5p	DCBLD2	hsa-miR-20a-5p	RBL1	hsa-miR-20a-5p	ZMAT3
hsa-miR-20a-5p	ABCG8	hsa-miR-20a-5p	CEP97	hsa-miR-20a-5p	TTPAL	hsa-miR-20a-5p	MFN1
hsa-miR-20a-5p	EPAS1	hsa-miR-20a-5p	PPP2R1A	hsa-miR-20a-5p	CTSA	hsa-miR-20a-5p	CAMK2N2
hsa-miR-20a-5p	SOCS5	hsa-miR-20a-5p	ZNF578	hsa-miR-20a-5p	NCOA3	hsa-miR-20a-5p	PSMD2
hsa-miR-20a-5p	KIAA1841	hsa-miR-20a-5p	ZNF665	hsa-miR-20a-5p	ARFGEF2	hsa-miR-20a-5p	WDR53
hsa-miR-20a-5p	WDR92	hsa-miR-20a-5p	ZNF331	hsa-miR-20a-5p	ZNFX1	hsa-miR-4485-3p	GPR37L1
hsa-miR-20a-5p	PPP3R1	hsa-miR-20a-5p	ZNF264	hsa-miR-20a-5p	KCNB1	hsa-miR-4485-3p	MTMR12
hsa-miR-20a-5p	FBXO48	hsa-miR-20a-5p	ZNF805	hsa-miR-20a-5p	PTGIS	hsa-miR-4485-3p	DUSP8
hsa-miR-20a-5p	OSTM1	hsa-miR-20a-5p	ZNF417	hsa-miR-20a-5p	PARD6B	hsa-miR-4485-3p	CLIP1
hsa-miR-20a-5p	SESN1	hsa-miR-20a-5p	FAM102A	hsa-miR-20a-5p	RAB22A	hsa-miR-664a-3p	CREB1
hsa-miR-20a-5p	CDK19	hsa-miR-20a-5p	GOLGA2	hsa-miR-20a-5p	POLR3A	hsa-miR-664a-3p	PPM1A
hsa-miR-20a-5p	RPF2	hsa-miR-20a-5p	CERCAM	hsa-miR-20a-5p	FAM213A	hsa-miR-664a-3p	RPS6KA5
hsa-miR-20a-5p	TRAF3IP2	hsa-miR-20a-5p	NUP188	hsa-miR-20a-5p	PTEN	hsa-miR-664a-3p	HLF
hsa-miR-20a-5p	MAP7	hsa-miR-20a-5p	C9orf78	hsa-miR-20a-5p	TNKS2	hsa-miR-664a-3p	DYNLL2
hsa-miR-20a-5p	MAP3K5	hsa-miR-20a-5p	SEC16A	hsa-miR-20a-5p	ALDH18A1	hsa-miR-664a-3p	ADCYAP1R1

hsa-miR-664a-3p	CDK13	hsa-miR-664a-3p	G6PC	hsa-miR-664a-5p	AEN	hsa-miR-664a-5p	RNF2
hsa-miR-664a-3p	POF1B	hsa-miR-664a-3p	TSPAN2	hsa-miR-664a-5p	CAPN15	hsa-miR-664a-5p	LPGAT1
hsa-miR-664a-3p	NAV2	hsa-miR-664a-3p	BEND4	hsa-miR-664a-5p	CRAMP1	hsa-miR-664a-5p	NPR1
hsa-miR-664a-3p	GPR26	hsa-miR-664a-3p	KIAA1211	hsa-miR-664a-5p	CASP10	hsa-miR-664a-5p	ADAR
hsa-miR-664a-3p	SUB1	hsa-miR-664a-3p	VLDLR	hsa-miR-664a-5p	DNPEP	hsa-miR-664a-5p	EFNA1
hsa-miR-664a-3p	ZBTB34	hsa-miR-664a-3p	KANK2	hsa-miR-664a-5p	NSD1	hsa-miR-664a-5p	VHLL
hsa-miR-664a-3p	SIGLEC10	hsa-miR-664a-3p	KRTAP13-2	hsa-miR-664a-5p	NQO2	hsa-miR-664a-5p	FMC1
hsa-miR-664a-3p	SPPL3	hsa-miR-664a-3p	PCGF3	hsa-miR-664a-5p	RSRC1	hsa-miR-664a-5p	NOM1
hsa-miR-664a-3p	RAN	hsa-miR-664a-3p	ARID1A	hsa-miR-664a-5p	RRM2	hsa-miR-664a-5p	MECP2
hsa-miR-664a-3p	SEMA3E	hsa-miR-664a-3p	ADAP2	hsa-miR-664a-5p	SLC35F6	hsa-miR-664a-5p	TP53INP1
hsa-miR-664a-3p	ZNF487	hsa-miR-664a-3p	TLDC1	hsa-miR-664a-5p	ALDH6A1	hsa-miR-664a-5p	UBE2D3
hsa-miR-664a-3p	RS1	hsa-miR-664a-3p	CBX6	hsa-miR-664a-5p	PDE4C	hsa-miR-664a-5p	METTL8
hsa-miR-664a-3p	PPP1R15B	hsa-miR-664a-3p	RANGAP1	hsa-miR-664a-5p	ZNF429	hsa-miR-664a-5p	ALOX5AP
hsa-miR-664a-3p	SERBP1	hsa-miR-664a-3p	HPGD	hsa-miR-664a-5p	PROSER3	hsa-miR-664a-5p	PLEKHG2
hsa-miR-664a-3p	CD2AP	hsa-miR-664a-3p	UNK	hsa-miR-664a-5p	SSBP2	hsa-miR-664a-5p	UBE2N
hsa-miR-664a-3p	PHIP	hsa-miR-664a-3p	BTD	hsa-miR-664a-5p	IBA57	hsa-miR-664a-5p	DTWD2
hsa-miR-664a-3p	MAPK8	hsa-miR-664a-3p	MED23	hsa-miR-664a-5p	IGF2BP3	hsa-miR-664a-5p	PHAX
hsa-miR-664a-3p	WEE2	hsa-miR-664a-3p	RNMT	hsa-miR-664a-5p	ARHGEF39	hsa-miR-664a-5p	LYRM7
hsa-miR-664a-3p	EN2	hsa-miR-664a-3p	CACNA2D3	hsa-miR-664a-5p	TRMT10B	hsa-miR-664a-5p	WDR77
hsa-miR-664a-3p	TMLHE	hsa-miR-664a-3p	ZNF667	hsa-miR-664a-5p	CD3EAP	hsa-miR-664a-5p	BACE2
hsa-miR-664a-3p	ARSI	hsa-miR-664a-3p	ARL6IP6	hsa-miR-664a-5p	MRPL17	hsa-miR-664a-5p	COL9A2
hsa-miR-664a-3p	DCAF17	hsa-miR-664a-3p	HSPA1B	hsa-miR-664a-5p	RPLP0	hsa-miR-664a-5p	KIF18B
hsa-miR-664a-3p	GNS	hsa-miR-664a-3p	PTPRT	hsa-miR-664a-5p	ZCCHC8	hsa-miR-664a-5p	ORAI2
hsa-miR-664a-3p	TMED5	hsa-miR-664a-3p	MAT1A	hsa-miR-664a-5p	PIWIL1	hsa-miR-664a-5p	FAM71F2
hsa-miR-664a-3p	MFSD14A	hsa-miR-664a-3p	SLC35G1	hsa-miR-664a-5p	VKORC1L1	hsa-miR-664a-5p	PACS2
hsa-miR-664a-3p	ZBTB44	hsa-miR-664a-5p	NRIP2	hsa-miR-664a-5p	ARSK	hsa-miR-664a-5p	CHRN1
hsa-miR-664a-3p	EXOS	hsa-miR-664a-5p	LPCAT3	hsa-miR-664a-5p	ALG10B	hsa-miR-664a-5p	TVP23C

hsa-miR-664a-5p	ZSWIM7	hsa-miR-664a-5p	POLQ	hsa-miR-664b-3p	ZNF507	hsa-miR-664b-3p	PRR26
hsa-miR-664a-5p	ERO1A	hsa-miR-664a-5p	LRTOMT	hsa-miR-664b-3p	LBR	hsa-miR-664b-3p	TMEM236
hsa-miR-664a-5p	CTSS	hsa-miR-664a-5p	OSTM1	hsa-miR-664b-3p	MAP3K21	hsa-miR-664b-3p	EIF2S3
hsa-miR-664a-5p	RANBP6	hsa-miR-664a-5p	ENPP1	hsa-miR-664b-3p	YAE1D1	hsa-miR-664b-3p	TPR
hsa-miR-664a-5p	MPI	hsa-miR-664a-5p	GATA6	hsa-miR-664b-3p	TMED4	hsa-miR-664b-3p	TROVE2
hsa-miR-664a-5p	C15orf40	hsa-miR-664a-5p	DSC3	hsa-miR-664b-3p	TSPAN6	hsa-miR-664b-3p	SLC41A1
hsa-miR-664a-5p	CERS4	hsa-miR-664a-5p	ZNF468	hsa-miR-664b-3p	RBM41	hsa-miR-664b-3p	FCMR
hsa-miR-664a-5p	ZNF878	hsa-miR-664a-5p	ZNF419	hsa-miR-664b-3p	CXorf56	hsa-miR-664b-3p	PRKAA2
hsa-miR-664a-5p	BACH1	hsa-miR-664a-5p	ZSCAN22	hsa-miR-664b-3p	TENM1	hsa-miR-664b-3p	MAP3K7
hsa-miR-664a-5p	CFAP298	hsa-miR-664a-5p	ZNF324B	hsa-miR-664b-3p	SPTY2D1	hsa-miR-664b-3p	UFL1
hsa-miR-664a-5p	C21orf58	hsa-miR-664a-5p	AAR2	hsa-miR-664b-3p	SLC6A5	hsa-miR-664b-3p	ACER3
hsa-miR-664a-5p	CXorf36	hsa-miR-664a-5p	STK4	hsa-miR-664b-3p	FANCF	hsa-miR-664b-3p	PPP2R1B
hsa-miR-664a-5p	SPN	hsa-miR-664a-5p	P2RX3	hsa-miR-664b-3p	SLC5A12	hsa-miR-664b-3p	EIF4EBP2
hsa-miR-664a-5p	NLRC5	hsa-miR-664a-5p	LPP	hsa-miR-664b-3p	CD44	hsa-miR-664b-3p	SMIM10
hsa-miR-664a-5p	SMIM14	hsa-miR-664b-3p	CYFIP2	hsa-miR-664b-3p	VPSS3	hsa-miR-664b-3p	ZNF185
hsa-miR-664a-5p	PQLC2	hsa-miR-664b-3p	CHD4	hsa-miR-664b-3p	PKIA	hsa-miR-664b-3p	RBM12B
hsa-miR-664a-5p	OTUD3	hsa-miR-664b-3p	SYNM	hsa-miR-664b-3p	LZIC	hsa-miR-664b-3p	KLF10
hsa-miR-664a-5p	SH3BGRL3	hsa-miR-664b-3p	PPIL3	hsa-miR-664b-3p	PDLIM3	hsa-miR-664b-3p	SAMD12
hsa-miR-664a-5p	ABHD15	hsa-miR-664b-3p	EPHB1	hsa-miR-664b-3p	BASP1	hsa-miR-664b-3p	FAM84B
hsa-miR-664a-5p	RSL1D1	hsa-miR-664b-3p	MSL2	hsa-miR-664b-3p	TNFSF8	hsa-miR-664b-3p	PAK4
hsa-miR-664a-5p	LDHD	hsa-miR-664b-3p	ZCCHC14	hsa-miR-664b-3p	AKIP1	hsa-miR-664b-3p	MDM2
hsa-miR-664a-5p	DARS2	hsa-miR-664b-3p	SELENOI	hsa-miR-664b-3p	IPO7	hsa-miR-664b-3p	ACSS3
hsa-miR-664a-5p	SERPINC1	hsa-miR-664b-3p	SLC30A6	hsa-miR-664b-3p	BRAP	hsa-miR-664b-3p	REEP5
hsa-miR-664a-5p	RRP7A	hsa-miR-664b-3p	TMEM63C	hsa-miR-664b-3p	FBXW8	hsa-miR-664b-3p	DCP2
hsa-miR-664a-5p	RNF24	hsa-miR-664b-3p	CALM1	hsa-miR-664b-3p	TMEM233	hsa-miR-664b-3p	DMXL1
hsa-miR-664a-5p	FBXL2	hsa-miR-664b-3p	PGLS	hsa-miR-664b-3p	CAMKK2	hsa-miR-664b-3p	FAM13B
hsa-miR-664a-5p	LRRC58	hsa-miR-664b-3p	UQCRCF1	hsa-miR-664b-3p	ZNF107	hsa-miR-664b-3p	DDAH1

hsa-miR-664b-3p	MPZL3	hsa-miR-664b-3p	TADA2A	hsa-miR-664b-3p	GLO1	hsa-miR-7704	IP6K1
hsa-miR-664b-3p	PRDM10	hsa-miR-664b-3p	CCDC25	hsa-miR-664b-3p	TAF8	hsa-miR-7704	COMMD5
hsa-miR-664b-3p	DEK	hsa-miR-664b-3p	ZFAND1	hsa-miR-664b-3p	SERINC3	hsa-miR-7704	ZNF426
hsa-miR-664b-3p	MDC1	hsa-miR-664b-3p	RNASEL	hsa-miR-664b-3p	ARFGEF2	hsa-miR-7704	LDLR
hsa-miR-664b-3p	RBBP4	hsa-miR-664b-3p	MIEF1	hsa-miR-664b-3p	PARD6B	hsa-miR-7704	RPH3AL
hsa-miR-664b-3p	ZNF362	hsa-miR-664b-3p	SNRPB2	hsa-miR-7704	G3BP1	hsa-miR-7704	NTSR1
hsa-miR-664b-3p	SMIM12	hsa-miR-664b-3p	ANKRD50	hsa-miR-7704	FLYWCH1	hsa-miR-7704	IFNAR1
hsa-miR-664b-3p	NDFIP2	hsa-miR-664b-3p	MAML3	hsa-miR-7704	CENPO	hsa-miR-7704	TBC1D25
hsa-miR-664b-3p	ITGBL1	hsa-miR-664b-3p	FBXW7	hsa-miR-7704	KMT2B	hsa-miR-7704	MAZ
hsa-miR-664b-3p	LRP10	hsa-miR-664b-3p	WWC2	hsa-miR-7704	NUPL2	hsa-miR-7704	RGS12
hsa-miR-664b-3p	FZD2	hsa-miR-664b-3p	GTF2H5	hsa-miR-7704	SDF4	hsa-miR-7704	C8orf58
hsa-miR-664b-3p	GSKIP	hsa-miR-664b-3p	DPH3	hsa-miR-7704	NMNAT1	hsa-miR-7704	GDE1
hsa-miR-664b-3p	SHMT1	hsa-miR-664b-3p	AZ12	hsa-miR-7704	ANKRD33B	hsa-miR-7704	APOL6
hsa-miR-664b-3p	MDGA2	hsa-miR-664b-3p	MAPK6	hsa-miR-7704	VDR	hsa-miR-7704	CDS2
hsa-miR-664b-3p	ANKRD17	hsa-miR-664b-3p	KIAA1841	hsa-miR-7704	KCNH1	hsa-miR-7704	SIPA1
hsa-miR-664b-3p	PCLAF	hsa-miR-664b-3p	PLEK	hsa-miR-7704	UBQLN4	hsa-miR-7704	TEX261
hsa-miR-664b-3p	AKAP8	hsa-miR-664b-3p	OLIG3	hsa-miR-7704	MEF2D	hsa-miR-7704	TOMM70
hsa-miR-664b-3p	TGOLN2	hsa-miR-664b-3p	TMEM241	hsa-miR-7704	ZNF488	hsa-miR-7704	UBE2S
hsa-miR-664b-3p	ZNF514	hsa-miR-664b-3p	ZCCHC2	hsa-miR-7704	ARC	hsa-miR-7704	PTGES2
hsa-miR-664b-3p	STARD7	hsa-miR-664b-3p	APPL1	hsa-miR-7704	PPIC	hsa-miR-7704	FIBCD1
hsa-miR-664b-3p	APP	hsa-miR-664b-3p	ZNF616	hsa-miR-7704	FGF19	hsa-miR-7704	HLA-DOA
hsa-miR-664b-3p	GPBP1	hsa-miR-664b-3p	SSC5D	hsa-miR-7704	POU3F1	hsa-miR-7704	CDKN1A
hsa-miR-664b-3p	TRAPPC13	hsa-miR-664b-3p	ZNF264	hsa-miR-7704	PLEKHM1	hsa-miR-7704	CPNE5
hsa-miR-664b-3p	SETD5	hsa-miR-664b-3p	MAP3K2	hsa-miR-7704	TRIM56	hsa-miR-7704	SNCG
hsa-miR-664b-3p	NCAPG	hsa-miR-664b-3p	HLA-DRB1	hsa-miR-7704	POLR2E	hsa-miR-7704	SLC22A12
hsa-miR-664b-3p	RCC2	hsa-miR-664b-3p	MAPK14	hsa-miR-7704	KDM6B		

8.4. Gene ontology categorization and enrichment analysis

8.4.1. Intracellular upregulated miRNA target genes GO categorization

Table 14: Biological processes of intracellular upregulated miRNA targets (Top 50).

GO biological process complete	Homo sapiens - REFLIST (20851)	Target gene (98)	over/ under	fold Enrichment	raw p value	FDR
regulation of protein export from nucleus (GO:0046825)	42	4	+	20.26	6.32E-05	9.95E-03
positive regulation of nucleocytoplasmic transport (GO:0046824)	69	5	+	15.42	2.52E-05	4.61E-03
stress-activated protein kinase signaling cascade (GO:0031098)	124	7	+	12.01	2.74E-06	8.56E-04
regulation of nucleocytoplasmic transport (GO:0046822)	117	6	+	10.91	2.45E-05	4.54E-03
positive regulation of intracellular protein transport (GO:0090316)	186	8	+	9.15	3.62E-06	1.01E-03
regulation of lipid biosynthetic process (GO:0046890)	200	8	+	8.51	6.04E-06	1.50E-03
positive regulation of intracellular transport (GO:0032388)	228	8	+	7.47	1.52E-05	3.05E-03
regulation of intracellular protein transport (GO:0033157)	271	9	+	7.07	6.67E-06	1.63E-03
signal transduction by protein phosphorylation (GO:0023014)	417	12	+	6.12	7.73E-07	3.24E-04
positive regulation of cellular protein localization (GO:1903829)	345	9	+	5.55	4.26E-05	7.06E-03
MAPK cascade (GO:0000165)	404	10	+	5.27	2.43E-05	4.54E-03
positive regulation of transport (GO:0051050)	942	18	+	4.07	4.35E-07	2.04E-04
peptidyl-amino acid modification (GO:0018193)	898	16	+	3.79	4.99E-06	1.28E-03
organophosphate metabolic process (GO:0019637)	898	16	+	3.79	4.99E-06	1.26E-03
protein phosphorylation (GO:0006468)	969	17	+	3.73	2.98E-06	9.10E-04
positive regulation of phosphorus metabolic process (GO:0010562)	1169	19	+	3.46	2.17E-06	7.18E-04
positive regulation of phosphate metabolic process (GO:0045937)	1169	19	+	3.46	2.17E-06	7.04E-04
phosphate-containing compound metabolic process (GO:0006796)	2167	35	+	3.44	2.60E-11	5.17E-08

small molecule metabolic process (GO:0044281)	1748	28	+	3.41	5.87E-09	6.22E-06
phosphorus metabolic process (GO:0006793)	2194	35	+	3.39	3.66E-11	6.47E-08
positive regulation of cellular protein metabolic process (GO:0032270)	1633	26	+	3.39	2.71E-08	2.16E-05
regulation of cellular localization (GO:0060341)	1010	16	+	3.37	2.10E-05	4.08E-03
positive regulation of protein metabolic process (GO:0051247)	1716	27	+	3.35	1.73E-08	1.53E-05
positive regulation of phosphorylation (GO:0042327)	1095	17	+	3.3	1.45E-05	2.96E-03
positive regulation of intracellular signal transduction (GO:1902533)	1050	16	+	3.24	3.34E-05	5.85E-03
cellular response to endogenous stimulus (GO:0071495)	1160	17	+	3.12	3.00E-05	5.36E-03
response to endogenous stimulus (GO:0009719)	1436	21	+	3.11	3.02E-06	9.05E-04
phosphorylation (GO:0016310)	1304	19	+	3.1	1.03E-05	2.33E-03
positive regulation of protein modification process (GO:0031401)	1250	18	+	3.06	2.13E-05	4.08E-03
regulation of cellular protein metabolic process (GO:0032268)	2691	38	+	3	1.31E-10	1.90E-07
regulation of protein modification process (GO:0031399)	1891	26	+	2.93	4.75E-07	2.16E-04
positive regulation of signal transduction (GO:0009967)	1675	23	+	2.92	2.64E-06	8.41E-04
positive regulation of molecular function (GO:0044093)	1837	25	+	2.9	1.01E-06	3.75E-04
regulation of phosphate metabolic process (GO:0019220)	1841	25	+	2.89	1.05E-06	3.81E-04
regulation of phosphorus metabolic process (GO:0051174)	1842	25	+	2.89	1.06E-06	3.76E-04
regulation of protein metabolic process (GO:0051246)	2835	38	+	2.85	5.92E-10	7.85E-07
cellular nitrogen compound biosynthetic process (GO:0044271)	1571	21	+	2.84	1.19E-05	2.46E-03
cellular catabolic process (GO:0044248)	1825	24	+	2.8	3.20E-06	9.42E-04
cellular response to organic substance (GO:0071310)	2368	31	+	2.79	7.57E-08	5.01E-05
intracellular signal transduction (GO:0035556)	1694	22	+	2.76	1.10E-05	2.37E-03
positive regulation of cell communication (GO:0010647)	1855	24	+	2.75	4.23E-06	1.16E-03
regulation of protein phosphorylation (GO:0001932)	1469	19	+	2.75	5.21E-05	8.46E-03
positive regulation of signaling (GO:0023056)	1862	24	+	2.74	4.51E-06	1.19E-03
organic substance catabolic process (GO:1901575)	1786	23	+	2.74	7.61E-06	1.81E-03
regulation of phosphorylation (GO:0042325)	1642	21	+	2.72	2.29E-05	4.34E-03

regulation of cellular component organization (GO:0051128)	2436	31	+	2.71	1.43E-07	8.43E-05
organic substance biosynthetic process (GO:1901576)	2802	35	+	2.66	2.43E-08	2.04E-05
response to oxygen-containing compound (GO:1901700)	1610	20	+	2.64	5.60E-05	8.99E-03
biosynthetic process (GO:0009058)	2861	35	+	2.6	4.13E-08	3.13E-05
regulation of intracellular signal transduction (GO:1902531)	1833	22	+	2.55	3.69E-05	6.31E-03

Table 15: Molecular functions of intracellular upregulated miRNA targets.

GO molecular function complete	Homo sapiens - REFLIST (20851)	Target gene (98)	over/ under	fold Enrichment	raw p value	FDR
mannose-6-phosphate isomerase activity (GO:0004476)	2	2	+	> 100	1.29E-04	2.12E-02
MAP kinase activity (GO:0004707)	20	3	+	31.91	1.64E-04	2.52E-02
intramolecular oxidoreductase activity (GO:0016860)	53	4	+	16.06	1.47E-04	2.33E-02
protein serine/threonine kinase activity (GO:0004674)	438	10	+	4.86	4.73E-05	8.66E-03
protein kinase activity (GO:0004672)	585	13	+	4.73	4.27E-06	1.36E-03
transferase activity, transferring phosphorus-containing groups (GO:0016772)	937	20	+	4.54	1.49E-08	2.37E-05
phosphotransferase activity, alcohol group as acceptor (GO:0016773)	691	14	+	4.31	5.03E-06	1.33E-03
kinase activity (GO:0016301)	772	15	+	4.13	3.68E-06	1.25E-03
transferase activity (GO:0016740)	2353	36	+	3.26	5.52E-11	1.31E-07
adenyl ribonucleotide binding (GO:0032559)	1571	23	+	3.11	8.96E-07	8.53E-04
ATP binding (GO:0005524)	1511	22	+	3.1	1.79E-06	1.06E-03
adenyl nucleotide binding (GO:0030554)	1583	23	+	3.09	1.02E-06	8.09E-04
transition metal ion binding (GO:0046914)	1121	15	+	2.85	2.49E-04	3.70E-02
purine ribonucleotide binding (GO:0032555)	1926	25	+	2.76	2.38E-06	1.03E-03
purine ribonucleoside triphosphate binding (GO:0035639)	1859	24	+	2.75	4.39E-06	1.30E-03
purine nucleotide binding (GO:0017076)	1940	25	+	2.74	2.70E-06	1.07E-03
ribonucleotide binding (GO:0032553)	1943	25	+	2.74	2.78E-06	1.02E-03
catalytic activity, acting on a protein (GO:0140096)	2274	29	+	2.71	4.03E-07	4.79E-04
nucleotide binding (GO:0000166)	2180	27	+	2.64	2.03E-06	1.07E-03
nucleoside phosphate binding (GO:1901265)	2181	27	+	2.63	2.05E-06	9.73E-04
carbohydrate derivative binding (GO:0097367)	2287	28	+	2.6	1.54E-06	1.05E-03
catalytic activity (GO:0003824)	5866	66	+	2.39	1.10E-15	5.24E-12
small molecule binding (GO:0036094)	2591	29	+	2.38	7.62E-06	1.65E-03
enzyme binding (GO:0019899)	2306	25	+	2.31	6.12E-05	1.08E-02

anion binding (GO:0043168)	2892	31	+	2.28	6.13E-06	1.39E-03
ion binding (GO:0043167)	6393	52	+	1.73	4.69E-06	1.31E-03
heterocyclic compound binding (GO:1901363)	5999	48	+	1.7	2.72E-05	5.40E-03
organic cyclic compound binding (GO:0097159)	6088	48	+	1.68	4.72E-05	8.99E-03
protein binding (GO:0005515)	14135	84	+	1.26	7.67E-05	1.30E-02
binding (GO:0005488)	16492	93	+	1.2	2.59E-05	5.37E-03
molecular_function (GO:0003674)	18332	98	+	1.14	5.98E-06	1.50E-03

Table 16: Cellular components associated with intracellular upregulated miRNA targets.

GO cellular component complete	Homo sapiens - REFLIST (20851)	Target genes (98)	over/ under	fold Enrichment	raw p value	FDR
catalytic complex (GO:1902494)	1402	20	+	3.04	7.83E-06	1.31E-03
nucleoplasm (GO:0005654)	3990	42	+	2.24	8.79E-08	4.40E-05
endomembrane system (GO:0012505)	4659	42	+	1.92	7.63E-06	1.39E-03
cytosol (GO:0005829)	5311	46	+	1.84	6.48E-06	1.30E-03
organelle lumen (GO:0043233)	6112	52	+	1.81	1.05E-06	3.00E-04
intracellular organelle lumen (GO:0070013)	6112	52	+	1.81	1.05E-06	2.63E-04
membrane-enclosed lumen (GO:0031974)	6112	52	+	1.81	1.05E-06	2.33E-04
nuclear lumen (GO:0031981)	4986	42	+	1.79	4.10E-05	5.87E-03
cytoplasm (GO:0005737)	11740	85	+	1.54	1.24E-10	2.49E-07
intracellular membrane-bounded organelle (GO:0043231)	11071	80	+	1.54	5.23E-09	3.49E-06
nucleus (GO:0005634)	7598	54	+	1.51	2.01E-04	2.37E-02
membrane-bounded organelle (GO:0043227)	12783	87	+	1.45	2.00E-09	2.00E-06
intracellular organelle (GO:0043229)	12896	81	+	1.34	1.39E-05	2.14E-03
organelle (GO:0043226)	13901	87	+	1.33	7.62E-07	2.54E-04
intracellular (GO:0005622)	14726	90	+	1.3	5.29E-07	2.12E-04
cellular_component (GO:0005575)	18964	98	+	1.1	1.42E-04	1.77E-02

8.4.2. Intracellular downregulated miRNA target genes GO categorization

Table 17: Biological processes of downregulated miRNA targets (Top 50).

GO biological process complete	Homo sapiens - REFLIST (20851)	Target genes (325)	over/under	Fold Enrichment	raw p value	FDR
SMAD protein complex assembly (GO:0007183)	7	4	+	36.66	1.65E-05	3.76E-04
stress-induced premature senescence (GO:0090400)	8	4	+	32.08	2.45E-05	5.33E-04
cellular response to leucine (GO:0071233)	10	5	+	32.08	2.19E-06	6.23E-05
'de novo' pyrimidine nucleobase biosynthetic process (GO:0006207)	7	3	+	27.5	3.97E-04	5.90E-03
germ cell migration (GO:0008354)	7	3	+	27.5	3.97E-04	5.89E-03
positive regulation of Arp2/3 complex-mediated actin nucleation (GO:2000601)	10	4	+	25.66	4.83E-05	9.75E-04
cellular response to leucine starvation (GO:1990253)	10	4	+	25.66	4.83E-05	9.73E-04
response to leucine (GO:0043201)	13	5	+	24.68	6.00E-06	1.52E-04
positive regulation of ER-associated ubiquitin-dependent protein catabolic process (GO:1903071)	8	3	+	24.06	5.39E-04	7.69E-03
regulation of vascular associated smooth muscle cell apoptotic process (GO:1905459)	8	3	+	24.06	5.39E-04	7.68E-03
vesicle fusion with Golgi apparatus (GO:0048280)	8	3	+	24.06	5.39E-04	7.67E-03
regulation of vascular associated smooth muscle contraction (GO:0003056)	9	3	+	21.39	7.11E-04	9.71E-03
cellular response to insulin-like growth factor stimulus (GO:1990314)	9	3	+	21.39	7.11E-04	9.70E-03
regulation of store-operated calcium channel activity (GO:1901339)	9	3	+	21.39	7.11E-04	9.69E-03
negative regulation of tyrosine phosphorylation of STAT protein (GO:0042532)	12	4	+	21.39	8.57E-05	1.62E-03
histone H4-K20 methylation (GO:0034770)	9	3	+	21.39	7.11E-04	9.68E-03
coronary artery morphogenesis (GO:0060982)	9	3	+	21.39	7.11E-04	9.67E-03
pyrimidine nucleobase biosynthetic process (GO:0019856)	9	3	+	21.39	7.11E-04	9.67E-03
negative regulation of epidermal growth factor-activated receptor activity (GO:0007175)	14	4	+	18.33	1.41E-04	2.48E-03
G1 phase (GO:0051318)	21	6	+	18.33	2.81E-06	7.76E-05
mitotic G1 phase (GO:0000080)	21	6	+	18.33	2.81E-06	7.75E-05
negative regulation of vascular associated smooth muscle cell proliferation (GO:1904706)	18	5	+	17.82	2.21E-05	4.88E-04

positive regulation of macrophage derived foam cell differentiation (GO:0010744)	18	5	+	17.82	2.21E-05	4.88E-04
positive regulation of transcription from RNA polymerase II promoter involved in cellular response to chemical stimulus (GO:1901522)	24	6	+	16.04	5.43E-06	1.40E-04
positive regulation of actin nucleation (GO:0051127)	16	4	+	16.04	2.17E-04	3.56E-03
mitotic cell cycle arrest (GO:0071850)	17	4	+	15.1	2.65E-04	4.23E-03
regulation of fibroblast apoptotic process (GO:2000269)	17	4	+	15.1	2.65E-04	4.23E-03
pyrimidine nucleobase metabolic process (GO:0006206)	17	4	+	15.1	2.65E-04	4.23E-03
intrinsic apoptotic signaling pathway in response to oxidative stress (GO:0008631)	17	4	+	15.1	2.65E-04	4.22E-03
positive regulation of muscle cell apoptotic process (GO:0010661)	26	6	+	14.81	8.08E-06	1.99E-04
release of cytochrome c from mitochondria (GO:0001836)	22	5	+	14.58	5.05E-05	1.01E-03
regulation of smooth muscle cell apoptotic process (GO:0034391)	22	5	+	14.58	5.05E-05	1.01E-03
glycogen catabolic process (GO:0005980)	18	4	+	14.26	3.20E-04	4.98E-03
T cell lineage commitment (GO:0002360)	23	5	+	13.95	6.07E-05	1.19E-03
nucleobase biosynthetic process (GO:0046112)	19	4	+	13.51	3.83E-04	5.77E-03
cellular response to low-density lipoprotein particle stimulus (GO:0071404)	19	4	+	13.51	3.83E-04	5.77E-03
cellular response to leptin stimulus (GO:0044320)	19	4	+	13.51	3.83E-04	5.76E-03
interleukin-6-mediated signaling pathway (GO:0070102)	19	4	+	13.51	3.83E-04	5.76E-03
mRNA transcription (GO:0009299)	19	4	+	13.51	3.83E-04	5.75E-03
glucan catabolic process (GO:0009251)	19	4	+	13.51	3.83E-04	5.74E-03
protein localization to cell-cell junction (GO:0150105)	19	4	+	13.51	3.83E-04	5.74E-03
response to leptin (GO:0044321)	24	5	+	13.37	7.24E-05	1.39E-03
negative regulation of cyclin-dependent protein serine/threonine kinase activity (GO:0045736)	29	6	+	13.27	1.39E-05	3.23E-04
signal transduction in absence of ligand (GO:0038034)	34	7	+	13.21	2.70E-06	7.51E-05
extrinsic apoptotic signaling pathway in absence of ligand (GO:0097192)	34	7	+	13.21	2.70E-06	7.50E-05
negative regulation of cellular senescence (GO:2000773)	20	4	+	12.83	4.54E-04	6.62E-03
positive regulation of transforming growth factor beta production (GO:0071636)	20	4	+	12.83	4.54E-04	6.61E-03
cellular polysaccharide catabolic process (GO:0044247)	20	4	+	12.83	4.54E-04	6.61E-03

negative regulation of receptor signaling pathway via JAK-STAT (GO:0046426)	20	4	+	12.83	4.54E-04	6.60E-03
regulation of myeloid cell apoptotic process (GO:0033032)	30	6	+	12.83	1.65E-05	3.76E-04

Table 18: Molecular functions of intracellular downregulated miRNA targets (Top 50).

GO molecular function complete	Homo sapiens - REFLIST (20851)	Target genes (325)	over/ under	Fold Enrichment	raw p value	FDR
histone methyltransferase activity (H4-K20 specific) (GO:0042799)	5	3	+	38.49	1.89E-04	1.35E-02
mannosyl-oligosaccharide 1,2-alpha-mannosidase activity (GO:0004571)	7	3	+	27.5	3.97E-04	2.39E-02
leucine binding (GO:0070728)	7	3	+	27.5	3.97E-04	2.36E-02
I-SMAD binding (GO:0070411)	14	6	+	27.5	4.04E-07	4.92E-05
inositol tetrakisphosphate phosphatase activity (GO:0052743)	7	3	+	27.5	3.97E-04	2.33E-02
CCR5 chemokine receptor binding (GO:0031730)	8	3	+	24.06	5.39E-04	2.92E-02
DEAD/H-box RNA helicase binding (GO:0017151)	8	3	+	24.06	5.39E-04	2.88E-02
mannosyl-oligosaccharide mannosidase activity (GO:0015924)	9	3	+	21.39	7.11E-04	3.52E-02
phospholipase activator activity (GO:0016004)	12	4	+	21.39	8.57E-05	7.28E-03
cyclin-dependent protein serine/threonine kinase inhibitor activity (GO:0004861)	12	4	+	21.39	8.57E-05	7.15E-03
1-phosphatidylinositol-3-kinase regulator activity (GO:0046935)	16	5	+	20.05	1.37E-05	1.39E-03
activin-activated receptor activity (GO:0017002)	10	3	+	19.25	9.14E-04	4.22E-02
lipase activator activity (GO:0060229)	14	4	+	18.33	1.41E-04	1.08E-02
inositol phosphate phosphatase activity (GO:0052745)	14	4	+	18.33	1.41E-04	1.06E-02
phosphatidylinositol 3-kinase regulator activity (GO:0035014)	20	5	+	16.04	3.41E-05	3.38E-03
insulin-like growth factor receptor binding (GO:0005159)	16	4	+	16.04	2.17E-04	1.50E-02
MAP kinase kinase kinase activity (GO:0004709)	26	6	+	14.81	8.08E-06	8.36E-04
phosphatidylinositol bisphosphate phosphatase activity (GO:0034593)	24	4	+	10.69	8.34E-04	3.93E-02
protein serine/threonine kinase inhibitor activity (GO:0030291)	31	5	+	10.35	2.11E-04	1.47E-02
transforming growth factor beta receptor binding (GO:0005160)	25	4	+	10.27	9.55E-04	4.37E-02
phosphatidylinositol phosphate phosphatase activity (GO:0052866)	33	5	+	9.72	2.73E-04	1.76E-02
phosphotyrosine residue binding (GO:0001784)	42	6	+	9.17	8.90E-05	7.18E-03
histone-lysine N-methyltransferase activity (GO:0018024)	44	6	+	8.75	1.12E-04	8.91E-03
SNAP receptor activity (GO:0005484)	37	5	+	8.67	4.41E-04	2.47E-02

protein tyrosine kinase binding (GO:1990782)	101	12	+	7.62	1.73E-07	2.16E-05
cyclin-dependent protein serine/threonine kinase regulator activity (GO:0016538)	51	6	+	7.55	2.34E-04	1.57E-02
protein phosphorylated amino acid binding (GO:0045309)	53	6	+	7.26	2.84E-04	1.80E-02
translation initiation factor activity (GO:0003743)	53	6	+	7.26	2.84E-04	1.78E-02
p53 binding (GO:0002039)	67	7	+	6.7	1.40E-04	1.09E-02
histone methyltransferase activity (GO:0042054)	59	6	+	6.52	4.82E-04	2.63E-02
SMAD binding (GO:0046332)	80	8	+	6.42	6.25E-05	5.84E-03
oxidoreductase activity, acting on the CH-CH group of donors (GO:0016627)	62	6	+	6.21	6.14E-04	3.11E-02
promoter-specific chromatin binding (GO:1990841)	62	6	+	6.21	6.14E-04	3.08E-02
receptor tyrosine kinase binding (GO:0030971)	73	7	+	6.15	2.29E-04	1.56E-02
Rac GTPase binding (GO:0048365)	74	7	+	6.07	2.47E-04	1.61E-02
protein-lysine N-methyltransferase activity (GO:0016279)	64	6	+	6.01	7.17E-04	3.52E-02
lysine N-methyltransferase activity (GO:0016278)	65	6	+	5.92	7.73E-04	3.72E-02
protein kinase inhibitor activity (GO:0004860)	65	6	+	5.92	7.73E-04	3.68E-02
ubiquitin binding (GO:0043130)	77	7	+	5.83	3.10E-04	1.91E-02
collagen binding (GO:0005518)	68	6	+	5.66	9.63E-04	4.36E-02
ubiquitin-like protein ligase binding (GO:0044389)	320	28	+	5.61	9.69E-13	2.71E-10
kinase inhibitor activity (GO:0019210)	69	6	+	5.58	1.03E-03	4.59E-02
ubiquitin protein ligase binding (GO:0031625)	301	26	+	5.54	8.48E-12	1.49E-09
activating transcription factor binding (GO:0033613)	85	7	+	5.28	5.40E-04	2.86E-02
phosphoprotein binding (GO:0051219)	86	7	+	5.22	5.76E-04	2.95E-02
phosphatase binding (GO:0019902)	198	15	+	4.86	1.13E-06	1.25E-04
ubiquitin-like protein binding (GO:0032182)	95	7	+	4.73	9.99E-04	4.49E-02
protein phosphatase binding (GO:0019903)	153	11	+	4.61	4.80E-05	4.66E-03
kinase regulator activity (GO:0019207)	224	16	+	4.58	1.03E-06	1.17E-04
protein kinase binding (GO:0019901)	685	48	+	4.5	1.64E-17	1.30E-14
protein serine/threonine kinase activity (GO:0004674)	438	30	+	4.39	4.56E-11	6.79E-09

Table 19: Cellular components associated with intracellular downregulated miRNA targets (Top 50).

GO cellular component complete	Homo sapiens - REFLIST (20851)	Target genes (325)	over/under	Fold Enrichment	raw p value	FDR
heteromeric SMAD protein complex (GO:0071144)	8	5	+	40.1	9.61E-07	5.34E-05
SMAD protein complex (GO:0071141)	10	5	+	32.08	2.19E-06	1.04E-04
TOR complex (GO:0038201)	15	4	+	17.11	1.76E-04	4.96E-03
eukaryotic 48S preinitiation complex (GO:0033290)	15	4	+	17.11	1.76E-04	4.89E-03
translation preinitiation complex (GO:0070993)	18	4	+	14.26	3.20E-04	8.22E-03
phosphatidylinositol 3-kinase complex (GO:0005942)	29	6	+	13.27	1.39E-05	5.26E-04
serine/threonine protein kinase complex (GO:1902554)	88	9	+	6.56	1.85E-05	6.50E-04
protein kinase complex (GO:1902911)	104	10	+	6.17	1.05E-05	4.12E-04
autophagosome (GO:0005776)	101	9	+	5.72	5.05E-05	1.74E-03
melanosome (GO:0042470)	106	9	+	5.45	7.15E-05	2.43E-03
pigment granule (GO:0048770)	106	9	+	5.45	7.15E-05	2.39E-03
RNA polymerase II transcription regulator complex (GO:0090575)	171	14	+	5.25	1.10E-06	5.94E-05
lamellipodium (GO:0030027)	205	15	+	4.69	1.69E-06	8.48E-05
transferase complex, transferring phosphorus-containing groups (GO:0061695)	262	18	+	4.41	3.70E-07	2.12E-05
membrane raft (GO:0045121)	333	21	+	4.05	1.52E-07	1.01E-05
membrane microdomain (GO:0098857)	334	21	+	4.03	1.59E-07	1.03E-05
cell-substrate junction (GO:0030055)	425	26	+	3.92	8.69E-09	7.25E-07
ruffle (GO:0001726)	181	11	+	3.9	1.96E-04	5.23E-03
membrane region (GO:0098589)	347	21	+	3.88	2.89E-07	1.70E-05
mitochondrial outer membrane (GO:0005741)	200	12	+	3.85	1.13E-04	3.49E-03
focal adhesion (GO:0005925)	417	25	+	3.85	2.47E-08	1.83E-06
organelle outer membrane (GO:0031968)	226	13	+	3.69	8.87E-05	2.91E-03
outer membrane (GO:0019867)	228	13	+	3.66	9.65E-05	3.07E-03
extrinsic component of membrane (GO:0019898)	310	17	+	3.52	1.35E-05	5.21E-04

cell leading edge (GO:0031252)	430	22	+	3.28	2.16E-06	1.06E-04
anchoring junction (GO:0070161)	839	42	+	3.21	7.31E-11	8.61E-09
transcription regulator complex (GO:0005667)	427	21	+	3.16	6.59E-06	2.75E-04
nuclear membrane (GO:0031965)	305	15	+	3.16	1.38E-04	4.07E-03
cell cortex (GO:0005938)	308	15	+	3.12	1.53E-04	4.38E-03
cell-cell junction (GO:0005911)	502	20	+	2.56	1.80E-04	4.93E-03
nuclear envelope (GO:0005635)	478	19	+	2.55	2.67E-04	6.95E-03
perinuclear region of cytoplasm (GO:0048471)	740	29	+	2.51	1.41E-05	5.23E-04
cytosol (GO:0005829)	5311	197	+	2.38	5.77E-40	1.16E-36
whole membrane (GO:0098805)	1748	64	+	2.35	3.06E-10	3.41E-08
catalytic complex (GO:1902494)	1402	51	+	2.33	2.66E-08	1.90E-06
envelope (GO:0031975)	1238	45	+	2.33	2.16E-07	1.35E-05
organelle envelope (GO:0031967)	1238	45	+	2.33	2.16E-07	1.31E-05
mitochondrial envelope (GO:0005740)	787	28	+	2.28	1.02E-04	3.19E-03
mitochondrial membrane (GO:0031966)	739	26	+	2.26	2.19E-04	5.76E-03
mitochondrion (GO:0005739)	1661	56	+	2.16	8.86E-08	6.12E-06
extracellular exosome (GO:0070062)	2098	69	+	2.11	4.96E-09	4.73E-07
cell surface (GO:0009986)	947	31	+	2.1	1.42E-04	4.13E-03
extracellular vesicle (GO:1903561)	2119	69	+	2.09	5.93E-09	5.40E-07
extracellular organelle (GO:0043230)	2121	69	+	2.09	6.07E-09	5.28E-07
plasma membrane region (GO:0098590)	1230	40	+	2.09	1.57E-05	5.62E-04
endosome (GO:0005768)	992	32	+	2.07	1.30E-04	3.87E-03
nuclear outer membrane-endoplasmic reticulum membrane network (GO:0042175)	1156	36	+	2	1.29E-04	3.90E-03
endoplasmic reticulum membrane (GO:0005789)	1133	35	+	1.98	1.84E-04	4.98E-03
membrane protein complex (GO:0098796)	1334	40	+	1.92	9.32E-05	3.01E-03
protein-containing complex (GO:0032991)	5543	164	+	1.9	1.44E-19	3.59E-17
cell junction (GO:0030054)	2066	60	+	1.86	3.77E-06	1.68E-04

8.4.3. Exosomal upregulated miRNA target genes GO categorization

Table 20: GO biological processes associated with target genes of upregulated *hsa-miR-7704*.

GO BP	Genes mapped	Percent hits against total genes
cellular component organization or biogenesis (GO:0071840)	2	4.30%
cellular process (GO:0009987)	11	23.40%
multi-organism process (GO:0051704)	1	2.10%
localization (GO:0051179)	5	10.60%
biological regulation (GO:0065007)	7	14.90%
response to stimulus (GO:0050896)	4	8.50%
signaling (GO:0023052)	2	4.30%
developmental process (GO:0032502)	4	8.50%
multicellular organismal process (GO:0032501)	3	6.40%
metabolic process (GO:0008152)	6	12.80%

Table 21: GO molecular functions associated with target genes of upregulated *hsa-miR-7704*.

GO MF	Genes mapped	Percent hits against total genes
transcription regulator activity (GO:0140110)	3	6.40%
molecular transducer activity (GO:0060089)	2	4.30%
binding (GO:0005488)	11	23.40%
molecular function regulator (GO:0098772)	1	2.10%
catalytic activity (GO:0003824)	7	14.90%
transporter activity (GO:0005215)	1	2.10%

Table 22: GO cellular components associated with target genes of upregulated *hsa-miR-7704*.

GO CC	Genes mapped	Percent hits against total genes
membrane part (GO:0044425)	4	8.50%
membrane (GO:0016020)	6	12.80%
organelle part (GO:0044422)	7	14.90%
extracellular region part (GO:0044421)	1	2.10%
membrane-enclosed lumen (GO:0031974)	4	8.50%
protein-containing complex (GO:0032991)	7	14.90%
extracellular region (GO:0005576)	1	2.10%
cell (GO:0005623)	16	34.00%
cell part (GO:0044464)	16	34.00%
organelle (GO:0043226)	12	25.50%

8.4.4. Exosomal downregulated miRNA target genes GO categorization

Table 23: Biological processes of downregulated exosomal miRNA target genes (Top 50).

GO biological process complete	Homo sapiens - REFLIST (20851)	Target genes (325)	over/ under	Fold Enrichment	raw <i>p</i> value	FDR
regulation of phosphatidylinositol 3-kinase activity (GO:0043551)	59	5	+	11.86	9.15E-05	2.78E-03
positive regulation of phosphatidylinositol 3-kinase activity (GO:0043552)	36	3	+	11.66	2.65E-03	4.08E-02
positive regulation of phosphatidylinositol 3-kinase signaling (GO:0014068)	87	6	+	9.65	5.29E-05	1.80E-03
regulation of phosphatidylinositol 3-kinase signaling (GO:0014066)	126	7	+	7.77	4.64E-05	1.61E-03
phosphatidylinositol-mediated signaling (GO:0048015)	79	4	+	7.09	2.90E-03	4.41E-02
positive regulation of macrophage apoptotic process (GO:2000111)	3	2	+	93.29	4.93E-04	1.11E-02
negative regulation of fibroblast apoptotic process (GO:2000270)	7	3	+	59.97	4.05E-05	1.44E-03
positive regulation of myeloid cell apoptotic process (GO:0033034)	9	2	+	31.1	2.64E-03	4.08E-02
regulation of macrophage apoptotic process (GO:2000109)	10	2	+	27.99	3.15E-03	4.71E-02
regulation of fibroblast apoptotic process (GO:2000269)	17	3	+	24.7	3.65E-04	8.62E-03
positive regulation of leukocyte apoptotic process (GO:2000108)	31	3	+	13.54	1.78E-03	3.05E-02
negative regulation of lymphocyte apoptotic process (GO:0070229)	31	3	+	13.54	1.78E-03	3.04E-02
neuron apoptotic process (GO:0051402)	50	4	+	11.2	5.84E-04	1.27E-02
regulation of leukocyte apoptotic process (GO:2000106)	88	6	+	9.54	5.62E-05	1.89E-03
activation of cysteine-type endopeptidase activity involved in apoptotic process (GO:0006919)	90	6	+	9.33	6.32E-05	2.10E-03
positive regulation of cysteine-type endopeptidase activity involved in apoptotic process (GO:0043280)	137	9	+	9.19	1.01E-06	6.51E-05
extrinsic apoptotic signaling pathway (GO:0097191)	99	5	+	7.07	8.80E-04	1.77E-02
regulation of cysteine-type endopeptidase activity involved in apoptotic process (GO:0043281)	219	10	+	6.39	5.69E-06	2.85E-04

intrinsic apoptotic signaling pathway (GO:0097193)	154	7	+	6.36	1.54E-04	4.22E-03
apoptotic signaling pathway (GO:0097190)	293	11	+	5.25	1.15E-05	5.14E-04
positive regulation of apoptotic signaling pathway (GO:2001235)	180	6	+	4.66	2.15E-03	3.50E-02
positive regulation of apoptotic process (GO:0043065)	657	20	+	4.26	7.14E-08	6.10E-06
negative regulation of apoptotic process (GO:0043066)	915	25	+	3.82	1.12E-08	1.31E-06
apoptotic process (GO:0006915)	918	22	+	3.35	8.27E-07	5.46E-05
regulation of apoptotic process (GO:0042981)	1566	37	+	3.31	9.32E-11	1.90E-08
regulation of apoptotic signaling pathway (GO:2001233)	408	9	+	3.09	2.99E-03	4.53E-02
negative regulation of interleukin-23 production (GO:0032707)	2	2	+	> 100	2.97E-04	7.30E-03
interleukin-2 production (GO:0032623)	10	3	+	41.98	9.50E-05	2.87E-03
regulation of interleukin-23 production (GO:0032667)	8	2	+	34.98	2.17E-03	3.52E-02
cellular response to interleukin-7 (GO:0098761)	31	3	+	13.54	1.78E-03	3.05E-02
response to interleukin-7 (GO:0098760)	31	3	+	13.54	1.78E-03	3.04E-02
cellular response to interleukin-6 (GO:0071354)	37	3	+	11.35	2.85E-03	4.36E-02
positive regulation of interleukin-12 production (GO:0032735)	39	3	+	10.76	3.28E-03	4.84E-02
positive regulation of interleukin-1 beta production (GO:0032731)	54	4	+	10.37	7.67E-04	1.59E-02
regulation of interleukin-12 production (GO:0032655)	59	4	+	9.49	1.05E-03	2.01E-02
positive regulation of interleukin-6 production (GO:0032755)	91	6	+	9.23	6.70E-05	2.20E-03
positive regulation of interleukin-1 production (GO:0032732)	62	4	+	9.03	1.25E-03	2.33E-02
regulation of interleukin-6 production (GO:0032675)	141	7	+	6.95	9.12E-05	2.78E-03
mitotic cell cycle arrest (GO:0071850)	17	3	+	24.7	3.65E-04	8.63E-03
cell cycle arrest (GO:0007050)	145	11	+	10.62	1.53E-08	1.70E-06
G1/S transition of mitotic cell cycle (GO:0000082)	129	7	+	7.59	5.34E-05	1.81E-03
cell cycle G1/S phase transition (GO:0044843)	131	7	+	7.48	5.86E-05	1.96E-03
negative regulation of G1/S transition of mitotic cell cycle (GO:2000134)	107	5	+	6.54	1.23E-03	2.30E-02
negative regulation of cell cycle G1/S phase transition (GO:1902807)	110	5	+	6.36	1.38E-03	2.51E-02
regulation of G1/S transition of mitotic cell cycle (GO:2000045)	155	7	+	6.32	1.60E-04	4.37E-03

regulation of cell cycle arrest (GO:0071156)	111	5	+	6.3	1.43E-03	2.60E-02
regulation of cell cycle G1/S phase transition (GO:1902806)	176	7	+	5.57	3.37E-04	8.06E-03
negative regulation of mitotic cell cycle (GO:0045930)	312	10	+	4.49	1.04E-04	3.06E-03
negative regulation of cell cycle (GO:0045786)	579	17	+	4.11	1.19E-06	7.33E-05
positive regulation of cell cycle (GO:0045787)	393	11	+	3.92	1.50E-04	4.15E-03
mitotic cell cycle phase transition (GO:0044772)	289	8	+	3.87	1.30E-03	2.41E-02
cell cycle phase transition (GO:0044770)	297	8	+	3.77	1.54E-03	2.74E-02
positive regulation of cell cycle process (GO:0090068)	297	8	+	3.77	1.54E-03	2.73E-02
negative regulation of cell cycle process (GO:0010948)	329	8	+	3.4	2.85E-03	4.36E-02
regulation of mitotic cell cycle (GO:0007346)	640	15	+	3.28	6.75E-05	2.20E-03
regulation of cell cycle (GO:0051726)	1210	24	+	2.78	6.32E-06	3.12E-04
cell cycle process (GO:0022402)	1069	20	+	2.62	8.97E-05	2.75E-03
regulation of cell cycle process (GO:0010564)	770	14	+	2.54	1.41E-03	2.55E-02
mitotic cell cycle (GO:0000278)	772	14	+	2.54	1.44E-03	2.60E-02
cell cycle (GO:0007049)	1390	23	+	2.32	1.87E-04	4.94E-03
regulation of vascular associated smooth muscle contraction (GO:0003056)	9	2	+	31.1	2.64E-03	4.10E-02
regulation of smooth muscle cell proliferation (GO:0048660)	139	7	+	7.05	8.37E-05	2.60E-03

Table 24: Molecular functions of downregulated exosomal miRNA target genes.

GO molecular function complete	Homo sapiens - REFLIST (20851)	Target genes (325)	over/under	Fold Enrichment	raw <i>p</i> value	FDR
cyclin-dependent protein serine/threonine kinase inhibitor activity (GO:0004861)	12	4	+	46.65	4.15E-06	1.32E-03
I-SMAD binding (GO:0070411)	14	4	+	39.98	6.89E-06	1.93E-03
protein serine/threonine kinase inhibitor activity (GO:0030291)	31	5	+	22.57	5.31E-06	1.58E-03
cyclin-dependent protein serine/threonine kinase regulator activity (GO:0016538)	51	5	+	13.72	4.80E-05	9.93E-03
protein kinase inhibitor activity (GO:0004860)	65	6	+	12.92	1.13E-05	2.99E-03
kinase inhibitor activity (GO:0019210)	69	6	+	12.17	1.55E-05	3.89E-03
protein kinase regulator activity (GO:0019887)	193	10	+	7.25	1.94E-06	6.60E-04
kinase regulator activity (GO:0019207)	224	11	+	6.87	9.70E-07	3.55E-04
kinase binding (GO:0019900)	773	26	+	4.71	7.56E-11	1.20E-07
protein kinase binding (GO:0019901)	685	23	+	4.7	1.10E-09	8.76E-07
protein domain specific binding (GO:0019904)	713	20	+	3.93	2.56E-07	1.01E-04
protein-containing complex binding (GO:0044877)	1278	32	+	3.5	5.71E-10	5.43E-07
enzyme binding (GO:0019899)	2306	49	+	2.97	1.31E-12	3.12E-09
enzyme regulator activity (GO:0030234)	1085	21	+	2.71	3.64E-05	8.66E-03
signaling receptor binding (GO:0005102)	1716	33	+	2.69	1.63E-07	7.74E-05
transferase activity (GO:0016740)	2353	40	+	2.38	1.64E-07	7.08E-05
nucleotide binding (GO:0000166)	2180	33	+	2.12	3.75E-05	8.50E-03
nucleoside phosphate binding (GO:1901265)	2181	33	+	2.12	3.77E-05	8.16E-03
catalytic activity (GO:0003824)	5866	80	+	1.91	9.16E-11	1.09E-07
protein binding (GO:0005515)	14135	138	+	1.37	6.39E-13	3.04E-09
binding (GO:0005488)	16492	144	+	1.22	1.36E-09	9.27E-07

Table 25: Cellular components of downregulated exosomal miRNA target genes.

GO cellular component complete	Homo sapiens - REFLIST (20851)	Target genes (325)	over/under	Fold Enrichment	raw p value	FDR
heteromeric SMAD protein complex (GO:0071144)	8	4	+	69.97	1.15E-06	1.36E-04
SMAD protein complex (GO:0071141)	10	4	+	55.98	2.31E-06	2.01E-04
SCAR complex (GO:0031209)	10	3	+	41.98	9.50E-05	4.42E-03
apical junction complex (GO:0043296)	144	7	+	6.8	1.03E-04	4.70E-03
ruffle (GO:0001726)	181	8	+	6.19	6.27E-05	3.22E-03
lamellipodium (GO:0030027)	205	9	+	6.14	2.28E-05	1.23E-03
apical plasma membrane (GO:0016324)	368	12	+	4.56	1.78E-05	9.88E-04
apical part of cell (GO:0045177)	439	14	+	4.46	4.43E-06	3.55E-04
cell leading edge (GO:0031252)	430	13	+	4.23	1.71E-05	9.77E-04
cell-substrate junction (GO:0030055)	425	12	+	3.95	6.89E-05	3.45E-03
anchoring junction (GO:0070161)	839	23	+	3.84	4.38E-08	9.74E-06
perinuclear region of cytoplasm (GO:0048471)	740	19	+	3.59	1.88E-06	1.89E-04
plasma membrane region (GO:0098590)	1230	25	+	2.84	2.58E-06	2.15E-04
cell surface (GO:0009986)	947	18	+	2.66	1.71E-04	7.61E-03
membrane protein complex (GO:0098796)	1334	25	+	2.62	1.03E-05	7.39E-04
whole membrane (GO:0098805)	1748	32	+	2.56	7.65E-07	9.57E-05
nuclear outer membrane-endoplasmic reticulum membrane network (GO:0042175)	1156	21	+	2.54	8.87E-05	4.23E-03
catalytic complex (GO:1902494)	1402	25	+	2.5	2.36E-05	1.24E-03
cytosol (GO:0005829)	5311	94	+	2.48	7.18E-22	1.44E-18
endoplasmic reticulum membrane (GO:0005789)	1133	20	+	2.47	1.93E-04	8.39E-03
cytoplasmic vesicle (GO:0031410)	2449	40	+	2.29	5.61E-07	8.02E-05
intracellular vesicle (GO:0097708)	2454	40	+	2.28	5.79E-07	7.72E-05

extracellular vesicle (GO:1903561)	2119	34	+	2.25	7.60E-06	5.86E-04
extracellular organelle (GO:0043230)	2121	34	+	2.24	7.70E-06	5.71E-04
extracellular exosome (GO:0070062)	2098	33	+	2.2	1.46E-05	8.61E-04
bounding membrane of organelle (GO:0098588)	2164	34	+	2.2	1.04E-05	7.20E-04
cell junction (GO:0030054)	2066	31	+	2.1	8.26E-05	4.03E-03
protein-containing complex (GO:0032991)	5543	82	+	2.07	2.83E-13	1.13E-10
vesicle (GO:0031982)	3937	56	+	1.99	1.43E-07	2.60E-05
organelle membrane (GO:0031090)	3630	50	+	1.93	2.12E-06	2.02E-04
endomembrane system (GO:0012505)	4659	61	+	1.83	5.12E-07	7.89E-05
nucleoplasm (GO:0005654)	3990	51	+	1.79	1.45E-05	8.78E-04
cytoplasm (GO:0005737)	11740	135	+	1.61	6.11E-20	6.11E-17
nucleus (GO:0005634)	7598	87	+	1.6	7.50E-08	1.50E-05
organelle lumen (GO:0043233)	6112	69	+	1.58	1.26E-05	8.40E-04
intracellular organelle lumen (GO:0070013)	6112	69	+	1.58	1.26E-05	8.13E-04
membrane-enclosed lumen (GO:0031974)	6112	69	+	1.58	1.26E-05	7.87E-04
nuclear lumen (GO:0031981)	4986	56	+	1.57	2.23E-04	9.51E-03
intracellular membrane-bounded organelle (GO:0043231)	11071	120	+	1.52	4.26E-12	1.42E-09
membrane-bounded organelle (GO:0043227)	12783	132	+	1.45	2.32E-13	1.16E-10
membrane (GO:0016020)	9943	100	+	1.41	2.16E-06	1.97E-04
intracellular organelle (GO:0043229)	12896	129	+	1.4	4.10E-11	1.03E-08
organelle (GO:0043226)	13901	135	+	1.36	1.60E-11	4.59E-09
intracellular (GO:0005622)	14726	142	+	1.35	5.35E-14	3.57E-11
cellular anatomical entity (GO:0110165)	18790	149	+	1.11	4.57E-07	7.63E-05